

Cerebellar Codings for Control of Compensatory Eye Movements

Cerebellaire coderingen voor controle van compensatoire oogbewegingen

Proefschrift

ter verkrijging van de graad van doctor aan de
Erasmus Universiteit Rotterdam
op gezag van de
rector magnificus

Prof.dr. S.W.J. Lamberts

en volgens besluit van het College voor Promoties.

De openbare verdediging zal plaatsvinden op
woensdag 24 september 2008 om 15.45 uur

door

Martijn Schonewille

geboren te Rotterdam



Promotiecommissie

Promotor: Prof.dr. C.I. de Zeeuw

Overige leden: Prof.dr. M.A. Frens
Dr. T.J. Ruigrok
Dr. J. van der Steen

Copromotor: Dr. F.E. Hoebeek

TABLE OF CONTENTS

Ch. 1	General Introduction	
1.1	Compensatory Eye Movements	6
1.2	Anatomical Pathways	9
1.3	Spiking Activity in the Cerebellum	12
1.4	Molecular Pathways Related to Motor Adaptation	15
1.5	Scope of Thesis	16
Ch. 2	Anatomical Pathways	
	Zonal Organization of the Mouse Flocculus: Physiology, Input and Output	29
Ch. 3	Purkinje Cell Activity in Relation to Behaviour	
3.1	Purkinje Cells in Awake Behaving Animals Operate in Stable Upstate Membrane Potential	51
3.2	Regular Patterns in Cerebellar Purkinje Cell Simple Spike Trains	73
3.3	Increased Noise Level of Purkinje Cell Activities Minimizes Impact of their Modulation during Sensorimotor Control	91
Ch. 4	Plasticity of the Parallel Fiber to Purkinje Cell Synapse in Motor Learning	
4.1	Challenging the Marr-Albus-Ito Hypothesis	117
4.2	Role of Calcineurin in Pf-PC LTP and Cerebellar Motor Learning	127
Ch. 5	Molecular layer interneurons	
	Role of GABAergic Interneurons in Cerebellar Motor Learning	141
Ch. 6	Discussion	
6.1	Basic Principles in Purkinje Cell Activity and Motor Learning	186
6.2	Causes of Purkinje Cell Activity	188
6.3	Consequences of Purkinje Cell Activity	191
6.4	Conclusions and perspectives	193
	Summary	198
	Samenvatting	200
	Dankwoord	202
	Curriculum Vitae	206
	List of Publications	207

Chapter 1

General Introduction

Introduction

This thesis focuses on the control of the cerebellum on motor behaviour, and more specifically on the role of the cerebellar Purkinje cells in exerting this control. As the cerebellum is an online control system, we look at both motor performance and learning, trying to identify components involved at the molecular, cellular and network level.

To study the cerebellum we used the vestibulocerebellum, with visual and vestibular stimulation as input and eye movements as recorded output. The advantage of the vestibulocerebellum over other parts is that the input given is highly controllable, while the output can be reliably measured, and performance and learning can be easily studied. In addition, we conducted electrophysiological recordings from the vestibulocerebellum, in particular of Purkinje cells in the flocculus. Combining the spiking behaviour of Purkinje cells with visual input and eye movement output allowed us to study how the cerebellum functions and using genetically modified animals we could determine the role of different elements in this system.

To provide some insights in the techniques used and the theory behind them, we will discuss the following topics in this introduction: compensatory eye movements, the anatomy of pathways to, within and out of the flocculus, the cellular physiology of Purkinje cells in relation to performance and the plasticity mechanisms related to motor learning.

1.1 Compensatory eye movements

Compensatory eye movements are designed to prevent retinal slip, the slip of images over the retina resulting in a degraded image. In the mice the two main reflexes that compensate for head movements are the VOR and the OKR (Fig. 1A-B). The vestibulo-ocular reflex (VOR) is a reflex based on head movement, detected by the semicircular canals (angular movement) or the otoliths (linear movement). The optokinetic reflex (OKR) generates eye movements based on retinal slip, and therefore is a feedback system, where the VOR is a feedforward system. Together VOR and OKR aim to minimise the retinal slip caused by moving through an environment (Fig. 1C) (Baarsma and Collewijn, 1974; De Zeeuw et al., 1998b; Delgado-Garcia, 2000; van Alphen et al., 2001)

Vestibulo-Ocular Reflex

Three semi-circular canals (SCC) detect angular head movements around one vertical and two horizontal axes (Fig. 2). The canals are filled with endolymph which moves relative to the canal when the head rotates. This movement in combination with its viscosity causes a deviation of the cupular membrane. The apical part of the hair cells located on this cupula has cilia ('hairs') and these will be pushed by the endolymph, leading to depolarization of the cell. The distribution of the cilia is asymmetrical, with the largest (kinocilium) on one side. Movement of the cilia towards the kinocilium will cause an increased inflow of potassium (Johnstone et al., 1963), resulting on the basal side in an increase in neurotransmitter release, while movement away from the kinocilium has the opposite effect, resulting in a decrease in release. Endolymphic calcium appears to control the influx of potassium (Crawford et al., 1991a; Lumpkin and Hudspeth, 1995; Sauer et al., 1999).

The viscosity and inertia of the endolymph and the elastic properties of the

cupula make the SCC work as low-pass for angular acceleration. Over a broad range of frequencies, particularly those generated by the animal's normal behaviour, the system response is proportional to the angular velocity with a high-pass filter function (Jones and Milsum, 1971). From the SCC the head velocity signal is carried to the brainstem through the vestibular nerve, projecting to several (vestibular) nuclei (Siegborn and Grant, 1983; Newlands and Perachio, 2003). In order to move the eye ball in its orbit several forces including e.g. viscous drag of the eye ball, elastic forces of connective tissue have to be overcome by the eye muscles and therefore encoded in the signal sent to them. Since this includes both a position and a velocity component, an integration step is needed to drive the eye muscles. This integration occurs in the nucleus prepositus hypoglossi and adjacent part of the vestibular nucleus for vertical axis eye movements (in cats: Cheron and Godaux, 1987), while it occurs in the interstitial nucleus of Cajal for eye movements around both horizontal axes (in monkeys: Crawford et al., 1991b; in cats: Fukushima and Kaneko, 1995). This integrator is 'leaky', i.e. it is not functioning perfectly, and as a result the eye when placed eccentrically in the light will drift back to the null position in the dark. This drift has a time constant of ~20s for humans, monkeys and cats, but only ~3s (indicating it is more 'leaky') in mice. In addition to the brainstem the cerebellum is also suggested to play a role in this integration, since selective lesions caused a reduction in the time constant of the cat from 20s to 3s (Robinson, 1974; Cannon and Robinson, 1987). In humans, inducing a change in VOR phase in either lag or lead direction resulted in a post-saccadic drift. This led to the hypothesis that changes in VOR phase can be instigated by changing the time constant of this neural integrator (Tiliket et al., 1994)

In addition to the time constant of the velocity to position neural integrator, the VOR also has a time constant. This time constant is measured by providing a velocity step in the dark and fitting a single exponential to the evoked eye movements. The time constant of the VOR is relatively small (van Alphen et al., 2001) when compared to other (higher order) animals (Curthoys, 1982), which could be beneficial for the mice because it shifts the range of frequencies it optimally responds to towards the higher frequencies. Higher frequencies are likely to be more common for the fast-moving mouse in its small environment.

Optokinetic Reflex

The optokinetic reflex (OKR) is driven by retinal slip and aimed at reducing this slip, making it a negative feedback system (Fig. 2). The generation of the OKR starts in the retina where direction selective retinal ganglion cells respond to retinal slip in a preferred direction. It is supplementary to the VOR since the cells in the retina work best at lower frequencies, while the VOR functions better at higher frequencies. Higher primates have a fovea, an area on the retina with higher spatial resolution they use this to track objects moving in their field of vision, a system called smooth pursuit. Lower animals have a visual streak (e.g. rabbits) or a rather homogenous distribution of photoreceptors over their retina (e.g. mice).

The absence of a fovea in mice dismissed the need for a slow pursuit system, and thus slow moving objects in a stationary background will not be tracked. In contrast, moving the entire background can easily generate compensatory eye movements. In fact, at low frequencies the gain (ratio between eye and stimulus velocity) is close to 1, a value that drops with increasing frequency. OKR gain and phase also depend strongly on the velocity of the stimulus, as increasing velocity reduces the response. This low-

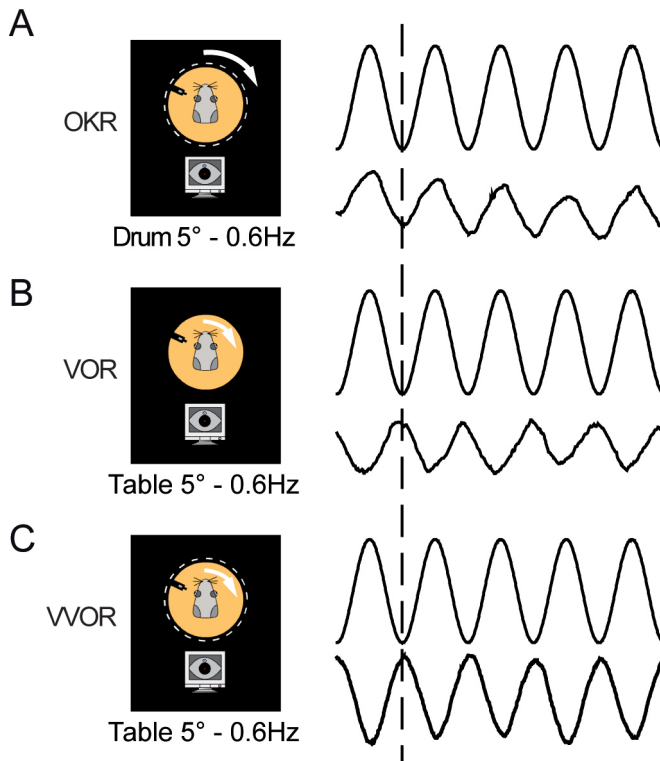


Figure 1. Compensatory eye movement recordings in mice. The two compensatory eye movements can be individually evoked in immobilized mice by either (A) rotating the dotted (white) surrounding of the mouse in the light (optokinetic response, OKR) or (B) rotating the turntable (yellow) in the dark (vestibulo-ocular response, VOR). Combining turntable rotation with light (C), the situation in every day life, will induced the visually-enhanced VOR, (VVOR). Stimulation induced eye movements can be tracked with an infrared camera, allowing for reproducible assessments of gain and phase of the eye movements. Low pass filter characterized OKR will complement high pass filter VOR,

pass filter-like behaviour makes the OKR an excellent complementary system for the VOR, since the OKR and VOR work best at low and high frequencies respectively. In the “natural” situation all movement of background will be the result of head movements of the mouse, of which the high frequencies will be compensated by the VOR and the residual low frequencies (or high frequencies at low velocity) by the OKR (Fig. 1).

Interaction between VOR and OKR

In every day (mouse) life VOR and OKR are not needed individually but work together to maintain the visual image stable in the retina during movement in a natural surrounding. The two reflexes are complementary and their sum is referred to in literature as visually enhanced (or visuo-) vestibular ocular reflex (VVOR) (Fig. 1). The three neuron relay of vestibular information to eye muscles can be modified through the visual input that feeds back into vestibular neurons, through cerebellum and inferior olive (Fig. 2). This system makes the cerebellum, in particular the flocculus, a candidate location for adaptation of the VOR according to visual feedback (Ito, 1982a). This suggests that the VOR should be modifiable with altered combination of visual and vestibular input, which was found to be true (Gonshor and Jones, 1973). In fact, the control over the VOR is so strong that its direction (or phase) can be completely reversed with prisms (Gonshor and Jones, 1976; Jones and Davies, 1976; Robinson, 1976).

Although the flocculus has a clear role in OKR, its role in VOR is debated. There are several contradicting studies; lesions of the flocculus resulted in either an increase in VOR gain (Robinson, 1976; Partsalis et al., 1995), a decrease (Keller and Precht, 1978; Ito et

al., 1982; Nagao, 1983) or had no clear effect (Barmack and Pettorossi, 1985). Chemical lesions had a similar, diffuse outcome; both a decrease (Van Neerven et al., 1989) and no effect on VOR gain (McElligott et al., 1998) were observed. Furthermore, in Lurcher mice, mice with a mutation resulting in a loss of Purkinje cells and therefore a loss of cerebellar output, the VOR gain is slightly higher than in their wild type littermates (Van Alphen et al., 2002; Katoh et al., 2005). While the role of the flocculus in baseline VOR is much debated, studies into its role in adaptation are more conclusive. Whether it was through physical lesion (Nagao, 1983) or chemical lesion (McElligott et al., 1998; Shutoh et al., 2006), all studies showed that impaired floccular function resulted in impaired adaptation.

This putative role of the flocculus in modifying the VOR was further experimentally confirmed in the same Lurcher mice. This mutation resulted in the loss of the ability to change the VOR, giving the flocculus a central role in this adaptation (Van Alphen et al., 2002; Katoh et al., 2005).

Experiments using chemical lesioning of the flocculus have demonstrated that the flocculus is indeed involved in the initial generation of the memory trace (McElligott et al., 1998; Nagao and Kitazawa, 2003). The question whether it remains in the flocculus or not has not been conclusively answered.

1.2 Anatomical Pathways

Compensatory eye movements are the result of activity in motoneurons that activate the extraocular eye muscles, which receive input from both vestibular nucleus neurons. These nuclei convey both visual and vestibular information and, important for this thesis, are under control of the cerebellar flocculus (Fig. 2). The flocculus is the part of the cerebellum involved in OKR, VOR and the adaptation of the VOR. While the output of the flocculus is restricted to cerebellar and vestibular nuclei, the input to the flocculus comes from more dispersed areas, like inferior olive, multiple vestibular nuclei and multiple pontine nuclei. Inputs from the inferior olive enter as climbing fibres, innervating Purkinje cells, while all other inputs enter as mossy fibres, innervating granule cells (Fig. 2).

Climbing fibres

Climbing fibre input to the flocculus originates from the contralateral inferior olive (Fig. 2), in particular the dorsal cap (DC) and the ventral lateral outgrowth (VLO). Cells in the caudal dorsal cap (CDC) modulate optimally the visual stimulus rotating around the vertical axis, while those in the ventral lateral outgrowth and rostral dorsal cap (RDC) respond best to rotations around the horizontal axis perpendicular to the plane of the ipsilateral anterior semicircular canals. The topographic organization in the inferior olive is continued in the flocculus (Voogd et al., 1996), shown in e.g. monkeys (Voogd et al., 1987), cats (Sato and Kawasaki, 1984) and rabbits (De Zeeuw et al., 1994). In rats, two zones (2 and 4) of Purkinje cells in the flocculus are innervated by the CDC and two (1 and 3) by the VLO (Ruigrok et al., 1992). This topographic separation of vertical and horizontal axis pathways is present throughout most of the visual pathway. The above described retinal slip signals reach the inferior olive through subsequently the ipsilateral dorsal tegmental nucleus and the pretectal nucleus of the optic tract for slip around the vertical axis (Gioli et al., 1988; Soodak and Simpson, 1988). In contrast, horizontal axis directed retinal slip passes through contralateral medial terminal nucleus and ipsilateral visual tegmental relay zone of the accessory optic system (Gioli et al., 1984; Soodak and

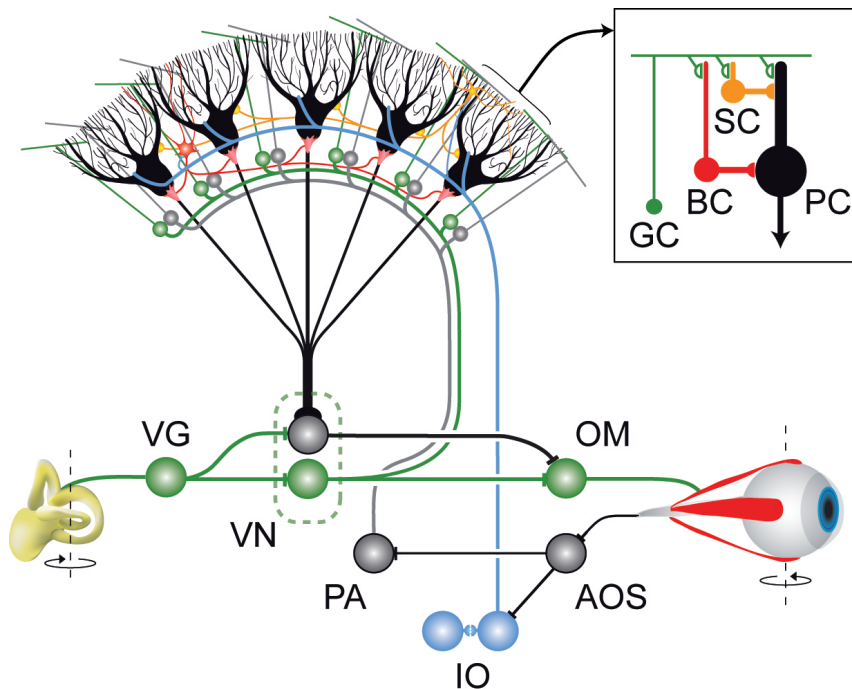


Figure 2. Schematic drawing of intra- and extracerebellar connections.

Purkinje cells (PC; black) in the flocculus of the vestibulo-cerebellum converge upon neurons in the vestibular nuclei (VN), through which they can influence the output of the oculomotor neurons (OM) that drive the eye movements. The Purkinje cells are innervated by two main inputs: they receive vestibular and eye movement signals through the mossy fiber-parallel fiber system (represented by green and grey inputs, respectively), and retinal slip signals through climbing fibers derived from the inferior olive (IO; blue). The parallel fibers, which all originate from the granule cells (GC), innervate the dendritic trees of both Purkinje cells and molecular layer interneurons (basket cells, BC: red and stellate cells, SC: yellow), thereby providing a feedforward inhibitory connection (see inset). VG, AOS and PA indicate vestibular ganglion cells, accessory optic system, and pontine areas, respectively.

Simpson, 1988).

Mossy fibres

In contrast to climbing fibre input the mossy fibre input targets granules cells, is of bilateral origin and comes from various different sources. Mossy fibres originate from the vestibulum, spinal cord and brainstem and carry information from the periphery and the cerebral cortex. It has been found that the flocculus receives mossy fibre projections from 4 main sources (cat: Sato et al., 1983; monkey: Langer et al., 1985a; rat: Ruigrok, 2003): (1) Perihypoglossal nucleus: dense projections originate from discrete areas of the rostral pole of the intercalated nucleus, the ventral part of the prepositus hypoglossal nucleus and the adjacent reticular formation. (2) Vestibular nuclear complex: secondary vestibular fibres come from discrete areas in the vestibular nuclei: the ventromedial and dorsomedial parts of the medial and inferior nucleus, the central area of the superior nucleus, the ventromedial part of the lateral nucleus, the group y and the interstitial nucleus of the vestibular nerve. (3) Medullary reticular formation: the strongest projection of mossy fibres arises from the accessory group of the paramedian reticular nucleus. (4) Pontine reticular formation and raphe nucleus: dense projections originate

from a narrow zone which involves the caudal part of the dorsal nucleus of the raphe, the inferior and superior central nucleus of the raphe and the medial part of the nucleus reticularis tegmenti pontis.

Mossy fibres are excitatory and most use glutamate as a neurotransmitter (for review see Voogd et al., 1996). Monoaminergic input consists mainly of serotonin and noradrenaline: serotonergic fibres originate in the nucleus pontis oralis and nucleus reticularis (para)gigantocellularis (Bishop et al., 1985), while noradrenergic input comes from the locus coeruleus (van Neerven et al., 1990). Injecting beta-antagonists into the flocculus blocked adaptation, while a beta-agonist enhanced the adaptation (van Neerven et al., 1990; van Neerven et al., 1991)

Furthermore there is evidence for the presence of both cholinergic input particularly in the vestibulocerebellum and predominantly from the medial vestibular nucleus (MVN) and nucleus prepositus hypoglossi (PrH) (Barmack et al., 1992) and of corticotropin-releasing factor from climbing fibres (Palkovits et al., 1977) and mossy fibres (Cummings and King, 1990). Cholinergic receptors have been found on granule cells and unipolar brush cells (Jaarsma et al., 1996).

Cerebellar cortical circuit

Whereas the climbing fibres mainly directly innervate Purkinje cells, the information carried by mossy fibres does not directly go to Purkinje cells, but instead innervates granule cells. Granule cells are the most abundant cell type in the brain, receiving single mossy fibre input from excitatory synapses on their dendrites. These dendrites terminate in a structure known as the glomerulus. Granule cell axons travel through the Purkinje cell layer to the molecular layer where they bifurcate and continue as parallel fibres to contact large number of Purkinje cells, and stellate and basket cells. Before bifurcating the ascending granule cell axon also contacts Purkinje and Golgi cells. These Golgi cells are inhibitory cells, located in the granular layer, that project back to the granule cells, with synapses in the above mentioned glomeruli. This creates an inhibitory feedback loop, effectively controlling the output of granule cells. Additional to this feedback loop the stellate cells and basket cells provide feed forward inhibition onto Purkinje cells. Stellate cells are located in the distal part of the molecular layer and inhibit the distal Purkinje cell dendrites; basket cells reside in the more proximal part of the molecular layer and owe their name to the basket-like synapse they form around the soma/axon hillock of Purkinje cells, suggesting they have a firm control on Purkinje cell activity (Eccles et al., 1967; Marr, 1969; Albus, 1971).

Floccular output pathway

The Purkinje cell axons carry the only signal going out of the cerebellar cortex. The projection targets of Purkinje cells are strongly related to the floccular zone they are in, as demonstrated in rabbit (De Zeeuw et al., 1994), monkey (Langer et al., 1985b), cat (Sato et al., 1988). Their target cells (floccular target neurons, FTNs) are in several cerebellar and vestibular nuclei, nuclei that also project to the flocculus. However, the FTNs do not project to the flocculus, but (in)directly project to the oculomotor nuclei (Sato et al., 1988). Remarkably, only a very small portion of for instance the MVN receives direct floccular input: only ~1% of all cells receive multiple boutons (Sekirnjak et al., 2003) and ~10% is inhibited by floccular stimulation (Sato et al., 1988).

In addition to the above described four zones in the rabbit flocculus there is a

fifth zone that does not receive visually modulated climbing fibre input. This zone is suggested to be related to head movements, since stimulation of this zone evokes short-latency head-movements (De Zeeuw and Koekkoek, 1997). The five zones can be visualized by acetylcholinesterase staining since its staining in fact delineates the borders between the zones (Voogd and Bigaré, 1980; Tan et al., 1995). This organization in the rabbit does not differ significantly between species, like for example: cat (Voogd, 1964; McCrea et al., 1979; Sato et al., 1982), primate (Haines, 1977; Langer et al., 1985b) and rat (Balaban et al., 2000). In general zones 1 and 3, modulating to horizontal axis (135°) visual stimulation, project to superior vestibular nucleus (SVN), group Y and ventral dentate nucleus (VDN). Zone 2 and 4, where Purkinje cells receive climbing fibre activity during contralateral movement of a visual stimulus during vertical axis rotation, project to the MVN and weakly to the lateral vestibular nucleus (LVN) for rabbit (De Zeeuw et al., 1994), monkey (Langer et al., 1985b), and cat (Sato et al., 1982).

Although there clearly is considerable amount of knowledge regarding the afferent and efferent projections of the flocculus in primates, cats, rabbits and rats, remarkable little is known about the flocculus in the mouse. Genetic tools such as knockouts and transgenics have rendered the mouse increasingly important as a laboratory animal model, especially in behavioural experiments and floccular recordings from a correctly identified zone in mutant mice would be an auspicious tool to study cerebellar function. The question therefore is: how is the mouse flocculus with its afferent and efferent connections organized?

1.3 Spiking activity in the cerebellar cortex

This thesis attempts to correlate cerebellar coding in spike activity with motor control. Traditionally, the focus in cellular recordings has been on the Purkinje cells, as they are the only cell projecting out of the cerebellar cortex, are cells with a high firing rate and therefore easy to find, and allow for confirmed single unit recordings. A consistently present pause in simple spikes after a complex spike, the climbing fibre pause, confirms that the recording is from only one Purkinje cell (Thach, 1967). Because Purkinje cells are the sole output cells, the result of cerebellar cortical information processing has to be in its spiking activities. The high average simple spike firing rate of Purkinje cells (~50Hz) could be seen as an optimal basis for information transfer, with a range of firing frequencies 'available'. Purkinje cells appear to use this range as they are known to fire highly irregularly (see e.g. Armstrong and Rawson, 1979).

Input to Purkinje cells

As described above, when it comes to sensorimotor information the cerebellum primarily receives 2 types of input: mossy fibres and climbing fibres. The climbing fibres directly innervate Purkinje cells, causing complex spikes that will be discussed separately in detail below. Mossy fibres contact granule cells, the most abundant cell type in the brain. Granule cells are small, and under inhibitory control of Golgi cells. As a result granule cells typically have a low average firing rate (<1Hz) but can temporarily reach very high frequencies (up to 250Hz) (Chadderton et al., 2004).

The axons of granule cells, ascending and parallel fibres, terminate on most other cell types in the cerebellar cortex, including Purkinje cells, stellate cells, basket cells and Golgi cells. Golgi cells primarily project back to granule cells and fire at moderately high

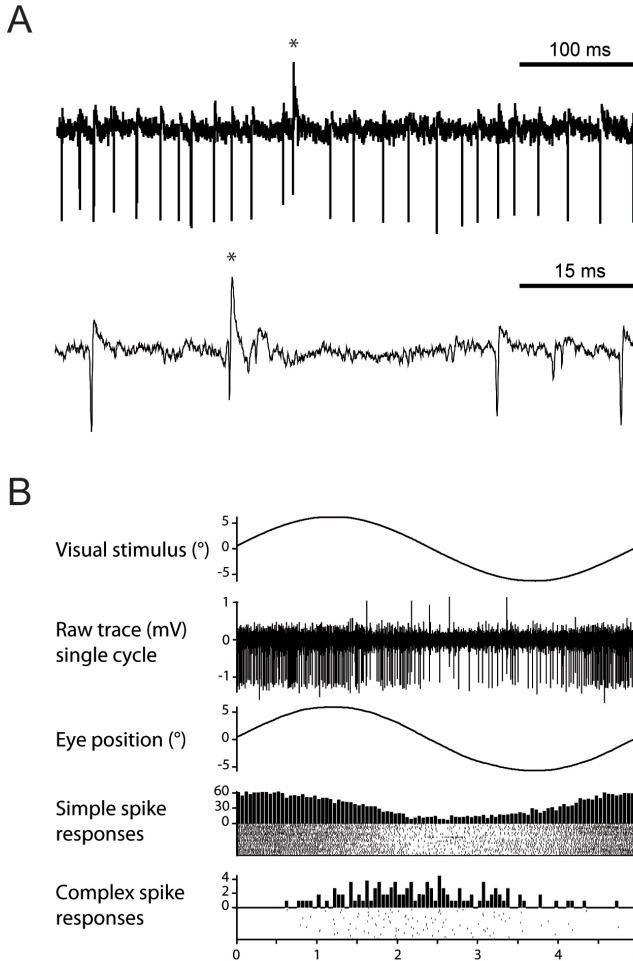


Figure 3. Purkinje cell activity recordings.

A) Extracellular recordings of Purkinje cells activity with two spike types: simple spikes and complex spikes (*). Note the clearly higher frequency of simple spikes ($\sim 50\text{Hz}$) compared to complex spikes ($\sim 1\text{Hz}$). B) Recording of a floccular (VA) Purkinje cell during sinusoidally rotating visual stimulation, showing modulation of both simple and complex spikes. Ipsilateral rotation (here: down) is related to a decrease in simple spike firing rate, while the complex spike frequency increases. Histograms further demonstrate this reciprocal relationship (example from this thesis).

frequencies: cat, 2 to 50 Hz (Edgley and Lidieth, 1987); monkey, 10–80 Hz (Miles et al., 1980); anaesthetized rats 8–30 Hz (Simpson et al., 2005; Holtzman et al., 2006); mouse $\sim 3\text{Hz}$ (Barmack and Yakhnitsa, 2008) and irregular firing with a coefficient of variance of ~ 0.9 (Vos et al., 1999).

Stellate and basket cells, or molecular layer interneurons (MLIs), have been suggested to receive, in addition to parallel fibre input, climbing fibre collaterals (Eccles et al., 1966b). Because MLIs receive the same inputs as Purkinje cells theoretically they should be capable of demonstrating comparable plasticity forms, a hypothesis that was confirmed recently (Mittmann et al., 2005) who made clear that the effect of coactivation of parallel and climbing fibre on Purkinje cell output depends on the balance between excitation and feed-forward inhibition through MLIs. Both MLIs project their inhibitory input onto a sagittal band of Purkinje cells. Both MLIs also have been found to display moderate/high firing frequencies in rat slice of $\sim 12\text{Hz}$ (Hausser and Clark, 1997) and $\sim 10\text{Hz}$ for stellate and $\sim 5\text{Hz}$ for basket cells in vivo (Barmack and Yakhnitsa, 2008). In fact, the only obvious difference between SC and BC is the location and size

of their axonal endings. Stellate cells terminate on Purkinje cell dendrites with 'normal' synapses, while basket cells derive their name from their basket-shaped axon terminal. This pinceau (Bishop, 1993) is a very large terminal wrapped around the soma and axon hillock, suggesting a strong control on Purkinje cell firing. The fact that MLIs harbour a combination of parallel and climbing fibre inputs with a strong control on Purkinje cell simple spike firing, poses an interesting question: To what extent are MLIs involved in Purkinje cell firing and motor behaviour?

Simple Spikes

Purkinje cells are one of the few cell types that can be instantly recognized, based on the types of spikes they fire: simple spikes at approx. 50Hz and complex spikes at approx. 1Hz (Fig 3A). The latter will be discussed below; the former is basically a normal action potential. Simple spikes are the result of a combination of 3 elements: intrinsic activity, excitatory inputs and inhibitory inputs. The intrinsic activity of Purkinje cells is very high, in slices with all inputs blocked it reaches 30-50 Hz: in rat ~40Hz (Hausser and Clark, 1997; Williams et al., 2002). This tonic intrinsic firing is related to the presence of resurgent sodium current (Raman and Bean, 1997, 1999).

Although a single Purkinje cell is contacted by ~175,000 parallel fibres (Napper and Harvey, 1988), the proportion of simple spikes in the background firing rate caused by excitatory inputs is not clear. In fact, recent evidence indicates a large portion of the parallel fibre contacts is silent, and stimulation of granule cells led in only ~10% of the cases to a recordable effect in Purkinje cells (Isope and Barbour, 2002). Despite the unclear potential of parallel fibre input, sensorimotor activity can temporarily drive the firing rate up, e.g. to 100-150Hz during arm movements (Gilbert and Thach, 1977) or to ~80Hz during eye movements (Fig. 3B) (Goossens et al., 2004) in responsive Purkinje cells. In fact, in slices the maximum firing rate observed was ~290Hz (Khaliq and Raman, 2005). Similarly, either the absence of excitation and/or an increase in inhibitory input can decrease simple spike firing rate dramatically. During sensorimotor stimuli, e.g. visual stimulus, this can be down to ~20Hz, and more abrupt activity can cause brief cessation of firing. Recent experiments even provide evidence that suggests that Purkinje cells have two states, depolarized/firing and hyperpolarized/silent. Since sensory input through climbing fibres can function as a switch between the two states, it was suggested that this could have a key role in short-term processing and storage of sensory information.

So not only do Purkinje cells have this extremely large range of frequencies to transfer information, they tend to use it too. Despite the intrinsic regular firing generation, Purkinje cells are known to be highly irregular with observed CV values ranging from 0.5 to 1 (Armstrong and Rawson, 1979; Goossens et al., 2004). The eminent question remaining thus is: what is the relation between Purkinje cell firing and behaviour?

Complex spikes

Climbing fibres, originating from the inferior olive, innervate Purkinje cells with a very large number of contact points. This large number of synapses (in rat ~250, Rossi et al., 1993; Shinoda et al., 2000) have a high release probability (Dittman and Regehr, 1998; Silver et al., 1998) and thus cause a massive depolarization of the Purkinje cell. Each climbing fibre innervates 5-10 Purkinje cells in a sagittal band (Sugihara et al., 2001; Sugihara et al., 2004), while each Purkinje cell is -in adult animals- innervated by only one climbing fibre. Because sagittal bands of Purkinje cells converge onto the same neurons

in the deep cerebellar or vestibular nucleus the complex spike signal may well have a strong impact even there. Purkinje cells receiving input from the same olivary neuron would fire complex spikes synchronously, a phenomenon that could be enhanced by the electrotonic coupling in the inferior olive (Llinas and Yarom, 1981). The dendrites of inferior olive cells are coupled by gap junctions, and this coupling under control of inhibitory input (De Zeeuw et al., 1993) and excitatory input (de Zeeuw et al., 1990).

The depolarization caused by climbing fibre activity results in a typical spike shape. A number of spikelets ride on a (~20ms) calcium wave (Eccles et al., 1966a) (Llinas and Sugimori, 1980a). This typical spike shape is the result of the following events, as reviewed by Schmolesky et al. (2002): 1) First the hundreds of contacts points of a single climbing fibre simultaneously release glutamate after an inferior olive neuron fires an action potential. This glutamate activates AMPA receptors and causes an EPSP. Because of the large number and spread of synapses the depolarizations lead to a dendritic calcium wave (Llinas and Sugimori, 1980b). The calcium waves requires P/Q and T-type voltage gated calcium channels (Pouille et al., 2000). This depolarization spreads to the axon hillock where it causes a sodium action potential, comparable to the simple spike (Ito, 1984; Stuart and Hausser, 1994). Conversely, sodium action potentials hardly travel into the dendrite (Lasser-Ross and Ross, 1992; Stuart and Hausser, 1994), presumably rather than due to the low number of sodium channels this is the result of the dendritic geometry of the Purkinje cell (Vetter et al., 2001). 2) The before mentioned dendritic calcium wave, caused by voltage gated calcium channels, typically has a number of spikelets riding on it. These spikelets are probably caused by resurgent sodium current (Raman and Bean, 1997). Interestingly, a recent study by Davie et al. (2008) shows that dendritic spikelets are not required for, nor directly linked to, somatic spikelets in the complex spikes. 3) A slow repolarization and a slow afterhyperpolarization constitute the final part of the complex spike. In addition to a role for the before mentioned voltage gated calcium channels and resurgent sodium channels, the involvement of calcium-dependent potassium (BK and SK) channels has also been demonstrated (Edgerton and Reinhart, 2003; Womack and Khodakhah, 2003).

The role of the complex spike is strongly debated, for review see (Simpson et al., 1996; De Zeeuw et al., 1998a). Some see it as a timing device, where the inferior olive organizes movement in time and space (Llinas, 1988; Welsh et al., 1995). Others consider it to be a teacher signal used to induced plasticity as originally proposed by Marr (1969) and Albus (1971), a mechanism that will be discussed more extensively below. Although there is a significant amount of evidence, also from other cerebellar learning tasks (Koekkoek et al., 2003) supporting the involvement of teacher signal controlled plasticity in motor learning, the issue is still heavily debated. We will attempt to shed some more light on the issue in this thesis.

1.4 Molecular pathways related to motor adaptation

Pf-PC LTD and LTP at the molecular level

The large influx of calcium during a complex spike is considered to be highly relevant for motor learning. Ever since the late 1960s and early 1970s cerebellar learning has been hypothesized to depend upon changes in synaptic strength of the parallel fibre-Purkinje cell synapse (Pf-PC), based on anatomy and modelling. Marr (1969) suggested that the climbing fibre functions as a teaching signal, used to calibrate synaptic strength so that it

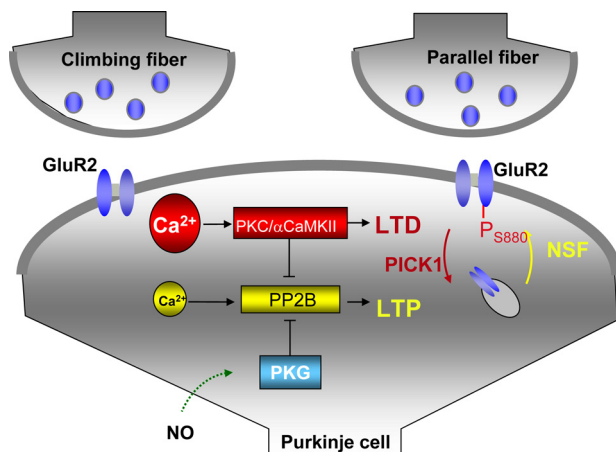


Figure 4. Molecular pathways in parallel fibre to Purkinje cell plasticity. Schematic drawing with, for reasons of clarity, climbing fibre (CF) and PF terminals contacting the same postsynaptic compartment. The cascade leading to LTD induction is depicted in darker grey. A large calcium transient, requiring climbing fibre activity, promotes PKC activation, which phosphorylates GluR2. GluR2 endocytosis requires binding of GluR2 to protein interacting with C-kinase1 (PICK1). The LTP cascade is shown in lighter grey: lower calcium transients promote phosphatase activation (only PP2B is directly calcium-regulated). GluR2 insertion requires GluR2 binding to NSF (adapted from Hansel et al., 2005)

will ultimately function correctly on its own, without olivary input. Subsequently, Albus (1971) extended and adjusted this theory by emphasizing an important role for the mossy fibre – granule cell – Golgi cell relay in pattern discrimination and by stating that the climbing fibre teaching should weaken -not strengthen- concomitant active parallel fibre contacts. Ito and colleagues (Ito, 1982b; Ito and Kano, 1982) extended the evidence for this theory by demonstrating that conjunctive climbing and parallel fibre stimulation decreases the postsynaptic excitation in Purkinje cell dendrites after parallel fibre stimulation (Fig. 4). Later the role of calcium in this process was confirmed (Miyakawa et al., 1992). Calcium enters the Purkinje cell through P/Q and T-type calcium channels after climbing fibre activity (Pouille et al., 2000; Schmolesky et al., 2002), but also from parallel fibre activated mGluR1 receptors, that cause inositol-triphsphate (IP₃) mediated calcium release from intracellular stores (Schoepp et al., 1990). In addition, parallel fibre activates diacylglycerol (DAG), and together DAG and calcium activate protein kinase C (PKC). When PKC is inhibited Pf-PC LTD does not occur; placing PKC in the cascade leading to LTD (Linden and Connor, 1991; Narasimhan and Linden, 1996). In addition to PKC other kinases are present in Purkinje cells. Protein kinase G is presumably involved through a different pathway, related to nitric oxide (NO) synthesis. NO is a very small molecule that spreads fast and far (Reynolds and Hartell, 2001); it activates guanylyl cyclase, which converts GTP into cGMP (Marcoli et al., 2006). The cGMP in turn activates PKG, which blocks dephosphorylation of AMPA receptors (Ito and Karachot, 1990; Hartell, 1994), comparable to PKC. As a result, blocking PKG causes a strong reduction of LTD (Feil et al., 2003). Additionally, and more recently, also calcium/calmodulin-dependent protein kinase II (CamKII) was demonstrated to be intimately involved in Purkinje cell plasticity. This kinase can function as a memory switch, as calcium causes a prolonged activation of CamKII (Lisman et al., 2002). Recent evidence indicates that kinases like PKC can act directly upon the GluR2 subunit of the AMPA receptor (Chung et al., 2003). Moreover, PKC activates Protein Interacting with C Kinase 1 (PICK1), which in turn also targets the C-terminal end of the GluR2 subunit (Xia et al., 1999). Both appear to be required for AMPA internalization and thus PF-PC LTD (Steinberg et al., 2006), leading to the interesting question: Is the observed phenotype in LTD-deficient mice caused by kinase mutations persistently present in mice that are LTD-deficient as a result of mutations downstream,

closer to the actual AMPA receptor internalization?

The phosphorylating function of kinases is counteracted by dephosphorylation by phosphatases. Very recent work confirms a role for phosphatases in Purkinje cells, by demonstrating that e.g. protein phosphatase 2B (PP2B) is required for parallel fibre to Purkinje cell long term potentiation (Pf-PC LTP). Evidence for the role of phosphatases in plasticity originates predominantly from the hippocampus, where similar interactions may occur at the systems level even though LTP and LTD are mediated by molecular processes that are opposite to those in the cerebellum (for review see Jorntell and Hansel, 2006). In contrast to that in cerebellar Purkinje cells, induction of LTP in hippocampal pyramidal cells is mediated by kinase pathways such as that of CamKII, whereas LTD in these cells is dependent on phosphatases such as PP2B (Zeng et al., 2001). Particularly in light of the discovery of large percentages of parallel fibre contacts that are silent an interesting question arises: what is the contribution of phosphatases and thereby of Pf-PC LTP to Purkinje cell activity and motor behaviour?

LTD and LTP in behaviour

A number of the molecules involved in the pathway leading to LTD have been used to generate genetically manipulated mice, in order to confirm their involvement in an intact system and to further elucidate the proposed role of LTD in motor learning. One of the first attempts was made with mice with a global deletion of the mGluR1 receptor, which resulted in a very severe cerebellar phenotype accompanied by absence of LTD and impaired climbing fibre elimination, and characterized by ataxia and impaired conditioned eye blink response (Aiba et al., 1994). Re-introduction of mGluR1 specifically in the Purkinje cells rescued the cerebellar symptoms (Kano et al., 1997). However, injecting mice with autoantibodies against mGluR1 from patients with paraneoplastic cerebellar ataxia affect both plasticity and 'normal' activity of Purkinje cells, suggesting that mGluR1 is involved in more than LTD (Coesmans et al., 2003). In an attempt to create a mouse with a more specifically affected plasticity, Chen and colleagues made a PKCgamma knockout mouse, but the phenotype was not very straightforward as motor performance in locomotion was affected, but motor learning in eye blink conditioning was not hampered (Chen et al., 1995). Moreover, cell physiological analysis demonstrated that in these mice Pf-PC LTD was not affected, but climbing fibre elimination was (Chen et al., 1995; Kano et al., 1995), suggesting that other PKC isoforms can compensate for the absence of gamma in the induction of LTD.

To avoid compensation by other kinases and a-specific non-Purkinje cell effects, De Zeeuw et al. (De Zeeuw et al., 1998c) created mice with a short PKC inhibitory peptide under control of a Purkinje cell specific promoter (L7-PKCi). The mice heterozygous for the mutation displayed impaired LTD, delayed climbing fibre elimination, normal motor performance and impaired VOR adaptation. Additional evidence supporting the role of LTD in VOR adaptation was obtained with mice with a Purkinje cell specific deletion of cGMP-dependent protein kinase (cGKI or PKG). These mice were also found to have reduced LTD, normal climbing fibre elimination, normal motor performance but impaired VOR adaptation. Taken together these studies demonstrate a strong correlation between LTD and motor learning, albeit solely based on kinase mutations that are abundantly present and potentially affect other pathways in Purkinje cells. A similar phenotype, impaired LTD and motor learning, was found in mice homozygous for a mutation deleting alphaCamKII globally (Hansel et al., 2006). Deletion of alphaCamKIV resulted in a loss

of LTD maintenance, and a more subtle impairment of VOR adaptation (Boyden et al., 2006).

Although the accumulated evidence linking Pf-PC LTD to motor learning is very convincing, there is still reason to be cautious. This thesis attempts to provide the next step in understanding the cerebellar contribution to motor learning.

Scope of thesis

The general aim of this thesis was to investigate the mechanisms underlying motor performance and adaptation at the molecular, cellular and network level. In particular we examine the role of Purkinje cell activity in cerebellar control of motor behaviour. First we give an introduction on compensatory eye movements, anatomical pathways, Purkinje cell activity and molecular pathways in the cerebellum (Chapter 1).

Chapter 2 describes how we made a functional map of the flocculus, the part of the cerebellum related to eye movements. The flocculus was divided into 5 functional zones based on Purkinje cells displaying climbing fibre responses selectively during optokinetic stimulation around the horizontal or vertical axis. The origin of their climbing fibre inputs, the nuclei receiving their output and a biochemical marker linked to specific zones are described.

In Chapter 3 we study the relation between Purkinje cell simple spike activity and behaviour. First, we examined the acclaimed role of bistability of the Purkinje cell membrane potential, and its role in storage of sensory information. Here we provide evidence suggesting several factors (genetic manipulation, anaesthesia) can disturb normal simple spike timing, and describe that Purkinje cells of awake behaving normal mice show very little sign of bistability (Ch. 3.1). Secondly, we demonstrated in normal mice the occurrence of patterns, periods of regular sized inter simple spike intervals, and their strong correlation with behaviour (Ch. 3.2). Finally, we investigated the role of the temporal structure of Purkinje cell simple spikes and their relation to motor behaviour. We describe how a mutation in the P/Q type voltage gated calcium channel in the tottering mutant results in highly irregular simple spike firing and the relation of this disturbance to the ataxic phenotype of these mutants (Ch. 3.3).

Chapter 4 investigates the molecular pathways involved in cerebellar adaptation processes. We studied the role of proteins involved in the plasticity at the parallel fibre to Purkinje cell synapse (PF-PC LTD) (Ch. 4.1). In 3 different mouse mutants that did not display PF-PC LTD -considered to be required for normal adaptation-, we did not find any motor performance or adaptation deficits. Next, we initiated a new approach by studying a Pf-PC LTP-deficient mutant mouse. These mice demonstrated learning deficits in both VOR adaptation and eye blink conditioning, and increased simple spike regularity (Ch. 4.2).

Then we shifted our focus towards the role of the molecular layer interneurons, by studying mice in which inhibition of Purkinje cells is genetically and selectively removed (Ch. 5). The mutant mice showed a robustly affected consolidation of motor adaptation, not being able to successfully complete a long-term adaptation paradigm. Close examination of the simple spike temporal structure revealed a consistent and clear difference in the regularity of firing, which was higher compared to littermates, particularly on small timescales.

In Chapter 6 we discuss the major findings in this thesis, and address the causes and consequences of Purkinje cell simple spike firing, in view of the possibility of temporal and frequency coding. We make an attempt at integrating this with our findings concerning the role of synaptic plasticity and Purkinje cell inhibition in motor adaptation.

Overall, this thesis aims to evaluate several existing theories, and at the same time explores new directions of research that could be further addressed in the near future.

Reference List

- Aiba A, Kano M, Chen C, Stanton ME, Fox GD, Herrup K, Zwingman TA, Tonegawa S (1994) Deficient cerebellar long-term depression and impaired motor learning in mGluR1 mutant mice. *Cell* 79:377-388.
- Albus JS (1971) A theory of cerebellar function. *Math Biosci* 10:25-61.
- Armstrong DM, Rawson JA (1979) Activity patterns of cerebellar cortical neurones and climbing fibre afferents in the awake cat. *J Physiol* 289:425-448.
- Baarsma E, Collewijn H (1974) Vestibulo-ocular and optokinetic reactions to rotation and their interaction in the rabbit. *J Physiol* 238:603-625.
- Balaban CD, Schuerger RJ, Porter JD (2000) Zonal organization of flocculo-vestibular connections in rats. *Neuroscience* 99:669-682.
- Barmack NH, Pettorossi VE (1985) Effects of unilateral lesions of the flocculus on optokinetic and vestibuloocular reflexes of the rabbit. *J Neurophysiol* 53:481-496.
- Barmack NH, Yakhnitsa V (2008) Functions of interneurons in mouse cerebellum. *J Neurosci* 28:1140-1152.
- Barmack NH, Baughman RW, Eckenstein FP, Shojaku H (1992) Secondary vestibular cholinergic projection to the cerebellum of rabbit and rat as revealed by choline acetyltransferase immunohistochemistry, retrograde and orthograde tracers. *J Comp Neurol* 317:250-270.
- Bishop GA (1993) An analysis of HRP-filled basket cell axons in the cat's cerebellum. I. Morphometry and configuration. *Anat Embryol (Berl)* 188:287-297.
- Bishop GA, Ho RH, King JS (1985) Localization of serotonin immunoreactivity in the opossum cerebellum. *J Comp Neurol* 235:301-321.
- Boyden ES, Katoh A, Pyle JL, Chatila TA, Tsien RW, Raymond JL (2006) Selective engagement of plasticity mechanisms for motor memory storage. *Neuron* 51:823-834.
- Cannon SC, Robinson DA (1987) Loss of the neural integrator of the oculomotor system from brain stem lesions in monkey. *J Neurophysiol* 57:1383-1409.
- Chadderton P, Margrie TW, Häusser M (2004) Integration of quanta in cerebellar granule cells during sensory processing. *Nature* 428:856-860.
- Chen C, Kano M, Abeliovich A, Chen L, Bao S, Kim JJ, Hashimoto K, Thompson RF, Tonegawa S (1995) Impaired motor coordination correlates with persistent multiple climbing fiber innervation in PKC gamma mutant mice. *Cell* 83:1233-1242.
- Cheron G, Godaux E (1987) Disabling of the oculomotor neural integrator by kainic acid injections in the prepositus-vestibular complex of the cat. *J Physiol* 394:267-290.
- Chung HJ, Steinberg JP, Huganir RL, Linden DJ (2003) Requirement of AMPA receptor GluR2 phosphorylation for cerebellar long-term depression. *Science* 300:1751-1755.
- Coesmans M, Smitt PA, Linden DJ, Shigemoto R, Hirano T, Yamakawa Y, van Alphen AM, Luo C, van der Geest JN, Kros JM, Gaillard CA, Frens MA, de Zeeuw CI (2003) Mechanisms underlying cerebellar motor deficits due to mGluR1-autoantibodies. *Ann Neurol* 53:325-336.
- Crawford AC, Evans MG, Fettiplace R (1991a) The actions of calcium on the mechano-electrical transducer current of turtle hair cells. *J Physiol* 434:369-398.

- Crawford JD, Cadera W, Vilis T (1991b) Generation of torsional and vertical eye position signals by the interstitial nucleus of Cajal. *Science* 252:1551-1553.
- Cummings S, King JS (1990) Coexistence of corticotropin releasing factor and enkephalin in cerebellar afferent systems. *Synapse* 5:167-174.
- Curthoys IS (1982) The response of primary horizontal semicircular canal neurons in the rat and guinea pig to angular acceleration. *Exp Brain Res* 47:286-294.
- Davie JT, Clark BA, Hausser M (2008) The origin of the complex spike in cerebellar Purkinje cells. *J Neurosci* 28:7599-7609.
- De Zeeuw CI, Koekkoek SKE (1997) Signal processing in the C2-module of the flocculus and its role in head movement control. In: *The cerebellum form structure to control*. (De Zeeuw CI, Strata P, Voogd J, eds), pp 299-320. Rotterdam: Elsevier.
- De Zeeuw CI, Wentzel P, Mugnaini E (1993) Fine structure of the dorsal cap of the inferior olive and its GABAergic and non-GABAergic input from the nucleus prepositus hypoglossi in rat and rabbit. *J Comp Neurol* 327:63-82.
- de Zeeuw CI, Holstege JC, Ruigrok TJ, Voogd J (1990) Mesodiencephalic and cerebellar terminals terminate upon the same dendritic spines in the glomeruli of the cat and rat inferior olive: an ultrastructural study using a combination of [3H]leucine and wheat germ agglutinin coupled horseradish peroxidase anterograde tracing. *Neuroscience* 34:645-655.
- De Zeeuw CI, Wylie DR, DiGiorgi PL, Simpson JI (1994) Projections of individual Purkinje cells of identified zones in the flocculus to the vestibular and cerebellar nuclei in the rabbit. *J Comp Neurol* 349:428-447.
- De Zeeuw CI, Simpson JI, Hoogenraad CC, Galjart N, Koekkoek SK, Ruigrok TJ (1998a) Microcircuitry and function of the inferior olive. *Trends Neurosci* 21:391-400.
- De Zeeuw CI, van Alphen AM, Koekkoek SK, Buharin E, Coesmans MP, Morpurgo MM, van den Burg J (1998b) Recording eye movements in mice: a new approach to investigate the molecular basis of cerebellar control of motor learning and motor timing. *Otolaryngol Head Neck Surg* 119:193-203.
- De Zeeuw CI, Hansel C, Bian F, Koekkoek SK, van Alphen AM, Linden DJ, Oberdick J (1998c) Expression of a protein kinase C inhibitor in Purkinje cells blocks cerebellar LTD and adaptation of the vestibulo-ocular reflex. *Neuron* 20:495-508.
- Delgado-Garcia JM (2000) Why move the eyes if we can move the head? *Brain Res Bull* 52:475-482.
- Dittman JS, Regehr WG (1998) Calcium dependence and recovery kinetics of presynaptic depression at the climbing fiber to Purkinje cell synapse. *J Neurosci* 18:6147-6162.
- Eccles JC, Llinas R, Sasaki K (1966a) The excitatory synaptic action of climbing fibres on the Purkinje cells of the cerebellum. *J Physiol* 182:268-296.
- Eccles JC, Llinas R, Sasaki K (1966b) The inhibitory interneurons within the cerebellar cortex. *Exp Brain Res* 1:1-16.
- Eccles JC, Ito M, Szentagothai J (1967) *The cerebellum as a neuronal machine*. Berlin-heidelberg-New York: springer.
- Edgerton JR, Reinhart PH (2003) Distinct contributions of small and large conductance Ca^{2+} -activated K^{+} channels to rat Purkinje neuron function. *J Physiol* 548:53-69.
- Edgley SA, Lidieth M (1987) The discharges of cerebellar Golgi cells during locomotion in the cat. *J Physiol* 392:315-332.
- Feil R, Hartmann J, Luo C, Wolfgruber W, Schilling K, Feil S, Barski JJ, Meyer M,

- Konnerth A, De Zeeuw CI, Hofmann F (2003) Impairment of LTD and cerebellar learning by Purkinje cell-specific ablation of cGMP-dependent protein kinase I. *J Cell Biol* 163:295-302.
- Fukushima K, Kaneko CR (1995) Vestibular integrators in the oculomotor system. *Neurosci Res* 22:249-258.
- Gilbert PF, Thach WT (1977) Purkinje cell activity during motor learning. *Brain Res* 128:309-328.
- Giolli RA, Blanks RH, Torigoe Y (1984) Pretectal and brain stem projections of the medial terminal nucleus of the accessory optic system of the rabbit and rat as studied by anterograde and retrograde neuronal tracing methods. *J Comp Neurol* 227:228-251.
- Giolli RA, Torigoe Y, Blanks RH, McDonald HM (1988) Projections of the dorsal and lateral terminal accessory optic nuclei and of the interstitial nucleus of the superior fasciculus (posterior fibers) in the rabbit and rat. *J Comp Neurol* 277:608-620.
- Gonshor A, Jones GM (1973) Proceedings: Changes of human vestibulo-ocular response induced by vision-reversal during head rotation. *J Physiol* 234:102P-103P.
- Gonshor A, Jones GM (1976) Extreme vestibulo-ocular adaptation induced by prolonged optical reversal of vision. *J Physiol* 256:381-414.
- Goossens HH, Hoebeek FE, Van Alphen AM, Van Der Steen J, Stahl JS, De Zeeuw CI, Frens MA (2004) Simple spike and complex spike activity of floccular Purkinje cells during the optokinetic reflex in mice lacking cerebellar long-term depression. *Eur J Neurosci* 19:687-697.
- Haines DE (1977) Cerebellar corticonuclear and corticovestibular fibers of the flocculonodular lobe in a prosimian primate (*Galago senegalensis*). *J Comp Neurol* 174:607-630.
- Hansel C (2005) When the B-team runs plasticity: GluR2 receptor trafficking in cerebellar long-term potentiation. *PNAS* 102: 18245-18246
- Hansel C, de Jeu M, Belmeguenai A, Houtman SH, Buitendijk GH, Andreev D, De Zeeuw CI, Elgersma Y (2006) α CaMKII is essential for cerebellar LTD and motor learning. *Neuron* 51:835-843.
- Hartell NA (1994) cGmp acts within cerebellar Purkinje cells to produce long term depression via mechanisms involving Pkc and Pkg. *Neuroreport* 5:833-836.
- Hausser M, Clark BA (1997) Tonic synaptic inhibition modulates neuronal output pattern and spatiotemporal synaptic integration. *Neuron* 19:665-678.
- Holtzman T, Rajapaksa T, Mostofi A, Edgley SA (2006) Different responses of rat cerebellar Purkinje cells and Golgi cells evoked by widespread convergent sensory inputs. *J Physiol* 574:491-507.
- Isope P, Barbour B (2002) Properties of unitary granule cell-->Purkinje cell synapses in adult rat cerebellar slices. *J Neurosci* 22:9668-9678.
- Ito M (1982a) Cerebellar control of the vestibulo-ocular reflex--around the flocculus hypothesis. *Annu Rev Neurosci* 5:275-296.
- Ito M (1982b) Experimental verification of Marr-Albus' plasticity assumption for the cerebellum. *Acta Biol Acad Sci Hung* 33:189-199.
- Ito M (1984) *The cerebellum and neural control*: Raven Press, New York.
- Ito M, Kano M (1982) Long-lasting depression of parallel fiber-Purkinje cell transmission induced by conjunctive stimulation of parallel fibers and climbing fibers in the

- cerebellar cortex. *Neurosci Lett* 33:253-258.
- Ito M, Karachot L (1990) Messengers mediating long-term desensitization in cerebellar Purkinje cells. *Neuroreport* 1:129-132.
- Ito M, Jastreboff PJ, Miyashita Y (1982) Specific effects of unilateral lesions in the flocculus upon eye movements in albino rabbits. *Exp Brain Res* 45:233-242.
- Jaarsma D, Dino MR, Cozzari C, Mugnaini E (1996) Cerebellar choline acetyltransferase positive mossy fibres and their granule and unipolar brush cell targets: a model for central cholinergic nicotinic neurotransmission. *J Neurocytol* 25:829-842.
- Johnstone CG, Schmidt RS, Johnstone BM (1963) Sodium and Potassium in Vertebrate Cochlear Endolymph as Determined by Flame Microspectrophotometry. *Comp Biochem Physiol* 13:335-341.
- Jones GM, Milsum JH (1971) Frequency-response analysis of central vestibular unit activity resulting from rotational stimulation of the semicircular canals. *J Physiol* 219:191-215.
- Jones GM, Davies P (1976) Adaptation of cat vestibulo-ocular reflex to 200 days of optically reversed vision. *Brain Res* 103:551-554.
- Jorntell H, Hansel C (2006) Synaptic memories upside down: bidirectional plasticity at cerebellar parallel fiber-Purkinje cell synapses. *Neuron* 52:227-238.
- Kano M, Hashimoto K, Kurihara H, Watanabe M, Inoue Y, Aiba A, Tonegawa S (1997) Persistent multiple climbing fiber innervation of cerebellar Purkinje cells in mice lacking mGluR1. *Neuron* 18:71-79.
- Kano M, Hashimoto K, Chen C, Abeliovich A, Aiba A, Kurihara H, Watanabe M, Inoue Y, Tonegawa S (1995) Impaired synapse elimination during cerebellar development in PKC gamma mutant mice. *Cell* 83:1223-1231.
- Katoh A, Yoshida T, Himeshima Y, Mishina M, Hirano T (2005) Defective control and adaptation of reflex eye movements in mutant mice deficient in either the glutamate receptor delta2 subunit or Purkinje cells. *Eur J Neurosci* 21:1315-1326.
- Keller EL, Precht W (1978) Persistence of visual response in vestibular nucleus neurons in cerebellectomized cat. *Exp Brain Res* 32:591-594.
- Khaliq ZM, Raman IM (2005) Axonal propagation of simple and complex spikes in cerebellar Purkinje neurons. *J Neurosci* 25:454-463.
- Koekkoek SK, Hulscher HC, Dortland BR, Hensbroek RA, Elgersma Y, Ruigrok TJ, De Zeeuw CI (2003) Cerebellar LTD and learning-dependent timing of conditioned eyelid responses. *Science* 301:1736-1739.
- Langer T, Fuchs AF, Scudder CA, Chubb MC (1985a) Afferents to the flocculus of the cerebellum in the rhesus macaque as revealed by retrograde transport of horseradish peroxidase. *J Comp Neurol* 235:1-25.
- Langer T, Fuchs AF, Chubb MC, Scudder CA, Lisberger SG (1985b) Floccular efferents in the rhesus macaque as revealed by autoradiography and horseradish peroxidase. *J Comp Neurol* 235:26-37.
- Lasser-Ross N, Ross WN (1992) Imaging voltage and synaptically activated sodium transients in cerebellar Purkinje cells. *Proc R Soc Lond B Biol Sci* 247:35-39.
- Linden DJ, Connor JA (1991) Participation of postsynaptic PKC in cerebellar long-term depression in culture. *Science* 254:1656-1659.
- Lisman J, Schulman H, Cline H (2002) The molecular basis of CaMKII function in synaptic and behavioural memory. *Nat Rev Neurosci* 3:175-190.

- Llinas R, Sugimori M (1980a) Electrophysiological properties of in vitro Purkinje cell somata in mammalian cerebellar slices. *J Physiol* 305:171-195.
- Llinas R, Sugimori M (1980b) Electrophysiological properties of in vitro Purkinje cell dendrites in mammalian cerebellar slices. *J Physiol* 305:197-213.
- Llinas R, Yarom Y (1981) Properties and distribution of ionic conductances generating electroresponsiveness of mammalian inferior olivary neurones in vitro. *J Physiol* 315:569-584.
- Llinas RR (1988) The intrinsic electrophysiological properties of mammalian neurons: insights into central nervous system function. *Science* 242:1654-1664.
- Lumpkin EA, Hudspeth AJ (1995) Detection of Ca²⁺ entry through mechanosensitive channels localizes the site of mechanoelectrical transduction in hair cells. *Proc Natl Acad Sci U S A* 92:10297-10301.
- Marcoli M, Maura G, Cervetto C, Giacomini C, Oliveri D, Candiani S, Pestarino M (2006) Nitric oxide-evoked cGMP production in Purkinje cells in rat cerebellum: an immunocytochemical and pharmacological study. *Neurochem Int* 49:683-690.
- Marr D (1969) A theory of cerebellar cortex. *J Physiol* 202:437-470.
- McCrea RA, Baker R, Delgado-Garcia J (1979) Afferent and efferent organization of the prepositus hypoglossi nucleus. *Prog Brain Res* 50:653-665.
- McElligott JG, Beeton P, Polk J (1998) Effect of cerebellar inactivation by lidocaine microdialysis on the vestibuloocular reflex in goldfish. *J Neurophysiol* 79:1286-1294.
- Miles FA, Fuller JH, Braitman DJ, Dow BM (1980) Long-term adaptive changes in primate vestibuloocular reflex. III. Electrophysiological observations in flocculus of normal monkeys. *J Neurophysiol* 43:1437-1476.
- Mittmann W, Koch U, Hausser M (2005) Feed-forward inhibition shapes the spike output of cerebellar Purkinje cells. *J Physiol* 563:369-378.
- Miyakawa H, Lev-Ram V, Lasser-Ross N, Ross WN (1992) Calcium transients evoked by climbing fiber and parallel fiber synaptic inputs in guinea pig cerebellar Purkinje neurons. *J Neurophysiol* 68:1178-1189.
- Nagao S (1983) Effects of vestibulocerebellar lesions upon dynamic characteristics and adaptation of vestibulo-ocular and optokinetic responses in pigmented rabbits. *Exp Brain Res* 53:36-46.
- Nagao S, Kitazawa H (2003) Effects of reversible shutdown of the monkey flocculus on the retention of adaptation of the horizontal vestibulo-ocular reflex. *Neuroscience* 118:563-570.
- Napper RM, Harvey RJ (1988) Number of parallel fiber synapses on an individual Purkinje cell in the cerebellum of the rat. *J Comp Neurol* 274:168-177.
- Narasimhan K, Linden DJ (1996) Defining a minimal computational unit for cerebellar long-term depression. *Neuron* 17:333-341.
- Newlands SD, Perachio AA (2003) Central projections of the vestibular nerve: a review and single fiber study in the Mongolian gerbil. *Brain Res Bull* 60:475-495.
- Palkovits M, Mezey E, Hamori J, Szentagothai J (1977) Quantitative histological analysis of the cerebellar nuclei in the cat. I. Numerical data on cells and on synapses. *Exp Brain Res* 28:189-209.
- Partsalis AM, Zhang Y, Highstein SM (1995) Dorsal Y group in the squirrel monkey. II. Contribution of the cerebellar flocculus to neuronal responses in normal and adapted animals. *J Neurophysiol* 73:632-650.

- Pouille F, Cavelier P, Desplantez T, Beekenkamp H, Craig PJ, Beattie RE, Volsen SG, Bossu JL (2000) Dendro-somatic distribution of calcium-mediated electrogenesis in purkinje cells from rat cerebellar slice cultures. *J Physiol* 527 Pt 2:265-282.
- Raman IM, Bean BP (1997) Resurgent sodium current and action potential formation in dissociated cerebellar Purkinje neurons. *J Neurosci* 17:4517-4526.
- Raman IM, Bean BP (1999) Ionic currents underlying spontaneous action potentials in isolated cerebellar Purkinje neurons. *J Neurosci* 19:1663-1674.
- Reynolds T, Hartell NA (2001) Roles for nitric oxide and arachidonic acid in the induction of heterosynaptic cerebellar LTD. *Neuroreport* 12:133-136.
- Robinson DA (1974) The effect of cerebellectomy on the cat's vestibulo-ocular integrator. *Brain Res* 71:195-207.
- Robinson DA (1976) Adaptive gain control of vestibuloocular reflex by the cerebellum. *J Neurophysiol* 39:954-969.
- Rossi F, Borsello T, Vaudano E, Strata P (1993) Regressive modifications of climbing fibres following Purkinje cell degeneration in the cerebellar cortex of the adult rat. *Neuroscience* 53:759-778.
- Ruigrok TJ (2003) Collateralization of climbing and mossy fibers projecting to the nodulus and flocculus of the rat cerebellum. *J Comp Neurol* 466:278-298.
- Ruigrok TJ, Osse RJ, Voogd J (1992) Organization of inferior olivary projections to the flocculus and ventral paraflocculus of the rat cerebellum. *J Comp Neurol* 316:129-150.
- Sato Y, Kawasaki T (1984) Functional localization in the three floccular zones related to eye movement control in the cat. *Brain Res* 290:25-31.
- Sato Y, Kawasaki T, Ikarashi K (1982) Zonal organization of the floccular Purkinje cells projecting to the vestibular nucleus in cats. *Brain Res* 232:1-15.
- Sato Y, Kawasaki T, Ikarashi K (1983) Afferent projections from the brainstem to the three floccular zones in cats. II. Mossy fiber projections. *Brain Res* 272:37-48.
- Sato Y, Kanda K, Kawasaki T (1988) Target neurons of floccular middle zone inhibition in medial vestibular nucleus. *Brain Res* 446:225-235.
- Sauer G, Richter CP, Klinke R (1999) Sodium, potassium, chloride and calcium concentrations measured in pigeon perilymph and endolymph. *Hear Res* 129:1-6.
- Schmolesky MT, Weber JT, De Zeeuw CI, Hansel C (2002) The making of a complex spike: ionic composition and plasticity. *Ann N Y Acad Sci* 978:359-390.
- Schoepp D, Bockaert J, Sladeczek F (1990) Pharmacological and functional characteristics of metabotropic excitatory amino acid receptors. *Trends Pharmacol Sci* 11:508-515.
- Sekirnjak C, Vissel B, Bollinger J, Faulstich M, du Lac S (2003) Purkinje cell synapses target physiologically unique brainstem neurons. *J Neurosci* 23:6392-6398.
- Shinoda Y, Sugihara I, Wu HS, Sugiuchi Y (2000) The entire trajectory of single climbing and mossy fibers in the cerebellar nuclei and cortex. *Prog Brain Res* 124:173-186.
- Shutoh F, Ohki M, Kitazawa H, Itohara S, Nagao S (2006) Memory trace of motor learning shifts transsynaptically from cerebellar cortex to nuclei for consolidation. *Neuroscience* 139:767-777.
- Siegborn J, Grant G (1983) Brainstem projections of different branches of the vestibular nerve. An experimental study by transganglionic transport of horseradish

- peroxidase in the cat. I. The horizontal ampullar and utricular nerves. *Arch Ital Biol* 121:237-248.
- Silver RA, Momiyama A, Cull-Candy SG (1998) Locus of frequency-dependent depression identified with multiple-probability fluctuation analysis at rat climbing fibre-Purkinje cell synapses. *J Physiol* 510 (Pt 3):881-902.
- Simpson JJ, Wylie DR, De Zeeuw CI (1996) On climbing fiber signals and their consequence(s). *Behav Brain Sci* 19:380-394.
- Simpson JJ, Hulscher HC, Sabel-Goedknecht E, Ruigrok TJ (2005) Between in and out: linking morphology and physiology of cerebellar cortical interneurons. *Prog Brain Res* 148:329-340.
- Soodak RE, Simpson JJ (1988) The accessory optic system of rabbit. I. Basic visual response properties. *J Neurophysiol* 60:2037-2054.
- Steinberg JP, Takamiya K, Shen Y, Xia J, Rubio ME, Yu S, Jin W, Thomas GM, Linden DJ, Huganir RL (2006) Targeted in vivo mutations of the AMPA receptor subunit GluR2 and its interacting protein PICK1 eliminate cerebellar long-term depression. *Neuron* 49:845-860.
- Stuart G, Hausser M (1994) Initiation and spread of sodium action potentials in cerebellar Purkinje cells. *Neuron* 13:703-712.
- Sugihara I, Wu HS, Shinoda Y (2001) The entire trajectories of single olivocerebellar axons in the cerebellar cortex and their contribution to Cerebellar compartmentalization. *J Neurosci* 21:7715-7723.
- Sugihara I, Ebata S, Shinoda Y (2004) Functional compartmentalization in the flocculus and the ventral dentate and dorsal group y nuclei: an analysis of single olivocerebellar axonal morphology. *J Comp Neurol* 470:113-133.
- Tan J, Gerrits NM, Nanhoe R, Simpson JJ, Voogd J (1995) Zonal organization of the climbing fiber projection to the flocculus and nodulus of the rabbit: a combined axonal tracing and acetylcholinesterase histochemical study. *J Comp Neurol* 356:23-50.
- Thach WT, Jr. (1967) Somatosensory receptive fields of single units in cat cerebellar cortex. *J Neurophysiol* 30:675-696.
- Tiliket C, Shelhamer M, Roberts D, Zee DS (1994) Short-term vestibulo-ocular reflex adaptation in humans. I. Effect on the ocular motor velocity-to-position neural integrator. *Exp Brain Res* 100:316-327.
- van Alphen AM, Stahl JS, De Zeeuw CI (2001) The dynamic characteristics of the mouse horizontal vestibulo-ocular and optokinetic response. *Brain Res* 890:296-305.
- Van Alphen AM, Schepers T, Luo C, De Zeeuw CI (2002) Motor performance and motor learning in Lurcher mice. *Ann N Y Acad Sci* 978:413-424.
- Van Neerven J, Pompeiano O, Collewyn H (1989) Depression of the vestibulo-ocular and optokinetic responses by intrafloccular microinjection of GABA-A and GABA-B agonists in the rabbit. *Arch Ital Biol* 127:243-263.
- van Neerven J, Pompeiano O, Collewyn H (1991) Effects of GABAergic and noradrenergic injections into the cerebellar flocculus on vestibulo-ocular reflexes in the rabbit. *Prog Brain Res* 88:485-497.
- van Neerven J, Pompeiano O, Collewyn H, van der Steen J (1990) Injections of beta-noradrenergic substances in the flocculus of rabbits affect adaptation of the VOR gain. *Exp Brain Res* 79:249-260.
- Vetter P, Roth A, Hausser M (2001) Propagation of action potentials in dendrites

- p depends on dendritic morphology.
- J Neurophysiol*
- 85:926-937.
- Voogd J (1964) The cerebellum of the cat. Structure and fibre connexions. In: *Anatomy*. Leiden: Rijksuniversiteit Leiden.
- Voogd J, Bigaré F (1980) Topographical distribution of olivary and corticonuclear fibers in the cerebellum. The inferior olivary nucleus Raven Press New York:207-305.
- Voogd J, Gerris NM, Hess DT (1987) Parasagittal organization of the cerebellum in macaques. An analysis based on acetylcholinesterase histochemistry. In: *Cerebellum and neuronal plasticity* (Glickstein M, Stein JF, eds), pp 19-40. New York: Plenum New York.
- Voogd J, Gerrits NM, Ruigrok TJ (1996) Organization of the vestibulocerebellum. *Ann N Y Acad Sci* 781:553-579.
- Vos BP, Maex R, Volny-Luraghi A, De Schutter E (1999) Parallel fibers synchronize spontaneous activity in cerebellar Golgi cells. *J Neurosci* 19:RC6.
- Welsh JP, Lang EJ, Sugihara I, Llinas R (1995) Dynamic organization of motor control within the olivocerebellar system [see comments]. *Nature* 374:453-457.
- Williams SR, Christensen SR, Stuart GJ, Hausser M (2002) Membrane potential bistability is controlled by the hyperpolarization-activated current I(H) in rat cerebellar Purkinje neurons in vitro. *J Physiol* 539:469-483.
- Womack MD, Khodakhah K (2003) Somatic and dendritic small-conductance calcium-activated potassium channels regulate the output of cerebellar purkinje neurons. *J Neurosci* 23:2600-2607.
- Xia J, Zhang X, Staudinger J, Huganir RL (1999) Clustering of AMPA receptors by the synaptic PDZ domain-containing protein PICK1. *Neuron* 22:179-187.
- Zeng H, Chattarji S, Barbarosie M, Rondi-Reig L, Philpot BD, Miyakawa T, Bear MF, Tonegawa S (2001) Forebrain-specific calcineurin knockout selectively impairs bidirectional synaptic plasticity and working/episodic-like memory. *Cell* 107:617-629.

Chapter 2

Zonal Organization of the Mouse Flocculus: Physiology, Input and Output

Adapted from J Comp Neurol. 2006 Aug 1;497(4):670-82.

M. Schonewille, C. Luo, T.J. Ruigrok, J. Voogd, M.T. Schmolesky, M. Rutteman, F.E. Hoebeek, M.T. De Jeu, C.I. De Zeeuw.

Abstract

The zones of the flocculus have been mapped in many species with a noticeable exception, the mouse. Here, the functional map of the mouse was constructed via extracellular recordings followed by tracer injections of biotinylated-dextran-amine and immunohistochemistry for heat-shock protein-25. Zones were identified based on the Purkinje cell complex spike modulation occurring in response to optokinetic stimulation. In zones 1 and 3 Purkinje cells responded best to rotation about a horizontal axis oriented at 135° ipsilateral azimuth, whereas in zones 2 and 4 they responded best to rotation about the vertical axis. The tracing experiments showed that Purkinje cells of zone 1 projected to the parvicellular part of lateral cerebellar nucleus and superior vestibular nucleus, while Purkinje cells of zone 3 projected to group Y and the superior vestibular nucleus. Purkinje cells of zones 2 and 4 projected to the magnocellular and parvicellular parts of the medial vestibular nucleus, while some also innervated the lateral vestibular nucleus or nucleus prepositus hypoglossi. The climbing fiber inputs to Purkinje cells in zones 1 and 3 were derived from neurons in the ventrolateral outgrowth of the contralateral inferior olive, whereas those in zones 2 and 4 were derived from the contralateral caudal dorsal cap. Purkinje cells in zones 1 and 2, but not in zones 3 and 4, were positively labeled for heat-shock protein-25. The present study illustrates that Purkinje cells in the murine flocculus are organized in discrete zones with specific functions, specific input – output relations, and a specific histochemical signature.

Introduction

The flocculus of the cerebellum plays an important role in the control of compensatory eye movements (De Zeeuw et al., 2003). As we aim in this thesis to unravel the cerebellar codings using (mutant) mice, correlating floccular Purkinje cell activity with stimulation, we first set out to map the organization of the flocculus in the mouse. The anatomical and/or physiological zones of the flocculus have been mapped for various species, including monkey (Lisberger and Fuchs, 1978), cat (Groenewegen and Voogd, 1977), rabbit (De Zeeuw et al., 1994a; Van der Steen et al., 1994; Tan et al., 1995b), and rat (Ruigrok et al., 1992; Sugihara et al., 2004). The organization of the flocculus in mammals generally follows that of the cerebellar cortex in that sagittal zones of Purkinje cells project to specific parts of the cerebellar and vestibular nuclei (Yamamoto et al., 1978; Voogd and Bigaré, 1980; Sato et al., 1982b, a; Tan et al., 1995b; Balaban et al., 2000; Sugihara et al., 2004) and that they receive their climbing fibers from a specific group of neurons in the contralateral inferior olive (IO) (Groenewegen and Voogd, 1977; Groenewegen et al., 1979; Ruigrok et al., 1992; Tan et al., 1995c; Sugihara et al., 2004). In most mammals the zones can be morphologically discriminated by using acetylcholinesterase staining as a biochemical marker and/or by tracing the climbing fiber inputs anterogradely from the olive (Voogd and Bigaré, 1980; Tan et al., 1995c). To date, little is known about the floccular organization in the mouse; so far no biochemical marker has been correlated to their zones and the topography of their climbing fiber projections has not been elucidated.

Climbing fibers potentials evoke complex spikes in Purkinje cells of the cerebellar cortex (Eccles et al., 1966; Thach, 1967). In the flocculus of both rabbits and mice, the complex spike activity of Purkinje cells is modulated optimally in response to rotational optokinetic stimulation about either the vertical axis (VA) or the horizontal axis (HA)

that is approximately perpendicular to the ipsilateral anterior semicircular canal (Graf et al., 1988; Goossens et al., 2004; Hoebeek et al., 2005). In zones 1 and 3 of the rabbit flocculus, complex spike activity is optimally modulated in response to optokinetic stimulation about the HA oriented at 45° contralateral azimuth/135° ipsilateral azimuth, while complex spike activities of Purkinje cells in zones 2 and 4 are optimally modulated in response to optokinetic stimulation about the vertical axis (De Zeeuw et al., 1994a). Whether the distribution of Purkinje cells with different preferred axes of optokinetic modulation in mice follows the same zonal pattern as in rabbits is unknown.

Purkinje cells in the flocculus are known to project to various parts of the cerebellar and vestibular nuclei, as demonstrated in primate (Haines, 1977; Langer et al., 1985), cat (Voogd, 1964; McCreary et al., 1979; Sato et al., 1982b), rabbit (Alley, 1977; Yamamoto and Shimoyama, 1977; Balaban, 1987), and rat (Balaban et al., 2000). These studies used degeneration and/or tracing of large groups of axons, mostly of multiple zones. Until recently studies on the efferent projection of individual zones of the flocculus were mostly done with retrograde axonal labeling from injections in the vestibular nuclei (Yamamoto et al., 1978; Sato et al., 1982a; Tan et al., 1995b) and therefore did not provide detailed information on the precise termination of the Purkinje cell axons. The only study using anterograde axonal transport from discrete injections of individual Purkinje cells is the study by De Zeeuw et al. (1994a). However, the Purkinje cell projections from this study could not be directly correlated to the specific olivary origins of the climbing fiber inputs to the flocculus due to the use of biocytin, which is exclusively an anterograde tracer.

To overcome this limitation as well as to find out whether and how the flocculus of the mouse is organized in zones, we placed small injections of biotinylated-dextran-amine (BDA), which acts as both an anterograde and a retrograde tracer, into areas that were identified electrophysiologically by recording climbing fiber responses of Purkinje cells during optokinetic stimulation. Although this technique is not as accurate as intra- or juxtacellular injections in Purkinje cells, it closely approaches this level, and in addition it labeled small areas of Purkinje cells as well as their climbing fiber inputs, thus allowing us to trace both the afferent and efferent projections of identified floccular zones in the same experiment. In addition, we investigated to what extent immunoreactivity for heat-shock protein-25 (HSP25), which has recently been demonstrated to reveal distinct bands in the vestibulocerebellum of mice (Armstrong et al., 2000), could be correlated to the physiological identity and projection pattern of these zones. Thus in conjunction, the current study provides a full description of the anatomical and physiological organization of the flocculus of the mouse, which nowadays with the advent of transgenics, is the first mammal of choice.

Experimental Procedures

All procedures adhered to the NIH Guide for the Care and Use of Laboratory Animals according to the principles expressed in the declaration of Helsinki and were approved by a national committee overseeing animal welfare.

Surgery. Eighteen adult C57BL/6 mice were prepared for neurophysiological experiments under anesthesia consisting of a 1:2 mixture of O₂, N₂O, and 1.5% isoflurane. An acrylic head fixation pedestal was fixed to the skull by M1 screws, and a recording chamber

was made following a craniotomy (diameter ~3 mm) of the left occipital bone (Goossens et al., 2001). The animals were allowed to recover for 5 days before the start of the recording and injection sessions.

Recordings and Injections. The animals were restrained in a custom made plastic tube, which was placed in the center of a random dotted drum that could be rotated around a variety of vertical or horizontal axes in space (Stahl et al., 2000; van Alphen et al., 2001). Extracellular Purkinje cell activity was recorded using filament containing borosilicate glass pipettes (OD 2.0 mm, ID 1.16 mm, tip diameter 2.0 μ m) filled with 2M NaCl. For amplification, data acquisition, and analysis, we used Cyberamp (CED, Cambridge, UK), Spike 2 software (CED) and custom-written Matlab routines (Mathworks, USA), respectively. Optokinetic stimulation consisted of a full-field random-dotted black and white drum (dot size 2°, distance to head 45 cm) rotating sinusoidally with 5° amplitude at 0.4 Hz around both the vertical axis (VA) and the horizontal axis (HA) that is perpendicular to the ipsilateral anterior semicircular canal (at a 45° angle clockwise from the rostrocaudal midline). A floccular zone was identified by its complex spike responses to this optokinetic stimulation (De Zeeuw et al., 1994a); for tuning curves in mice see (Hoebeek et al., 2005), and subsequently the recording pipette was exchanged for a pipette (tip diameter 2 μ m) that was filled with 10% BDA. After the floccular zone was re-identified based on the complex spike modulation recorded with the BDA pipette, an iontophoretic injection was made using a constantly monitored anodal current of 1-4 μ A, pulsed 7 seconds on, 7 seconds off, for a period of 10 minutes. Following the injection, the brain was covered with gramicidin-containing ointment and sealed with bone wax (Hoebeek et al., 2005).

Tissue processing. After 5-7 days the mice were deeply anesthetized with pentobarbital (200 mg/kg) and perfused transcardially with 4% paraformaldehyde. The brains were postfixed for 1 hour in 4% paraformaldehyde, embedded in gelatin (11%) and sectioned transversally at 40 μ m with a freezing microtome. Sections were serially collected in four glass vials in which subsequent rinsing and incubation procedures were performed. Vials 1 and 3 were incubated for both BDA and HSP25 staining, whereas vials 2 and 4 only served for BDA histochemistry. All sections were rinsed for 30 min in Tris buffered saline (TBS, pH 7.6), incubated for 90 min in a solution of TBS / 0.05% Triton-X100 / 10% normal horse serum to block non-specific protein-binding sites, incubated overnight at 4°C in avidin-biotin-peroxidase complex (Vector Laboratories, Inc. Burlingame, Ca), rinsed again, and finally incubated in diaminobenzidine (75 mg/100 ml). In vials 1 and 3, cobalt ions were added to the incubation bath in order to obtain a black reaction product. The reaction was stopped after 15-20 minutes by rinsing in TBS. Vials 1 and 3 were subsequently incubated with the rabbit-anti-mouse HSP25 antibody (1:10.000, SPA-801, StressGen, Victoria, BC, Canada) diluted in TBS containing 0.5% Triton-X100 and 2% normal serum. After 48 hours incubation in the dark at 4°C, the sections were rinsed in TBS (3 times) and then incubated 90 min with the secondary antibody biotinylated goat-anti-rabbit antibody (1:200, Vector Laboratories, Burlingame, CA). After this incubation, the sections were rinsed in TBS for 60 minutes, and incubated again 90 min with the Avidin-Biotin-Complex (Vector Laboratories, Inc., Burlingame, CA) in TBS with 0.5% Triton-X100. This step was followed by 3 x 5 min rinsing in TBS and 3 x 5 min in 0.1 M Tris buffer (pH 7.6). This time, the complex was visualized by diaminobenzidine (DAB,

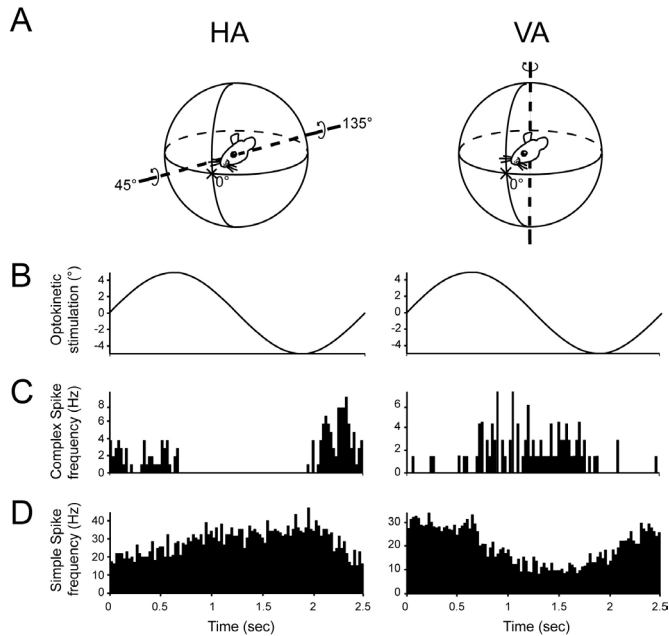


Figure 1. Complex spike and simple spike activities of Purkinje cells in the flocculus are modulated by HA or VA visual field rotation.

A, This panel shows the spatial orientation of the optokinetic stimulation used to determine the preferred axis for each Purkinje cell. The visual field was rotated around the ipsilateral 135° posterior - contralateral 45° anterior axis in the horizontal plane (HA; left column) or the vertical axis (VA; right column). Arrows in A indicate the direction of rotation that results in increased complex spike activity in the left flocculus. B, Sinusoidal optokinetic stimulation was presented at 0.4 Hz. C, Examples of peristimulus time histograms of complex spike activity of two Purkinje cells showing an optimal response to HA (left) or VA (right) optokinetic stimulation. D, As in C but for simple spikes; note reciprocal modulation in that increased simple spike activity is accompanied by decreased complex spike activity and vice versa. The histograms in C and D show the average firing frequency over 40 cycles per bin (bin width is 25 msec).

75mg/100 ml) only, thus resulting in a brown precipitate at places where HSP25 was present. Sections of vials 2 and 4 in which only BDA was visualized as a brown precipitate, served as additional sections for analysis and plotting. The sections were mounted, air-dried, counterstained with thionin, dehydrated through graded alcohol series, cleared in xylene, and cover-slipped with Permount (Fisher Scientific). The HSP25 antibody used in this study was generated against recombinant mouse HSP25. The specificity for HSP25 has been extensively tested through preadsorption with recombinant HSP25 and comparison with HSP25 mRNA distribution in murine fixed brain sections in previous studies (Maatkamp et al., 2004). Furthermore, the same results were obtained with goat polyclonal antibody raised against the C-terminal portion of human HSP27, the human orthologue of HSP25. Consistent with previous studies both antibodies predominantly stained motoneurons in spinal cord and brainstem, and to lesser degree astrocytes and blood vessels (Maatkamp et al., 2004).

Histological analysis. The histological material was analyzed with a Leica DMR light microscope equipped with a DC 300 digital camera. Photo panels were constructed in CorelDraw after some correction for brightness and contrast in Corel Photo-Paint (both version 11). Graphical plots of anterograde and retrograde labeling in the cerebellar

and vestibular nuclei were made with an Olympus BH-2 microscope equipped with a Lucivid miniature monitor (Microbrightfield, Colchester, VT) and a motorized X, Y and Z stage drive, and Neurolucida software (Microbrightfield). Similar plots were made of retrograde labeling within the inferior olivary complex from which a standardized diagram was prepared of the caudal inferior olivary nucleus (Ruigrok et al., 1992). Olivary labeling was subsequently entered within this standardized diagram. To map the flocculus, digital prints were prepared of all consecutive sections from the caudal-most to the rostral-most part of the flocculus. In all sections four reference points were indicated which served to construct a map of the unfolded flocculus (Ruigrok et al., 1992; Balaban et al., 2000) (see Figure 3). The unfolded flocculus map was transformed by custom-written Matlab routines.

Results

Purkinje cell recordings and injections

Most of the complex spike activities of the Purkinje cells in the flocculus of the mouse responded optimally to optokinetic stimulation along either the VA or the HA perpendicular to the ipsilateral anterior semicircular canal (Figure 1). In all these cases the simple spikes modulated out of phase with respect to the complex spike activities (Figure 1C, D). The 18 small BDA injections that were made were distributed throughout the entire caudal-rostral and medio-lateral extent of the areas in the flocculus that responded to optokinetic stimulation (Figure 2, 3). The cells that modulated optimally to the HA were clustered either in a zone located caudally in the flocculus (referred to as zone 1) or in a zone located in its rostral half (referred to as zone 3) (see Figure 3D-E). In contrast, the VA cells were all located in between or rostrally to these zones (referred to as zone 2 and zone 4). Caudal to zone 1, no cells were found that responded to optokinetic stimulation; in this area, which probably corresponds to the C2-zone (see De Zeeuw et al., 1994a; De Zeeuw and Koekkoek, 1997), no injections were made. Among the eighteen BDA injections that were made in the floccular areas that showed responses to optokinetic stimulation, four were made into zone 1, eight in zone 2, five in zone 3, and one in zone 4 (Table 1). Two of these injections, i.e. nr 17770-8 in zone 1 and nr 15733-1 in zone 3, extended somewhat into the ventral paraflocculus. A large part of the Purkinje cells that were located in the three most caudal zones, i.e. zone C2, zone 1 and zone 2, were positively labeled for HSP-25 (Figure 3B, C). In contrast, none of the Purkinje cells in zones 3 and 4 showed any immunoreactivity for HSP-25. In conjunction, these data indicate that the vast majority of Purkinje cells in the flocculus of the mouse respond to optokinetic stimulation about axes that run through the horizontal semicircular canal or ipsilateral anterior semicircular canal, that these cells are organized in parasagittal zones, and that they can be partly identified by immuno-histochemical staining.

Projections from the inferior olive to the flocculus

The data described above indicate that the complex spike activities of Purkinje cells in zones 1 and 3 modulate optimally around an axis that is perpendicular to the preferred axis of Purkinje cells in zones 2 and 4. These results suggest that the climbing fibers that evoke these different activities originate from different clusters of neurons in the inferior olive. We therefore investigated whether the BDA injections in zones 1 and 3 resulted in different sets of retrogradely labeled neurons than those in zones 2 and 4. This

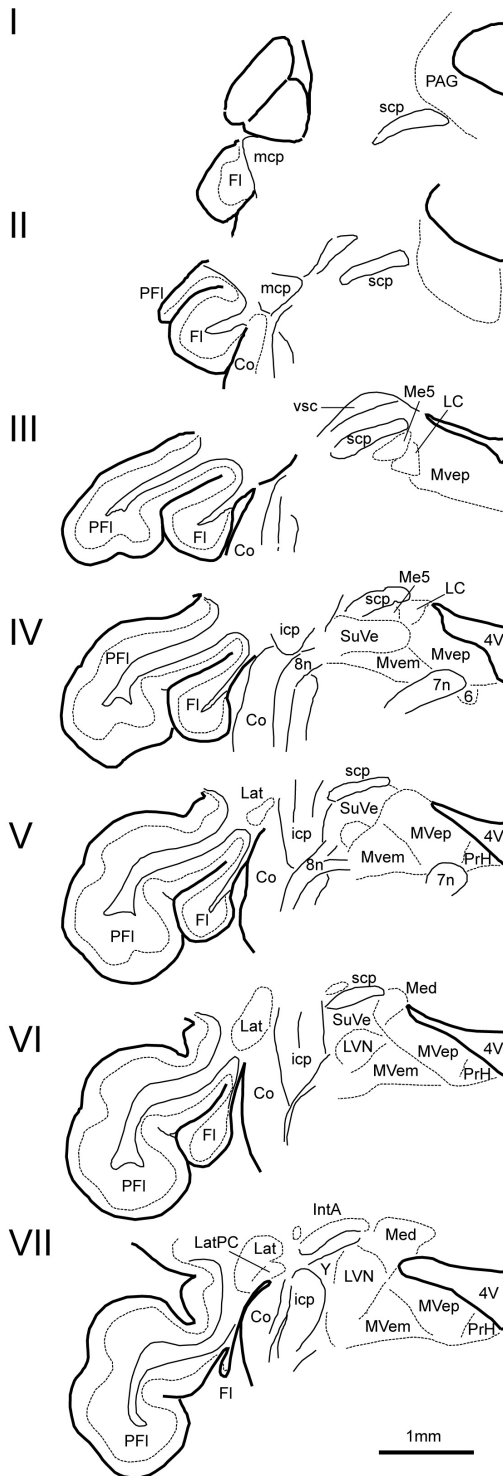


Figure 2. Series of drawings indicating the position and shape of the flocculus and paraflocculus in relation to the cerebellar and vestibular nuclei.

Drawings were based on every fifth 40µm section of mouse 15733-2, and display the entire flocculus from its most rostral tip (I) down to its most caudal tip (VII). For abbreviations, see list.

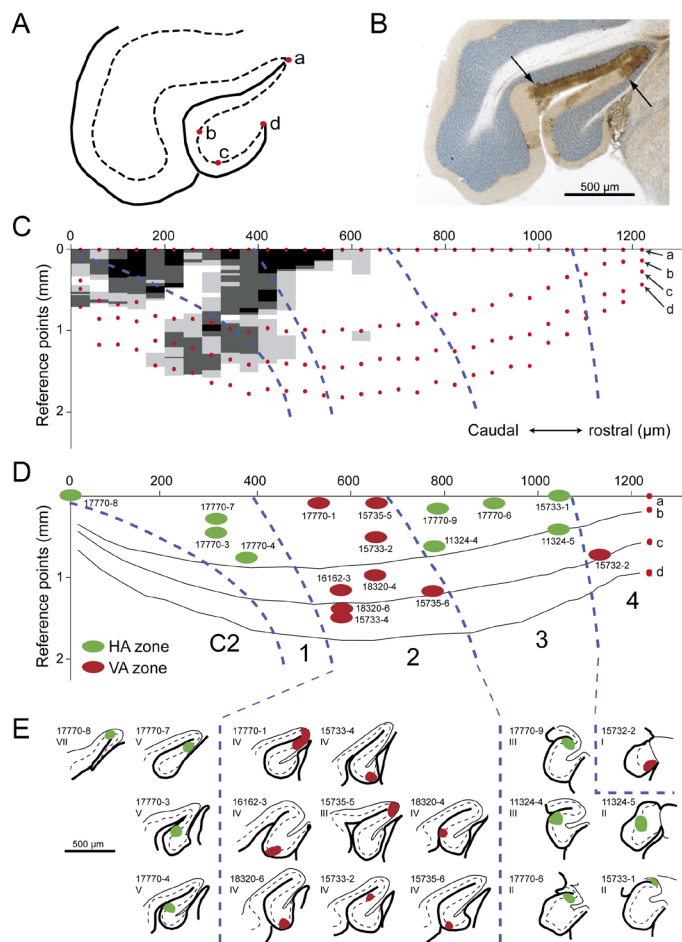


Figure 3. The flocculus of the mouse can be divided into five functional zones.

A, Schematic representation of the flocculus showing the four reference points (a, b, c and d) used in each floccular section (40 μ m) for analysis. B, Example of HSP25 staining (brown) in the (para)flocculus (borders of the HSP25-immunopositive area are indicated by arrows). C, Schematic representation showing the HSP25 expression pattern (from gray to black in increasing intensity) in the flocculus of the mouse with reference points a-d unfolded along the y-axis and consecutive sections presented in the rostrocaudal direction along the x-axis. Blue lines indicate the borders of the functional zones identified by electrophysiological recordings. D, BDA injection sites in HA (green) and VA (red) zones superimposed on the scheme presented in C. The numbers refer to the animals involved. Note that HSP25 labeling is restricted to zones 1, 2, and C2. E, Plots of original sections indicating the size and position of the BDA injections of all studied cases. Case numbers are indicated and Roman numbers refer to the approximate level of the plot relative to the series shown in Figure 2.

prediction did hold (Table 1). The injections of BDA in zones 1 and 3 resulted in labeled neurons in the contralateral ventrolateral outgrowth (VLO) (Figure 4), whereas those in zones 2 and 4 resulted in retrogradely labeled neurons in the contralateral caudal dorsal cap (CDC) (Figure 5). In all cases the injections were relatively small and the number of retrogradely labeled neurons never exceeded 15. In 1 case, mouse 15735-5, the cluster of retrogradely labeled neurons in the caudal dorsal cap extended into a more rostral area approaching the rostral dorsal cap and VLO. Note that the injection site in this case was located near the border between zones 2 and 3 (Figure 3D). In 3 cases we did not observe any retrogradely labeled neuron in the inferior olive (Table 1). Thus, collectively from these results we conclude that the sources of the climbing fiber projections to the different floccular zones in the mouse are compatible with the preferred complex spike modulations of their Purkinje cells. The climbing fiber projections to both HA zones (1 and 3) are derived from the same olivary subnucleus, the VLO, while those to the VA zones (2 and 4) are both derived from a different subnucleus, the caudal DC.

Purkinje cell projections

The specific climbing fiber inputs as well as the preferred complex spike and simple

Mouse	Phys.	Zone	Ipsilateral projection	Contralateral inferior olive
17770-3	HA	1	LatPC, SuVe	no labeling
17770-4	HA	1	LatPC, SuVe	VLO
17770-7	HA	1	LatPC, SuVe	VLO
17770-8	HA	1	no projection	VLO
18320-4	VA	2	no projection	CDC
15735-6	VA	2	MVep, some in LVN	no labeling
15733-4	VA	2	MVep, MVem, some in LVN	CDC
18320-6	VA	2	MVep, MVem	CDC
15733-2	VA	2	no projection	no labeling
17770-1	VA	2	MVem, MVep, some in PrH	CDC
16162-3	VA	2	MVep	CDC
15735-5	VA	2	SuVe and MVem, MVep	CDC
11324-4	HA	3	SuVe and MVep, group Y	VLO
15733-1	HA	3	group Y	VLO
11324-5	HA	3	SuVe, group Y	VLO
17770-6	HA	3	SuVe, group Y	VLO
17770-9	HA	3	SuVe, group Y	VLO
15732-2	VA	4	MVem, MVep, some in LVN	CDC

Table 1. List of mice. Complex spike responses to HA or VA optokinetic stimulations, Injection, projection sites of BDA-labeled floccular Purkinje cells, and retrogradely labeled neurons in the contralateral IO.

spike modulations of the Purkinje cell zones described above would theoretically be most effective were it maintained in the nuclei receiving Purkinje cell inputs as well. We therefore investigated whether the BDA injections in the flocculus that provided the zone-specific retrograde labeling in the different olivary subnuclei, also showed anatomically discrete anterograde labeling of Purkinje cell axons and terminals.

The injections into the HA zones 1 and 3 demonstrated similar, yet not identical, projection patterns. Labeled fibers originating from zone 1 followed the floccular peduncle from which they turned caudally towards the parvicellular aspect of the lateral cerebellar nucleus (LatPC) where a dense axonal terminal plexus was observed in a confined narrow region (Figures 4C and 6A). Other fibers followed an arching route through the LatPC passing just dorsal to the inferior cerebellar peduncle and Y-nucleus. At that point the fibers turned rostromedially and reached the superior vestibular nucleus (SuVe) where a few fibers and terminals were found. The fibers of zone 3 followed the same route as the fibers of zone 1, but they provided more terminal boutons in the SuVe and showed terminals in the dorsal part of group Y instead of the LatPC (Figure 5).

The injections into VA zones 2 and 4 demonstrated projection patterns that clearly

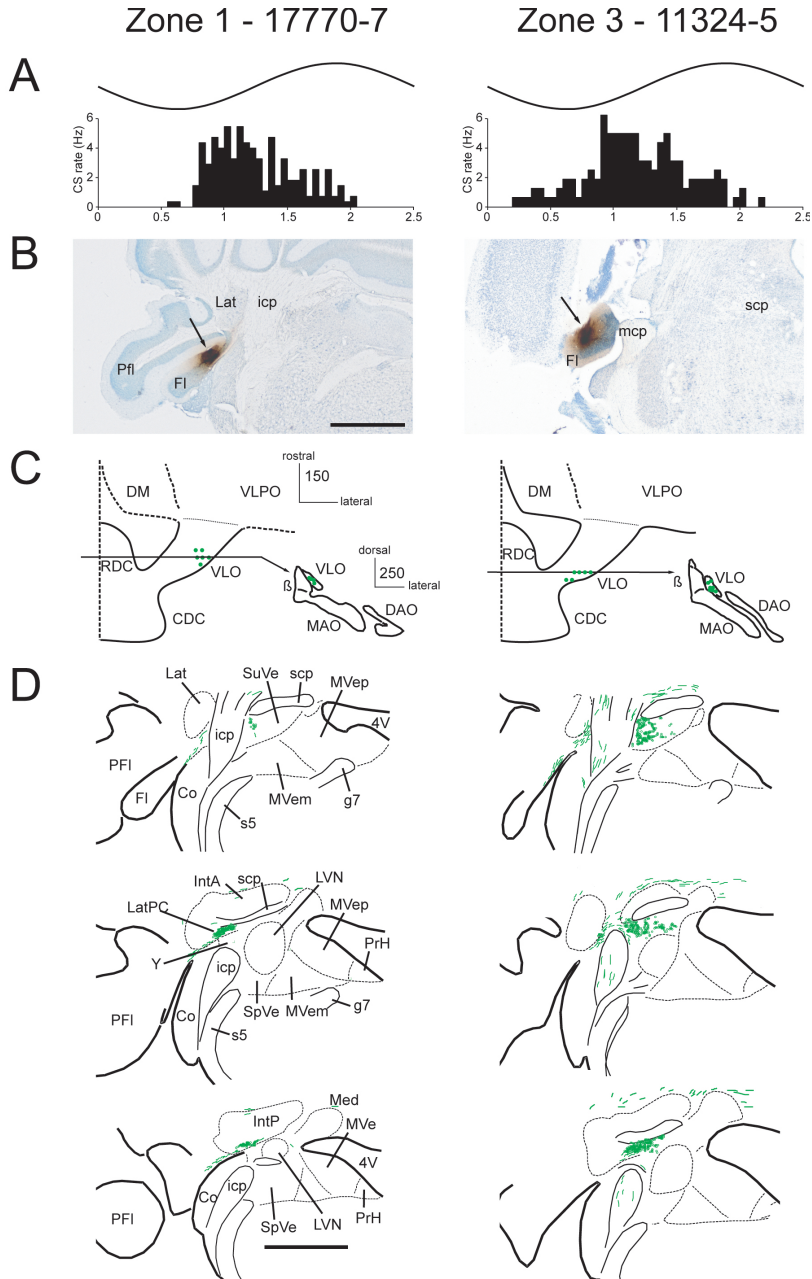


Figure 4. Floccular zones 1 and 3, responding optimally to HA optokinetic stimulation, receive specific climbing fiber inputs and project to discrete regions in the midbrain.

A, Peri stimulus time histogram of the complex spikes modulation (bottom) demonstrating the response to sinusoidal HA stimulation (top). B, Micrographs showing examples of BDA injection sites in zones 1 and 3 in the mouse flocculus. C, Reconstructions of corresponding retrograde labeling in the contralateral inferior olive illustrate that the injections in zones 1 and 3 labeled olivary neurons (dots) in the ventrolateral outgrowth (VLO). Insets show a reconstruction of the coronal view at the rostrocaudal level indicated by the line. D, Reconstructions of corresponding projection patterns shows that the injection in zone 1 resulted in Purkinje cells projecting to LatPC and SuVe, while the injection in zone 3 resulted in Purkinje cells projecting to group Y and SuVe. For abbreviations, see list.

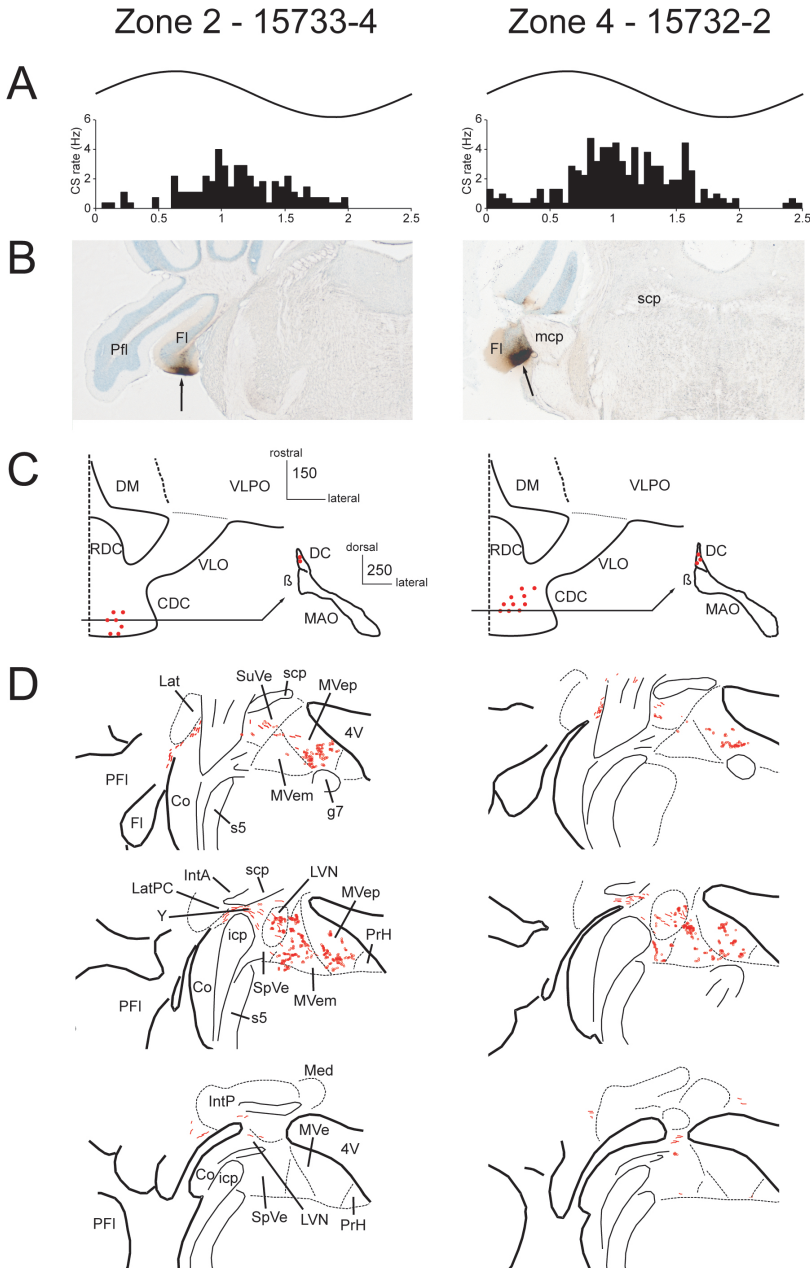


Figure 5. Floccular zones 2 and 4, responding optimally to VA optokinetic stimulation, receive specific climbing fiber inputs and project to discrete regions in the midbrain.

A, Peri stimulus time histogram of the complex spikes modulation (bottom) demonstrating the response to sinusoidal VA stimulation (top). B, Micrographs showing examples of BDA injection sites in zones 2 and 4 in the mouse flocculus. C, Reconstructions of corresponding retrograde labeling in the contralateral inferior olive illustrate that the injections in zone 2 and 4 labeled olivary neurons (dots) in the caudal dorsal cap (CDC). Insets show a reconstruction of the coronal view at the rostrocaudal level indicated by the line. D, Reconstructions of corresponding projection patterns shows that the injection in zones 2 and 4 (VA) resulted in Purkinje cells projecting to MVem and MVep, and in some cases to lesser extent also to the LVN or PrH. For abbreviations, see list.

diverged from those of zones 1 and 3 (Table 1). Purkinje cell axons derived from zone 2 coursed ventrally to the LatPC and passed group Y without providing terminals to these regions. They descended ventromedially to terminate within the magnocellular and parvicellular parts of the medial vestibular nucleus (MVem and MVep). Occasionally, terminals were observed within the lateral vestibular nucleus (LVN) and sparsely in the nucleus prepositus hypoglossi (PrH) (nr. 17770-1: Figure 6F). Axon terminals were observed in all these regions, but the terminal arborizations were much more extensive in the MVem and MVep than in the LVN or PrH. Within the MVem many labeled terminals were distributed around large somata and proximal dendrites (Figure 6G). In the case in which the injection site was close to the border with zone 3 (nr. 15735-5), some of the fibers also projected to the SuVe. The labeled Purkinje cell axons derived from zone 4 demonstrated a similar pattern of terminal arborizations as those of zone 2; most labeling was observed in the MVem and MVep, some in the LVN, and no axonal varicosities were seen within the confines of the LatPC or group Y.

These data allow us to conclude that the Purkinje cell projections from HA zones (1 and 3) diverge from those of VA zones (2 and 4) and that the specifics of these projection patterns match remarkably well with the characteristics of the climbing fiber inputs described above.

Discussion

In the present study, for the first time, we demonstrated that subpopulations of Purkinje cells reside in anatomically and physiologically discrete zones in the mouse flocculus. In addition, we have shown that the individual zones of Purkinje cells receive climbing fiber inputs from different regions of the inferior olive and project to different sets of nuclei and subnuclei, thereby retaining structural and functional separation at all three levels of the cerebellar modules.

Zones in the mouse flocculus

The mouse flocculus was found to have four parasagittal zones that responded to optokinetic stimulation about particular axes in space (zones 1 to 4) and one zone that was non-responsive to optokinetic stimulation (C2 zone). Zones 1 and 3 contained Purkinje cells responding optimally to visual field rotation around the 45° contralateral azimuth - 135° ipsilateral azimuth HA, while Purkinje cells located in zones 2 and 4 showed a maximal response to rotation around the VA. These data agree with the divisions that have been found in the rabbit flocculus following both zone-specific recordings and zone-specific stimulations. De Zeeuw and colleagues (De Zeeuw et al., 1994a) showed a near-identical organization of zones in the rabbit flocculus following recordings of complex spike and simple spike activities, while Van der Steen and colleagues (Van der Steen et al., 1994) were able to evoke binocular eye movements about the same HA and VA axes in space by electrical microstimulation of the corresponding zones. In these studies the sites of the recordings or stimulations were marked by a tracer and/or electrical lesion and subsequently correlated to anatomical zones, the borders of which were visualized with the use of acetylcholine-esterase (AChE) (Tan et al., 1995a). In mice, however, neither AChE nor any other biochemical marker tested to date clearly labels the borders between the zones in the vestibulocerebellum (De Zeeuw et al., 2003). However, Armstrong and colleagues have recently made note of HSP-25 patterning in

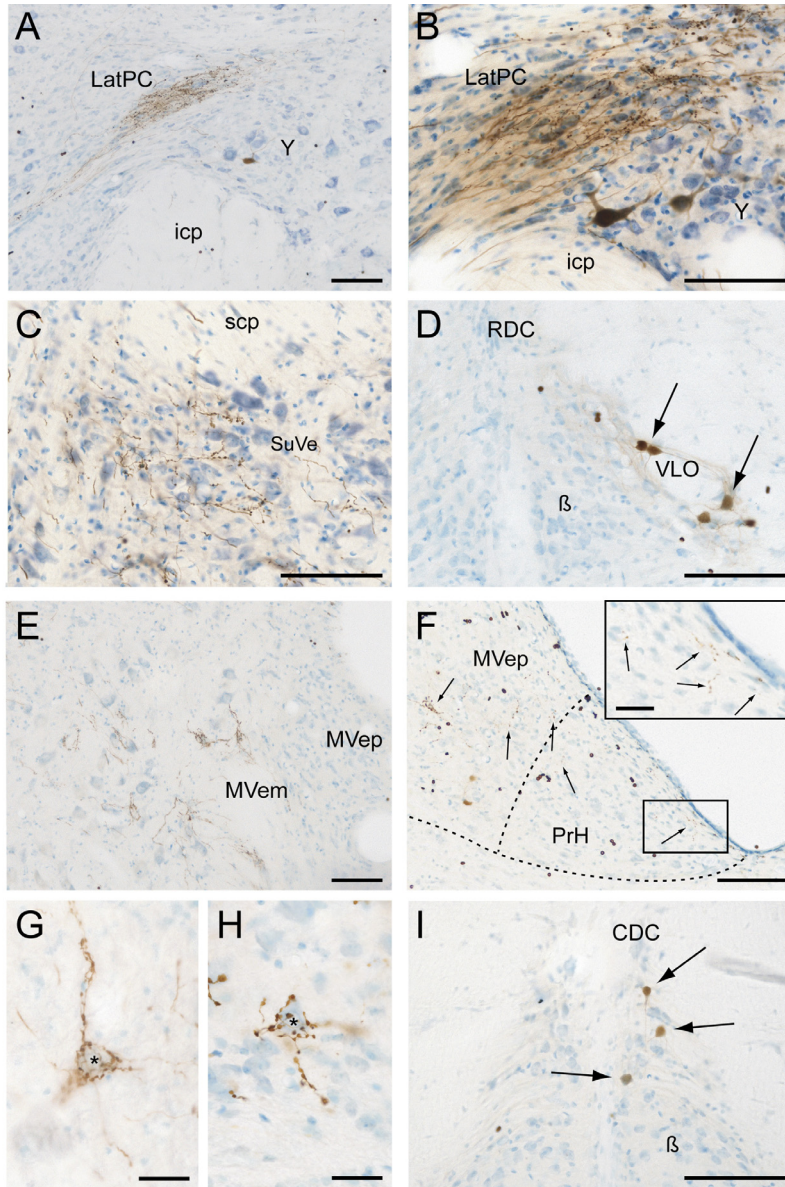


Figure 6. Micrographs showing labeling characteristics after BDA injections into identified zones of the mouse flocculus.

A, Anterograde labeling of Purkinje cell axons and terminals within the LatPC following injection in zone 1 (case 17770-7). B, Purkinje cell terminal arborizations are labeled within LatPC and group Y after BDA injection in zone 3 (case 11324-5). C, Same case also shows efferent labeling within the lateral part of the SuVe. D, Retrograde labeled neurons (arrows) are present in the VLO after BDA injection in zone 3 of the contralateral flocculus (case 17770-6). E, Varicose fibers and terminals in the MVem are labeled after injection into zone 2 of the flocculus (case 15733-4). F, Anterograde labeling of Purkinje cell axons and terminals within the PrH following injection in zone 2 (case 17770-1). G and H, These panels show examples of vestibular nucleus neurons (asterisks) that are surrounded by labeled terminal fibers after BDA injections into zone 2 (case 15733-4) and zone 4 (case 15732-2), respectively. I, Retrograde labeling of olivary neurons (arrows) in the CDC after BDA injection into zone 4 of the flocculus (case 15732-2). Scale bars represent 25 μ m in G, H and inset of F and 100 μ m in all other panels. For abbreviations, see list.

the vestibulocerebellum (Armstrong et al., 2000). Therefore, we tested the usefulness of Hsp-25 as a morphological marker for zonal borders and found that this protein is expressed by Purkinje cells in HA zone 1, VA zone 2, and the non-HA / non-VA zone C2, but not by those in zones 3 and 4. Thus, although we have not been able to find a specific morphological marker for either the VA zones or HA zones, we did find a marker to segregate the two most rostral zones from the three caudal zones in mice.

The most rostral floccular VA zone (zone 4), which we have found both in mice and rabbits, has not been described for the cat at the physiological level. (Sato and Kawasaki, 1984) found three zones in the flocculus of the cat following electrical stimulation; stimulation of a caudal zone produced downward eye movements, while stimulation of a middle and rostral zone produced ipsilateral horizontal and upward eye movements, respectively. Thus, the organization of these zones suggests that the caudal zone of the cat flocculus corresponds to zone 1 of the mouse flocculus, the middle zone to zone 2 and the rostral zone to zone 3. It appears likely though that the cat flocculus also has a rostral VA zone, because it can be found at the anatomical level following anterograde tracing of its climbing fibers (Gerrits and Voogd, 1982). Possibly, the rostral VA zone was missed in the physiological study in the cat, because it is too narrow to be reliably detected by electrical stimulation. In support of this point, it should be noted that in rabbits too zone 4 could not be detected by electrical stimulation (Van der Steen et al., 1994), while it was evident following single unit recordings of modulating Purkinje cells (De Zeeuw et al., 1994a).

Similarly, Gerrits and Voogd (Gerrits, 1985) found the existence of the C2 zone in the cat flocculus based on its 3D-structure, its relation with adjacent cerebellar structures, and its connections. Presumably the cat C2 zone is like that in mice and rabbits in that it is not directly involved in the optokinetic reflex. The function of the C2 zone could be related to head movements, as stimulation of this zone in the flocculus evokes short-latency head movements (De Zeeuw and Koekkoek, 1997).

Climbing fiber input to the mouse flocculus

The observation that complex spike activities in the mouse flocculus can be divided into discrete zones based on their responses to optokinetic stimulation around particular axes in space agreed well with the finding that these zones receive their climbing fiber inputs from different olivary subnuclei. We showed that Purkinje cells in HA zones 1 and 3 receive their climbing fibers from the VLO, while those in VA zones 2 and 4 receive their climbing fibers from the caudal DC. These data largely agree with the findings by Tan and colleagues (Tan et al., 1995c) in rabbit, except that zones 1 and 3 in that species also receive inputs from the rostral DC. The zonal organization of the olivocerebellar projection to the flocculus in the mouse also shows a pattern similar to that in the rat (Ruigrok et al., 1992; Sugihara et al., 2004); zones FD and FD' in the rat correspond to zones 1 and 3 and are innervated by the VLO, while zones FE and FE' are innervated by the dorsal cap and correspond to zone 2 and zone 4, respectively. Thus, one can conclude that the VLO and caudal DC in animals in the grandorder glires are generally involved in vertical and horizontal optokinetic eye movements, respectively, and that the olivary projections to the flocculus in the mouse resemble those that have been described for rats and rabbits.

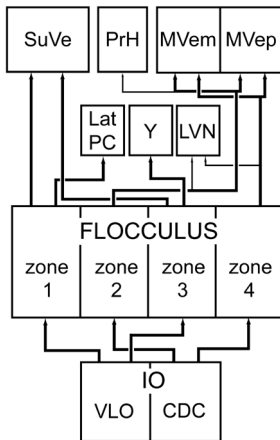


Figure 7. Summary of afferent and efferent pathways of Purkinje cells in the mouse flocculus. Line width indicates the relative strength of the projection. For abbreviations, see list.

Purkinje cell projections of the mouse flocculus

The organization of the output of the flocculus in mice was as zone-specific as that of its climbing fiber input and its Purkinje cell activities. Our findings reveal that Purkinje cells of zone 1 project to the LatPC and/or SuVe, that Purkinje cells of zone 3 project to group Y and/or SuVe, and that those of zone 2 and 4 project to the MVem and MVep, and occasionally to the LVN and PrH. These results largely agree with degeneration and tracing studies in rabbits (Yamamoto et al., 1978; Yamamoto, 1979; De Zeeuw et al., 1994a; Tan et al., 1995b), cats (Voogd, 1964; Sato et al., 1982b, a; Carleton and Carpenter, 1983; Dietrichs, 1983; Langer et al., 1985), monkeys (Balaban et al., 1981; Carleton and Carpenter, 1983; Langer et al., 1985) and rats (Bernard, 1987; Umetani, 1992; Balaban et al., 2000). The present study indicates that cells in the VA zone 2 project directly to neurons in the PrH. However, this projection was only clearly seen in case 17770-1 (Table 1), where the injection involved the medial part of the ventral paraflocculus. Purkinje cells in this area have been reported to be in labeled after injection in the PrH (Balaban et al., 2000). A projection from the flocculus to the PrH has been suggested before in the rabbit (Yamamoto et al., 1978), but De Zeeuw and colleagues (1994a) were unable to confirm this, let alone to determine from which zone it was derived. In addition, we observed a projection from zone 3, but not zone 1, to group Y in mice, while in rabbits both zones have been found to project to the dorsal part of group Y (De Zeeuw et al., 1994a). Thus, there may be subtle differences between mice and other mammals, but the main topographical organization appears very similar.

The results of this study in mice are comparable to previous studies in that there are 4 floccular zones for 2 preferred axes of optokinetic stimulation. These findings raise the question as to why there are 2 functional zones for each axis. A possible explanation may be found in the relatively subtle differences in the projections within the sets of HA zones and VA zones. For example, while Purkinje cells of zone 1 and zone 3 receive input from the same part of the inferior olive and respond both optimally to the same HA axis of optokinetic stimulation, the Purkinje cells in zone 1 project to the SuVe and LatPC whereas those in zone 3 project to the SuVe and the dorsal part of group Y. In all animals studied so far the LatPC is known to provide an inhibitory feedback to the inferior olive (De Zeeuw et al., 1994b), but whether this connection also holds for group Y is less

clear (Partsalis et al., 1995). Similarly, the Purkinje cells in zone 2 may be involved in an inhibitory feedback to the olive via the PrH (De Zeeuw et al., 1993), but such projection has never been shown for zone 4. Thus, it appears possible that Purkinje cells zones 1 and 2 may be especially relevant for the closed loop systems in optokinetic control, while those of zones 3 and 4 may be more relevant for the open loop pathways (see also De Zeeuw et al., 1994a).

Finally, the current study provides the first direct evidence for mammals that the specific output connections of the floccular zones perfectly match their specific climbing fiber inputs. We have been able to directly show this relation by combining anterograde and retrograde transport of a single tracer, BDA. Fortunately, the speed and efficiency of the anterograde and retrograde transport of BDA were sufficiently comparable to allow us to identify both labeled neurons in the inferior olive and sites of Purkinje cell terminations in the cerebellar and vestibular nuclei in single sections following single injections. Whenever the source of the climbing fibers was not discrete, for example when an injection site was close to the border between two zones, the Purkinje cell projections were similarly more diffuse. Therefore, the current data allow us to conclude that the olivocerebellar modules as originally described by Voogd and colleagues (Voogd and Glickstein, 1998) hold valid and reach an extremely high level of precise topography.

Abbreviations

AChE	acetylcholinesterase
BDA	biotinylated dextran amine
CDC	caudal dorsal cap
DC	dorsal cap
DM	dorsomedial group
Fl	flocculus
FRN's	flocculus receiving neurons
HA	horizontal axis
HSP25	heat-shock protein-25
icp	inferior cerebellar peduncle
IntA	anterior interposed nucleus of the cerebellum
IntP	posterior interposed nucleus of the cerebellum
IO	inferior olive
LatPC	parvicellular part of lateral cerebellar nucleus
LVN	lateral vestibular nucleus
Med	medial cerebellar nucleus
MVe	medial vestibular nucleus
MVem	magnocellular part of medial vestibular nucleus
MVep	parvicellular part of medial vestibular nucleus
OKR	optokinetic reflex
PFI	paraflocculus
PrH	nucleus prepositus hypoglossi
RDC	rostral dorsal cap
scp	superior cerebellar peduncle
SuVe	superior vestibular nucleus
VA	vertical axis
VLO	ventrolateral outgrowth
VOR	vestibulo-ocular reflex
WGA-HRP	wheat germ agglutinated horseradish peroxidase

Reference list

- Alley K (1977) Anatomical basis for interaction between cerebellar flocculus and brainstem. In: *Control of Gaze by Brainstem Neurons* (Baker R, Berthoz A, eds), pp 109-117. Amsterdam: Elsevier.
- Armstrong CL, Krueger-Naug AM, Currie RW, Hawkes R (2000) Constitutive expression of the 25-kDa heat shock protein Hsp25 reveals novel parasagittal bands of purkinje cells in the adult mouse cerebellar cortex. *J Comp Neurol* 416:383-397.
- Balaban CD (1987) Distribution of inferior olivary projections to the vestibular nuclei of albino rabbits. *Neuroscience* 24:119-134.
- Balaban CD, Ito M, Watanabe E (1981) Demonstration of zonal projections from the cerebellar flocculus to vestibular nuclei in monkeys (*Macaca fuscata*). *Neurosci Lett* 27:101-105.
- Balaban CD, Schuerger RJ, Porter JD (2000) Zonal organization of flocculo-vestibular connections in rats. *Neuroscience* 99:669-682.
- Bernard JF (1987) Topographical organization of olivocerebellar and corticonuclear connections in the rat--an WGA-HRP study: I. Lobules IX, X, and the flocculus. *J Comp Neurol* 263:241-258.
- Carleton SC, Carpenter MB (1983) Afferent and efferent connections of the medial, inferior and lateral vestibular nuclei in the cat and monkey. *Brain Res* 278:29-51.
- De Zeeuw CI, Koekkoek SKE (1997) Signal processing in the C2-module of the flocculus and its role in head movement control. In: *The cerebellum form structure to control*. (De Zeeuw CI, Strata P, Voogd J, eds), pp 299-320. Rotterdam: Elsevier.
- De Zeeuw CI, Wentzel P, Mugnaini E (1993) Fine structure of the dorsal cap of the inferior olive and its GABAergic and non-GABAergic input from the nucleus prepositus hypoglossi in rat and rabbit. *J Comp Neurol* 327:63-82.
- De Zeeuw CI, Wylie DR, DiGiorgi PL, Simpson JI (1994a) Projections of individual Purkinje cells of identified zones in the flocculus to the vestibular and cerebellar nuclei in the rabbit. *J Comp Neurol* 349:428-447.
- De Zeeuw CI, Gerrits NM, Voogd J, Leonard CS, Simpson JI (1994b) The rostral dorsal cap and ventrolateral outgrowth of the rabbit inferior olive receive a GABAergic input from dorsal group Y and the ventral dentate nucleus. *J Comp Neurol* 341:420-432.
- De Zeeuw CI, Koekkoek SK, van Alphen AM, Luo C, Hoebeek F, van der Steen J, Frens MA, Sun JC, Goossens HHLM, Jaarsma D, Coesmans MPH, Schmolesky MT, de Jeu MTG, Galjart N (2003) Gain and phase control of compensatory eye movements by the flocculus of the vestibulocerebellum. In: *Handbook of auditory research*, pp 375-422: Springer Verlag.
- Dietrichs E (1983) The cerebellar corticonuclear and nucleocortical projections in the cat as studied with anterograde and retrograde transport of horseradish peroxidase. V. The posterior lobe vermis and the flocculo-nodular lobe. *Anat Embryol* 167:449-462.
- Eccles JC, Sasaki K, Strata P (1966) The profiles of physiological events produced by a parallel fibre volley in the cerebellar cortex. *Exp Brain Res* 2:18-34.
- Gerrits NM (1985) Brainstem Control of the Cerebellar Flocculus. In: pp 1-89. Leiden: Leiden University.

- Gerrits NM, Voogd J (1982) The climbing fiber projection to the flocculus and adjacent paraflocculus in the cat. *Neuroscience* 7:2971-2991.
- Goossens HH, Hoebeek FE, Van Alphen AM, Van Der Steen J, Stahl JS, De Zeeuw CI, Frens MA (2004) Simple spike and complex spike activity of floccular Purkinje cells during the optokinetic reflex in mice lacking cerebellar long-term depression. *Eur J Neurosci* 19:687-697.
- Goossens J, Daniel H, Rancillac A, van der Steen J, Oberdick J, Crepel F, De Zeeuw CI, Frens MA (2001) Expression of protein kinase C inhibitor blocks cerebellar long-term depression without affecting Purkinje cell excitability in alert mice. *J Neurosci* 21:5813-5823.
- Graf W, Simpson JJ, Leonard CS (1988) Spatial organization of visual messages of the rabbit's cerebellar flocculus. II. Complex and simple spike responses of Purkinje cells. *J Neurophysiol* 60:2091-2121.
- Groenewegen HJ, Voogd J (1977) The parasagittal zonation within the olivocerebellar projection. I. Climbing fiber distribution in the vermis of cat cerebellum. *J Comp Neurol* 174:417-488.
- Groenewegen HJ, Voogd J, Freedman SL (1979) The parasagittal zonation within the olivocerebellar projection. II. Climbing fiber distribution in the intermediate and hemispheric parts of cat cerebellum. *J Comp Neurol* 183:551-601.
- Haines DE (1977) Cerebellar corticonuclear and corticovestibular fibers of the flocculonodular lobe in a prosimian primate (Galago senegalensis). *J Comp Neurol* 174:607-630.
- Hoebeek FE, Stahl JS, van Alphen AM, Schonewille M, Luo C, Rutteman M, van den Maagdenberg AM, Molenaar PC, Goossens HH, Frens MA, De Zeeuw CI (2005) Increased noise level of purkinje cell activities minimizes impact of their modulation during sensorimotor control. *Neuron* 45:953-965.
- Langer T, Fuchs AF, Chubb MC, Scudder CA, Lisberger SG (1985) Floccular efferents in the rhesus macaque as revealed by autoradiography and horseradish peroxidase. *J Comp Neurol* 235:26-37.
- Lisberger SG, Fuchs AF (1978) Role of primate flocculus during rapid behavioral modification of vestibuloocular reflex. II. Mossy fiber firing patterns during horizontal head rotation and eye movement. *J Neurophysiol* 41:764-777.
- Maatkamp A, Vlug A, Haasdijk E, Troost D, French PJ, Jaarsma D (2004) Decrease of Hsp25 protein expression precedes degeneration of motoneurons in ALS-SOD1 mice. *Eur J Neurosci* 20:14-28.
- McCrea RA, Baker R, Delgado-Garcia J (1979) Afferent and efferent organization of the prepositus hypoglossi nucleus. *Prog Brain Res* 50:653-665.
- Partsalis AM, Zhang Y, Highstein SM (1995) Dorsal Y group in the squirrel monkey. I. Neuronal responses during rapid and long-term modifications of the vertical VOR. *J Neurophysiol* 73:615-631.
- Ruigrok TJ, Osse RJ, Voogd J (1992) Organization of inferior olivary projections to the flocculus and ventral paraflocculus of the rat cerebellum. *J Comp Neurol* 316:129-150.
- Sato Y, Kawasaki T (1984) Functional localization in the three floccular zones related to eye movement control in the cat. *Brain Res* 290:25-31.
- Sato Y, Kawasaki T, Ikarashi K (1982a) Zonal organization of the floccular Purkinje cells projecting to the group y of the vestibular nuclear complex and the lateral

- cerebellar nucleus in cats. *Brain Res* 234:430-434.
- Sato Y, Kawasaki T, Ikarashi K (1982b) Zonal organization of the floccular Purkinje cells projecting to the vestibular nucleus in cats. *Brain Res* 232:1-15.
- Stahl JS, van Alphen AM, De Zeeuw CI (2000) A comparison of video and magnetic search coil recordings of mouse eye movements [In Process Citation]. *J Neurosci Methods* 99:101-110.
- Sugihara I, Ebata S, Shinoda Y (2004) Functional compartmentalization in the flocculus and the ventral dentate and dorsal group y nuclei: an analysis of single olivocerebellar axonal morphology. *J Comp Neurol* 470:113-133.
- Tan J, Simpson JI, Voogd J (1995a) Anatomical compartments in the white matter of the rabbit flocculus. *J Comp Neurol* 356:1-22.
- Tan J, Epema AH, Voogd J (1995b) Zonal organization of the flocculovestibular nucleus projection in the rabbit: a combined axonal tracing and acetylcholinesterase histochemical study. *J Comp Neurol* 356:51-71.
- Tan J, Gerrits NM, Nanhoe R, Simpson JI, Voogd J (1995c) Zonal organization of the climbing fiber projection to the flocculus and nodulus of the rabbit: a combined axonal tracing and acetylcholinesterase histochemical study. *J Comp Neurol* 356:23-50.
- Thach WT, Jr. (1967) Somatosensory receptive fields of single units in cat cerebellar cortex. *J-Neurophysiol* 30:675-696.
- Umetani T (1992) Efferent projections from the flocculus in the albino rat as revealed by an autoradiographic orthograde tracing method. *Brain Res* 586:91-103.
- van Alphen AM, Stahl JS, De Zeeuw CI (2001) The dynamic characteristics of the mouse horizontal vestibulo-ocular and optokinetic response. *Brain Res* 890:296-305.
- Van der Steen J, Simpson JI, Tan J (1994) Functional and anatomic organization of three-dimensional eye movements in rabbit cerebellar flocculus. *J Neurophys* 72:31-46.
- Voogd J (1964) The cerebellum of the cat. Structure and fibre connexions. In: *Anatomy*. Leiden: Rijksuniversiteit Leiden.
- Voogd J, Bigaré F (1980) Topographical distribution of olivary and corticonuclear fibers in the cerebellum. The inferior olivary nucleus Raven Press New York:207-305.
- Voogd J, Glickstein M (1998) The anatomy of the cerebellum. *Trends Neurosci* 21:370-375.
- Yamamoto M (1979) Topographical representation in rabbit cerebellar flocculus for various afferent inputs from the brainstem investigated by means of retrograde axonal transport of horseradish peroxidase. *Neurosci Lett* 12:29-34.
- Yamamoto M, Shimoyama I (1977) Differential localization of rabbit's flocculus Purkinje cells projecting to the medial and superior vestibular nuclei, investigated by means of the HRP retrograde axonal transport. *Neuroscience* 5:279-283.
- Yamamoto M, Shimoyama I, Highstein SM (1978) Vestibular nucleus neurons relaying excitation from the anterior canal to the oculomotor nucleus. *Brain Res* 148:31-42.

Chapter 3

Purkinje cell activity in relation to behavior

Chapter 3

Paragraph 1

Purkinje Cells in Awake Behaving Animals Operate in Stable Upstate Membrane Potential

Adapted from Nat Neurosci. 2006 Apr;9(4):459-61.

M. Schonewille, S. Khosrovani, B.H. Winkelman, F.E. Hoebeek, M.T. De Jeu, I.M. Larsen, J. Van der Burg, M.T. Schmolesky, M.A. Frens, C.I. De Zeeuw.

Abstract

Bistability of membrane potentials has been described for various neurons in the brain. Recently, evidence has been provided that complex spikes can alter the state of the membrane potential of Purkinje cells suggesting a mechanism by which somatosensory stimulation can act as a toggle switch to control the triggering of simple spikes and thereby motor behavior. Yet, all forms of bistability have only been demonstrated under anesthesia. Using intracellular and extracellular recordings we show that bistability of Purkinje cell activity as well as the toggle phenomenon are virtually absent in animals during motor performance or motor learning in the awake state, whereas both are prominently present under anesthetics. We conclude from our study that the membrane potential of Purkinje cells is effectively constrained to the upstate level under physiological circumstances.

Introduction

After unravelling the floccular map in the mouse we continued with the first step in investigating Purkinje cell activity in relation to behaviour. We first focused on the relative newly described phenomenon of bistability, as it could potentially be a generally used mechanism in the brain. Cellular bistability or multistable states of the membrane potential have been demonstrated both *in vitro* and *in vivo* for different types of neurons throughout the brain and various functions have been proposed for this phenomenon. For example, bistability found in prefrontal cortex neurons could explain the ability to rapidly generate generalized responses to novel stimuli in working memory tasks (Branchereau et al., 1996; Durstewitz et al., 2000), while reports suggest that bistability in the nucleus accumbens may provide a selective gate for the transfer of information by increasing the probability of action potential firing in the upstate mode (O'Donnell and Grace, 1995; O'Donnell et al., 1999). Similarly, bistability in Purkinje cells has been proposed to play a key role in short-term processing and storage of sensorimotor information in the cerebellar cortex (Williams et al., 2002; Loewenstein et al., 2005). However, all recordings of bistability to date have been obtained either in slices or in anesthetized animals. Since anesthetics can directly or indirectly affect the membrane potential (MacIver and Kendig, 1991), and since stable intracellular recordings in awake behaving animals present technical complications, it remains to be elucidated whether the functional roles of bistability proposed above hold valid in normal behaving animals under physiological conditions.

Here we investigate to what extent anaesthesia can enhance bistability, whether extracellular recordings in awake behaving animals show signs of bistability and/or whether such signs emerge under sensory stimulation or motor learning paradigms. To do this we recorded intracellular and/or extracellular activity of the Purkinje cells in the mouse vestibulocerebellum, which is known to control compensatory eye movements (Ito, 1982; Lisberger, 1998; De Zeeuw et al., 2003). In this system, relationships between sensory input, motor output, and Purkinje cell activities can be rigorously defined during both motor performance and motor learning (De Zeeuw et al., 1995; Simpson et al., 1996; Goossens et al., 2004). Moreover, the characteristic complex spike and simple spike activities of Purkinje cells, which are controlled by their climbing fibre and parallel fiber inputs, respectively, show typical interactions which may be useful for drawing conclusions from the extracellular responses about the intracellular state. Not only do

Purkinje cells consistently show a pause of about 10 to 100 ms in simple spike activity directly following a single complex spike (normally referred to as climbing fibre pause (Armstrong, 1974; Schmolesky et al., 2002), but they also show, under anaesthesia, a toggle switch phenomenon in that single complex spikes can bring the membrane potential to either an upstate or downstate level and thereby switch the simple spike activity on or off, respectively (Loewenstein et al., 2005). Thus, if the toggling phenomenon is present under physiological conditions, the complex spike activities relaying error signals originating in the inferior olive (De Zeeuw et al., 1998), would almost certainly have a strong impact on motor behaviour by directly modifying the simple spike firing frequency (Loewenstein et al., 2005).

In the present study we demonstrate via combined intracellular and extracellular recordings of single Purkinje cells that one can indeed accurately and consistently deduce shifts in the membrane potential from extracellularly recorded activity. We looked for signs of bistability and toggling through comparative analysis of the inter-simple spike distribution characteristics and by quantifying the periods of quiescence in simple spike activity and their relation to the occurrence of complex spikes. Our recordings during natural visual and vestibular stimulation indicate that bistability and the toggling phenomenon are prominent under anaesthesia and in mutants with altered Ca^{2+} conductance, but that they are virtually absent in awake wild type mice, not even when we challenge the system by motor learning paradigms.

Experimental procedures

All experiments were conducted in accordance with the European Communities Council Directive (86/609/EEC) and were reviewed and approved by the national ethics committee.

Intracellular recordings

C57BL/6 wild type and homozygous tottering mice (4-5 weeks old) were prepared for experiments under isoflurane or ketamine/xylazine anesthesia (Goossens et al., 2001). In short, a pedestal was mounted on the head of a mouse using dental acrylic and the head was fixed by bolting the pedestal to a metal bar. A craniotomy (1x1 mm) was made in the occipital bone above Crus 2 and/or the vermis of the cerebellum, and the dura was carefully removed. Borosilicate glass patch pipettes (OD 1.5 mm, ID 1.2 mm, 4-6 M Ω) containing standard intracellular solution (in mM: KCl 9, KOH 10, MgCl₂ 3.48, NaCl 4, KGluconate 120, HEPES 10, sucrose 17.5, Na₂ATP 4, Na₃GTP 0.4, pH 7.2, osmolarity 290-310 mOsm/kg) were advanced into the top layer of the cerebellar cortex in 1-5 μm steps (SM IV, Luigs & Neumann, Ratingen, Germany), with slight positive pressure applied to the tip described elsewhere (Margrie et al., 2002). The exposed area was covered with artificial cerebrospinal fluid (NaCl 148, KCl 3.0, CaCl₂·2H₂O 1.4, MgCl₂·6H₂O 0.8, Na₂HPO₄·7H₂O 0.8, NaH₂PO₄·H₂O 0.2). Recordings were amplified (MultiClamp 700A, Axon Instr., Foster City, USA), filtered at 3-10 kHz and sampled at 10-20 kHz (DIGIDATA 1322A, Axon Instr.). Somatic and dendritic recordings with a minimal duration of 1 min were used and all membrane potentials were corrected for the junction potential (8 mV). Double recordings were performed using an extracellular electrode attached to a patching electrode with the patching electrode reaching approximately 10 μm deeper. For optimal attachment first two-component epoxy adhesive was used to bind the

electrodes at the part closest to the tip, and after drying dental cement was applied for additional support.

Extracellular recordings

C57BL/6 mice and homozygous *tottering* mice (3-12 months old) were prepared under isoflurane anaesthesia for chronic neurophysiological experiments by mounting a pedestal as described above. A recording chamber was built around craniotomies in both left and right occipital bones with a maximal diameter of 3 mm (Goossens et al., 2001). For the experiment the animal was anesthetized with isoflurane or ketamine/xylazine and the head was fixed by bolting the pedestal to a metal bar. When recording from awake mice, mice were briefly anesthetized with isoflurane, restrained in a custom made plastic tube and a 20 min acclimatization period preceded the recordings. Extracellular Purkinje cell activity was recorded using borosilicate glass electrodes (OD 2.0 mm, ID 1.16 mm, 4-8 M Ω). Electrodes were advanced into the cerebellum by a hydraulic micro-drive (Narishige, Tokyo, Japan). Recordings were made from left and right Crus I and II, paramedian lobule, and (para)flocculus. Approximately two-thirds of the Purkinje cells recorded were non-floccular, and no difference was found between floccular and non-floccular Purkinje cells in any of the calculated parameters (obviously, all recordings during optokinetic and vestibular stimulation were from floccular Purkinje cells). Purkinje cells were identified by the brief pause in simple spike activity following each complex spike. The raw electrode signal was amplified, filtered (CyberAmp, CED, Cambridge, UK), digitized (CED) and stored on disk for off-line analysis. Minimum duration of recordings was 2 min for spontaneous activity and 15 continuous cycles for recordings with optokinetic stimulation. Following each recording session the brain was covered with gramicidin-containing ointment and the chamber was sealed with bone wax.

Recordings under anaesthesia

For intra- and extracellular recordings under anaesthesia, commonly used anaesthetics ketamine/xylazine and isoflurane were used. Ketamine/xylazine anaesthesia was induced by an i.p. injection of 0.1 ml of a mixture containing 50 and 8 mg/kg body weight ketamine and xylazine, respectively. Anaesthesia was maintained with subsequent injections of 0.05 ml of the same mixture. Isoflurane anaesthesia was induced by inhalation of 4.0% isoflurane in a 2:1 mixture of NO₂ and O₂ for approximately 1-2 min, and was maintained with 1.0-1.5% isoflurane. Depth of anaesthesia was monitored in both groups by testing corneal and pinch reflexes, observing whisker and tail movements and breathing rate. Body temperature was maintained at ~37° using a homeothermic blanket (FHC, Bowdoinham, Me., USA).

Optokinetic and vestibular stimulation

For extracellular recordings during motor performance and motor learning tasks we recorded from the left flocculus under optokinetic (and vestibular) stimulation as previously described (Hoebeek et al., 2005). In short, optokinetic stimulation (OKR) consisted of either a planetarium or a random-dotted drum (dot size 2°) rotating sinusoidally around the vertical axis running through the animals' head with a fixed peak velocity (8°/s) at different frequencies ranging from 0.05 to 0.4 Hz. This stimulation will cause slip of the image over the retina, generating an error signal that results in

an increased complex spike firing frequency. Mismatched optokinetic and vestibular stimulation (VVT) consisted of a vertical axis whole body rotation in combination with horizontal axis optokinetic stimulation, both with 5° amplitude at 0.4 Hz. This stimulation will result in an adaptation of eye movements; after this training the animal will make vertical eye movements during vestibular stimulation in the horizontal plane in the dark. Stimulus velocities were measured and controlled by a 1401plus unit (CED). The left flocculus was first located by recording Purkinje cell activity during sensory motor behaviour. For optokinetic stimulation, only Purkinje cells that showed optimal complex spike modulation for stimulus rotations around the vertical axis were used. For combined optokinetic and vestibular stimulation all modulating floccular Purkinje cells were used. The position of the left eye was measured using a video set-up (Stahl et al., 2000; Stahl, 2004) (sampling rate 240 Hz; ETL-200, ISCAN, Burlington, MA, USA).

Data analysis

Off-line analysis was performed in Matlab (version 6.5, Mathworks, USA). Simple spikes and complex spikes were detected and discriminated using custom-made Matlab routines based on principal component analysis (Goossens et al., 2004). For intracellular recordings, transitions between states were detected using two thresholds, one for entering the downstate and one for entering the overstate. Only state changes with a minimum duration of 100 ms were registered. To avoid defining noise or individual complex spikes as a short upstate, we removed pairs of down-up and up-down transitions that occurred within 50 ms. In extracellular data, complex spike induced transitions were defined using two 100 ms intervals before and after each complex spike, starting at -102 and 25 ms respectively. If an interval contained simple spikes it was classified as upstate, otherwise as silent state. Complex spike toggling efficiency was defined as the fraction state changes given the total set of complex spikes. The ISSI distribution of each Purkinje cell was characterized by calculating the mean, CV (standard deviation divided by the mean), skewness and kurtosis proper. The CV indicates the relative width of the distribution; skewness indicates the asymmetry of the distribution, a positive value being a tail to the right (longer ISSIs indicating silent states); and kurtosis is a measure for the peakedness of the distribution, the higher the value the more 'peaky' the distribution is, indicating a strong preference for one firing frequency. Skewness and kurtosis were bootstrap bias corrected (Efron and Tibshirani, 1993) using 2000 sets of randomly selected ISSIs. Because the ISSIs due to a silent state are several orders longer and more variable in duration than upstate ISSIs, we used the logarithm of the ISSIs to calculate the skewness and kurtosis, which makes the distributions independent of time-scale and relatively symmetric (Bhumbra and Dyball, 2004).

Additional silent state ISSIs will positively skew the distribution and could even render the distribution bimodal. We therefore tested all ISSI distributions for unimodality with a dip test (Hartigan, 1985) using R software (version 2.1.0, <http://www.r-project.org>). In addition to comparing the shape of ISSI distributions, we also searched directly for long pauses in simple spike firing, since the downstate and the overstate are characterized by the absence of simple spike firing. We analyzed all ISSIs for each cell with different minimum silent periods that could be considered a pause (range 50 – 2000 ms). For each cell, silent states were analyzed by calculating for the entire range of pauses the percentage of total recording time the cell was pausing, and for each group the percentage of cells with at least one pause was calculated. In order to analyze

Purkinje cell activity during sensory motor behaviour simple spike raster plots were made. Simple and complex spike activity was modulated by optokinetically induced motor activity, which alters the ISSI distributions by inducing both shorter and longer ISSIs. Therefore we corrected each ISSI for the average firing rate during the part of the stimulus cycle that was encompassed by that ISSI using:

$$ISSI_{res}(i) = \langle ISSI \rangle \int_{u_i}^{u_{i+1}} R(\phi_t) dt$$

where $ISSI_{res}(i)$ is the i^{th} rescaled inter-simple spike interval, R is the stimulus-conditional average firing rate function, ϕ_t is the phase of the stimulus at time t and u_i is the i^{th} simple spike time. The continuous rate function R was obtained with a kernel density estimation algorithm using a Gaussian kernel with $SD=50$ ms. This rescaling procedure removes the linear effect of the stimulus on the firing rate and transforms the ISSIs, in the ideal case of inhomogeneous Poisson firing, into a Poisson process with unit rate (Brown et al., 2002). The distributions of the ISSIs before and after correction were used to calculate all used parameters, with the exception of the toggling, as the rescaling disturbs the original temporal relation between complex spikes and ISSIs.

Statistical analysis

All data are presented as mean \pm SEM. Statistical analysis was done using ANOVA (for normally distributed data), Mann-Whitney (for non-parametric data) or Chi-square test (for binominal data) and values were considered significantly different when $p < 0.05$.

Results

Bistability is present in Purkinje cells of anesthetized mice

To confirm the occurrence of bistability of Purkinje cells, which has so far only been shown in anesthetized rats and guinea pigs (Williams et al., 2002; Loewenstein et al., 2005), we performed whole-cell patch recordings in vivo in mice under isoflurane or ketamine/xylazine anaesthesia. Under isoflurane all Purkinje cells ($n = 6$) showed a bistable or multistable membrane potential (Fig. 1a). The upstate of the membrane potential (on average -52 ± 1 mV, mean \pm SEM) always occurred in conjunction with continuous firing of action potentials (mean firing frequency overall 40 ± 7 Hz; upstate 80 ± 22 Hz), whereas the downstate (-62 ± 3 mV) was completely silent but for complex spikes. In 5 out of 6 recorded Purkinje cells we observed a third state, which was even more depolarized (-37 ± 1 mV). The third state, hereafter referred to as the “overstate”, was quiescent but it occasionally displayed small spikelets (~ 3 -4 mV). While the upstate usually occurred after a downstate, the overstate always occurred after the upstate. Shifts from a particular state to a more depolarized state were often associated with the occurrence of a complex spike (from down- to upstate in 57 ± 16 % of the cases and from upstate to overstate in 57 ± 17 %; as opposed to 13 ± 8 % from up- to downstate and 17 ± 17 % from overstate to either upstate or downstate). Most of the time (68 ± 12 %) the cells were in the upstate; downstate and overstate covered 25 ± 12 % and 7 ± 5 % of the time, while their average duration lasted 1.1 ± 0.3 s and 0.8 ± 0.5 s, respectively.

Under ketamine/xylazine anaesthesia 6 out of 10 Purkinje cells showed a bistable or multistable membrane potential (Fig. 1b). Here too, the upstate of the membrane potential (on average -51 ± 1 mV) was correlated with continuous firing of action potentials (mean firing frequency overall 68 ± 9 Hz, same for upstate), while the downstate ($-61 \pm$

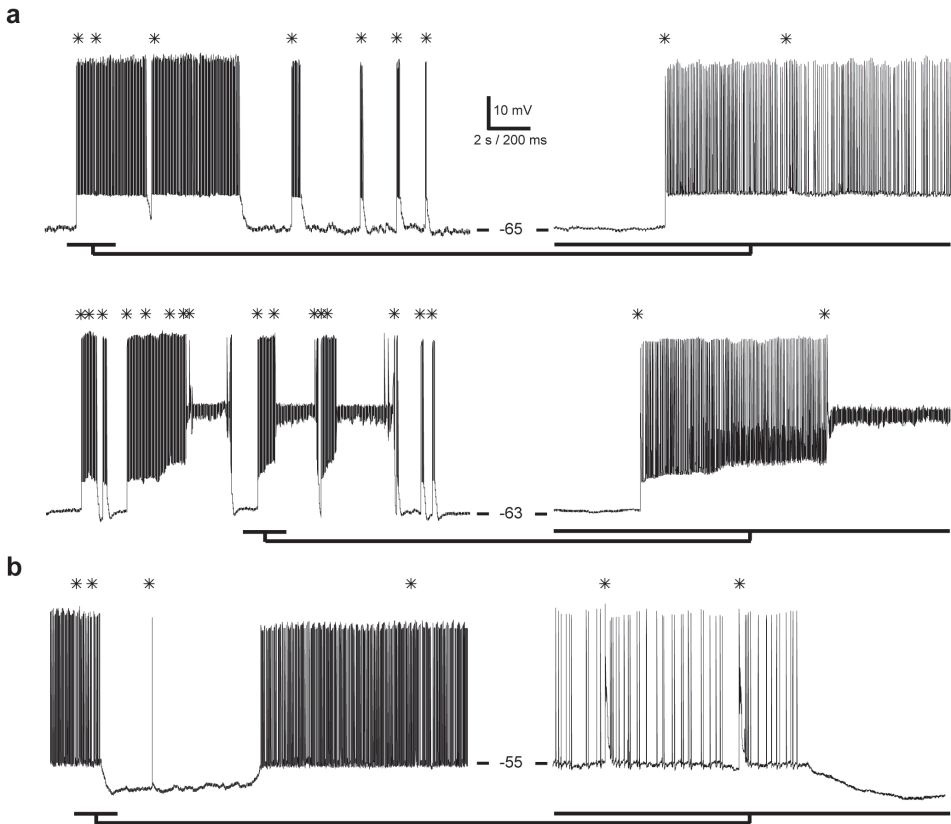


Figure 1. Membrane potential bistability of Purkinje cells *in vivo* under anesthesia.

(a) Top panel left: whole-cell recording of a Purkinje cell in an isoflurane anesthetized mouse showing two states of membrane potential; a hyperpolarized downstate and a depolarized upstate (asterisks indicate complex spikes). Right: enlargement of a transition from down- to upstate related to a complex spike. Bottom panel left: example of a Purkinje cell in an isoflurane anesthetized mouse displaying three states: a downstate, an upstate and an even more depolarized overstate. Right: enlargement showing that both transitions to a higher state are related to the occurrence of a complex spike. (b) Purkinje cell recording from a ketamine/xylazine anesthetized mouse, typically operating mostly in the upstate (left) and showing a weaker temporal relation between the occurrence of complex spikes and transitions (right). Note that throughout all examples the upstate displays continuous firing whereas the downstate and overstate are silent, but for complex spikes.

2 mV) and overstate (-39 ± 3 mV) were silent. Moreover, the shifts showed the same characteristics as described for the experiments under isoflurane in that the higher states usually occurred after a gradual stepwise elevation and that these elevations were relatively often associated with complex spike activities (down- to upstate 45 ± 14 % and up- to overstate 86 ± 11 %). The average duration of individual downstates (1.2 ± 0.5 s) and individual overstates (1.1 ± 0.8 s) did not differ from those found under isoflurane ($P = 0.91$ and $P = 0.74$, resp.). However, the percentage of time that the membrane potential was in the downstate (3 ± 2 %) as well as the percentage of cells displaying an overstate (20%) were both significantly lower ($P = 0.022$ and $P = 0.035$, resp.) than those under isoflurane (25 ± 12 % and 83%, respectively).

These data show that Purkinje cells in mice can show multiple stable states under various forms of anaesthesia, that the transitions to down- and overstate are more prominent under isoflurane than ketamine/xylazine, and that under both forms of

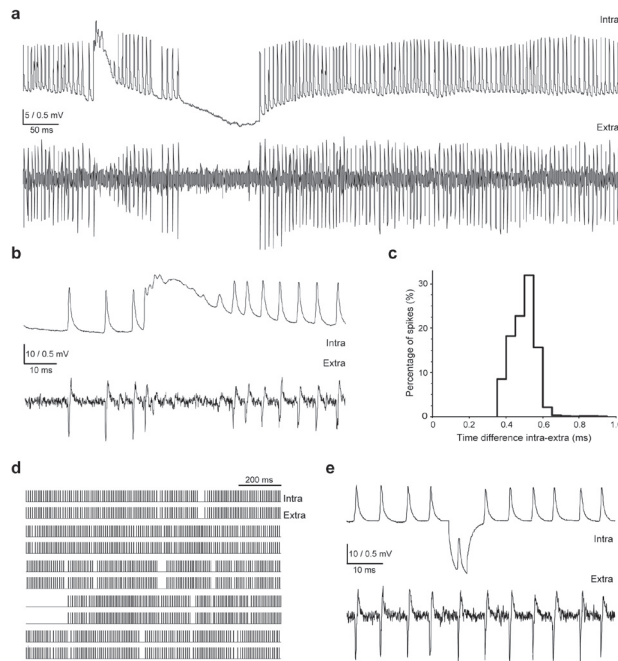


Figure 2. Dual recordings match action potentials of intracellular recordings with complex and simple spikes of extracellular recordings. (a) Simultaneous intracellular and extracellular recordings of the same Purkinje cell show a perfect match between action potentials (top) and simple spikes (bottom). (b) Enlargement of a complex spike, displaying the typical slow (calcium) wave in the intracellular recording and the complex spike waveform and climbing fiber pause in the extracellular recording. (c) Histogram of the time difference between intracellular action potentials and extracellular simple spikes. (d) Analysis of approximately 6 seconds of dual recording with each simple spike represented by a vertical bar. Together with (c) these figures demonstrate a 100% match at a time resolution of 1.0 ms. (e) Intracellular negative current injection is not seen in the extracellular recording excluding the possibility that the dual recordings result in cross-talk between the two electrodes.

anaesthesia the complex spikes can elicit simple spike firing by shifting the membrane potential from down- to upstate.

Action potentials of intracellular recordings correspond to simple spikes of extracellular recordings

While it is well established that the complex spike is an all or none response of the Purkinje cell to climbing fibre activation (Thach, 1967; Schmolesky et al., 2002), much less is known about how well extracellularly recorded events correspond to the sub- and suprathreshold potentials that can be observed with the use of the whole-cell recordings such as those described above. We therefore recorded simultaneously both intracellularly and extracellularly the activity of single Purkinje cells *in vivo* under ketamine/xylazine anesthesia ($n = 2$) using double electrode recordings (extracellular recording electrodes were attached to patch electrodes that reached 10 μm deeper) (Fig. 2a-b). The recording traces showed a perfect match in that every simple and complex spike recorded intracellularly corresponded to a single spike recorded extracellularly and vice versa (resulting in a 100% match at a time resolution of 1.0 ms; Fig. 2c-d). Thus, during downstate silent periods identified using the intracellular data, no extracellular simple spikes were recorded. Moreover, the prolonged silent periods observed in the extracellular recordings corresponded exclusively to down- or overstate

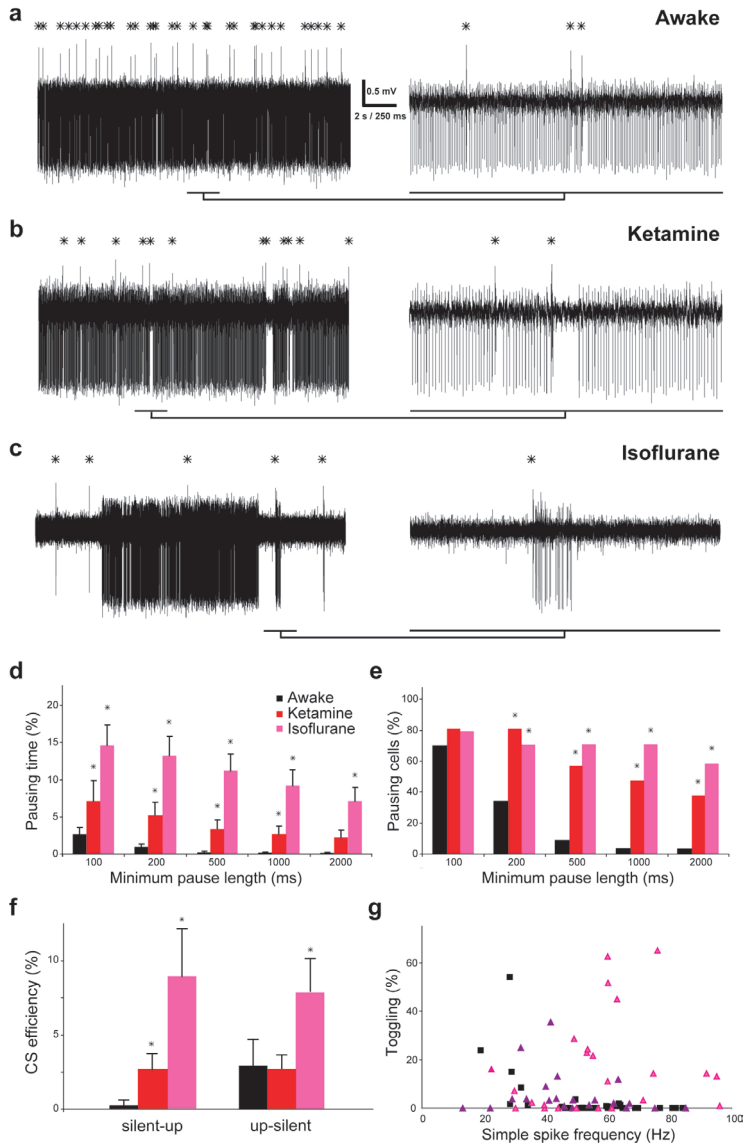


Figure 3. Extracellular recordings display a dramatic induction of the occurrence of simple spike pauses and toggling signs by anesthetics.

(a) Typical extracellular recording of spontaneous Purkinje cell activity in an awake mouse (left, 20 s overview) displaying little or no signs of pauses or toggling (right, 2 s enlargement). Asterisks indicate complex spikes. (b) Purkinje cell recorded extracellularly in mice under ketamine/xylazine anesthesia showing pauses in simple spike firing. (c) Extracellular recording of a Purkinje cell in a mouse under isoflurane anesthesia displaying a highly irregular firing pattern consisting of pauses and bursts. (d) Histogram comparing the percentage of total recording time that individual cells were pausing for different minimum pause lengths. Independent of the pause length Purkinje cells recorded under ketamine/xylazine ($n = 21$) as well as under isoflurane ($n = 24$) spent significantly more time in pause than cells in awake mice ($n = 36$). (e) Histogram comparing the percentage of cells showing one or more pause(s) for different minimum pause lengths. Both ketamine/xylazine and isoflurane show a significantly higher percentage of cells for minimum pause lengths of 200 to 2000 ms. (f) Histogram displaying the percentage of all complex spikes triggering a change in simple spike firing of the Purkinje cell, either from a silent state to the upstate (silent-up) or in the opposite direction (upstate - silent). (g) Scatterplot displaying for each cell the percentage of all transitions (i.e. both from an upstate to a silent state or vice versa), related to the average simple spike firing frequency over the entire range.

Table 1. Overview of basic characteristics of spontaneous simple spike activities

Simple spike characteristics	Firing frequency (Hz)	Coefficient of Variance	Skewness	Kurtosis	CF pause (ms)
Awake spontaneous (n = 36)	55 ± 3	0.5 ± 0.0	0.2 ± 0.1	5 ± 0	15 ± 1
Isoflurane (n = 24)	57 ± 4	4.4 ± 0.8 ***	2.3 ± 0.5 **	31 ± 7 **	15 ± 1
Ketamine/xylazine (n = 21)	50 ± 4	1.7 ± 0.5 *	1.2 ± 0.4 *	20 ± 4 **	18 ± 1

(* : P < 0.05; ** : P < 0.01; *** : P < 0.001)

periods of the intracellular recordings. To exclude the possibility that cross-talk between the two electrodes caused the perfect match, we gave short negative current pulses similar in size to the spikes recorded intracellularly. These current injections resulted in a hyperpolarization in the intracellular recording, while no deflection occurred in the extracellular recording (Fig. 2e). The maximum duration of an ISSI during a downstate or overstate period was over 5 s, and the vast majority (> 90 %) of all downstate and overstate ISSIs were greater than 200 ms. In contrast, no simple spike pause in the upstate was longer than 200ms.

Thus operationally we determined that any silent period observed in an extracellular recording that is longer than 200 ms, most likely reflects a downstate or overstate. Together these data indicate that simple spikes of extracellular recordings always correspond to action potentials of intracellular recordings, and that the state of the membrane potential of a Purkinje cell can be deduced from the temporal patterns of simple spike activities that have been recorded with extracellular methods.

Extracellular recordings show low level of bistability in spontaneous awake state

Whereas whole-cell recordings in awake behaving animals impose technical problems, stable extracellular recordings of Purkinje cells are quite feasible in the awake state (Goossens et al., 2004). Thus, since the temporal pattern of simple spike activities provides, as explained above, information about the state of the membrane potential, extracellular recordings offer a means to compare the occurrence of bistability in awake animals with that in anesthetized animals. Therefore we conducted extracellular recordings of Purkinje cell activity in awake mice (n = 36 cells) as well as in mice anesthetized with either isoflurane (n = 24) or ketamine/xylazine (n = 21). As mentioned above, silent states will introduce ISSIs that are up to several orders longer in duration than ISSIs during the upstate. These long ISSIs affect the upper tail of the ISSI distribution. We examined the shape of the ISSI distribution using skewness and kurtosis as indicators of asymmetry and peakedness, respectively. We expected additional silent state ISSIs to positively skew the distribution. Because the variance of silent state ISSIs scales with their mean duration, we used the logarithm of the ISSIs. In addition, as a measure of spike train regularity, we calculated the coefficient of variation (CV), and since multiple

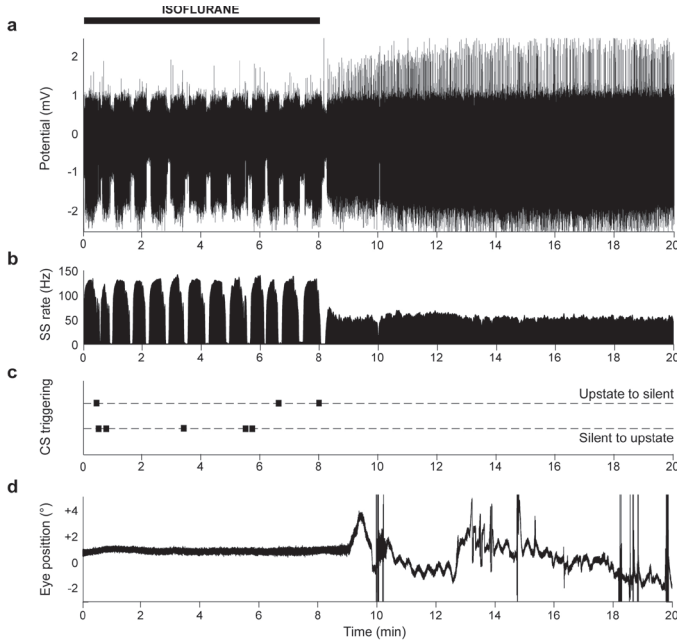


Figure 4. Cessation of anesthesia during extracellular recordings eliminates pauses and signs of toggling in Purkinje cell firing behavior.

(a) Extracellular Purkinje cell recording of a mouse starting under isoflurane anesthesia, which is ceased after 8 min. (b) Simple spike firing frequency during anesthesia consists of pauses and high frequency bursts; after cessation of the application of isoflurane this firing behaviour is no longer present. (c) Signs of toggling (time points depicted by squares) can be found in both directions during application of isoflurane, but no longer occur after cessation of isoflurane. (d) Recordings of eye position during the experiment show that compensatory eye movements start approximately 1 min after the cessation of isoflurane, confirming that the mouse recovered from anesthetics.

firing states can lead to a bimodal log-ISSI distribution, we tested for unimodality using a dip test (Hartigan, 1985).

While the simple spike firing frequencies and climbing fibre pauses did not vary significantly between Purkinje cells of awake mice and mice under both types of anaesthetics (both $P > 0.50$ and both $P > 0.07$, respectively), the regularity of simple spike activities in awake mice was much greater than that found in anesthetized mice (Fig. 3a-c). Their Coefficient of Variance (CV), skewness, and kurtosis were all significantly smaller (for numbers and significance levels see Table 1). Furthermore, the dip test indicated that the percentages of cells with bi-/multimodal ISSI (Fig. 7b), a strong indicator of multiple firing states, was significantly increased in anesthetized mice. If bistability were present in awake animals, one would expect to find a significant number of ISSI pauses with a duration exceeding 200 ms, as seen in anesthetized mice. However, pauses longer than 200 ms hardly occurred in awake mice. Both the total percentage of time spent in a pause state and the total percentage of cells that showed one or more pauses greater than 200 ms were substantially lower in awake animals than in those anesthetized (Fig. 3d-e). All values (i.e. CV, skewness and kurtosis) were compared for Purkinje cells in the different areas Crus I and II, paramedian lobule and (para)flocculus and no differences were observed (data not shown). In addition, we found little evidence for the toggling switch phenomenon mediated by the complex spikes in awake animals (Fig. 3f). When we examined the instances at which a pause in simple spike activities of at least 100 ms occurred before or after a complex spike, we found that complex spikes rarely triggered a change in simple spike activities from silent to upstate ($0.3 \pm 0.1\%$) and in a limited number of cases from upstate to silent ($2.9 \pm 1.6\%$). These percentages were significantly lower than those obtained under isoflurane (silent to upstate $9.3 \pm 3.0\%$, $P < 0.001$; upstate to silent $7.7 \pm 2.2\%$, $P = 0.026$) or ketamine/xylazine (silent to upstate 2.5

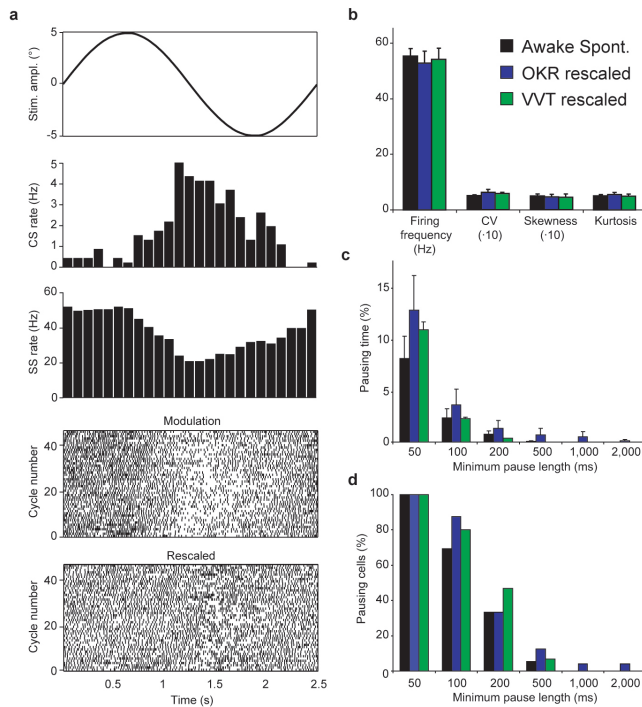


Figure 5. Subjecting the animal to a motor performance or motor learning task does not lead to significantly greater bistability in Purkinje cells.

(a) To correct for the modulation (middle, 100ms bin peri-stimulus time histogram) induced by optokinetic stimulation (top), the ISI distributions were rescaled. Peri-stimulus raster plots show the effect of the rescaling on the modulation (top: before, bottom: after). Rescaled ISI distributions of recordings reveal that distribution characteristics mean, CV, skewness and kurtosis do not significantly differ (b) or do not spend significantly more time in pause (c) when mice are subjected to optokinetic stimulation (OKR with peak velocity of 8°/s at 0.4 Hz; motor performance task) or visuovestibular training (VVT with combined optokinetic and vestibular stimulation both with an amplitude of 5° at 0.4 Hz; motor learning task) relative to spontaneously active conditions. (d) The percentage of cells with at least one pause within the examined range also did not differ between groups either.

$\pm 1.4\%$, $P = 0.046$). The occasional triggering from upstate to silent by a complex spike in awake animals was, in contrast to that in anesthetized animals, found to be directly related to the simple spike firing frequency, in that signs of toggling were only seen in cells with a relatively low simple spike firing frequency (Fig. 3g). The low firing frequency greatly enhances the chance of finding a 100ms, not representing a downstate.

Finally, if the use of anaesthesia increases bistability, cessation of such application should bring the same Purkinje cells to a stable upstate level resulting in regular simple spike firing without pauses or inter-spike intervals longer than 158 ms and without signs of toggling by the complex spikes. We therefore investigated the extracellular activities of individual Purkinje cells ($n = 2$) both during and after application of isoflurane, which can be administered by respiration and stopped abruptly at will. Fig. 4 shows an example of the recordings of a Purkinje cell in the paramedian lobule. While the regular pauses and signs of complex spike toggling described above were abundantly observed during application of isoflurane, they disappeared within one minute after stopping it (Fig. 4a-c). To verify that the animal switched from an anesthetized state to an awake state after this minute, we attempted to evoke compensatory eye movements during the entire experiment. These recordings showed that sinusoidal optokinetic stimulation indeed resulted in visual reflexes approximately one minute after application of isoflurane was stopped (Fig. 4d).

Together, the extracellular recordings described above indicate that anaesthetics can dramatically induce bistability in Purkinje cells and that this process is practically absent in the awake state.

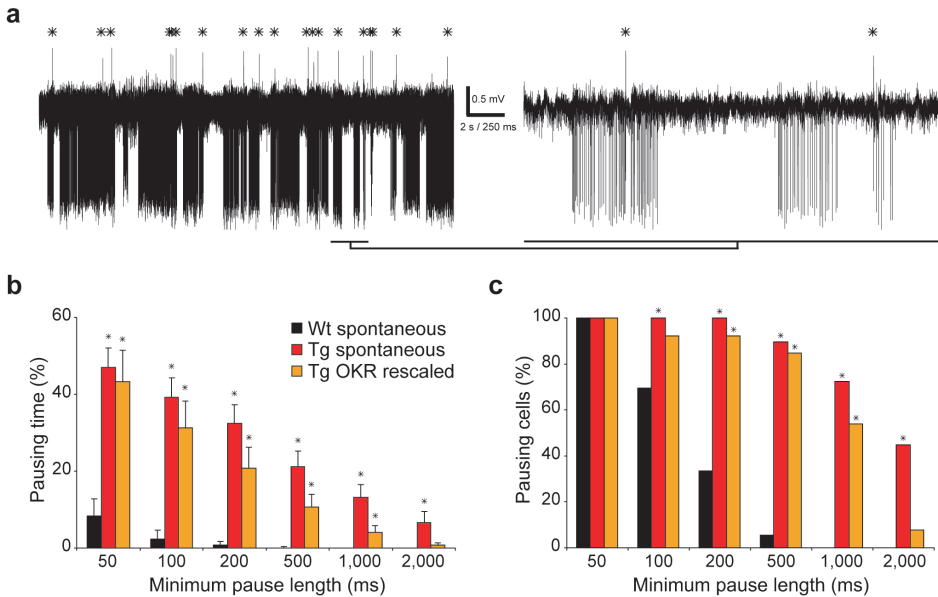


Figure 6. The *tottering* mutation causes changes in the simple spike firing pattern comparable to the effect of anesthetics. (a) Typical extracellular Purkinje cell recording trace with irregular simple spike firing (left) and putative toggling by the second complex spike in the enlargement (right, complex spikes marked by asterisks). (b) In line with the effect of anesthetics the *tottering* mutation also results in Purkinje cells that spend significantly more time in pauses. This effect was found in cells from animals with and without optokinetic stimulation. (c) The percentage of pausing cells was also higher in both of these groups compared to wild type mice.

Modulation of afferents to Purkinje cells does not alter their stability in awake state

While the data above demonstrate that pauses, as a sign of bistability, virtually do not occur in spontaneously active Purkinje cells in awake animals, they do not exclude the possibility that bistability may be enhanced by sensory modulation or learning paradigms. We therefore compared the temporal patterns of the simple and complex spike activities of Purkinje cell recordings from awake mice without stimulation ($n = 36$) with those during optokinetic stimulation (OKR modulation; $n = 24$) and visuovestibular training (VVT modulation; $n = 15$). Since optokinetic stimulation modulates the ISSIs (Fig. 5a) independent from the presence of complex spikes (Leonard, 1986) and thereby alters the ISSI distribution, we corrected each ISSI for the average firing rate during the part of the stimulus cycle encompassed by that ISSI (Fig. 5b). This rescaling procedure removes the linear effect of the stimulus on the firing rate. The skewness and kurtosis values of the rescaled ISSI distributions recorded during both optokinetic stimulation and visuovestibular training did not differ from those during spontaneous activity in awake mice (all P -values > 0.25). Moreover, the time that the cells were in pause and percentage of cells that showed pauses also did not differ significantly among the groups (all P -values > 0.16 , Fig. 5c-d). These results indicate that bistability of Purkinje cells in awake mice is neither enhanced by the sensory stimulation that modulates these cells nor by the motor performance or motor learning that is controlled by these cells.

Purkinje cells with abnormal voltage-gated calcium channels display bistable firing behaviour in awake state

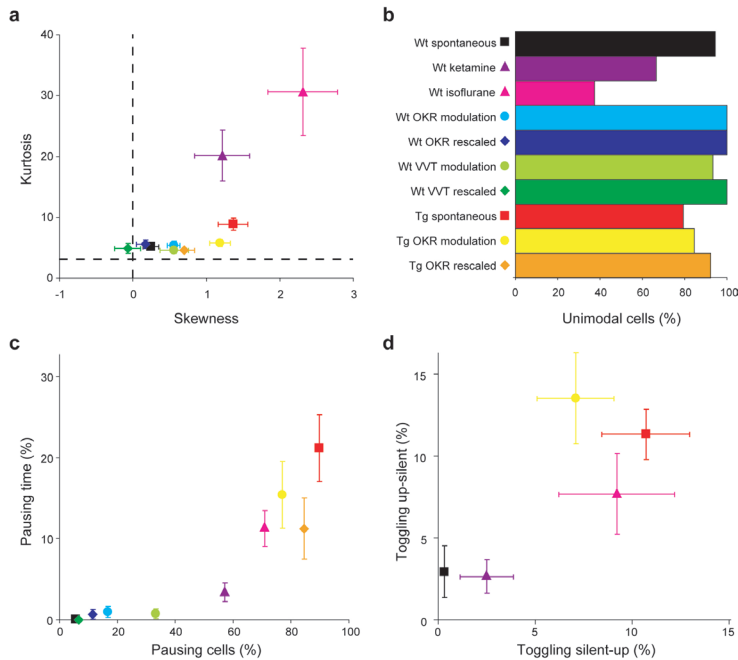


Figure 7. Silent states in Purkinje cells, suggestive for bistability, can be evoked by anesthetics or genetic mutations, but not by subjecting the animal to motor performance or motor learning tasks. (a) Skewness and kurtosis, two characteristics of the shape of ISSI distributions are both increased by anesthetics, while the tottering mutation mostly results in a higher skewness. Dashed lines indicate skewness and kurtosis value of a lognormal distribution. (b) The percentage of cells with a unimodal ISSI distribution was reduced by both anesthetics. (c) Using a minimum pause length of 500 ms (approximately 3 times the maximum ISSI found in the upstate), both the percentage of pausing time and pausing cells, as a sign for bistability, are higher as a result of either anesthetics or the tottering mutation. (d) The percentage of times a complex spike putatively triggered a change in simple spike firing in either direction, as a sign for toggling, is higher as a result of both anesthetics and the tottering mutation.

The findings presented above suggest that anaesthesia in general causes or promotes bistability and led us to hypothesize that there could be specific factors that can influence bistability. Since isoflurane potentiates the GABA_A-receptor current (Nakahiro et al., 1989; Hall et al., 1994) and is very effective in inducing bistability, we selected a mutant with enhanced inhibition to test this hypothesis. The tottering mouse, which suffers from a mutation in its voltage-gated P/Q-type calcium channels, appeared an interesting candidate, because its Purkinje cells show an increased susceptibility to inhibitory modulation by GABAergic interneurons (Zhou et al., 2003) and show irregular simple spike firing behavior (Ch. 3.3: Hoebeek et al., 2006). We therefore investigated bistability in tottering mice by analyzing the pauses and signs of toggling using extracellular recordings in the awake state (Fig. 6a-c). Purkinje cells of awake tottering mutants without ($n = 29$) and with optokinetic stimulation ($n = 13$) showed the same type of changes in simple spike firing patterns as the wild type animals under isoflurane anaesthesia. That is, the values for ISSI distribution parameters (CV, skewness and kurtosis), pausing time, and pausing cells (minimum pause length 100-1000 ms) were all significantly higher in both these conditions than in awake wild type animals (all P -values < 0.005). Moreover, we observed numerous cases in which the complex spike activities putatively triggered simple spike activities via a toggling process. During

spontaneous activity as well as motor performance the percentages of complex spikes related to transitions between upstate and pause in awake totterings were significantly higher than those in awake wild types (for both upstate to silent and silent to upstate, all P -values < 0.001 , Fig. 7d). These findings suggest that bistability is indeed enhanced in mutants in which inhibition is increased. To further test this hypothesis we compared the level of bistability in totterings with that in wild types using whole-cell recordings in vivo under isoflurane and ketamine/xylazine. Under ketamine/xylazine anaesthesia the Purkinje cells of the totterings spent significantly more time in the downstate as compared to those in wild types (percentage of total time in downstate $25 \pm 7\%$ vs. $3 \pm 2\%$, $P = 0.022$). The time spent in downstate as a result of isoflurane in normal mice, and that in tottering mice under ketamine is comparable. However, the use of isoflurane in tottering mice did not result in an additional effect on the time in downstate, which might be explained as a 'saturation' of the effect of inhibition. Together these data indicate that awake animals can show robust signs of bistability if their voltage-gated P/Q-type calcium channels are genetically affected. The fact that the influence on GABA-currents is one of the prominent features of both isoflurane application and the tottering mutation suggests that alterations in inhibition play an important role in bistability.

Discussion

We have demonstrated that Purkinje cells in mice shift between several membrane states when their intrinsic excitability is altered due to anaesthesia or particular genetic mutations. However, Purkinje cells in healthy awake behaving animals operate virtually exclusively in the upstate of the membrane potential. This propensity holds true in mice during spontaneous activity as well as during motor performance and motor learning.

Role of membrane stability in Purkinje cells in awake behaving animals

The recent discovery that bistability can occur in vivo in Purkinje cells of both rats and guinea pigs under various forms of anaesthesia and that climbing fibre activity evoked by sensory stimulation can trigger periods of simple spike bursts or quiescence under these circumstances has revived the debate about the possible roles of bistability of Purkinje cells (Loewenstein et al., 2005). In particular the findings by Loewenstein and colleagues have raised the possibility that Purkinje cell bistability may play a key role in short-term processing and storage of sensory information. We have therefore first set out experiments to investigate whether action potentials obtained with in vivo whole-cell recordings can be directly related to simple spike activities recorded extracellularly, and whether the temporal pattern of these simple spike activities provides information about the state of the membrane potential. By recording simultaneously whole-cell activities and extracellular activities of the same Purkinje cells under anaesthesia in mice we were able to show unequivocally that both questions can be answered positively. The double recordings demonstrated that extracellular single-unit recordings accurately represent the activity measured intracellularly and that extracellularly recorded silent states and thereby bistability are characterized by long pauses (> 158 ms) and toggling by the occurrence of a complex spike between a pause and an upstate. We subsequently employed the extracellular recording technique to investigate whether the occurrence of bistability in Purkinje cells is correlated to the presence of anaesthesia and/or to the behavioural state of the animal, i.e. spontaneously active, doing a motor performance

task, or being subjected to a task of cerebellar motor learning. These experiments showed that bistability in general hardly occurs in the awake state and that it can hardly be influenced by sensory stimulation or motor training paradigms in this state, while it is prominently present under isoflurane or ketamine/xylazine anaesthesia (summarized in Fig. 7). These data agree with extracellular recordings in other labs that investigated simple spike and complex spike behaviour in awake behaving and learning animals including those in monkeys, cats and rabbits (Thach, 1967; Sato et al., 1992; De Zeeuw et al., 1995; Simpson et al., 1996; Norris et al., 2004). Although most of these previous studies in awake behaving animals have also shown some irregularities in simple spike activities, detailed analyses with the current methods showed that the pauses of simple spikes hardly ever exceed 100 ms and that the silent periods after the complex spikes were perfectly in line with the normal climbing fiber pauses (data not shown), which are simply reflecting a refractory period rather than a change in the state of the membrane potential. Moreover, further inspection of the data obtained by other labs in other awake, behaving animals also showed virtually no sign of the toggling switch, which is so prominently present under anaesthesia. Even simple spike activities during desynchronized sleep (Hobson and McCarley, 1972; McCarley and Hobson, 1972), hardly demonstrate any sign of bistability. Thus, although we have no access to whole-cell recordings, let alone to double intracellular and extracellular recordings, of Purkinje cells in species other than mice, it is parsimonious to conclude that Purkinje cells in awake behaving animals in general operate virtually solely in the upstate and that this state of their membrane potential is not significantly modified by sensory stimulation, motor performance or motor learning. In contrast, the Purkinje cells of tottering mutants, which turned out to have a very high level of bistability even in the awake state (present study), are virtually unable to exert any cerebellar control on their motor behavior (Ch. 3.3: Hoebeek et al., 2005). Thus, one might argue that healthy Purkinje cells and a functional cerebellar cortical network are in fact designed to avoid bistability under normal physiological circumstances.

Mechanisms of bistability

Previous studies have shown that various conductances including non-inactivating sodium and calcium conductances, potassium conductances and h-currents (I_h) can play a role in generating bistability in Purkinje cells (Llinas and Sugimori, 1980a, 1980b; Li et al., 1993; Rapp et al., 1994; Williams et al., 2002; Loewenstein et al., 2005). Our data obtained with anaesthetics and genetic modification suggest that artificially enhancing the inhibitory input from the GABAergic interneurons and/or diminishing the excitatory drive through the mossy fibre - parallel fibre pathway could elicit a down state that is normally virtually absent. Isoflurane is known to potentiate the GABA_A receptor current (Nakahiro et al., 1989; Hall et al., 1994), while ketamine and xylazine act as NMDA-receptor blocker and alpha 2-adrenergic receptor agonist, respectively (Leppavuori and Putkonen, 1980; Wagner et al., 2001). This reasoning is further supported by studies which showed that isoflurane and alpha 2-adrenergic receptor agonists can also reduce the frequency and regularity of simple spike firing in vitro (Crepel et al., 1987; Parfitt et al., 1988; Antkowiak et al., 1997) and that loss of inhibitory input causes Purkinje cells to fire simple spikes more regularly (Hausser and Clark, 1997). Moreover, our findings of an increased level of bistability in the tottering is also compatible with this idea, because this mutant shows a reduction in the amplitude of the parallel fibre – Purkinje cell EPSC

and an increased susceptibility to inhibitory modulation by GABAergic interneurons (Matsushita et al., 2002; Zhou et al., 2003). A comparable relation between enhanced inhibition and increased irregularity, characterized also by longer ISSIs, has been described in the GluR62 knockout mouse (Ohtsuki et al., 2004; Yoshida et al., 2004). Thus, enhancing the inhibitory and/or diminishing the excitatory input to Purkinje cells at a non-physiological level may affect the various conductances such that an artificial downstate is generated, which in turn permits the complex spike to trigger or toggle a new upstate with simple spike bursts.

Acknowledgements

The authors thank Ing. J. van den Burg for excellent assistance. Research was supported by Neuro-Bsik (C.D.Z.), ZonMw (C.D.Z.), NWOALW (C.D.Z., M.F.), NWO-PIONIER (C.D.Z.), EEC (C.D.Z.), EUR (M.T.S.) and NWO-VIDI (M.F., B.W.).

Reference list

- Antkowiak B, Hentschke H, Kirschfeld K (1997) Effects of volatile anaesthetics on spontaneous action potential firing of cerebellar Purkinje cells in vitro do not follow the Meyer-Overton rule. *Br J Anaesth* 79:617-624.
- Armstrong DM (1974) Functional significance of connections of the inferior olive. *Physiol Rev* 54:358-417.
- Bhumra GS, Dyball RE (2004) Measuring spike coding in the rat supraoptic nucleus. *J Physiol* 555:281-296.
- Branchereau P, Van Bockstaele EJ, Chan J, Pickel VM (1996) Pyramidal neurons in rat prefrontal cortex show a complex synaptic response to single electrical stimulation of the locus coeruleus region: evidence for antidromic activation and GABAergic inhibition using in vivo intracellular recording and electron microscopy. *Synapse* 22:313-331.
- Brown EN, Barbieri R, Ventura V, Kass RE, Frank LM (2002) The time-rescaling theorem and its application to neural spike train data analysis. *Neural Comput* 14:325-346.
- Crepel F, Debono M, Flores R (1987) Alpha-adrenergic inhibition of rat cerebellar Purkinje cells in vitro: a voltage-clamp study. *J Physiol* 383:487-498.
- De Zeeuw CI, Wylie DR, Stahl JS, Simpson JJ (1995) Phase Relations of Purkinje Cells in the Rabbit Flocculus During Compensatory Eye Movements. *J of Neurophysiol* 74:2051-2063.
- De Zeeuw CI, Simpson JJ, Hoogenraad CC, Galjart N, Koekkoek SK, Ruigrok TJ (1998) Microcircuitry and function of the inferior olive. *Trends Neurosci* 21:391-400.
- De Zeeuw CI, Koekkoek SK, van Alphen AM, Luo C, Hoebeek F, van der Steen J, Frens MA, Sun JC, Goossens HHLM, Jaarsma D, Coesmans MPH, Schmolesky MT, de Jeu MTG, Galjart N (2003) Gain and phase control of compensatory eye movements by the flocculus of the vestibulocerebellum. In: *Handbook of auditory research*, pp 375-422: Springer Verlag.
- Durstewitz D, Seamans JK, Sejnowski TJ (2000) Neurocomputational models of working memory. *Nat Neurosci* 3 Suppl:1184-1191.
- Efron B, Tibshirani RJ (1993) *An introduction to the bootstrap*. London: Chapman and

Hall.

- Goossens HH, Hoebeek FE, Van Alphen AM, Van Der Steen J, Stahl JS, De Zeeuw CI, Frens MA (2004) Simple spike and complex spike activity of floccular Purkinje cells during the optokinetic reflex in mice lacking cerebellar long-term depression. *Eur J Neurosci* 19:687-697.
- Goossens J, Daniel H, Rancillac A, van der Steen J, Oberdick J, Crepel F, De Zeeuw CI, Frens MA (2001) Expression of protein kinase C inhibitor blocks cerebellar long-term depression without affecting Purkinje cell excitability in alert mice. *J Neurosci* 21:5813-5823.
- Hall AC, Lieb WR, Franks NP (1994) Stereoselective and non-stereoselective actions of isoflurane on the GABAA receptor. *Br J Pharmacol* 112:906-910.
- Hartigan JA, Hartigan, P.M. (1985) The Dip Test of Unimodality. *Ann Stat* 13:70-84.
- Hausser M, Clark BA (1997) Tonic synaptic inhibition modulates neuronal output pattern and spatiotemporal synaptic integration. *Neuron* 19:665-678.
- Hobson JA, McCarley RW (1972) Spontaneous discharge rates of cat cerebellar Purkinje cells in sleep and waking. *Electroencephalogr Clin Neurophysiol* 33:457-469.
- Hoebeek FE, Stahl JS, van Alphen AM, Schonewille M, Luo C, Rutteman M, van den Maagdenberg AM, Molenaar PC, Goossens HH, Frens MA, De Zeeuw CI (2005) Increased noise level of purkinje cell activities minimizes impact of their modulation during sensorimotor control. *Neuron* 45:953-965.
- Ito M (1982) Cerebellar control of the vestibulo-ocular reflex--around the flocculus hypothesis. *Annu Rev Neurosci* 5:275-296.
- Leonard CS (1986) Signal characteristics of cerebellar Purkinje cells in the rabbit flocculus during compensatory eye movements. In: *Physiology and Biophysics*, p 190. New York: New York University.
- Leppavuori A, Putkonen PT (1980) Alpha-adrenoceptive influences on the control of the sleep-waking cycle in the cat. *Brain Res* 193:95-115.
- Li SJ, Wang Y, Strahlendorf HK, Strahlendorf JC (1993) Serotonin alters an inwardly rectifying current (I_h) in rat cerebellar Purkinje cells under voltage clamp. *Brain Res* 617:87-95.
- Lisberger SG (1998) Physiologic basis for motor learning in the vestibulo-ocular reflex. *Otolaryngol Head Neck Surg* 119:43-48.
- Llinas R, Sugimori M (1980a) Electrophysiological properties of in vitro Purkinje cell dendrites in mammalian cerebellar slices. *J Physiol* 305:197-213.
- Llinas R, Sugimori M (1980b) Electrophysiological properties of in vitro Purkinje cell somata in mammalian cerebellar slices. *J Physiol* 305:171-195.
- Loewenstein Y, Mahon S, Chadderton P, Kitamura K, Sompolinsky H, Yarom Y, Hausser M (2005) Bistability of cerebellar Purkinje cells modulated by sensory stimulation. *Nat Neurosci* 8:202-211.
- MacIver MB, Kendig JJ (1991) Anesthetic effects on resting membrane potential are voltage-dependent and agent-specific. *Anesthesiology* 74:83-88.
- Margrie TW, Brecht M, Sakmann B (2002) In vivo, low-resistance, whole-cell recordings from neurons in the anaesthetized and awake mammalian brain. *Pflugers Arch* 444:491-498.
- Matsushita K, Wakamori M, Rhyu IJ, Arii T, Oda S, Mori Y, Imoto K (2002) Bidirectional alterations in cerebellar synaptic transmission of tottering and rolling Ca²⁺ channel mutant mice. *J Neurosci* 22:4388-4398.

- McCarley RW, Hobson JA (1972) Simple spike firing patterns of cat cerebellar Purkinje cells in sleep and waking. *Electroencephalogr Clin Neurophysiol* 33:471-483.
- Nakahiro M, Yeh JZ, Brunner E, Narahashi T (1989) General anesthetics modulate GABA receptor channel complex in rat dorsal root ganglion neurons. *Faseb J* 3:1850-1854.
- Norris SA, Greger B, Hathaway EN, Thach WT (2004) Purkinje cell spike firing in the posterolateral cerebellum: correlation with visual stimulus, oculomotor response, and error feedback. *J Neurophysiol* 92:1867-1879.
- O'Donnell P, Grace AA (1995) Synaptic interactions among excitatory afferents to nucleus accumbens neurons: hippocampal gating of prefrontal cortical input. *J Neurosci* 15:3622-3639.
- O'Donnell P, Greene J, Pabello N, Lewis BL, Grace AA (1999) Modulation of cell firing in the nucleus accumbens. *Ann N Y Acad Sci* 877:157-175.
- Ohtsuki G, Kawaguchi SY, Mishina M, Hirano T (2004) Enhanced inhibitory synaptic transmission in the cerebellar molecular layer of the GluRdelta2 knock-out mouse. *J Neurosci* 24:10900-10907.
- Parfitt KD, Freedman R, Bickford-Wimer PC (1988) Electrophysiological effects of locally applied noradrenergic agents at cerebellar Purkinje neurons: receptor specificity. *Brain Res* 462:242-251.
- Rapp M, Segev I, Yarom Y (1994) Physiology, morphology and detailed passive models of guinea-pig cerebellar Purkinje cells. *J Physiol (Lond)* 474:101-118.
- Sato Y, Miura A, Fushika H, Kawasaki T (1992) Short-term modulation of cerebellar purkinjecell activity after spontaneous climbing fiber input. *J Neurophysiol* 68:2051-2062.
- Schmolesky MT, Weber JT, De Zeeuw CI, Hansel C (2002) The making of a complex spike: ionic composition and plasticity. *Ann N Y Acad Sci* 978:359-390.
- Simpson JJ, Wylie DR, De Zeeuw CI (1996) On climbing fiber signals and their consequence(s). *Behav Brain Sci* 19:380-394.
- Stahl JS (2004) Eye movements of the murine p/q calcium channel mutant rocker, and the impact of aging. *J Neurophysiol* 91:2066-2078.
- Stahl JS, van Alphen AM, De Zeeuw CI (2000) A comparison of video and magnetic search coil recordings of mouse eye movements [In Process Citation]. *J Neurosci Methods* 99:101-110.
- Thach WT, Jr. (1967) Somatosensory receptive fields of single units in cat cerebellar cortex. *J Neurophysiol* 30:675-696.
- Wagner LE, 2nd, Gingrich KJ, Kullu JC, Yang J (2001) Ketamine blockade of voltage-gated sodium channels: evidence for a shared receptor site with local anesthetics. *Anesthesiology* 95:1406-1413.
- Williams SR, Christensen SR, Stuart GJ, Hausser M (2002) Membrane potential bistability is controlled by the hyperpolarization-activated current I(H) in rat cerebellar Purkinje neurons in vitro. *J Physiol* 539:469-483.
- Yoshida T, Katoh A, Ohtsuki G, Mishina M, Hirano T (2004) Oscillating Purkinje neuron activity causing involuntary eye movement in a mutant mouse deficient in the glutamate receptor delta2 subunit. *J Neurosci* 24:2440-2448.
- Zhou YD, Turner TJ, Dunlap K (2003) Enhanced G protein-dependent modulation of excitatory synaptic transmission in the cerebellum of the Ca²⁺ channel-mutant mouse, tottering. *J Physiol* 547:497-507.

Chapter 3

Paragraph 2

Regular Patterns in Cerebellar Purkinje Cell Simple Spike Trains

Adapted from PLoS ONE. 2007 May 30;2(5):e485.

S.L. Shin, F.E. Hoebeek, M. Schonewille, C.I. De Zeeuw, A. Aertsen, E. De Schutter.

Abstract

Cerebellar Purkinje cells (PC) *in vivo* are commonly reported to generate irregular spike trains, documented by high coefficients of variation of interspike-intervals (ISI). In strong contrast, they fire very regularly in the *in vitro* slice preparation. We studied the nature of this difference in firing properties by focusing on short-term variability and its dependence on behavioral state. Using an analysis based on CV_2 values, we could isolate precise regular spiking patterns, lasting up to hundreds of milliseconds, in PC simple spike trains recorded in both anesthetized and awake rodents. Regular spike patterns, defined by low variability of successive ISIs, comprised over half of the spikes, showed a wide range of mean ISIs, and were affected by behavioral state and tactile stimulation. Interestingly, regular patterns often coincided in nearby Purkinje cells without precise synchronization of individual spikes. Regular patterns exclusively appeared during the up state of the PC membrane potential, while single ISIs occurred both during up and down states. Possible functional consequences of regular spike patterns were investigated by modeling the synaptic conductance in neurons of the deep cerebellar nuclei (DCN). Simulations showed that these regular patterns caused epochs of relatively constant synaptic conductance in DCN neurons.

Our findings indicate that the apparent irregularity in cerebellar PC simple spike trains *in vivo* is most likely caused by mixing of different regular spike patterns, separated by single long intervals, over time. We propose that PCs may signal information, at least in part, in regular spike patterns to downstream DCN neurons.

Introduction

The cerebellum is crucial for the precise temporal control of motor related tasks [1] and conditioned behaviors [2]. Yet, it is not clear how the cerebellum may signal precise timing at the cellular level. Prior studies of spike time coding in the cerebellum have focused on the discharge of Purkinje cells (PCs), which form the sole output of cerebellar cortex. However, thus far these studies only considered mean firing rates of the simple spikes (SS) [3], [4] or complex spikes (CS) [5], [6]. Little attention has been paid to their fine-temporal structure, even though spike timing may encode additional information in other systems [7]–[12]. In fact, for two different strains of ataxic mice with mutations of voltage-gated calcium channels expressed in PCs it was recently reported that PCs show increased irregularity of firing [13], [14]. A common measure to characterize the temporal structure of spike trains is the coefficient of variation (CV) of the interspike intervals (ISIs). The CV of SS firing of PCs recorded *in vivo* is reported to be quite high [15], [16]: close to or even higher than 1, the CV of a Poisson process. Conversely, PCs in the *in vitro* slice preparation fire very regularly [17], [18]. To test whether this difference in firing properties is as large as is commonly assumed and to investigate its possible functional importance, we analyzed the fine-temporal structure of SS trains in different preparations and behavioral states in more detail, focusing on the short-term variability.

Experimental Procedures

Electrophysiological recordings in vivo

Rats. Sprague-Dawley rats (n=26, 300–500 g, Iffa Credo, Brussels, Belgium) were

anesthetized with a mixture of ketamine HCl (75 mg/kg; Ketalar, Parke-Davis, Warner Lambert Manufacturing, Dublin, Ireland) and xylazine HCl (3.9 mg/kg; Rompun, Bayer, Leverkusen, Germany) in normal saline (0.9% NaCl, Baxter, Lessine, Belgium) by intraperitoneal injection. A craniotomy exposing Crus I and II of the left cerebellar hemisphere was performed [16]. Supplemental doses (one-third initial dose) were given intramuscularly to maintain deep anesthesia as evidenced by the lack of a pinch withdrawal reflex and/or lack of whisking. Forty eight single unit recordings were made in the cerebellar cortex with tungsten microelectrodes (impedance ~ 10 MOhm, FHC, Bowdoinham, ME). Signals were filtered and amplified (bandpass=0.5–9 kHz; gain=5,000–10,000) using a multichannel neuronal acquisition processor (Plexon Inc., Austin, TX) and collected spike trains were analyzed off-line using NEX (Plexon Inc.). After recordings of spontaneous activity, 12 stimulus-evoked responses were recorded in 10 rats. Perioral receptive fields were explored as reported elsewhere [16]. The punctate stimulus was applied at a rate of 0.5 Hz. In a separate series of experiments reported in more detail in [19], 8 transverse pairs of nearby PCs were recorded using similar procedures. Electric lesions were made after recordings to measure the distance between pairs and the distance between the centers of lesions was measured. In the context of this paper, the data from all these experiments were re-analyzed. All experimental methods were approved by the University of Antwerp and conformed to European Union guidelines. Mice. Extracellular activity was recorded in the cerebellar flocculus and paramedian lobule using glass micropipettes filled with 2 M NaCl (tip diameter: 2–5 mm; impedance: 2.5 M Ω at 1 kHz) in either restrained awake or anesthetized (with mixture of ketamine (50 mg/kg) and xylazine (10 mg/kg)) C57BL/6 mice. The electrode tip was positioned on the cerebellar surface under visual guidance (Olympus VS-IV; Olympus Optical, Tokyo, Japan) using a micromanipulator (David Kopf Instruments, Tujunga, CA) and moved downward by a hydraulic microdrive (Trent Wells) equipped with a stepping motor (TL Elektronik SMS 87). The electrode signal was amplified and filtered (bandwidth 10–6000 Hz; Dagan 2400; Dagan, Minneapolis, MN) and sampled at 12.5 kHz (CED 1401plus, Spike2, Cambridge, UK). Single-unit PCs were identified on-line by the presence of a brief pause in simple spikes after the complex spike. In the off-line analysis, SSs and CSs were detected and discriminated using custom-made software implemented in Matlab (Mathworks, Natick, MA). All experimental methods were approved by Erasmus MC in Rotterdam, and conformed to European Union guidelines.

Spike timing analysis

Data analysis of extracellular recordings. Recordings were 83 to 1202 sec long and comprised 1,328 to 62,371 spikes. Analysis was carried out using Matlab and Excel (Microsoft). Short-term regularity was measured with $CV_2 = 2|ISI_{n+1} - ISI_n| / (ISI_{n+1} + ISI_n)$ [20]. The number of regular patterns was measured using a threshold value for CV_2 ranging from 0 to 2 with an increment of 0.02. In each PC the numbers were normalized by the maximum number of patterns to avoid an influence of the difference between firing rates. The strength of synchronization of regular patterns was measured using a standard score, the Z score of the amplitude of the central peak of the cross-correlogram [21]: $Z = (N_c - N_e) / (SD_e)$, with N_c the number of spikes in the central peak (bin=5 ms), N_e the mean number of spikes in a 2 sec window between –1 and 1 sec, and SD_e its standard deviation. To determine whether the observed synchronization (Z score of 3 or higher) reflected spike to spike precise synchronization or rather co-modulation of firing rates

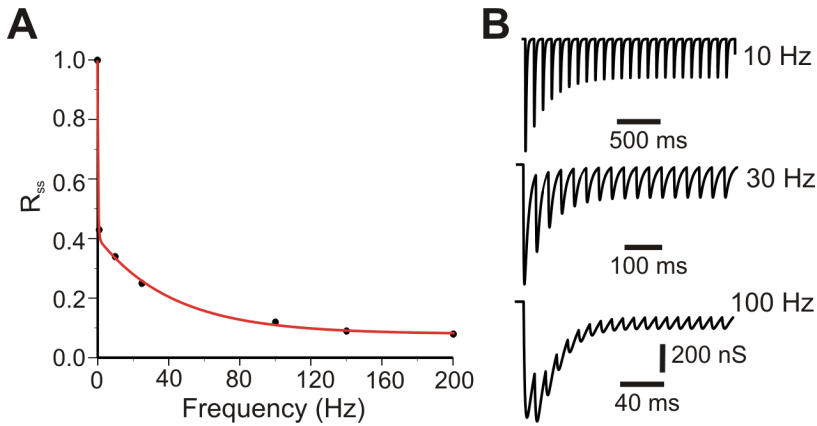


Figure 1. Simulation of PC to DCN synaptic conductance.

(A) Saturating level of release probability (R_{ss}) taken from Pedroarena and Schwarz (2003) could be modeled with a double exponential function (red line, see Materials and Methods for details). (B) Simulated synaptic conductance profiles in response to 10, 30 and 100 Hz PC firing, respectively. These results should be compared to Figure 7A of Pedroarena and Schwarz (2003).

[22], [23], simulated spike trains were generated by randomly shuffling the ISIs within blocks of 5 consecutive ISIs and the correlation analysis repeated for the shuffled spike trains. The correlation between CSs and patterns were analyzed in 32 PCs where CSs were well isolated. If the duration from the ends of patterns to CSs was longer than 1.2 times the pattern mean ISI, it was considered longer than the pattern mean ISI.

Data analysis of whole-cell clamp recordings

Three membrane potential traces recorded from 3 different anesthetized rats were analyzed to investigate the relation between spike patterns and the membrane potential [24]. The sampling frequencies of the original recordings (50, 50, and 20 kHz) were sampled down to 10 kHz without losing discriminative power. Spikes were sorted by setting thresholds at -38 mV, -42 mV, and -32 mV in cell1, cell2 and cell3 respectively. Spikes were further sorted as either CS or SS by checking the mean membrane potential between 2 and 4 ms after a spike. If the mean membrane potential was higher than -38 mV, -38 mV, and -40 mV in cell 1, 2, and 3 respectively, the spike was sorted as a CS. Mean firing rate of SS (CS) was 12.8 ± 5.2 Hz (1.1 ± 0.4 Hz). The threshold to distinguish UP from DOWN states was set to -55 mV. Regular patterns and single intervals were isolated as in the extracellular recordings. Data are represented as mean \pm SEM, unless otherwise stated. All p-values refer to Student's paired or unpaired t-test, unless otherwise specified.

Stochastic Modeling of Poisson processes

Both spontaneous and evoked spike trains were modeled using an inhomogeneous Poisson process (see also [25]) with 2 ms of dead time (which is equal to the detection window used in the electrophysiological recordings). The probability density of the process can be described as:

$$Pn(t) = r_n e^{-rnt} \Theta(t - 2)$$

where t denotes the time elapsed since the last spike, r_n is the mean firing rate at the

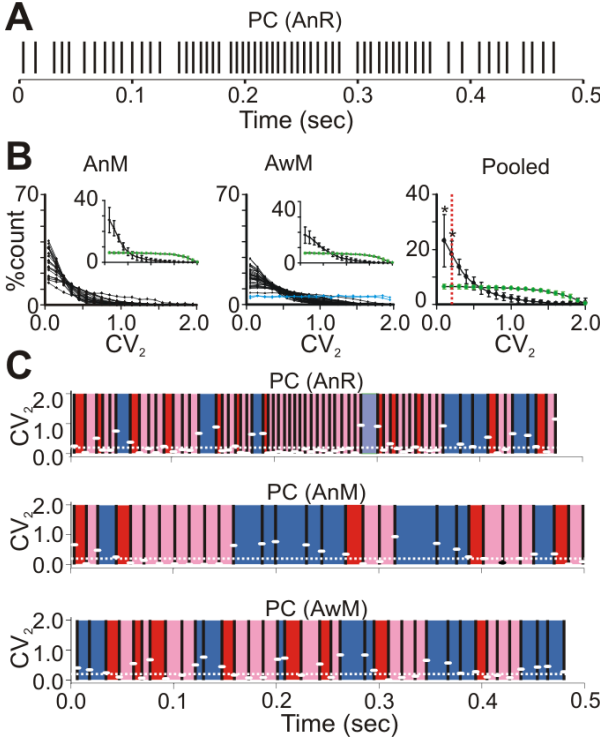


Figure 2. Regular patterns in cerebellar Purkinje cell simple spike trains.

(A) Raster plot of PC SS in an anesthetized rat (AnR). (B) CV₂ distributions of SS trains recorded from anesthetized mice (AnM, left), awake mice (AwM, middle), blue: neurons in cerebral motor cortex, and mean of 92 CV₂ distributions (Pooled, right) which were significantly different from those of inhomogeneous Poisson processes with similarly modulated firing rates ($p < 0.05$, χ^2 test; *: $p < 0.001$, χ^2 goodness of fit residual test; red line: CV₂ = 0.2). Insets and right panel: mean \pm s.e.m. (black: PC, grey: inhomogeneous Poisson process) (C) Extracting regular spiking patterns by setting CV₂ threshold at 0.2 (white dotted lines). White dashes: CV₂ values calculated from the two surrounding ISIs, medium grey: first ISI of regular patterns, light grey: successive ISIs in regular patterns, dark grey: ISIs not belonging to a regular pattern). (For color figure, see online version)

n-th ISI, estimated by

$$m = \frac{5}{\sum_{i=n-2}^{n+2} ISI_i}$$

where $n=3, 4, \dots$, number of spikes-2, $\Theta(t-2)$ is Heaviside function standing for 1 only when t is 2 ms or larger. The mean firing rates of realized spike trains (51.7 ± 2.4 Hz, $N=92$) were statistically similar to those of recorded SS trains (51.7 ± 2.4 Hz, $N=92$, $p > 0.6$). For evoked spike trains, firing rate was estimated from the rate distribution around stimulation time (bin size: 1 ms, lag=1 s). Based on these estimates, model spike times were created trial by trial. Then, a final spike train was constructed by concatenating spike times in consecutive trials. Simulations were performed using Matlab.

Synaptic Conductance Modeling

The dynamics of multiple pulse depression of the synapse between PCs and DCN neurons were described previously [26], [27]. The data reported in these papers are quantitatively different, even though they report the same phenomena, probably due to different experimental conditions (e.g. recording temperature). Our phenomenological model is based on the Pedroarena and Schwarz study [26], because it measured multiple pulse depression at more frequencies over a large range (from 1 to 200 Hz). The depression is assumed to be caused by changes of the presynaptic release probability (R). We fitted a deterministic model for R to the multiple pulse depression data. This deterministic approach is justified because the large number of release sites from which transmitter

	Number of PCs	Mean firing rate	%Long ISI (ISI>1 s)	CV	Mean CV ₂	Maximum pattern size
Anesthetized rats	48	45.5±4.1	0.41±0.11	3.93±0.49	0.51±0.03	28.9±4.4
Awake mice	37	51.0±2.7 (p>0.2)	0.01±0.00 (p<0.001)	1.39±0.38 (p<10 ⁻⁴)	0.39±0.02 (p<0.001)	13.0±0.6 (p<0.001)
Anesthetized mice	21	49.8±3.6 (p>0.4, p ⁺ >0.7)	0.02±0.01 (p<0.001, p ⁺ >0.1)	1.74±0.47 (p<0.05, p ⁺ >0.4)	0.30±0.02 (p<10 ⁻⁶ , p ⁺ <0.05)	24.9±2.8 (p>0.4, p ⁺ <0.001)

Table 1. Summary of spontaneous simple spike firing properties of all PCs reported in this study.

can reach all receptors [28] makes synaptic failures unlikely. We fitted equations for the steady state level of release probability R_{ss} and the time constant of depression τ to the data:

$$R_{ss}(r) = 0.08 + 0.60 e^{-2.84r} + 0.32 e^{-0.02r}$$

$$\tau(r) = 2 + 2500 e^{-0.274r} + 100 e^{-0.022r}$$

where r is the instantaneous firing rate computed as the inverse of the last interspike interval. R_{ss} and τ are updated at the time of occurrence of each spike n and R_n is then computed as:

$$R_n = R_{n-1} + (R_{ss} - R_{n-1})(1 - e^{-ISI_n/\tau})$$

with R_{n-1} is the release probability computed at the previous spike time, ISI_n is the interspike interval between the current spike and the previous spike. See Figure 1 for the accuracy of the fit of our model to the experimental data.

Synaptic conductance (G_{syn}) during spiking was modeled by a double exponential function multiplied by R_n and calculated over 200 ms with a resolution of 0.1 ms following each spike:

$$G_{syn}(t) = G_{pre} + A(G_{max}/(\tau_1 - \tau_2)) R_n (e^{-t/\tau_1} - e^{-t/\tau_2})$$

Here, G_{pre} is the synaptic conductance caused by previous spikes, $A=15.5$ is a constant to scale the maximum conductance to the experimental value of G_{max} (11.7 nS), τ_1 is 12 ms, and τ_2 is 1.2 ms. G_{max} , τ_1 , and τ_2 , were chosen to fit the multiple pulse depression traces shown in Figure 7 of Pedroarena et al [26]. The multiple pulse depression following 10, 30 and 100 Hz stimulation of the PC is shown in Figure 1.

Results

Simple spike trains contain precise regular spiking patterns

We analyzed spontaneous PC activity in 3 data sets: recordings from the cerebellar hemisphere of anesthetized rats (AnR, n=48) and from the flocculus or paramedian lobule of anesthetized (AnM, n=21) and awake (AwM, n=37) mice. Firing rates were similar for all data sets (Table 1). As expected, CVs of the spike trains were high: 3.93±0.49 (AnR), 1.74±0.47 (AnM) and 1.39±0.38 (AwM), consistent with previous reports [6], [16] and suggestive of highly irregular firing *in vivo*. Nevertheless, careful visual inspection of the individual spike trains revealed clear patterns of regular firing (Figure 2A).

To characterize these patterns we used a short range measure which compares two adjacent ISIs, i.e. the CV₂ (cf. Materials and Methods; [20]). Surprisingly, we found that in all data sets the mean CV₂ was low (AnR: 0.51±0.03, AnM: 0.30±0.02, AwM: 0.39±0.02), suggestive of much more regular firing at short time scales. In fact, most PCs showed a

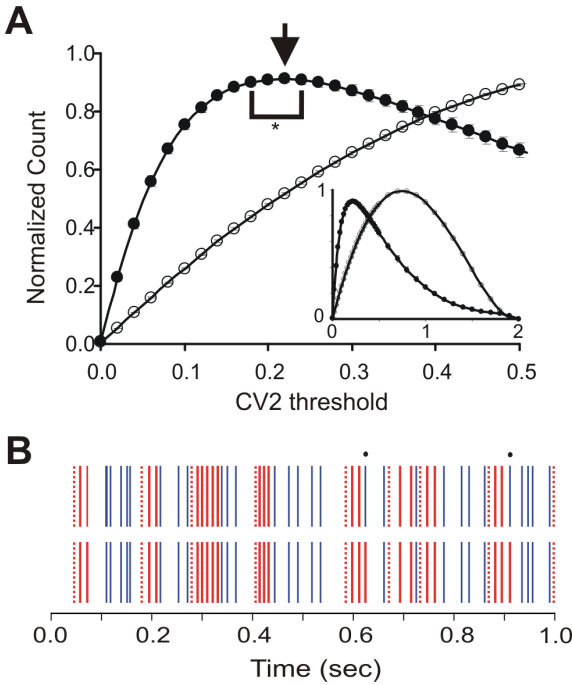


Figure 3. Effect of CV_2 threshold on patterns.

(A) Mean (\pm SEM) of normalized number of patterns in spike trains classified with different values of the CV_2 threshold, ranging from 0 to 0.5, in 92 PCs (filled circles) and in simulated spike trains from Poisson processes with similar firing rate profiles as in the PCs (open circles). Arrow: maximum number of patterns, *: range where there was no statistical difference ($p > 0.05$). Inset: same distribution but for all possible thresholds. (B) Raster plots with indication of the spike timings belonging to patterns (dotted lines: start of patterns, grey solid lines: following spikes in each pattern) and singles (black). Black dots: difference in classified patterns when threshold was 0.2 (upper trace) and 0.24 (lower trace). (For color figure, see online version)

skewed CV_2 distribution, with a high proportion of low CV_2 values (Figure 2B), indicating the presence of regularity in spiking patterns. This was in clear contrast to spontaneous spiking of neocortical neurons, which showed uniform CV_2 distributions as previously reported [20] (Figure 2B, blue) and which are similar to realizations of inhomogeneous Poisson processes (insets in Figure 2B, green).

We studied the properties of regular spiking patterns in PCs whose CV_2 distribution was significantly different from rate modulated Poisson (AnR: $n=38$, AnM: $n=21$, AwM: $n=33$, $p < 0.05$, χ^2 test) in more detail. Their pooled CV_2 distribution showed significantly more CV_2 values of 0.2 or lower ($p < 0.001$, χ^2 goodness of fit residual test) than the corresponding Poisson processes did (Figure 2B, rightmost panel). To isolate the regular spiking patterns in individual spike trains, we applied a threshold of 0.2 on the measured CV_2 values as illustrated in Figure 2C. Whenever the CV_2 value was below or equal to threshold (white dotted line), the associated two ISIs were considered part of a regular pattern (pink). If the next ISI also had a CV_2 value below or equal to threshold, it was included into the pattern (pink); if not, this next ISI was either single (i.e. not belonging to a pattern; blue) or the start of a new pattern (provided the next CV_2 value was again below or equal to threshold; red).

With this procedure, 57% (AnR), 67% (AnM) and 54% (AwM) of ISIs belonged to regular patterns. To verify the effect of the statistically defined CV_2 threshold of 0.2, we compared the number of patterns extracted using different thresholds (Figure 3). Thresholds in the range 0.18–0.24 generated statistically similar number of patterns as a threshold of 0.22, which generated the maximum number of patterns ($n=92$, $p > 0.1$).

The mean ISIs of patterns were not uniformly distributed. Most of the pattern ISIs were relatively short, so that the peaks of the overall ISI distributions mostly consisted

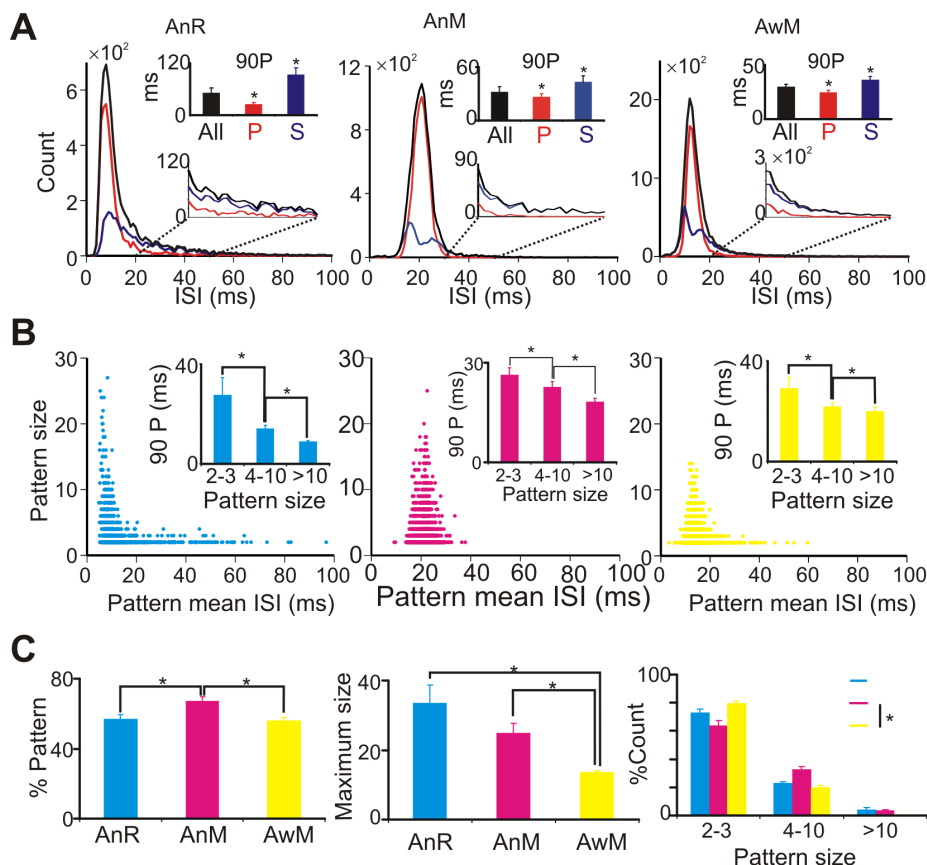


Figure 4. Characteristics of regular spike patterns.

(A) ISI distribution of overall ISIs (black), patterns (red) and singles (blue) from a representative sample PC spike train of AnR (left), AnM (middle) and AwM (right). Insets: magnified plot of indicated area (lower) and 90 P (90 percentile, upper) of each population, *: $p < 0.01$, Student t test. (B) The relation between pattern mean ISI and pattern size in AnR (left, cyan), AnM (middle, magenta) and AwM (right, yellow). Insets: maximum pattern mean ISI (90 percentile) of different pattern sizes. *: $p < 0.001$, Wilcoxon signed rank test. (C) Percentage ISIs belonging to patterns (upper, *: $p < 0.001$, Student t test), Average maximum pattern size (middle, *: $p < 0.001$, Student t test), and Pattern size distribution (lower, $p < 0.05$, χ^2 test). Cyan: AnR, magenta: AnM, yellow: AwM. (For color figure, see online version)

of regular patterns, while their tails comprised only single ISIs. As a result, the 90 percentile of ISI for patterns was significantly shorter than that of singles (Figure 4A).

Characteristics of regular spiking patterns change with behavioral state

Regular patterns can be characterized by two parameters: pattern size, defined as the number of ISIs in the pattern, and pattern mean ISI. Examples of the distribution of these two parameters are shown in Figure 4B. Observe that short patterns occurred with a wide range of mean ISIs, whereas long patterns contained only short ISIs (insets), though not the shortest. The wide range of pattern mean ISIs and the fact that the fraction of pattern spikes was only weakly (rats: linear correlation $R^2=0.371$ compared to a $R^2=0.666$ for 92 inhomogeneous Poisson processes) or not (mice: $R^2 < 0.1$) dependent on the mean firing rates of PCs make it unlikely that regular patterns were caused by refractoriness.

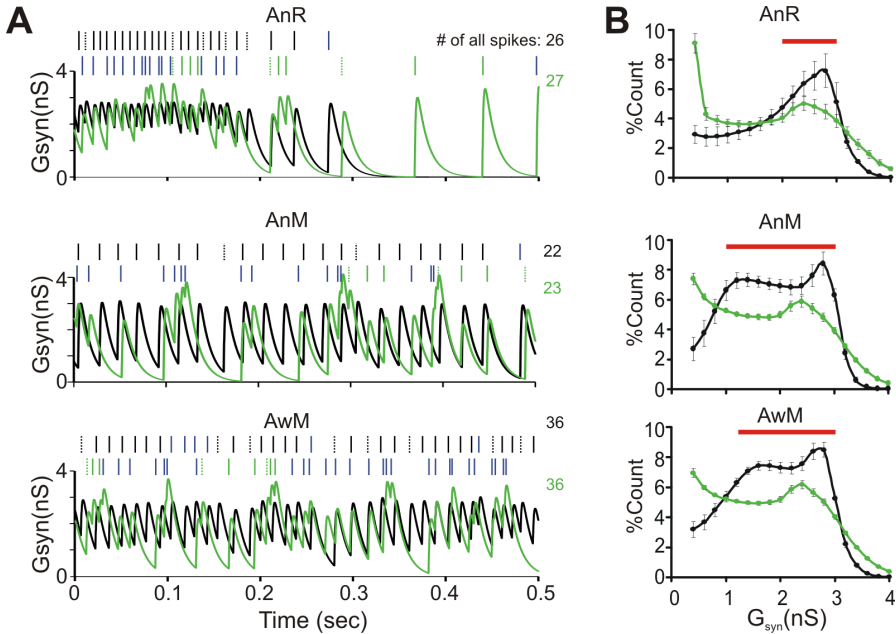


Figure 5. Simulated synaptic conductance in PC to DCN synapse caused by spontaneous PC spiking.

(A) A representative example of the simulated synaptic conductance (G_{syn}) induced by PC (black) of AnR (upper panel), AnM (middle panel) and AwM (lower panel), and by corresponding realizations of an inhomogeneous Poisson process (grey). Rasters: spikes belonging to patterns (black and grey dotted lines: start of patterns, black and grey solid lines: following spikes in patterns, darker grey lines: singles), numbers: number of all spikes in the 500 ms window. (B) Distribution of G_{syn} values for PCs (black) compared to Poisson processes (grey). Bin = 0.2 nS. Red bar: bins where PCs contained significantly more G_{syn} values. $p < 0.05$. (For color figure, see online version)

Pattern sizes showed a wide distribution. On average, 72% of patterns comprised only 2–3 ISIs, but many patterns were much longer (Figure 4B and 4C), lasting 45.0 ± 3.5 , 76.5 ± 6.3 , and 52.5 ± 3.1 ms for AnR, AnM, and AwM, respectively. The size of patterns depended on the CV_2 threshold used, but this did not affect the pattern mean ISI much (data not shown). Interestingly, we found a significant difference in the proportion of long patterns between anesthetized and awake rodents. In anesthetized rodents, $4.1 \pm 1.4\%$ (AnR) and $3.5 \pm 0.8\%$ (AnM) of patterns contained more than 10 ISIs, while in awake rodents (AwM) only $0.4 \pm 0.1\%$ did ($p < 0.01$), with maximum pattern sizes of 182, 61 and 21 ISIs, respectively (Figure 4C). This significant difference between pattern sizes of awake vs. anesthetized rodents indicates that regular patterns may be influenced by the behavioral state of the animal. Indeed, if regular spiking patterns were a specific signal by which PCs transmit information, one would predict faster changes in this signal, i.e. shorter patterns associated with a wider range of pattern mean ISIs, in awake, active animals than in anesthetized ones.

Simulation of the effects of regular spiking patterns on target neurons

PCs inhibit neurons in the downstream DCN; any information transmitted by regular PC spike patterns will be decoded at that level. PC synapses onto DCN neurons show fast synaptic depression [26], [27], a property that is known to endow synapses with low-pass filtering properties [29]. We developed a phenomenological model to reproduce

the previously reported frequency-dependent depression of this synapse [26] (cf. Materials and Methods), allowing us to predict the effects of regular PC spike patterns on synaptic conductance (G_{syn}) in DCN neurons. Specifically, we used this model to compare the G_{syn} evoked by recorded SS trains with that of simulated spike trains generated by inhomogeneous Poisson processes of the same modulated firing rates. Such Poisson processes have far fewer regular patterns: only 20% of ISIs belonged to patterns, 80% of which were of size 2 (cf. Fig. 2B). A representative example of conductance traces (Figure 5A) demonstrates that the long regular patterns in SS trains induced epochs with little fluctuation of G_{syn} , while Poisson spike trains generated much more variable G_{syn} (Figure 5A, green). In almost all cases, the distribution of G_{syn} of Poisson spike trains was significantly different from that of real SS trains (Figure 5B; Kolmogorov-Smirnov test, $p < 0.05$, bin 0.01 s, AnR 35/38 cells; AnM 33/33; AwM 20/21). Thus, the distribution of G_{syn} of PCs was mostly confined to a narrow range of values as is also evident from its CV, which was significantly lower for PCs (0.53 ± 0.03 , 0.47 ± 0.03 and 0.49 ± 0.03 for AnR, AnM and AwM, respectively) than for simulated spike trains from Poisson processes (0.66 ± 0.05 , 0.75 ± 0.04 , and 0.71 ± 0.03 , $p < 0.04$).

Spikes of regular patterns are correlated, but not precisely synchronized

In rats, each DCN neuron receives inhibition from 100 [30] up to 1000 [31] PCs. Anatomically, though, it is not clear whether all converging inputs are active at the same time. This convergence raises the question whether regular patterns in the afferent PCs coincide in time, causing periodic ripples in G_{syn} during their occurrence, or whether they are asynchronous, rendering G_{syn} more constant. We studied the correlation in time of regular patterns in 8 simultaneously recorded transverse pairs of PCs in AnR, separated by $69.8 \pm 9.4 \mu\text{m}$ (range: 50–100 μm). We found that the spikes belonging to patterns revealed central peaks in the cross-correlogram. These central peaks reflected

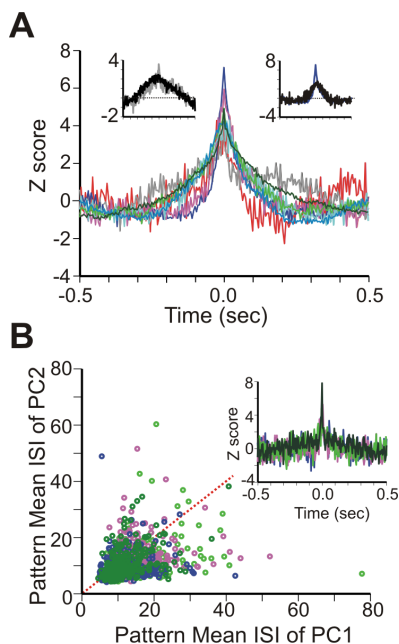


Figure 6. Coincident patterns in nearby PC pairs in AnR.

(A) Eight cross-correlograms of timings of spikes belonging to regular patterns extracted from recordings of nearby PC pairs, with each pair colored differently. Insets: cross-correlograms of the shuffled spike trains of two pairs (black) superimposed on original cross-correlogram of patterns (blue and gray: pairs showing strongest and weakest synchronization respectively). (B) The relation of pattern mean ISIs in 4 pairs in which pattern starts coincided significantly (inset: cross-correlograms of the first spikes of regular patterns in the 4 pairs). Red dotted line: diagonal. (For color figure, see online version)

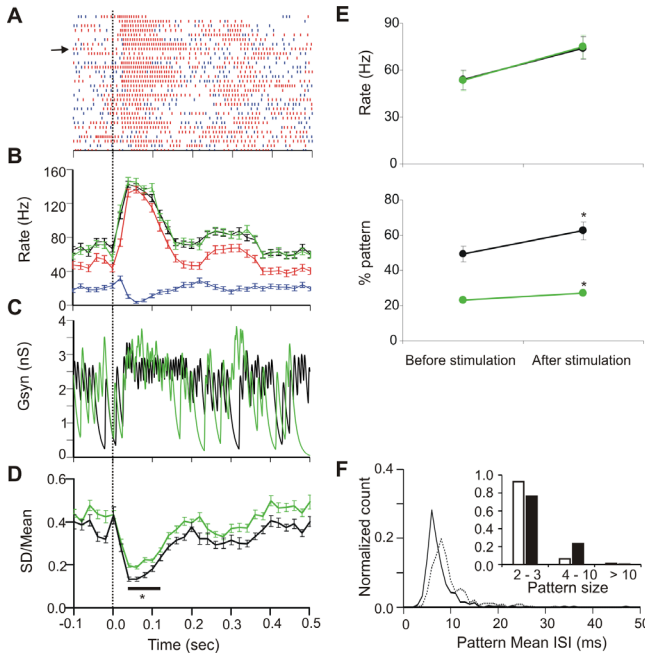


Figure 7. A representative example of regular patterns in tactile stimulus evoked PC SS responses.

(A) Peri-event raster plot of patterns (red) and singles (blue) during tactile stimulation in AnR. (B) Mean rate (\pm SEM) of overall spikes (black), realization of Poisson process (green), pattern spikes (red) and singles (blue). Bin = 20 ms. (C) Simulated G_{syn} for the trial indicated by arrow in (A) (bin = 1 ms). (D) CV (SD/Mean) of simulated G_{syn} (*: $p < 0.001$, Student t test, bin 20 ms). Black dotted line: stimulation time. (E) Mean firing rate (upper panel) and percent ISIs belonging to regular patterns (lower panel) in 200 ms before and after stimulation (upper panel) of simulated spike trains from inhomogeneous Poisson process (green) and from recorded PCs (black). *: $p < 0.005$, Wilcoxon signed ranks test. (F) Pattern mean ISI distribution before (dotted line) and after (solid line) tactile stimulation. Inset: Pattern size distribution before (open) and after (filled) stimulation. (For color figure, see online version)

significant synchronization as their Z scores were higher than 3 (Figure 6A, $z = 5.0 \pm 0.4$), but they were quite broad (full width at half peak (HW) = 70 ± 8.6 ms). No synchronization was observed in pairs of PCs on the same parallel fiber beam separated by more than 0.5 mm ($n = 20$, data not shown). We investigated several mechanisms that could explain the broad width of the central peaks. There was no significant relation between HW and the mean duration of patterns ($R^2 < 0.0001$). Broad peaks in cross-correlograms are often caused by firing rate co-modulation [23], implying that patterns would coincide because they occur more often during increased firing rates (Figure 4A). As properly shuffled spike trains (cf. Materials and Methods) overlapped the broad peaks largely (Figure 6A, inset), the central peaks observed can indeed be largely explained by firing rate co-modulation. In addition, we found in four of the pairs a significant, and much more precise, correlation of the start of patterns ($z = 5.6 \pm 0.9$, HW = 16.3 ± 2.4 ms, Figure 6B, inset). But although patterns in these four pairs started together, their mean ISIs were independent of each other ($R^2 = 0.17 \pm 0.03$, Figure 6B). We conclude that while for a fraction of patterns the start was precisely synchronized, overall pattern spikes were not precisely synchronized but tended to co-occur in a loose manner because of firing rate co-modulation.

Despite our lack of knowledge about detailed convergence patterns of PCs onto DCN neurons, convergence is more likely for adjacent pairs, where we observed coincident patterns, than for distant pairs which did not show synchronization. In the case of coincident converging patterns, the lack of spike synchronization caused by their different spike frequencies will further reduce the variability of their combined G_{syn} [32]. Otherwise, the averaged G_{syn} of perfectly synchronized PCs would have the same variability as that caused by single PCs. A similar reduction of variability also occurs in completely irregular spike trains generated by Poisson processes [32], but only when

there are many more active convergent inputs.

Tactile stimulation increases regularity of spiking

Next, the effect of sensory stimulation on regular patterns in the SS response was investigated. To this end, we analyzed responses to tactile stimulation in AnR (Figure 7) ($n=12$). Typically, PCs responded after a short delay with a significant increase in SS firing rate in a 200 ms window, from 53.8 ± 6.2 Hz to 74.2 ± 7.3 Hz ($p < 0.003$, Wilcoxon signed ranks test), as reported elsewhere [33]. In the same window, we also found a significantly increased proportion of ISIs belonging to regular patterns, from $49.3 \pm 4.5\%$ to $62.5 \pm 5.1\%$ ($p < 0.005$, Wilcoxon signed ranks test). Spike trains always become more regular at high firing rates because spikes cannot fire arbitrarily close together, due to the refractory period. Indeed, simulated Poisson processes with refractory period that show similar rate changes ($p > 0.2$; before: 53.3 ± 6.3 Hz, after: 75.0 ± 7.5

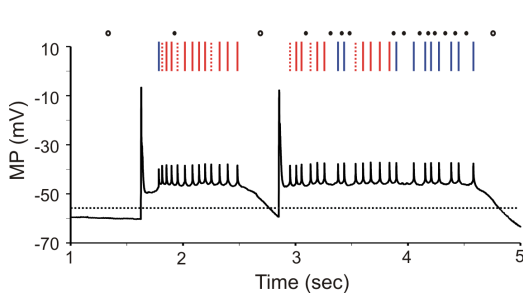


Figure 8. Regular patterns and singles related to the membrane potential (MP).

Dendritic patch-clamp recording of PC in anesthetized rat (data from Loewenstein et al. 2005). Voltage trace: large spikes are complex spikes, small ones are simple spikes. Dotted black line: threshold to define up and down-states (MP = -55 mV). Raster plot at top: simple spikes were sorted as either pattern spikes (dotted red lines: start of patterns, solid red lines: following spikes in each pattern) or single spikes (blue lines). All patterns were during up-state, but singles occurred both during up (filled circles) and down (open circles) states.

Hz; Figure 7E upper panel) as the experimental data revealed a slight but statistically significant increase of the fraction of ISIs belonging to regular patterns ($p < 0.005$; before: $23.1 \pm 0.7\%$, after: $27.1 \pm 0.8\%$; Figure 7E lower panel). However, this increase was proportionally ($18 \pm 2\%$) much smaller than the increase in PCs ($29 \pm 3\%$) ($p < 0.03$, Wilcoxon signed ranks test). We conclude that the increase in patterns in PCs was larger than expected from only the firing rate increase. Regular patterns following stimulation were also faster and lasted longer than before stimulation (Figure 7F).

To estimate the effect of this change of SS patterns on downstream DCN neurons, we again computed the predicted G_{syn} and compared these with the results obtained from spike trains realized from inhomogeneous Poisson processes (Figure 7C). The real SS train induced a steady current of about 4.5 nS, while the Poisson process produced a highly variable G_{syn} , despite the similar modulations of firing rates. The CV of G_{syn} induced by the real SS train dropped significantly ($p < 0.001$) during a period of 116.7 ± 19.0 ms after stimulus onset compared to the effect of Poisson spike trains (Figure 7D). This indicates that tactile stimulation further reduced the variability of G_{syn} in DCN neurons by an increased regularity of PC spike timing.

Regular patterns and singles in relation to the PC membrane potential

It has been shown that the membrane potential of PCs in anesthetized animals can be

bistable, showing up and down-states [24]. Although PCs in awake behaving animals probably operate predominantly in the up-state [34] and regular patterns in our data tended to last much shorter than the reported duration of up-states in the anesthetized preparation [24], the occurrence of patterns might in principle be related to the state of the membrane potential. We therefore applied our analysis method to whole-cell clamp recordings from PCs of anesthetized rats *in vivo* (data obtained from Loewenstein et al., 2005; Figure 8). As expected, patterns occurred only during up-states (Figure 8, red spikes), but a single up-state typically consisted of several patterns (4.8 ± 1.1 for the recording shown in Figure 8, 3.8 ± 0.3 for all recordings). Singles could occur during both up ($92.1 \pm 3.7\%$; Figure 8, filled dots) or down ($7.9 \pm 3.7\%$, Figure 8, open dots) states. Thus, the classification of SSs developed in this study allows for a subcategorization of spikes occurring during the up-state which may be relevant at short time scales.

CSs may toggle transitions between up and down-states [24]. This is also the case for start of the two up-states shown in Figure 8. We found that, except for patterns occurring at state transitions, the start or end of patterns was not related to CS firing. This is confirmed by the much higher frequency of starts of patterns (7.42 ± 4.30 Hz, AnR, $n=32$) than of CSs (0.72 ± 0.05 Hz).

Discussion

Taken together, our main findings indicate that (1) interesting fine-temporal properties of neuronal responses may be uncovered by analyzing regular pattern structure on a single trial basis; (2) PC simple spike trains contain distinctly more spike timing regularities than hitherto known; (3) the high CV in *in vivo* recordings is most likely caused by mixing of different regular spiking patterns, separated by single, typically longer, ISIs; (4) the onset of patterns can be synchronized in nearby PCs, but their member spikes are not synchronized; (5) most regular patterns are not influenced by complex spikes; (6) regular pattern properties change with behavioral state and tactile stimulation; and (7) regular patterns may cause epochs of close to constant synaptic conductance in downstream DCN neurons.

Our extracellular recordings do not provide conclusive evidence on the mechanisms causing regular patterns. However, as PCs fire highly regularly in slice preparations in which their synaptic inputs are blocked [17], [18] and since they show increased irregularity following mutations of their voltage gated Ca^{2+} channels [13], the endogenous properties of PCs are likely to contribute to their regularity of firing. However, the current observation that most patterns occur within the up-state, combined with the finding that PCs in awake behaving animals probably operate predominantly in the up-state [34] suggests that additional mechanisms such as short-term and long-term synaptic processes probably also play a role in controlling the start and end of a regular pattern, as well as its mean ISI. As CSs have little effect on patterns, it is most likely that parallel fiber inputs combined with molecular layer inhibition control the pattern properties. Furthermore, synaptic plasticity can adapt the effect of both the excitatory parallel fiber inputs and the inhibitory input from the basket cells and stellate cells on the SS patterns [35], [36]. Such mechanisms could explain why the onset of patterns was synchronized in only a subset of nearby PCs, and why even in those cases the pattern mean ISIs were different.

The regular patterns discovered in this study comprised a large part of the simple

spike trains and were shown to be modulated by behavioral state and stimulation, suggesting that they may have functional significance. Our simulations of the effect of regular patterns on G_{syn} in downstream DCN neurons indicate that they keep inhibitory conductance fairly constant. The interaction between regular patterns and G_{syn} may provide an explanation of why these synapses depress so strongly [26], [27] and forms the basis for our hypothesis on the function of regular patterns. It is generally assumed that cerebellar learning through induction of long-term depression at the parallel fiber to PC synapse leads to disinhibition of DCN neurons [35], [37]. In addition, DCN neurons respond strongly to disinhibition because of their post-inhibitory rebound spike [38], which may form a powerful timing signal [2], [39]. Correspondingly, the activity of DCN neurons in adult rodents consists of pauses, most likely caused by PC inhibition, mixed with transient periods of fast bursting [40]. The effectiveness of disinhibition to create a rebound spike depends on the synchronicity of the disinhibition, which we recently demonstrated to be significant among nearby PCs [19], and on the level of preceding inhibition. Because the inactivation of calcium channels expressed in the DCN neurons is strongly voltage dependent in the relevant potential range [41], these channels are very sensitive to even small changes in inhibitory input. Consequently, the level of inhibition preceding the rebound spike exerts a very strong effect on the amplitude of the rebound spike [42].

We hypothesize that regular patterns encode a specific level of inhibition in their firing rate and, as such, approximate a perfect firing rate code [43], which should be completely regular. When regular patterns from convergent PCs coincide, the summed inhibition will be relatively constant over the duration of the patterns and, consequently, keep the level of inactivation of calcium channels steady. Thereby, the firing rates of regular spike patterns in afferent PCs will control the amplitude of any rebound spike that follows in the next second. The occurrence of a rebound spike is evoked by synchronized pauses in the SS trains [19], [44], which are mostly not part of the regular patterns as they belong to the tail of the ISI distribution.

In conclusion, we propose that the regular patterns, which comprise the majority of spikes in PC SS trains, can control the amplitude of subsequent timing signals by modulating the amplitude of rebound spikes in downstream DCN neurons.

Acknowledgments

We thank Drs. Dana Cohen and Miguel Nicolelis for making the mice cortical recordings available and Drs Séverine Mahon and Mike Häusser for sharing the PC whole-cell clamp recordings. We thank Drs. Dieter Jaeger, Reinoud Maex, Martin Nawrot, Arnd Roth, Stefan Rotter and Cornelius Schwarz for comments on an earlier version of the manuscript.

Reference List

1. Ivry RB, Spencer RM (2004) The neural representation of time. *Curr Opin Neurobiol* 14: 225–232.
2. Koekkoek SK, Hulscher HC, Dortland BR, Hensbroek RA, Elgersma Y, et al. (2003) Cerebellar LTD and learning-dependent timing of conditioned eyelid responses. *Science* 301: 1736–1739.

3. Shidara M, Kawano K, Gomi H, Kawato M (1993) Inverse-dynamics model eye movement control by Purkinje cells in the cerebellum. *Nature* 365: 50–52.
4. Coltz JD, Johnson MT, Ebner TJ (1999) Cerebellar Purkinje cell simple spike discharge encodes movement velocity in primates during visuomotor arm tracking. *J Neurosci* 19: 1782–1803.
5. Kitazawa S, Kimura T, Yin PB (1998) Cerebellar complex spikes encode both destinations and errors in arm movements. *Nature* 392: 494–497.
6. Goossens HH, H FE, Van Alphen AM, Van Der Steen J, Stahl JS, et al. (2004) Simple spike and complex spike activity of floccular Purkinje cells during the optokinetic reflex in mice lacking cerebellar long-term depression. *Eur J Neurosci* 19: 687–697.
7. Rieke F, Warland D, de Ruyter van Steveninck RR, Bialek W (1997) *Spikes. Exploring the neural code.* Cambridge, MA: The MIT Press.
8. VanRullen R, Guyonneau R, Thorpe SJ (2005) Spike times make sense. *Trends Neurosci* 28: 1–4.
9. Vaadia E, Haalman I, Abeles M, Bergman H, Prut Y, et al. (1995) Dynamics of neuronal interactions in monkey cortex in relation to behavioural events. *Nature* 373: 515–518.
10. Riehle A, Grun S, Diesmann M, Aertsen A (1997) Spike synchronization and rate modulation differentially involved in motor cortical function. *Science* 278: 1950–1953.
11. Konishi M (2003) Coding of auditory space. *Annu Rev Neurosci* 26: 31–55.
12. Heil P (2004) First-spike latency of auditory neurons revisited. *Curr Opin Neurobiol* 14: 461–467.
13. Hoebeek FE, Stahl JS, van Alphen AM, Schonewille M, Luo C, et al. (2005) Increased noise level of Purkinje cell activities minimizes impact of their modulation during sensorimotor control. *Neuron* 45: 953–965.
14. Walter JT, Alvina K, Womack MD, Chevez C, Khodakhah K (2006) Decreases in the precision of Purkinje cell pacemaking cause cerebellar dysfunction and ataxia. *Nat Neurosci* 9: 389–397.
15. Goossens J, Daniel H, Rancillac A, van der Steen J, Oberdick J, et al. (2001) Expression of protein kinase C inhibitor blocks cerebellar long-term depression without affecting Purkinje cell excitability in alert mice. *J NeuroSci* 21: 5813.
16. Vos BP, Volny-Luraghi A, De Schutter E (1999) Cerebellar Golgi cells in the rat: receptive fields and timing of responses to facial stimulation. *Eur J Neurosci* 11: 2621–2634.
17. Hausser M, Clark BA (1997) Tonic synaptic inhibition modulates neuronal output pattern and spatiotemporal synaptic integration. *Neuron* 19: 665–678.
18. Raman IM, Bean BP (1999) Ionic currents underlying spontaneous action potentials in isolated cerebellar Purkinje neurons. *J Neurosci* 19: 1663–1674.
19. Shin SL, De Schutter E (2006) Dynamic synchronization of Purkinje cell simple spikes. *J Neurophysiol* 96: 3485–3491.
20. Holt GR, Softky WR, Koch C, Douglas RJ (1996) Comparison of discharge variability in vitro and in vivo in cat visual cortex neurons. *J Neurophysiol* 75: 1806–1814.
21. Vos BP, Maex R, Volny-Luraghi A, De Schutter E (1999) Parallel fibers synchronize spontaneous activity in cerebellar Golgi cells. *J NeuroSci* 19: RC6.
22. Eggermont JJ, Smith GM (1995) Rate covariance dominates spontaneous cortical

- unit-pair correlograms. *Neuroreport* 6: 2125–2128.
23. Maex R, Vos BP, De Schutter E (2000) Weak common parallel fibre synapses explain the loose synchrony observed between rat cerebellar golgi cells. *J Physiol* 523: (Pt 1)175–192.
 24. Loewenstein Y, Mahon S, Chadderton P, Kitamura K, Sompolinsky H, et al. (2005) Bistability of cerebellar Purkinje cells modulated by sensory stimulation. *Nat Neurosci* 8: 202–211.
 25. Shin SL, Rotter S, Aertsen A, De Schutter E (2007) Stochastic description of complex and simple spike firing in cerebellar Purkinje cells. *Eur J Neurosci* 25: 785–794.
 26. Pedroarena CM, Schwarz C (2003) Efficacy and short-term plasticity at GABAergic synapses between Purkinje and cerebellar nuclei neurons. *J Neurophysiol* 89: 704–715.
 27. Telgkamp P, Raman IM (2002) Depression of inhibitory synaptic transmission between Purkinje cells and neurons of the cerebellar nuclei. *J Neurosci* 22: 8447–8457.
 28. Telgkamp P, Padgett DE, Ledoux VA, Woolley CS, Raman IM (2004) Maintenance of high-frequency transmission at purkinje to cerebellar nuclear synapses by spillover from boutons with multiple release sites. *Neuron* 41: 113–126.
 29. Abbott LF, Regehr WG (2004) Synaptic computation. *Nature* 431: 796–803.
 30. De Zeeuw CI, Wylie DR, DiGiorgi PL, Simpson JI (1994) Projections of individual Purkinje cells of identified zones in the flocculus to the vestibular and cerebellar nuclei in the rabbit. *J Comp Neurol* 349: 428–447.
 31. Chan-Palay V (1977) *Cerebellar Dentate Nucleus*. New York: Springer-Verlag.
 32. Softky WR, Koch C (1993) The highly irregular firing of cortical cells is inconsistent with temporal integration of random EPSPs. *J Neurosci* 13: 334–350.
 33. Jaeger D, Bower JM (1994) Prolonged responses in rat cerebellar Purkinje cells following activation of the granule cell layer: an intracellular in vitro and in vivo investigation. *Exp Brain Res* 100: 200–214.
 34. Schonewille M, Khosrovani S, Hoebeek FE, De Jeu MTG, Larsen IM, et al. (2006) Purkinje cells in awake behaving animals operate at the upstate membrane potential. *Nat Neurosci* 9: 459–461.
 35. Ito M (2001) Cerebellar long-term depression: characterization, signal transduction, and functional roles. *Physiol Rev* 81: 1143–1195.
 36. Jorntell H, Ekerot CF (2003) Receptive field plasticity profoundly alters the cutaneous parallel fiber synaptic input to cerebellar interneurons in vivo. *J Neurosci* 23: 9620–9631.
 37. Ohyama T, Nores WL, Murphy M, Mauk MD (2003) What the cerebellum computes. *Trends Neurosci* 26: 222–227.
 38. Aizenman CD, Linden DJ (1999) Regulation of the rebound depolarization and spontaneous firing patterns of deep nuclear neurons in slices of rat cerebellum. *J Neurophysiol* 82: 1697–1709.
 39. Kistler WM, De Zeeuw CI (2002) Dynamical working memory and timed responses: the role of reverberating loops in the olivo-cerebellar system. *Neural Comput* 14: 2597–2626.
 40. LeDoux MS, Hurst DC, Lorden JF (1998) Single-unit activity of cerebellar nuclear cells in the awake genetically dystonic rat. *Neuroscience* 86: 533–545.
 41. Gauck V, Thomann M, Jaeger D, Borst A (2001) Spatial distribution of low- and

- high-voltage-activated calcium currents in neurons of the deep cerebellar nuclei. *J Neurosci* 21: RC158.
42. Koekkoek SKE, Yamaguchi K, Milojkovic BA, Dortland BR, Ruigrok TJH, et al. (2005) Deletion of FMR1 in Purkinje cells enhances parallel fiber LTD, enlarges spines, and attenuates eyelid conditioning in a manner which phenocopies human Fragile X syndrome. *Neuron* 47: 339–352.
 43. Koch C (1999) *Biophysics of computation: Information processing in single neurons*. New York: Oxford University Press.
 44. Steuber V, Mittmann W, Hoebeek FE, Silver RA, De Zeeuw CI, et al. (2007) Cerebellar LTD and pattern recognition by Purkinje cells. *Neuron* 54: 121–136.

Chapter 3

Paragraph 3

Increased Noise Level of Purkinje Cell Activities Minimizes Impact of their Modulation during Sensorimotor Control

Adapted from Neuron. 2005 Mar 24;45(6):953-65.

F.E. Hoebeek, J.S. Stahl, A.M. van Alphen, M. Schonewille, C. Luo, M. Rutteman, A.M. van den Maagdenberg, P.C. Molenaar, H.H. Goossens, M.A. Frens, C.I. De Zeeuw.

Abstract

While firing rate is well established as a relevant parameter for encoding information processing among neurons, the significance of other parameters awaits further elucidation. Here, we show that regularity of neuronal spike activities can play an important role during sensorimotor processing by investigating cerebellar function in *tottering* mutants, which suffer from a mutation in P/Q-type voltage gated calcium channels. While the modulation amplitude of the simple spike firing rate of their floccular Purkinje cells during optokinetic stimulation is indistinguishable from that in wild types, the regularity of firing is disrupted and the firing pattern of these spikes is totally aberrant. This irregularity is so robust that the effective functional output of the cerebellar cortex in *tottering* cannot be detected at the behavioural level in that the level of ataxia as measured by gain and phase values during compensatory eye movements is indistinguishable from that in wild types in which the flocculus is ablated. In addition, this phenotype observed in *tottering* can be largely mimicked in wild types by applying blockers of P/Q-type channels locally to their flocculus. Moreover, normal eye movements can be evoked in tottering when the flocculus is electrically stimulated with regular spike trains mimicking the firing pattern of normal simple spikes. To our knowledge the present study provides the first demonstration for the relevance of regularity of firing in Purkinje cells and one of the most dramatic demonstrations so far for the relevance of this parameter in neuronal information processing.

Introduction

The previous paragraphs have emphasized the significance of regular firing by demonstrating that Purkinje cells are nearly continuously active in the upstate and, despite being known as irregular, display short periods of very regular simple spike firing. As a proof of principal it would be of interest to investigate the impact on behavior of a highly irregular Purkinje cell firing pattern, e.g. as seen in the tottering mutant mice. Purkinje cell activities are modulated by sensorimotor activity, e.g. visual stimulation induced compensatory eye movements. Modulation of firing rate is usually considered as both a necessary and a sufficient parameter to correlate neuronal activities to sensorimotor behavior. Such relations have been demonstrated in many investigations of numerous systems varying from the sensory auditory and visual system to lower and higher motor systems (Frazor et al., 2004; Li et al., 1999). Theoreticians have pointed out the impact of noise levels (i.e. regularity of firing) in their neuronal network models (Mar et al., 1999; Steinmetz et al., 2001; Tiesinga et al., 2002), but it remains to be demonstrated at the experimental level to what extent a change in noise without a change in spike modulation can alter sensorimotor behaviour. The field of calcium channelopathies is likely to harbor a candidate demonstrating this dissociation between the impact of modulation of neuronal firing and that of noise of neuronal firing in, because various mutations in voltage-gated calcium channels result in both cell physiological and behavioural aberrations (Llinas et al., 1989; Mintz et al., 1992; Ophoff et al., 1996; Qian and Noebels, 2000; Cao et al., 2004). We focused on the *tottering* mutant (*tg*), which suffers from a point-mutation in the $\alpha 1_a$ -subunit of the P- and Q-type voltage-gated calcium channels that affects the extracellular membrane domain of the pore forming loop (Bourinet et al., 1999; Fletcher et al., 1996). The cerebellar Purkinje cells of these mutants show a complex combination of cellular abnormalities including

a reduction in Ca^{2+} channel current density (Wakamori et al., 1998), a reduction in the amplitude of the parallel fibre – Purkinje cell EPSC (Matsushita et al., 2002), and an increased susceptibility to inhibitory modulation by GABAergic interneurons (Zhou et al., 2003). The general importance of these deficits for motor behaviour is indicated by the fact that mutations in the $\alpha 1_a$ -subunit of the P- and Q-type channels do not only lead to various mouse models with motor coordination problems (Green and Sidman, 1962; Fletcher et al., 1996; Campbell et al., 1999; Stahl, 2004), but also to various human syndromes with ataxia including familial hemiplegic migraine, episodic ataxia type II, and spinocerebellar ataxia type VI (Ophoff et al., 1996; Zuchenko et al., 1997; Ducros et al., 1999). We therefore set out experiments in *tg* mutants to correlate the simple spike and complex spike activities of their Purkinje cells to their motor performance with special emphasis on measuring modulation and noise parameters of firing patterns. The flocculus of the vestibulocerebellum, which controls compensatory eye movements, was used as a model system to determine these correlations quantitatively. In this system relationships between sensory input, motor output, and intermediate Purkinje cell activities can be rigorously defined (De Zeeuw et al., 1995; Stahl and Simpson, 1995ab; Simpson et al., 1996; Goossens et al., 2004).

Experimental Procedures

Animal preparation

Data were collected from 32 *tg* mice and 32 wild type littermates (C57BL/6J background; Jackson laboratory, Bar Harbor, ME, USA), which were prepared for chronic experiments (Goossens et al., 2004; van Alphen et al., 2001). All preparations were done with approval of the European Communities Council Directive (86/609/EEC).

Eye movement recordings

The OKR was assessed by rotating a planetarium sinusoidally around both vertical and horizontal axes at various frequencies (0.05, 0.1, 0.2, 0.4, 0.8 and 1.6 Hz) and a fixed peak velocity ($8^\circ/\text{sec}$) (Stahl et al., 2000; van Alphen et al., 2001). The VOR and VVOR were assessed by rotating the animal sinusoidally around the vertical axis at various frequencies (0.1, 0.2, 0.4, 0.6, 0.8, and 1.0 Hz) and a fixed amplitude (10°) in the light. Stimuli were controlled and monitored by a 1401plus unit (CED, Cambridge, UK). The position of the left eye was measured using a video set-up (sampling rate 240 Hz; ETL-200, ISCAN, Burlington, MA, USA; Stahl et al., 2000; Stahl, 2004). For baseline compensatory eye movements (see Figure 1) the eye position signal was sampled at 500 Hz (1401plus unit, CED). Data were stored for off-line analysis using Spike 2 and Matlab (Mathworks Inc. Natick, MA, USA).

Single cell recordings

Extracellular Purkinje cell activities were recorded from either the flocculus or non-floccular regions in the hemisphere of the left cerebellar cortex (Goossens et al., 2004). The cells were recorded either during spontaneous activity in the light or during modulation due to optokinetic stimulation (see above). Signals were amplified, filtered, digitized and stored for off-line analysis. Purkinje cells were identified by a brief pause in simple spike activity following each complex spike. Once a floccular Purkinje cell was isolated, the preferred axis of rotation was determined by rotating the planetarium

around the vertical axis or a horizontal axis at 135° azimuth, ipsilateral to the side of recording (if necessary tuning curves were made using stimulations around multiple axes in space).

Floccular lesions and histology

After localizing the left flocculus by recording its typical complex spike response to optokinetic stimulation, it was lesioned by suction in 6 *tg* and 4 wild type animals. Eye movement recordings were done for two days pre-lesion and averaged and subsequently compared to post-lesion data (third day post-lesion). To check the damage the animals were anaesthetised and perfused, and subsequently Nissl and silver stainings were made of the cerebellum and brainstem (Jaarsma et al., 1992; Nadler and Evenson, 1983).

Electrical stimulation

Custom-made urethane-insulated tungsten electrodes were used to electrically stimulate the left floccular peduncle. Regular trains of pulses (200 ms, 400 ms, 600 ms, 800 ms, 1000 ms and 1500 ms trains; 80 μ s pulse duration; 100 Hz pulse frequency with various stimulation intensities) were used to evoke eye movements in the ipsilateral eye. Analyses of the short latencies as well as the eye movements during the various stimulus time courses were done using linear regression analysis (Van der Steen et al., 1994).

Injections of ω -Agatoxin IVA

The borders of the left flocculus were identified using the electrophysiological recordings described above. Subsequently, the recording electrode was replaced by a borosilicate glass electrode filled with 100 nM ω -Agatoxin IVA (diluted in 0.9% saline; Alomone Labs, Jerusalem, Israel) (Knight et al., 2003). Approximately 10 μ l of the ω -Agatoxin IVA solution was injected by pressure at multiple sites evenly distributed over the entire flocculus. Compensatory eye movements were measured before the localization of the flocculus and three days after the injection of the blocker in 4 wild type mice. As controls we injected the vehicle (saline) in 3 wild types and the ω -Agatoxin IVA solution in 2 *tg* mice. Juxtacellular recordings of Purkinje cell activities were made with the use of multiple barrel electrodes following iontophoretic injections of ω -Agatoxin IVA solution as described by Shields et al. (2004).

Data analysis

Off-line analysis of eye movements and neuronal firing rates was performed in Matlab (Mathworks) (Goossens et al., 2004; Stahl, 2004). Gain and phase values were determined by fitting sine functions to the slow-phase eye velocity traces. Simple spikes and complex spikes were discriminated using custom-made routines based on cluster analysis (Goossens et al., 2004). Simple spike PSTH's (100 bins per cycle) were compiled at each stimulus frequency (F) and fit by a sine function. Neuronal amplitude of modulation was calculated by dividing the amplitude of the fitted sine wave by its offset. The phase of the simple spike activity relative to the eye velocity (θ) was calculated from the difference of the phase of the sinusoidal fits to firing rate and eye velocity (De Zeeuw et al., 1995; Stahl and Simpson, 1995b). CV values of spontaneous spike activities were calculated by dividing the standard deviations of the interspike interval lengths by their means. Autocorrelograms of spiking data and interspike intervals during modulation were constructed using custom made routines in Matlab. A fixed bin size of 50 ms

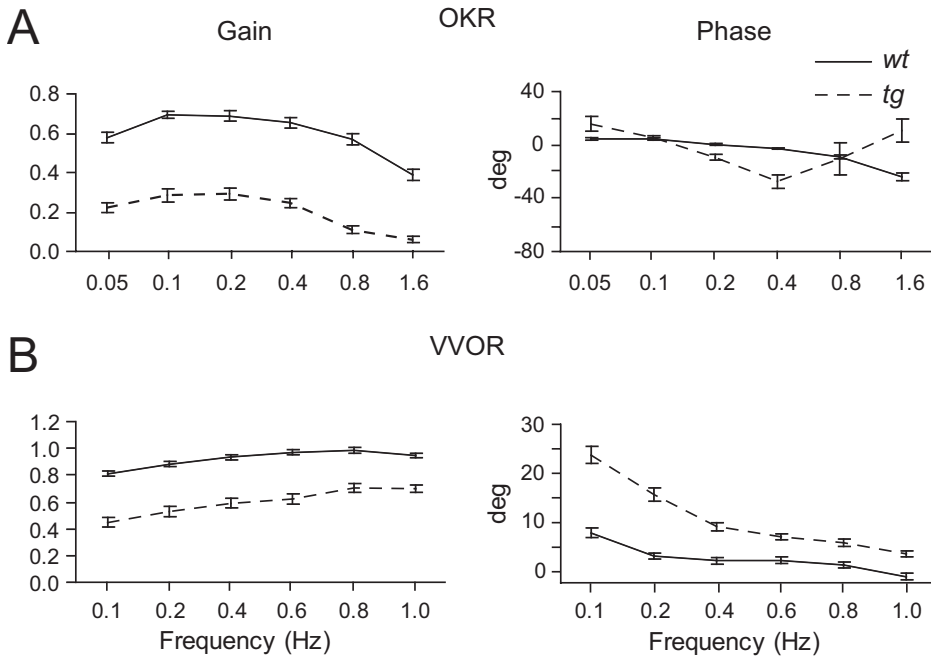


Figure 1. Compensatory eye movements under vision are impaired in tottering (*tg*) mice.

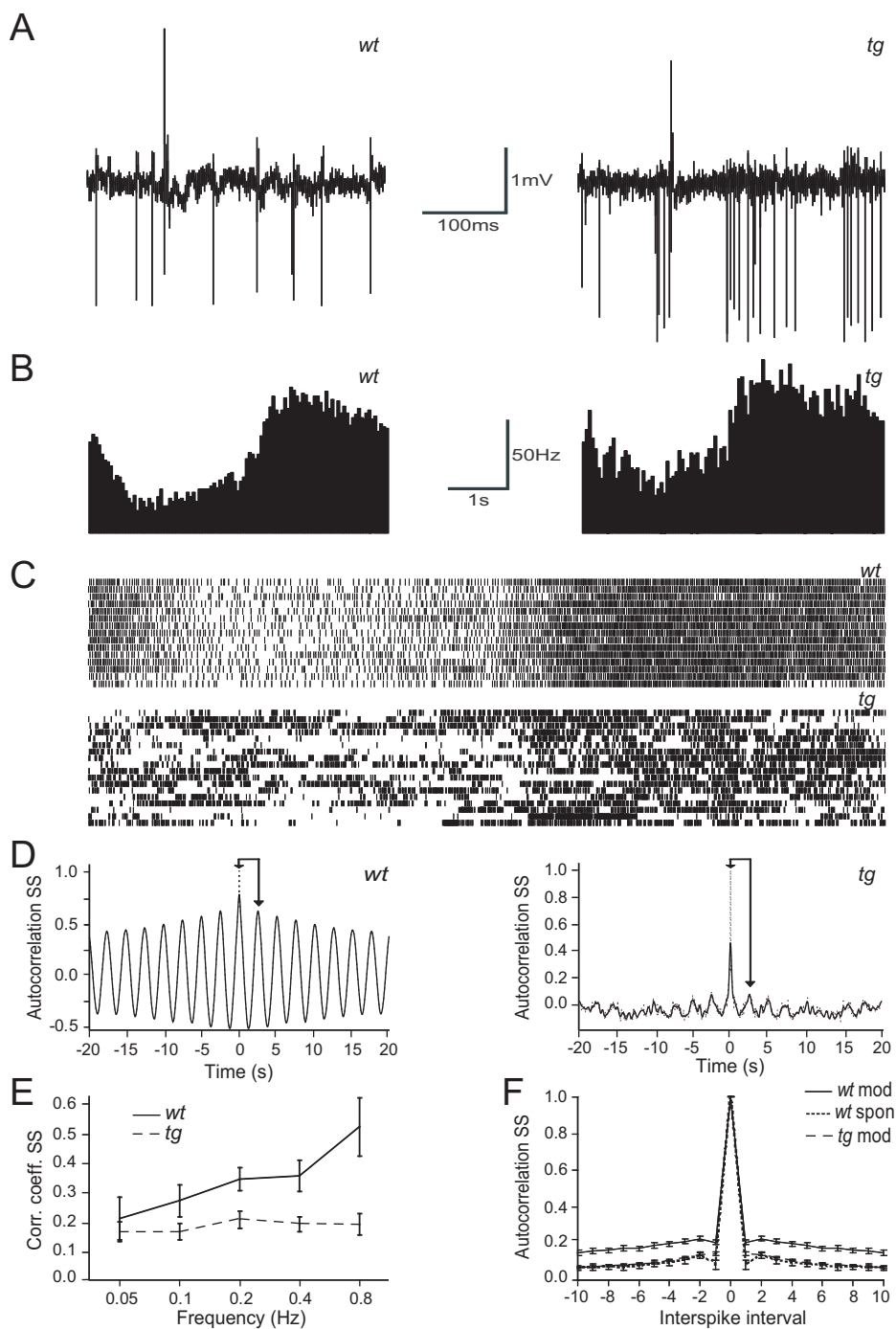
Gain values (left column) of *tg* mutants are decreased during the optokinetic reflex (OKR) (A) and vestibulo-ocular reflex in the light (VVOR) (C), but not during the vestibulo-ocular reflex in the dark (VOR) (B). Phase values (right column) of the *tg* mutants only show significant changes during VVOR. Solid lines and dashed lines indicate data of wild types (*wt*) and *tg* mutants, respectively.

and a 7th order low pass filter were used to calculate the correlogram coefficient of the spiking data (ratio of the amplitude of the first off-centre peak in the filtered data and the amplitude of the centre peak of the raw data). An increased noise level was defined as any significant increase in irregularity of spike firing within periods varying from 5 ms up to 1000 ms (as revealed by CV values or autocorrelograms). Epochs containing quick phases were analysed separately. Saccades were detected with a velocity threshold of 25°/s (for details see Van der Steen & Bruno, 1995). Data are presented as mean \pm SEM.

Results

Mutation in P/Q-type calcium channel leads to abnormal sensorimotor behaviour

The *tg* mutants under investigation showed the general ataxic behaviour during locomotion as described previously (eg. Campbell et al., 1999). To determine the level of ataxia at a quantitative level we investigated gain and phase during sinusoidal optokinetic and vestibular stimulation at frequencies varying from 0.05 Hz to 1.6 Hz in 5 *tg* mutants and 8 wild types (Figure 1). During the optokinetic reflex (OKR) the gain values of *tg* mice ranged from 0.06 to 0.32, while those in wild types ranged from 0.36 to 0.71; these values were significantly different ($p < 0.001$; repeated measures ANOVA). During the vestibulo-ocular reflex in the dark (VOR) the gain values of the *tg* mutants ranged from 0.26 to 0.77 and were not significantly different from those in wild types



($p = 0.4$; repeated measure ANOVA). During vestibular stimulation in the light (VVOR) the gain values in *tg* mice ranged from 0.48 to 0.74 and were significantly different ($p < 0.001$; repeated measures ANOVA) from those in wild types (ranging from 0.82 to 1.02). The phase leads of *tg* mutants differed from those in wild types during VVOR ($p < 0.001$; repeated measures ANOVA), but not during OKR and VOR ($p = 0.3$ and $p = 0.4$). These data indicate that compensatory eye movements under vision (i.e. OKR and VVOR), which are controlled by the flocculus of the vestibulocerebellum, are abnormal in *tg* mutants.

Purkinje cells with abnormal P/Q-type channels fire irregularly but modulate normally

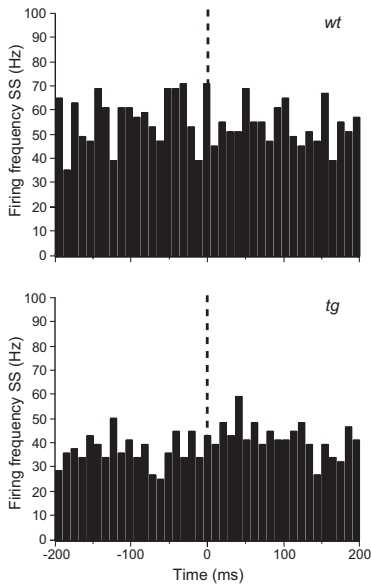
To find out whether the motor deficits in *tg* mice can be caused by abnormal firing of their Purkinje cells in the cerebellum we recorded their simple spikes and complex spikes in various cerebellar regions during spontaneous activity and in the flocculus during optokinetic stimulation. Extracellular recordings of Purkinje cells in *tg* mutants ($n = 86$ from 22 animals) and wild type mice ($n = 79$ from 14 animals) during spontaneous activity in the light did not reveal gross anomalies in amplitude, shape or duration of their simple spikes or complex spikes. However, the firing pattern of the simple spikes was much more irregular in *tg* mutants than in wild types (Figure 2A). This difference held equally true for all cerebellar regions from which we recorded, i.e. crus I and II, paramedian lobule, paraflocculus and the flocculus. The coefficient of variance (CV; for details see experimental procedures) of the spontaneous simple spike activities in the non-floccular regions in *tg* mice (2.18 ± 0.19) did not differ ($p = 0.4$; t-test) from that in the flocculus (2.57 ± 0.25) showing that the abnormal firing pattern was a general phenomenon. The average CV of the pooled simple spikes during spontaneous activity in *tg* (2.25 ± 0.16) was almost four times higher than that in wild types (0.63 ± 0.07). This difference was highly significantly different ($p = 3.93 \times 10^{-16}$; t-test). The increase in irregularity in *tg* mice was also reflected in a shorter climbing fibre pause (defined by the period between the start of the complex spike and the start of the first simple spike after this event). In *tg* and wild types the pause was 13.6 ± 0.55 ms and 16.4 ± 0.07 ms, respectively ($p < 0.05$; t-test). The reduction in pause length cannot be explained by a higher firing frequency of the simple spikes in *tg*, because the average firing frequency was in fact slightly lower (varying from 52 spks/s to 65 spks/s).

The irregular simple spike firing pattern can only explain the ataxic behaviour when it persists during the performance of movements. We therefore investigated the activities

Figure 2. Simple spike activities (SS) of Purkinje cells in *tg* mutants modulate normally during optokinetic stimulation, but fire irregularly.

(A) Extracellular recordings of spontaneous Purkinje cell activities of a wt (left panel) and a *tg* mouse (right panel). Note the increased irregularity of the simple spikes in *tg* (complex spikes go up, simple spikes go down). (B) Peri-Stimulus Time Histograms (PSTH) show that the modulation of the simple spike activities of a floccular Purkinje cell during optokinetic stimulation in *tg* is indistinguishable from that in wt (for population data see Figure 3B). (C) Raster plots of the same spikes that are presented in the PSTH's in B show that Purkinje cells in *tg* mice fire much more irregularly despite their normal modulation. Each small stripe represents a single spike and each row of stripes represents spike data of a complete stimulus cycle. (D) Autocorrelations during modulation show that the predictability of simple spikes in wt is much better than that in *tg* (stimulus at 0.4 Hz and 8°/s; bin size 50 ms). Unfiltered traces are indicated by striped lines and low pass filtered traces are indicated in solid lines; left column for wt and right column for *tg*. Arrows indicate values used for calculation of correlation coefficients (see methods). (E) Correlation coefficients during optokinetic stimulation in *tg* mice are lower than those of wild types and they are not influenced by stimulus frequency, in contrast to those of wild types. (F) Autocorrelation of simple spike intervals in wt during optokinetic modulation (solid line; wt mod) is significantly higher than that in wt during spontaneous activity (dotted line; wt spon) as well as than that in *tg* during modulation (dashed line; *tg* mod).

A



B

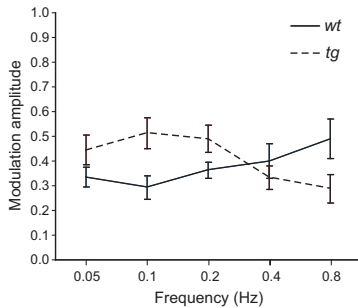


Figure 3. Saccade related and modulation related simple spike activities of floccular Purkinje cells in *tg* are indistinguishable from that in *wt*.

(A) Histograms of average simple spike activities occurring around the onset of fast phases which are superimposed at moment zero and indicated by vertical dotted lines (bin size 10 ms). Note that there was no significant correlation between spike data and saccadic eye movements neither for *wt* ($n = 51$) nor for *tg* ($n = 55$). (B) Average modulation amplitude of simple spike activities of all Purkinje cells that modulate optimally around the vertical axis; no significant difference was observed among *wt* and *tg* mice.

of floccular Purkinje cells in alert *tg* mutants ($n = 25$ from 10 animals) and wild types ($n = 14$ from 5 animals) that made compensatory eye movements in response to optokinetic stimulation (Figure 2B). During this behavioural paradigm too the simple spikes activities in the *tg* were much more irregular during both the on-phase and off-phase of modulation (for trace-by-trace plot in a raster diagram see Figure 2C). To quantify the level of irregularity during optokinetic modulation we calculated both the autocorrelogram coefficients of the simple spikes using a bin size of 50 ms (Figures 2D and E) and autocorrelogram coefficients of the interspike intervals on a spike by spike basis (Figure 2F). Both calculations showed that the autocorrelations were much lower in *tg* than in controls ($p < 0.001$ in both analyses; ANOVA). Moreover, while the correlation coefficient in wild types increased with increasing stimulus frequency, that of the *tg* mutants did not (Figure 2E). In addition the average autocorrelation of the interspike intervals in wild types during

modulation was significantly higher than that during spontaneous activity ($p < 0.001$; ANOVA), while that of the *tg* mutants was not ($p = 0.4$; ANOVA). Together these data demonstrate that Purkinje cells in *tg* mice fire much more irregularly during modulation than those in wild types and that the predictive power of a single interspike interval of a modulating Purkinje cell is significantly bigger in wild types than that in *tg* mice.

Two potential confounding factors during optokinetic stimulation might contribute to a difference in regularity of simple spike firing between wild types and *tg* mice. These include possible differences in simple spike activities associated with spontaneous saccadic eye movements as well as possible differences in depth of optokinetic modulation. Both factors were found to be irrelevant. Saccade - triggered spike averages showed no significant peaks in firing frequency before or after saccades neither in wild types nor in *tg* mutants ($p = 0.9$ and $p = 0.2$, respectively; Kolmogorov-Smirnov), and there was no difference among wild types and *tg* mice in the response of the Purkinje cells to spontaneous eye movements ($p = 0.2$; Kolmogorov-Smirnov) (Figure 3A). Sine waves

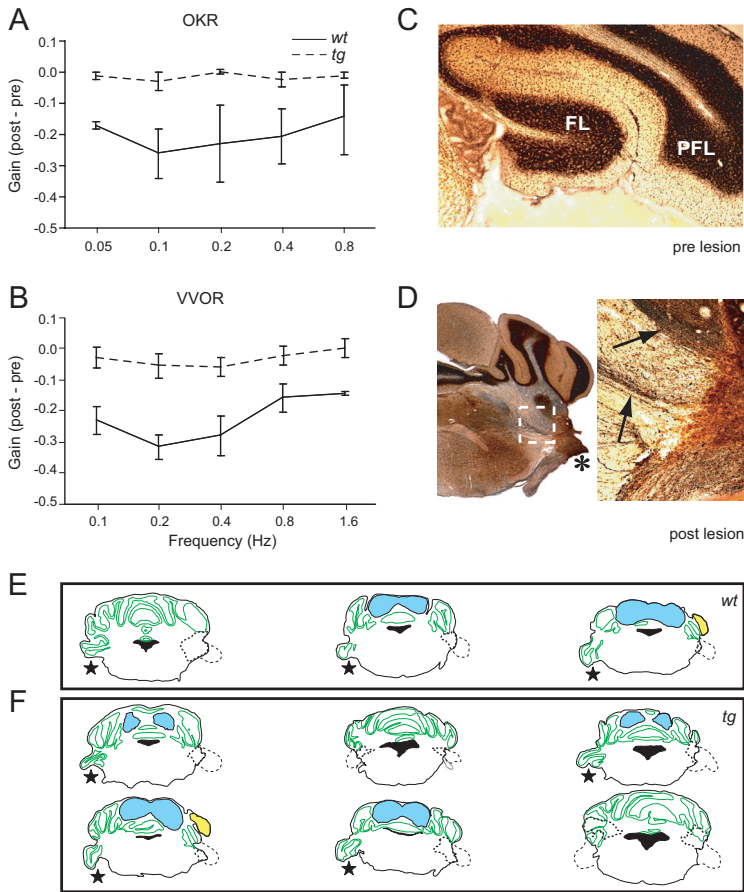


Figure 4. Flocculus of *tg* mutant does not contribute to compensatory eye movements.

(A and B) Gain values of *tg* mutants during OKR (A) and VVOR (B) are not decreased by ablation of their flocculus, whereas those in wild types are. (C and D) A silver-stained section of an intact flocculus and parafofoculus of a *tg* mouse in which no lesion was placed (C) and a silver stained section of degenerated fibers in the floccular peduncle of a *tg* mouse in which the flocculus was ablated (D). Asterisk in D indicates the location of the lesion. Inset in low magnification panel on the left corresponds to high magnification panel on the right. Arrows indicate borders of floccular peduncle.

fitted to the optokinetic simple spike responses showed that the average modulation amplitudes did not differ either ($p = 0.7$; non-orthogonal ANOVA) (Figure 3B).

Taken together we conclude from our floccular Purkinje cell recordings during optokinetic responses that a change in regularity of simple spike activities but not in modulation amplitude may explain the ataxic eye movement behaviour of *tg* mutants.

Output of modulating Purkinje cells in vestibulocerebellum of tg mutants is not functional

Even though OKR and VVOR gain values as well as the regularity of simple spike responses during these movements are affected in *tg*, the modulating Purkinje cells in their flocculus may still contribute, although less effectively than in wild types, to increase the gain of its compensatory eye movements. To determine the extent to which signal processing in the flocculus of the *tg* contributes to compensatory eye movements under vision, we ablated the flocculus of *tg* and wild type mice and evaluated their differences in pre- and post-lesion gain values (Figures 4A and B). In *tg* mutants we did not observe any significant decrease in OKR or VVOR gain values after the lesions ($p = 0.1$ and $p = 0.4$, respectively; ANOVA). In contrast, the same values did decrease significantly in

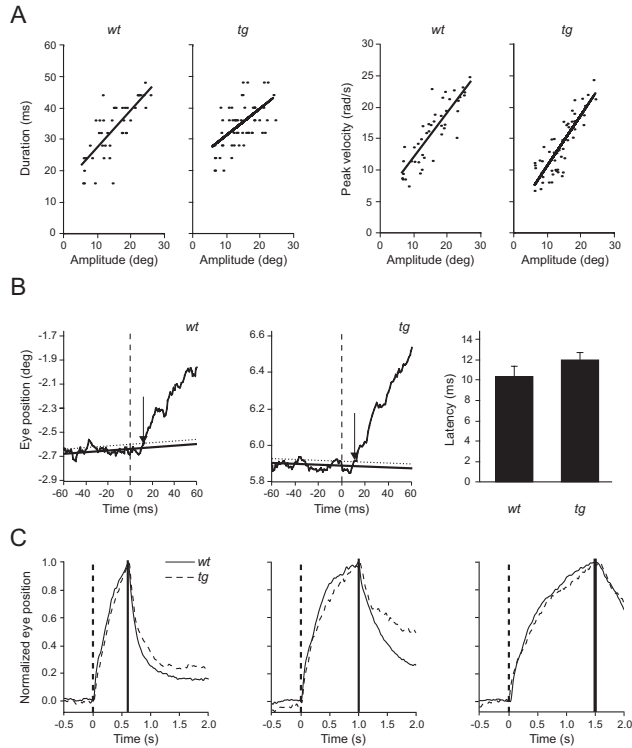


Figure 5. Oculomotor connections downstream of the flocculus appear functionally intact.

(A) dynamics of saccadic eye movements are unaffected in that the main sequence parameters in *tg* are not different from those in wt; data show representative of linear fits to the duration re amplitude (left panels) and peak velocity re amplitude (right panels). (B) Eye movements evoked by electrical stimulation in the flocculus show normal latencies in *tg* mutants. The left and middle panel show eye position traces before and after the onset (dashed line) of electrical stimulation in wt and *tg*, respectively. Solid straight lines indicate result of linear regression of the 200 ms period prior to the onset of the stimulus with (thin line) and without 1 SD (bold line). Arrows indicate crossings of eye position traces and SD lines, which are used for quantification of the latencies. Right panel indicates that the average latency of the eye movements following electrical stimulation of the flocculus in wt is indistinguishable from that in *tg*. (C) Left, middle and right panel show normalized eye positions following 600 ms, 1000 ms and 1500 ms stimulus protocols, respectively. Dashed and dotted vertical lines indicate onset and stop of the electrical stimulus, respectively. The finding that the eyes in *tg* mutants did not drift back during the application of the stimulus suggests that the neurotransmitter stores in its oculomotor synapses and neuromuscular junctions are not depleted.

wild types during OKR and VVOR ($p < 0.03$ and $p < 0.05$, respectively; ANOVA). For both OKR and VVOR we found that the gain values of the wild types after the lesions did not differ from those of the *tg* mutants before the lesions ($p = 0.3$ and $p = 0.2$, respectively; ANOVA). Both wild type and *tg* VOR gain values did not change after the lesion ($p = 0.1$ and $p = 0.9$, respectively; ANOVA). The completeness of the lesions was verified with the use of silver staining that revealed the degenerating fibers in the floccular peduncle (Figures 4C and D). These data indicate that the output of the flocculus in *tg* mutants does not contribute significantly to the gain of the optokinetic reflex or visually enhanced vestibulo-ocular reflex.

Connections downstream of cerebellar cortex are functionally intact

The recording and lesion experiments described above suggest that the floccular output

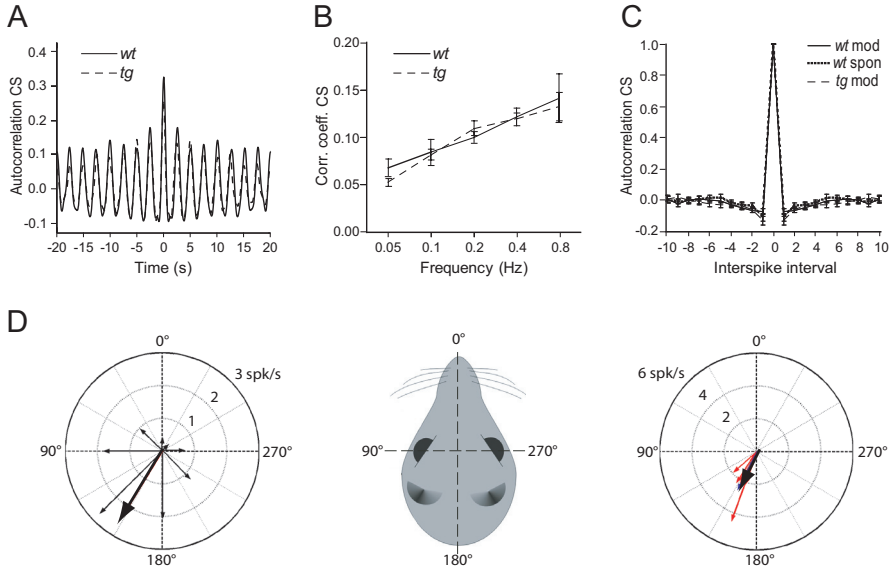


Figure 6. Olivary connections upstream of flocculus of *tg* mutants are functionally intact.

(A) Autocorrelations show that there is no difference in the predictability of complex spike activities (CS) during optokinetic modulation between wt and *tg* data (stimulus frequency 0.4 Hz; bin size 50 ms). Blue and red lines indicate low-pass filtered autocorrelation for wt and *tg*, respectively. (B) Correlation coefficients of wt and *tg* CS activities during modulation are equally dependent on stimulus frequency. (C) Autocorrelations of CS interspike intervals in wt during modulation did not differ from that in wt during spontaneous activity nor from that in *tg* mice during modulation. Note that all CS data presented in panels A, B and C show opposite results to the SS data presented in Figures 2D, E and F. (D) Tuning curves of climbing fibre responses of floccular Purkinje cells are normal in *tg* mutants. Left panel shows an example of the depth of modulation of the climbing fibre responses of a single cell for 8 different horizontal axes in space. Lengths of arrows indicate depth of modulation and the big arrow indicates vector for optimal modulation (close to 135° azimuth). Right panel shows these vectors for five different cells (blue arrow indicates average vector).

is functionally non-existent in the *tg* due to irregular simple spike activities. However, an alternative or additional explanation could be that the floccular output is impaired downstream at the level of the synaptic targets of its visual pathways in the vestibular nuclei, oculomotor nuclei and/or at the neuromuscular junctions of the eye muscles (Plomp et al., 2000). To find out whether such a functional barrier exists, we investigated whether saccadic eye movements are also impaired in *tg* mutants and whether normal eye movements can be evoked following electrical stimulation of their flocculus. Figure 5A shows the analyses of the main sequence parameters of spontaneous saccadic fast phases. The slopes of duration re amplitude (1.16 ± 0.21) as well as the offsets of the linear fits (15.3 ± 4.52) in *tg* mice did not differ from those in wild types (0.89 ± 0.17 and 19.6 ± 3.26 , respectively) ($p = 0.2$ and $p = 0.3$; t-test). Moreover, the slope (39.6 ± 1.78) and offset (7.43 ± 1.40) of the peak velocity to amplitude fits in *tg* did not differ either ($p = 0.2$ and $p = 0.9$, respectively; t-test) from those in wild types (36.7 ± 0.80 and 7.32 ± 1.59 , respectively). These data suggest that the relay functions of the oculomotor nuclei and associated neuromuscular junctions are at least intact for the short duration of fast saccadic eye movements. The short latencies of the eye movements that could be evoked by electrical stimulation of the vertical axis zone of the flocculus with a regular 100 Hz pulse train of a short duration of 200 ms confirmed this observation (Figure 5B). The average latency in *tg* mice (12.7 ± 1.4 ms) did not differ ($p = 0.5$; t-test) from that in

wild types (11.7 ± 0.7 ms). Moreover, the stimulus thresholds that were necessary to evoke these short-latency eye movements with a prominent temporal component were the same in both types of animals (varying from 10 μ A to 18 μ A in both groups). To further exclude the possibility that *tg* mutants suffer from a relatively strong depletion of neurotransmitters in one of their synaptic connections downstream of the flocculus, we also investigated their eye movements following stimuli with longer time courses up to 1500 ms (Figure 5C). Independent from the duration of the stimulation the dynamics of the movements elicited in the ipsilateral eye in *tg* mutants were comparable to those in wild types, and in both *tg* mutants and wild types these movements never stopped before the stimulus stopped. These results suggest that synaptic transmission in the optokinetic and vestibular system downstream of the flocculus is not functionally blocked in *tg* mutants and that their reduced visual compensatory eye movement performance is most likely not caused by such a barrier.

Olivary connections upstream of cerebellar cortex are functionally intact

Since P/Q-type calcium channels are also moderately expressed in the inferior olive neurons (Fletcher et al., 1996; Hillman et al., 1991; Stea et al., 1994; Westenbroek et al., 1995), the increased irregularity in simple spike activities may also be imposed by changes upstream of the flocculus, that is, in climbing fibre activities generated in the olive (De Zeeuw et al., 1998). This seems feasible since sudden increases or decreases of climbing fibre activities decrease and increase the simple spike frequency, respectively (Montarolo et al., 1982). We therefore also compared the complex spike activities (Figure 6). During spontaneous activity the mean firing frequency and CV of complex spikes in *tg* mice equalled 0.98 ± 0.04 spk/s and 0.78 ± 0.02 , respectively, while those in wild types equalled 0.90 ± 0.03 spk/s and 0.81 ± 0.02 ($p = 0.1$ and $p = 0.3$, respectively; t-test). During optokinetic stimulation the autocorrelograms of complex spike activities in *tg* mutants did not differ from those in wild types either, neither with regard to the analyses using 50 ms spike bins (Figures 6A and B) nor with regard to the analyses of the interspike intervals ($p = 0.4$ and $p = 0.1$, respectively; ANOVA) (Figure 6C). To further assess the integrative properties of the olivary neurons and its inputs from the accessory optic system (Simpson et al., 1996), we also investigated the preference of their climbing fiber responses for particular axes of optokinetic stimulation, i.e. their spatial tuning (Figure 6D). Apart from the neurons that modulated optimally about the vertical axis, we also identified numerous neurons that modulated optimally about the horizontal axis 135° ipsilateral to the azimuth. The bimodal vector distribution and the resulting vectors of the tuning curves in *tg* mutants did not differ from those in wild types and they resembled those described for other animals such as rabbits and pigeons (Graf et al., 1988; De Zeeuw et al., 1994; Wylie et al., 1995). Moreover, their complex spike activities were always in counter phase with the simple spike activities independent from the spatial axis used for stimulation. We conclude that both the spontaneous activities and integrative properties of the olivary neurons that ultimately determine the complex spike output of the floccular Purkinje cells are not affected in *tg* mutants, and that their simple spike irregularities are thus not indirectly caused by altered climbing fibre responses.

*Acute blockade of P/Q-type channels in flocculus of wild types partially mimics behavioural phenotype of *tg**

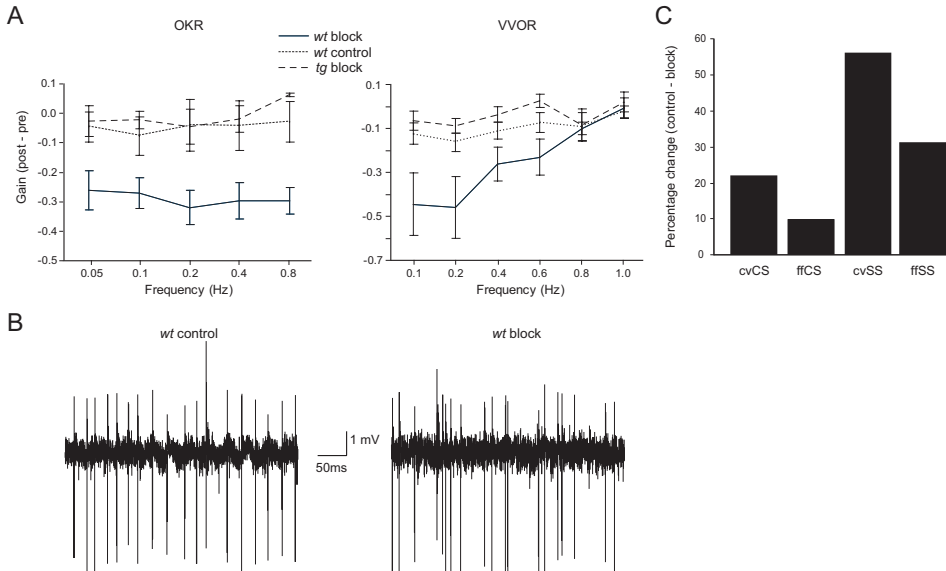


Figure 7. Phenotype of *tg* mutant can be largely mimicked by local injection of selective P/Q-type channel blocker. (A) OKR gain values in wt decreased after injection of ω -Agatoxin IVA into the flocculus (solid line; wt block), but not after injection of the solution vehicle (dotted line; wt control). Injection of the blocker into the flocculus in *tg* mice (dashed line; *tg* block) resulted in no change in OKR gain values. (B) Same as in A but for VVOR. (C) Histograms showing the differences in CV and firing frequency of complex spikes and simple spikes in wild type mice (cvCS, ffCS, cvSS and ffSS, respectively) following juxtacellular application of ω -Agatoxin IVA as compared to the control injection with the vehicle alone.

The data presented above suggest that the connections downstream and upstream of the cerebellar cortex are sufficiently intact in the *tg* mutants to allow functional synaptic transmission, but it remains to be demonstrated whether dysfunctional P/Q-type channels in the cerebellar cortex alone are sufficient to induce ataxic behaviour. Moreover, it is clear from cell physiological studies of *tg* mutants that their Purkinje cell activities must reflect both acute synaptic abnormalities and secondary compensatory effects (Wakamori et al., 1998; Matsushita et al., 2002; Zhou et al., 2003), but it remains to be demonstrated whether the simple spike irregularities that we observed can be attributed to both processes or the acute effects alone. We therefore investigated the impact of an acute and local, partial blockade of the P/Q-type channels in the vestibulocerebellum on the OKR and VVOR as well as on their simple spike and complex spike activities (Figure 7). In wild types injections of 100 nM ω -Agatoxin IVA, but not of the vehicle solution alone, into the flocculus resulted in a significant decrease of the OKR gain values at the entire frequency range ($p < 0.001$; ANOVA) (Figure 7A). For the VVOR injections of the P/Q-channel blocker also caused an overall significant gain reduction ($p < 0.02$; ANOVA), but the differences with the results following vehicle injections were relatively small at the higher frequencies (Figure 7B). The phase lead during VVOR was significantly enhanced ($p < 0.001$, ANOVA), whereas the phase lag during OKR was not affected ($p = 0.1$, ANOVA). In *tg* mutants the injections did not exert any significant effect ($p = 0.3$ and $p = 0.4$ for OKR and VVOR gain values, respectively; ANOVA). These data indicate that acute local application of P/Q-type channel blockers to the flocculus of a wild type mouse can be sufficient to mimic the eye movement performance of a *tg* mouse during OKR and VVOR.

Juxtacellular application of ω -Agatoxin IVA to Purkinje cells of both the flocculus and non-floccular regions in the cerebellar cortex of alert wild type mice resulted in three categories of cells: One type in which long silent periods of simple spikes occurred, while the complex spikes maintained ($n = 14$); a second type in which both the simple spikes and complex spikes maintained throughout the recordings ($n = 13$); and a third type in which only the simple spikes maintained ($n = 3$). All cells in the second category showed a clean climbing fiber pause throughout the recordings indicating a single unit (Simpson et al., 1996) and they could be readily used for further analysis. This analysis showed that the average firing frequency of their simple spike activities increased from 59 ± 11 spk/s up to 83 ± 16 spk/s and that their average CV tended to change concomitantly following injection of ω -Agatoxin IVA as compared to injection of the vehicle alone (Figure 7C). However, none of the average changes in simple spike responses was statistically significant when we considered this category alone ($p = 0.1$ and $p = 0.3$ for differences in CV and firing frequency, respectively; ANOVA). Yet, when we pooled the data sets of all three categories of cells, the change in CV, but not in firing frequency, was significant ($p < 0.02$ and $p = 0.4$, respectively; ANOVA). In contrast, the average change in CV of the complex spike activities after application of ω -Agatoxin IVA was not significant ($p = 0.2$; ANOVA). Thus, even though one cannot rule out the possibility that some of the cells of the first and third category were not a pure single unit (for technical reasons see Simpson et al., 1996), overall the data do support our hypothesis that an acute blockage of P/Q-channels enhances irregularity of the simple spike activities, and that this change in turn may cause deficits in motor coordination.

Discussion

The previous two paragraphs demonstrate the importance simple spike regularity; silent downstate of substantial length are virtually absent in awake behaving mice (Ch. 3.1) and in simple spike firing contains patterns of very regular firing (Ch. 3.2). Analysis of simple spike activities in *tottering* revealed highly irregular firing, comparable to recordings in bistable Purkinje cells. The current study extends the evidence demonstrating that highly irregular, or noisy, simple spike firing results in a dysfunctional cerebellum, a situation that does not occur under normal circumstances. The potential impact of noise on signal processing had been recognized by theoretical neuroscientists before, but experimental evidence in which a pure change in noise results in altered sensorimotor behaviour has been lacking. Here we provide such evidence by showing that a mutation in P/Q-type voltage gated calcium channels leads to irregular simple spike activities of Purkinje cells without any change in modulation of firing rate and that these irregularities cause deficits in cerebellar motor control such as that of compensatory eye movements. Thereby the present study puts forward the behavioural relevance of regularity of firing for signal coding in sensorimotor processing. Because similar mutations in this type of calcium channel underlie ataxia in human syndromes, the current data raise the possibility that pure aberrations in noise levels of neurons can be sufficient to induce neurological diseases.

Cellular basis of irregular simple spike firing pattern

The cell physiological aberrations that underlie the observed simple spike irregularities in the cerebellar flocculus during compensatory eye movements in tg may arise from three

possible sources: the optokinetic and/or vestibular mossy fiber inputs to the flocculus, the visual climbing fiber inputs to the flocculus, and/or intrinsic abnormalities of neurons in the floccular cerebellar cortex itself. The first possibility appears very unlikely because in situ hybridisation and immunocytochemical studies have shown that the distribution of P/Q channels within the nuclei that give rise to optokinetic and vestibular mossy fibers is very sparse (Stea et al., 1994; Westenbroek et al., 1995; Fletcher et al., 1996; Craig et al., 1998). The second option however appears quite possible, because P/Q-type channels are ubiquitously distributed in all neurons of all olivary subnuclei including the dorsal cap of Kooij and ventrolateral outgrowth, which are known to give rise to the climbing fibers that innervate the flocculus (Tan et al., 1995). We therefore investigated the shape of the complex spikes, their mean firing frequency and regularity of firing as well as the tuning curves and phase of their modulation during optokinetic stimulation about different axes in space. None of these values was abnormal and we conclude that the dynamic and integrative properties of neurons in the inferior olive that determine the ultimate complex spike output of the flocculus are not affected in *tg* mutants. Thus, simple spike irregularities in *tg* are probably neither caused by altered mossy fiber inputs nor by altered climbing fiber responses, and therefore must predominantly reflect the intrinsic, presynaptic and postsynaptic changes of neurons within the cerebellar cortex itself.

Because P/Q-type channels are widely and densely distributed throughout various layers of the cerebellar cortex (Fletcher et al., 1996; Hillman et al., 1991; Stea et al., 1994; Westenbroek et al., 1995), it appears likely that several abnormal cell physiological factors in the cerebellar cortex of *tg* mice converge and ultimately accumulate into an increase in irregularity of their simple spike activities. First, the intrinsic excitabilities of Purkinje cells and granule cells are likely altered in that their peak current amplitude, current density of P/Q-type VGCCs, and calcium influx are affected (Zhang et al., 1993; Randall and Tsien, 1995; Wakamori et al., 1998). Second, the synaptic connection between the granule and Purkinje cells is weakened in that the amplitude of their EPSC is smaller (Matsushita et al., 2002). Third, even though the climbing fiber-mediated EPSC is normal (Matsushita et al., 2002), the length of the climbing fiber pause turned out to be slightly reduced (present study). This decrease in pause length, which may be caused by a reduced activity of calcium-dependent potassium channels (Schmolesky et al., 2002; Sausbier et al., 2004), may affect the simple spike activities (Sato et al., 1993). Fourth and finally, more indirect compensatory mechanisms may occur in the cerebellar cortex of the *tg* mutant. For example, there may be a shift in neurotransmitter release reliability from P/Q-type channels to N-type channels as shown for the forebrain and hippocampus (Leenders et al., 2002; Qian and Noebels, 2000; Cao et al., 2004). Because an increased influence of the N-type channel leads to an increased susceptibility for inhibitory modulation by G protein-coupled receptors (Zhou et al., 2003) and because a single action potential of a cerebellar inhibitory interneuron is able to delay spontaneous intrinsic action potentials in Purkinje cells (Hausser and Clark, 1997), such an increased susceptibility would be predicted to prolong the silent periods that basket cells and stellate cells can impose on them. Thus in conjunction we conclude that a combination of multiple defects of different natures at various synapses in the cerebellar cortex can explain the enormously enhanced irregularity of the simple spike response in *tg* mutants.

Behavioural consequences of irregular simple spike activities

Our behavioural and neuronal observations that gain and phase values during compensatory eye movements under vision are affected and that simple spike activities in their flocculus are irregular while their modulation amplitude is normal raise the possibility that irregular simple spike activities of Purkinje cells are the prime cause of ataxia in *tg* mutants. This notion is well in line with the fact that the density of P/Q-type channels in the cerebellum is by far the highest when compared to all other brain structures involved in oculomotor behaviour (Fletcher et al., 1996; Hillman et al., 1991; Stea et al., 1994; Westenbroek et al., 1995). Even so, either acutely ongoing or developmental abnormalities in floccular target neurons of the visual pathways in the vestibular nuclei and/or in the oculomotor neuron junction with the eye muscles can in principle also affect the performance of their optokinetic reflex and/or visually enhanced vestibulo-ocular reflex. To overcome this potential caveat we investigated the dynamics of saccadic eye movements in *tg* mutants as well as their eye movements following electrical stimulation in the flocculus. The duration and velocity re amplitude profiles of their saccadic eye movements were normal. In this respect the phenotype of *tg* mutants diverges from that in rocker mice, which suffer from a different mutation in the same $\alpha 1_a$ -subunit of the P/Q-type channel and show deficits in both slow and fast phases of their eye movements (Stahl, 2004). Thus, strengthened by the specificity of the behavioural phenotype, the experiments on saccadic eye movements indeed indicate that neurons of the oculomotor nuclei in *tg* mice operate functionally normally. In addition, we demonstrated that the courses of the eye movements evoked by prolonged floccular stimulation appeared normal in *tg* mice indicating that a potential enhanced depletion of neurotransmitters at the oculomotor endplate is not apparent (see also Plomp et al., 2000; Qian and Noebels, 2000; Cao et al., 2004). Finally, equally important, we also demonstrated that the gain and phase values of the vestibulo-ocular reflex in the dark were not affected; these data also strongly indicate that the compensatory non-visual vestibular pathways to the oculomotor nuclei are not functionally impaired. Thus, all synaptic connections in the oculomotor pathway downstream of the flocculus are at least at the systems level functionally intact. These data however do not allow us to conclude that there are no changes at these synaptic inputs at the cell physiological level (Qian and Noebels, 2000). In fact, the total of cellular compensations may be such that the overall synaptic strengths in these connections are sufficiently preserved despite the shift away from the P/Q-type predominance mentioned above (Cao et al., 2004).

If Purkinje cell irregularities cause complete loss-of-function of the cerebellum in *tg*, ablations of their flocculus should not further decrease the gain values of their compensatory eye movements and their gain values with an intact flocculus should be similar to those of wild types with an ablated flocculus. On the other hand, if aberrations in neurons downstream of the cerebellar cortex contribute to ataxia in *tg* mutants, ablations of their flocculus should further decrease the gain values of their compensatory eye movements and their gain values with an intact flocculus does not need to be similar to those of wild types with an ablated flocculus. The outcome of our flocculectomy experiments in wild types and *tg* mutants, confirmed the first hypothesis and contradicted the second. Finally, if the abnormalities in the cerebellar cortex of the *tg* mutant are indeed sufficient to cause motor deficits, one expects that a local blockage of the P/Q-channels in the flocculus should be sufficient to impair at least in part the compensatory eye movements as well as the simple spike patterns in wild type

mice. This prediction was also largely upheld. The relatively small inconsistencies found between the phenotype of *tg* mutants and that of wild types treated with the P/Q-channel blocker ω -Agatoxin IVA (compare eg. VVOR data at highest frequencies) may be due to the longer-term secondary compensations that probably occur in the mutant only. Taken together, our eye movement recordings combined with our electrophysiological recordings, electrical stimulations, lesions and pharmacological blockage experiments indicate that the *tg* mutation in the α_{1a} -subunit of the P- and Q-type voltage-gated calcium channel leads to irregular simple spike firing patterns and that these irregular simple spike activities are sufficient to cause deficits in motor performance.

Functional implications

Our data obtained in *tg* mutants suggest that the noise level of neuronal firing patterns can be altered without any impact on their modulation and that such a change is sufficient to alternate motor behaviour. This possibility is further strengthened by our finding that the autocorrelation of the interspike intervals of the simple spike activities during modulation in wild types was not only much stronger than that during modulation in *tg* mutants but also than that during spontaneous activity in wild types. To the best of our knowledge this is one of the first times that such a relation has been found. Together the data suggest that the average firing rates and modulation amplitudes are thus not the sole deterministic parameters to explain cerebellar motor behaviour. It has been recognized by information theoreticians for quite some time that an optimal level of noise (i.e. irregularity) can be important for signal processing (Bialek et al., 1991; Mar et al., 1999; Steinmetz et al., 2001; Tiesinga et al., 2002). For example, models by Rieke and Chacron indicate that on the one hand noise will increase the trial-to-trial variability of a neural response to repeated presentations of a stimulus, but on the other hand it will also increase the variability of the spike train and thereby potentially lead to increased information capacity (Rieke et al., 1997; Chacron et al., 2003). Here, we showed that a mutation in the α_{1a} -subunit of the P/Q-type voltage-gated calcium channel leads to a noise level in the simple spike activities of Purkinje cells that is too high to allow effective signal transmission at its target nuclei in the cerebellar and vestibular nuclei during modulation. Apparently, at the level of individual Purkinje cell terminals many of the simple spikes in *tg* mutants fall outside the time window that is determined by the effective range of interspike intervals. This range may not only be determined by the properties of the synapses of the target neurons of the Purkinje cell terminals, but also by changes in intrinsic excitability of these neurons (Aizenman and Linden, 2000; Nelson et al., 2003).

Since patients suffering from ataxia in syndromes such as familial hemiplegic migraine, episodic ataxia type II, and spinocerebellar ataxia type VI have motor coordination problems that resemble those in *tg* mutants and because these syndromes are caused by comparable mutations in the same subunit (Ophoff et al., 1996; Baloh et al., 1997; Zuchenko et al., 1997; Ducros et al., 1999; Harno et al., 2003), irregular Purkinje cell activities may also contribute to the ataxia found in these patients. It should be noted, however, that the most severe forms of ataxia in these patients start to occur when the Purkinje cells start to degenerate (Gomez et al., 1997; Buttner et al., 1998), so the irregular Purkinje cell activities can only contribute to the motor coordination deficits during the first years of their disease. By elucidating the systems mechanism that may underlie part of their motor coordination problems, the current data raise the

possibility to design therapeutic neurostimulation protocols for patients with beginning forms of ataxia that result from similar mutations in their P/Q-type calcium channel (Ophoff et al., 1996). The fact that we were able to evoke eye movements by electrical stimulation in the flocculus of tg mutants further supports this possibility. The relevance of noise levels in firing patterns is probably not restricted to these pathological cases or to the area of the cerebellum. For example, Huxter and colleagues recently showed in hippocampal pyramidal cells that the time of firing and firing rate are dissociable and that they can represent two independent variables: respectively the animal's location within a place field and its speed of movement through the field (Huxter et al., 2003). Thus, proper modulation of neuronal activities is essential, but the absolute moment in time at which individual spikes occur can be equally crucial for signal processing in various brain regions under both pathological and physiological circumstances.

Acknowledgements

The authors thank Ings. J. van den Burg and L. Broos as well as B. Winkelman, M.Sc. and C. Andreescu, M.D. for excellent assistance, and Prof. Dr. P. Goadsby of University College London for providing us with protocols for the use of ω -Agatoxin-IVA *in vivo*. Research was supported by ZonMw (C.D.Z., A.v.d.M.), NWO-ALW (C.D.Z., M.F.), NWO-PIONIER (C.D.Z.), EEC (C.D.Z.), NWO-VIDI (M.F.) and NIH (J.S.).

Reference list

- Aizenman, C. D., and Linden, D. J. (2000). Rapid, synaptically driven increases in the intrinsic excitability of cerebellar deep nuclear neurons. *Nat Neurosci* 3, 109-111.
- Baloh, R.W., Yue, Q., Furman, J.M., and Nelson, S.F. (1997). Familial episodic ataxia: clinical heterogeneity in four families linked to chromosome 19p. *Ann Neurol* 41, 8-16.
- Bialek, W., Rieke, F., de Ruyter van Steveninck, R. R., and Warland, D. (1991). Reading a neural code. *Science* 252, 1854-1857.
- Bourinet, E., Soong, T. W., Sutton, K., Slaymaker, S., Mathews, E., Monteil, A., Zamponi, G. W., Nargeot, J., and Snutch, T. P. (1999). Splicing of alpha 1A subunit gene generates phenotypic variants of P- and Q-type calcium channels. *Nat Neurosci* 2, 407-415.
- Buttner, N., Geschwid, D., Jen, J. C., Perlman, S., Pulst, S. M., Baloh, R. W. (1998). Oculomotor phenotypes in autosomal dominant ataxias. *Arch Neurol* 55, 1353-1357.
- Campbell, D. B., North, J. B., and Hess, E. J. (1999). Tottering mouse motor dysfunction is abolished on the Purkinje cell degeneration (pcd) mutant background. *Exp Neurol* 160, 268-278.
- Cao, Y. Q., Piedras-Renteria, E. S., Smith, G. B., Chen, G., Harata, N. C., Tsien, R. W. (2003). Presynaptic Ca^{2+} channels compete for channel type-preferring slots in altered neurotransmission arising from Ca^{2+} channelopathy. *Neuron* 43, 387-400.
- Chacron, M. J., Longtin, A., and Maler, L. (2003). The effects of spontaneous activity, background noise, and the stimulus ensemble on information transfer in neurons. *Network* 14, 803-824.

- Craig, P. J., McAinsh, A. D., McCormack, A. L., Smith, W., Beattie, R. E., Priestley, J. V., Yip, J. L., Averill, S., Longbottom, E. R., Volsen, S. G. (1998) Distribution of the voltage-dependent calcium channel $\alpha(1A)$ subunit throughout the mature rat brain and its relationship to neurotransmitter pathways. *J Comp Neurol* 397, 251-267.
- De Zeeuw, C.I., Wylie, D.R., DiGiorgi, P.L., and Simpson, J.I. (1994) Projections of individual Purkinje cells of identified zones in the flocculus to the vestibular and cerebellar nuclei in the rabbit. *J. Comp. Neurol.* 349, 428-448.
- De Zeeuw, C.I., D.R. Wylie, J. Stahl, and J.I. Simpson (1995) Phase relations of floccular Purkinje cells during compensatory eye movements in the alert rabbit. *J. Neurophysiol.* 74, 2051-2063.
- De Zeeuw, C. I., Simpson, J. I., Hoogenraad, C. C., Galjart, N., Koekkoek, S. K., and Ruigrok, T. J. (1998). Microcircuitry and function of the inferior olive. *Trends Neurosci* 21, 391-400.
- Ducros, A., Denier, C., Joutel, A., Vahedi, K., Michel, A., Darcel, F., Madigand, M., Guerouaou, D., Tison, F., Julien, J., et al. (1999). Recurrence of the T666M calcium channel CACNA1A gene mutation in familial hemiplegic migraine with progressive cerebellar ataxia. *Am J Hum Genet* 64, 89-98.
- Fletcher, C. F., Lutz, C. M., O'Sullivan, T. N., Shaughnessy, J. D., Jr., Hawkes, R., Frankel, W. N., Copeland, N. G., and Jenkins, N. A. (1996). Absence epilepsy in tottering mutant mice is associated with calcium channel defects. *Cell* 87, 607-617.
- Frazor, R. A., Albrecht, D. G., Geisler, W. S., and Crane, A. M. (2004). Visual Cortex Neurons of Monkeys and Cats: Temporal Dynamics of the Spatial Frequency Response Function. *J Neurophysiol* 91, 2607-2627.
- Goossens, H. H., Hoebeek, F. E., Van Alphen, A. M., Van Der Steen, J., Stahl, J. S., De Zeeuw, C. I., and Frens, M. A. (2004). Simple spike and complex spike activity of floccular Purkinje cells during the optokinetic reflex in mice lacking cerebellar long-term depression. *Eur J Neurosci* 19, 687-697.
- Goossens, J., Daniel, H., Rancillac, A., van der Steen, J., Oberdick, J., Crepel, F., De Zeeuw, C. I., and Frens, M. A. (2001). Expression of protein kinase C inhibitor blocks cerebellar long-term depression without affecting Purkinje cell excitability in alert mice. *J Neurosci* 21, 5813-5823.
- Graf, W., Simpson, J. I., and Leonard, C. S. (1988). Spatial organization of visual messages of the rabbit's cerebellar flocculus. II. Complex and simple spike responses of Purkinje cells. *J Neurophysiol* 60, 2091-2121.
- Green, M. C., and Sidman, R. L. (1962). Tottering--a neuromuscular mutation in the mouse. And its linkage with oligosyndacylism. *J Hered* 53, 233-237.
- Harno, H., Hirvonen, T., Kaunisto, M.A., Aalto, H., Levo, H., Isotalo, E., Kallela, M., Kaprio, J., Palotie, A., Wessman, M., and Farkkila, M. (2003). Subclinical vestibulocerebellar dysfunction in migraine with and without aura. *Neurology* 61, 1748-1752.
- Hausser, M., Clark, B. A. (1997) Tonic synaptic inhibition modulates neuronal output pattern and spatiotemporal synaptic integration. *Neuron* 19, 665-678.
- Hillman, D., Chen, S., Aung, T. T., Cherksey, B., Sugimori, M., and Llinas, R. R. (1991). Localization of P-type calcium channels in the central nervous system. *Proc Natl Acad Sci U S A* 88, 7076-7080.
- Huxter, J., Burgess, N., and O'Keefe, J. (2003). Independent rate and temporal coding in hippocampal pyramidal cells. *Nature* 425, 828-832.
- Jaarsma, D., Postema, F., and Korf, J. (1992). Time course and distribution of neuronal

- degeneration in the dentate gyrus of rat after adrenalectomy: a silver impregnation study. *Hippocampus* 2, 143-150.
- Knight, Y. E., Bartsch, T., Kaube, H., Goadsby, P. J. (2002). P/Q-type calcium channel blockade in the periaqueductal gray facilitates trigeminal nociception: a functional genetic link for migraine? *J Neurosci* 22, RC213.
- Leenders, A. G., van den Maagdenberg, A. M., Lopes da Silva, F. H., Sheng, Z. H., Molenaar, P. C., Ghijsen, W. E. (2002). Neurotransmitter release from tottering mice nerve terminals with reduced expression of mutated P- and Q-type Ca²⁺-channels. *Eur J Neurosci* 15, 13-18.
- Li, Z., Morris, K. F., Baekey, D. M., Shannon, R., and Lindsey, B. G. (1999). Multimodal medullary neurons and correlational linkages of the respiratory network. *J Neurophysiol* 82, 188-201.
- Llinas, R., Sugimori, M., Lin, J. W., and Cherksey, B. (1989). Blocking and isolation of a calcium channel from neurons in mammals and cephalopods utilizing a toxin fraction (FTX) from funnel-web spider poison. *Proc Natl Acad Sci U S A* 86, 1689-1693.
- Mar, D. J., Chow, C. C., Gerstner, W., Adams, R. W., and Collins, J. J. (1999). Noise shaping in populations of coupled model neurons. *Proc Natl Acad Sci U S A* 96, 10450-10455.
- Matsushita, K., Wakamori, M., Rhyu, I. J., Arai, T., Oda, S. I., Mori, Y., and Imoto, K. (2002). Bidirectional Alterations in Cerebellar Synaptic Transmission of tottering and rolling Ca²⁺ Channel Mutant Mice. *J Neurosci* 22, 4388-4398.
- Mintz, I. M., Venema, V. J., Swiderek, K. M., Lee, T. D., Bean, B. P., and Adams, M. E. (1992). P-type calcium channels blocked by the spider toxin omega-Aga-IVA. *Nature* 355, 827-829.
- Montarolo, P. G., Palestini, M., and Strata, P. (1982). The inhibitory effect of the olivocerebellar input on the cerebellar Purkinje cells in the rat. *J Physiol* 332, 187-202.
- Nadler, J. V., and Evenson, D. A. (1983). Use of excitatory amino acids to make axon-sparing lesions of hypothalamus. *Methods Enzymol* 103, 393-400.
- Nelson, A. B., Krispel, C. M., Sekirnjak, C., and du Lac, S. (2003). Long-lasting increases in intrinsic excitability triggered by inhibition. *Neuron* 40, 609-620.
- Ophoff, R. A., Terwindt, G. M., Vergouwe, M. N., van Eijk, R., Oefner, P. J., Hoffman, S. M., Lamerdin, J. E., Mohrenweiser, H. W., Bulman, D. E., Ferrari, M., et al. (1996). Familial hemiplegic migraine and episodic ataxia type-2 are caused by mutations in the Ca²⁺ channel gene CACNL1A4. *Cell* 87, 543-552.
- Plomp, J. J., Vergouwe, M. N., Van den Maagdenberg, A. M., Ferrari, M. D., Frants, R. R., and Molenaar, P. C. (2000). Abnormal transmitter release at neuromuscular junctions of mice carrying the tottering alpha(1A) Ca(2+) channel mutation. *Brain* 123 Pt 3, 463-471.
- Qian, J., Noebels, J. L. (2000) Presynaptic Ca²⁺ channels and neurotransmitter release at the terminal of a mouse cortical neuron. *J Neurosci* 21, 3721-3728.
- Randall, A., Tsien, R. W. (1995). Pharmacological dissection of multiple types of Ca²⁺ channel currents in rat cerebellar granule neurons. *J Neurosci* 15, 2995-3012.
- Rieke, F., Warland, D., de Ruyter van Steveninck, R. R., and Bialek, W. (1997). *Spikes* (Massachusetts, MIT press).
- Sato, Y., Miura, A., Fushiki, H., Kawasaki, T. (1993) Barbiturate depresses simple spike

- activity of cerebellar Purkinje cells after climbing fiber input. *J Neurophysiol* 69, 1082-1090.
- Sausbier, M., Hu, H., Arntz, C., Feil, S., Kamm, S., Adelsberger, H., Sausbier, U., Sailer, C. A., Feil, R., Hofmann, F., Korth, M., Shipston, M. J., Knaus, H. G., Wolfer, D. P., Pedroarena, C. M., Storm, J. F., Ruth, P. (2004) Cerebellar ataxia and Purkinje cell dysfunction caused by Ca^{2+} -activated K^{+} channel deficiency. *Proc Natl Acad Sci U S A* 101, 9474-9478.
- Schmolesky, M. T., Weber, J. T., De Zeeuw, C. I., Hansel, C. (2002) The making of a complex spike: ionic composition and plasticity. *Ann N Y Acad Sci.* 978, 359-390.
- Simpson, J. I., Wylie, D. R., and De Zeeuw, C. I. (1996). On climbing fiber signals and their consequence(s). *Beh. Brain Sciences* 19, 380-394.
- Shields, K. G., Storer, R. J., Akerman, S. A., and Goadsby, P. J. Calcium channels modulate nociceptive transmission in the trigeminal nucleus of the cat. *Neuroscience* in press.
- Stahl, J. S. (2004). Eye movements of the murine p/q calcium channel mutant rocker, and the impact of aging. *J Neurophysiol* 91, 2066-2078.
- Stahl, J. S., and Simpson, J. I. (1995a). Dynamics of abducens nucleus neurons in the awake rabbit. *J Neurophysiol* 73, 1383-1395.
- Stahl, J. S., and Simpson, J. I. (1995b). Dynamics of rabbit vestibular nucleus neurons and the influence of the flocculus. *J Neurophysiol* 73, 1396-1413.
- Stahl, J. S., van Alphen, A. M., and De Zeeuw, C. I. (2000). A comparison of video and magnetic search coil recordings of mouse eye movements [In Process Citation]. *J Neurosci Methods* 99, 101-110.
- Stea, A., Tomlinson, W. J., Soong, T. W., Bourinet, E., Dubel, S. J., Vincent, S. R., and Snutch, T. P. (1994). Localization and functional properties of a rat brain $\alpha 1\text{A}$ calcium channel reflect similarities to neuronal Q- and P-type channels. *Proc Natl Acad Sci U S A* 91, 10576-10580.
- Steinmetz, P. N., Manwani, A., and Koch, C. (2001). Variability and coding efficiency of noisy neural spike encoders. *Biosystems* 62, 87-97.
- Tan, J., Gerrits, N. M., Nanhoe, R., Simpson, J. I., Voogd, J. (1995). Zonal organization of the climbing fiber projection to the flocculus and nodulus of the rabbit: a combined axonal tracing and acetylcholinesterase histochemical study. *J Comp Neurol* 356, 23-50.
- Tiesinga, P. H., Fellous, J. M., and Sejnowski, T. J. (2002). Attractor reliability reveals deterministic structure in neuronal spike trains. *Neural Comput* 14, 1629-1650.
- van Alphen, A. M., Stahl, J. S., and De Zeeuw, C. I. (2001). The dynamic characteristics of the mouse horizontal vestibulo-ocular and optokinetic response. *Brain Res* 890, 296-305.
- Van der Steen, J., Simpson, J. I., and Tan, J. (1994). Functional and anatomic organization of three-dimensional eye movements in rabbit cerebellar flocculus. *J Neurophysiol* 72, 31-46.
- Van der Steen, J., & Bruno, P. (1995). Unequal Amplitude Saccades Produced by Aniseikonic Patterns: Effects of Viewing Distance. *Vision Res* 35, 3459-3471.
- Wakamori, M., Yamazaki, K., Matsunodaira, H., Teramoto, T., Tanaka, I., Niidome, T., Sawada, K., Nishizawa, Y., Sekiguchi, N., Mori, E., et al. (1998). Single tottering mutations responsible for the neuropathic phenotype of the P-type calcium channel. *J Biol Chem* 273, 34857-34867.

- Westenbroek, R. E., Sakurai, T., Elliott, E. M., Hell, J. W., Starr, T. V., Snutch, T. P., and Catterall, W. A. (1995). Immunochemical identification and subcellular distribution of the alpha 1A subunits of brain calcium channels. *J Neurosci* 15, 6403-6418.
- Wylie, D. R., De Zeeuw, C. I., and Simpson, J. I. (1995). Temporal relations of the complex spike activity of Purkinje cell pairs in the vestibulocerebellum of rabbits. *J Neurosci* 15, 2875-2887.
- Zhang, J. F., Randall, A. D., Ellinor, P. T., Horne, W. A., Sather, W. A., Tanabe, T., Schwarz, T. L., Tsien, R. W. (1993) Distinctive pharmacology and kinetics of cloned neuronal Ca²⁺ channels and their possible counterparts in mammalian CNS neurons. *Neuropharmacol* 32, 1075-1088.
- Zhou, Y. D., Turner, T. J., and Dunlap, K. (2003). Enhanced G protein-dependent modulation of excitatory synaptic transmission in the cerebellum of the Ca²⁺ channel-mutant mouse, tottering. *J Physiol* 547, 497-507.
- Zhuchenko, O., Bailey, J., Bonnen, P., Ashizawa, T., Stockton, D.W., Amos, C., Dobyns, W.B., Subramony, S.H., Zoghbi, H.Y., and Lee, C.C. (1997). Autosomal dominant cerebellar ataxia (SCA6) associated with small polyglutamine expansions in the alpha 1A-voltage-dependent calcium channel. *Nat Genet* 15, 62-69.

Chapter 4

Plasticity of the parallel fibre to Purkinje cell synapse in motor learning

Chapter 4

Paragraph 1

Challenging the Marr-Albus-Ito Hypothesis

M. Schonewille, W. Amerika, Z. Gao, F.E. Hoebeek, M. de Jeu, D. Linden, R. Hugarir and C.I. De Zeeuw.

Abstract

Ever since Marr, Albus and Ito have put forward their hypothesis that long term depression at the parallel fiber to Purkinje cell synapse (PF-PC LTD) is the key element in cerebellar learning (Marr, 1969; Albus, 1971; Ito, 1982), this theory has dominated the field. So far most studies were aimed to block one or more of the central kinases involved in induction of PF-PC-LTD and to subsequently demonstrate that cerebellar motor learning is impaired (Aiba et al., 1994; Kim and Thompson, 1997; De Zeeuw et al., 1998; Koekkoek et al., 2003; Boyden et al., 2006; Hansel et al., 2006). However, these kinases operate relatively upstream in the molecular processes underlying LTD, and the behavioral impairments observed in these studies might thus have been due to deficits in processes other than LTD. We therefore created and tested 3 different mouse models in which the internalization of AMPA-receptors, which forms the actual site of expression of LTD, is directly affected (Steinberg et al., 2006). We show that neither short-term, one day adaptation (VOR gain-up, VOR gain-down, and OKR gain-up) nor long-term, six day adaptation (VOR phase-reverse) is affected in either of these mutants. These results provide strong evidence against the role of PF-PC LTD in adaptation of the vestibulo-ocular reflex (VOR) and thus contradict the longstanding hypothesis on cerebellar learning.

Introduction

Since the cerebellum is involved in both motor behavior and learning, mice with specific mutations targeted to eliminate motor learning could provide an excellent tool to study the related Purkinje cell activity. Synaptic plasticity including LTD and long-term potentiation (LTP) is generally considered to be the main mechanism in the central nervous system underlying learning. The theory of PF-PC LTD was originally based on models by Marr and Albus, which predicted that the cerebellar matrix consisting of the parallel fibers and orthogonally oriented climbing fibers is optimally designed for entraining and modifying the Purkinje cell output (Marr, 1969; Albus, 1971). Cell physiological data obtained by Ito confirmed this concept by showing that combined activation of these two inputs indeed resulted in a persistent depression of excitatory post-synaptic currents (EPSC) in Purkinje cells (Ito, 1982; Linden and Connor, 1995; Bear and Linden, 2000). Moreover, Ito and colleagues also showed that induction of LTD during visuovestibular training can in principle persistently modify the gain and phase of the simple spike activities of the floccular Purkinje cells that drive the VOR (Nagao, 1989) (for underlying circuitry see Fig. 1a). The potential correlation between LTD induction and VOR adaptation was subsequently supported by series of studies in mouse mutants in which both processes were blocked concomitantly (Aiba et al., 1994; Kim and Thompson, 1997; De Zeeuw et al., 1998; Feil et al., 2003; Koekkoek et al., 2003; Boyden et al., 2006; Hansel et al., 2006). For example, blockage of LTD by interfering in the PKC, PKG, α CamKII or α CamKIV pathways all resulted in impairment of VOR adaptation (De Zeeuw et al., 1998; Feil et al., 2003; Boyden et al., 2006; Hansel et al., 2006). Still, these studies were not conclusive (see also Raymond and Lisberger, 1997; Welsh et al., 2005), because all these kinases form central elements in the total of complex biochemical interactions inside the cytoplasm of Purkinje cells and they may thus also interact with proteins involved in one or more forms of plasticity other than postsynaptic parallel fiber LTD (see eg. Kano et al., 1996; Hansel et al., 2006).

Experimental Procedures

Eye movement recordings

All mice for eye movement recordings were between 12 and 30 weeks of age and were surgically prepared for experiments under general anesthesia of a mixture of isoflurane (Rhodia Organique Fine Ltd, Bristol, UK) and oxygen. A construct consisting of two nuts was attached to the frontal and parietal bones using Optibond prime and adhesive (Kerr, Bioggio, Switzerland) and Charisma (Heraeus Kulzer, Armonk, NY, USA). After a recovery period of 5 days the mouse was placed in a restrainer, with its head bolted to a bar. The restrainer was fixed onto the centre of the turntable. A cylindrical screen (diameter 63 cm) with a random-dotted pattern (each element 2°) surrounded the turntable (diameter 60 cm). The OKR and (V)VOR were evoked by rotating the surrounding screen and turntable, respectively, with an amplitude of 5° at different frequencies. The surrounding screen and the turntable were driven independently by AC servo-motors (Harmonic Drive AG, The Netherlands). Gain up and down adaptation was induced with 5° drum. The table and drum position signal were measured by potentiometers, filtered, digitized (CED Limited, UK), and stored on disk for off-line analysis. A CCD camera was fixed to the turntable in order to monitor the mouse's eyes. The eye movements were recorded at 240 Hz using an eye-tracking device (ISCAN Inc.). Video calibrations and subsequent eye movement computations were performed as described previously (Hoebbeck et al., 2005; Stahl et al., 2000).

Off-line analysis of eye movement recordings was performed in Matlab (MathWorks, Natick, MA) (Goossens et al., 2004). The gain and the phase of the eye movements were determined by fitting sine functions to the slow-phase eye velocity traces. Gain was computed as the ratio of eye velocity to stimulus velocity, whereas phase was expressed as the difference (in degrees) between the eye velocity and stimulus velocity traces.

In vitro electrophysiology

Male and female mutant and control mice (10 – 25 weeks of age) were anaesthetized with isoflurane (IVAX Pharmaceuticals, Runcorn, UK) and decapitated. The brains were removed and dissected in cold (0.5–4°C) oxygenated 'slicing' solution, containing (in mM): containing in mM: 124 NaCl, 5 KCl, 1.25 Na₂PO₄, 2 MgSO₄, 2 CaCl₂, 26 NaHCO₃ and 15 D-glucose; pH 7.4, when bubbled with 95% O₂ and 5% CO₂. Parasagittal slices (200 µm) were cut from the cerebellar vermis (HM 650V; Microm International GmbH, Walldorf, Germany) and incubated at 32°C for 40 minutes and thereafter at room temperature. After 20 minutes of incubation, the sucrose containing slicing solution was gradually replaced by a normal 'external' solution containing (in mM): 125 NaCl, 2.5 KCl, 2 CaCl₂, 1 MgCl₂, 25 NaHCO₃, 1.25 NaH₂PO₄, and 25 glucose; pH 7.4, when bubbled with 95% O₂ and 5% CO₂. Experiments were performed at room temperature in the presence of bath-applied 100 µM picrotoxin to block GABA_A receptors.

Slices were transferred to a submerged recording chamber and perfused with oxygenated external solution (1.5–2.5 ml/min). Patch-clamp recordings were made with Axopatch-200A or -200B amplifiers (Molecular Devices Corporation, Sunnyvale, CA) from visualized Purkinje cells. Whole-cell currents were recorded at room temperature (25 ± 1°C). Currents were filtered at 3kHz and digitized at 8kHz. For extracellular stimulation, glass pipettes were filled with external saline. Test responses were evoked at a frequency of 0.05 Hz using ca. 0.5–4 µA pulses that were applied for 500 (LTP) or 700 µs (LTD). Holding potentials were in the range of -60 to -75 mV. In all experiments, cells were

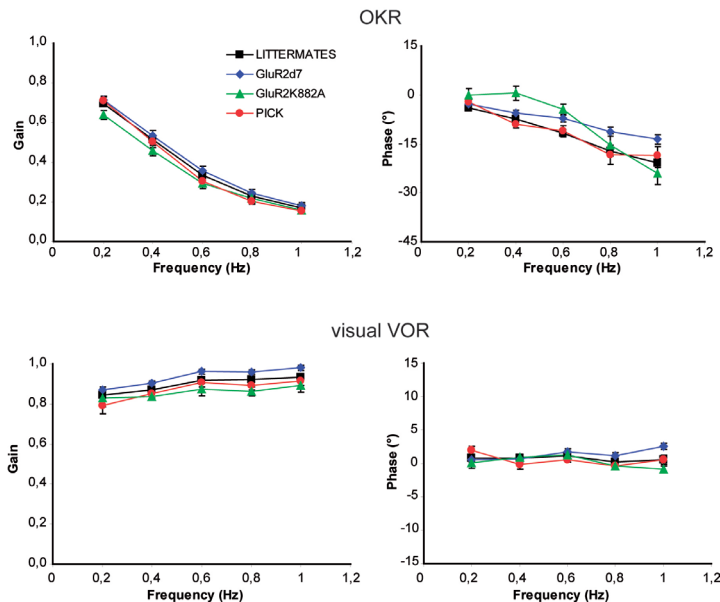


Figure 1. Basic performance is comparable to littermates in the LTD deficient mutants. The underlying circuit of compensatory eye movements is well documented and shown schematically (Fig. 1A). The optokinetic reflex (OKR) and visual vestibulo-ocular reflex (visual VOR) gain and phase values (Fig. 1B-C) of GluR2delta7, GluR2K882A and PICK1 were not significantly worse than wild type littermates. This shows that all mice have good vision and when visual stimulus is combined with vestibular stimulation mutant mice do not suffer from performance impairments that may affect training.

switched to current-clamp mode for tetanization. Recordings were excluded from the study if the series or input resistance varied by >15% over the course of the experiment. Paired PF-EPSCs were evoked by stimuli delivered with a glass pipette (containing external solution) located within the molecular cell layer (in a fixed position ~100-150 μm from the soma of the recorded Purkinje cell). PF-LTP was induced by PF stimulation at 1Hz for 5min.

Results

Here we investigated the role of PF-PC LTD in VOR-adaptation by testing three different mutant mice in which PF-PC LTD is affected at the actual site of plasticity itself, i.e. at the level of the glutamate receptors and related protein complex associated with the Purkinje cell membrane directly postsynaptic to the parallel fiber input (Steinberg et al., 2006). The mutants include the GluR2K882A knockin (KI) mouse, GluR2D7 KI mouse, and PICK1 knockout (KO) mouse. The GluR2K882A KI mouse contains a mutated form of GluR2, which incorporates a lysine mutation in the consensus recognition motif for PKC (S/T-X-K/R) and prevents thereby phosphorylation at S880 and internalization of the AMPA receptor (Kemp and Pearson, 1990; Wang and Linden, 2000; Xia et al., 2000; Chung et al., 2003; Steinberg et al., 2006). The GluR2D7 KI mutant is a homozygous KI mouse with a GluR2 AMPA receptor subunit that lacks the last seven amino acids; this mutation eliminates the C-terminal type II PDZ ligand and disrupts the interaction of GluR2 with PICK1 and GRIP1/2 (Xia et al., 2000; Steinberg et al., 2006). Finally, the homozygous PICK1 KO mouse lacks PICK1 and thereby the interface machinery that allows PKC to control the internalization of the AMPA receptor (Xia et al., 2000).

To find out as to whether these types of mutants are suited for detecting specific phenotypes in motor learning, we first made sure that they have no gross deficits in their

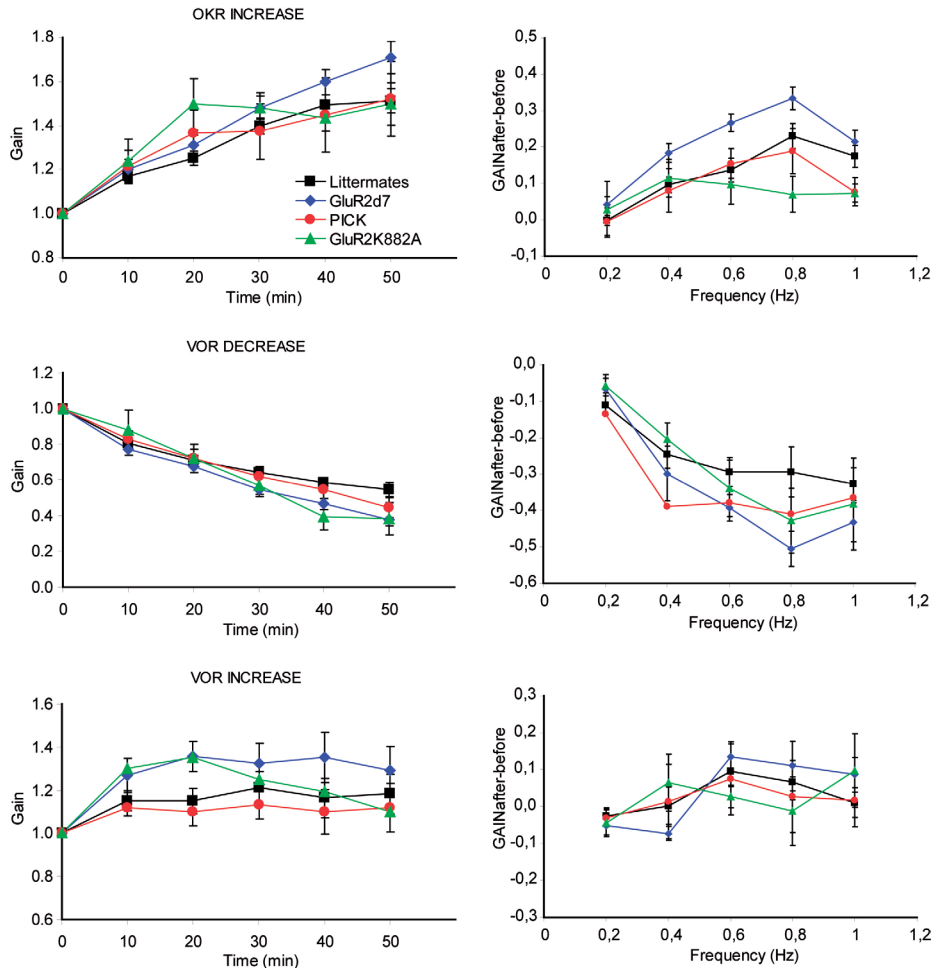


Figure 2. Short, one day, VOR and OKR gain adaptations were not affected in the mutated mice.

All short adaptations consisted of 5 times 10 min training, with recordings before, in between and after the training sessions, of which the gain values are shown. Columns show gain changes from normalized baseline gain over the training period (left), normalized gain after 50 min of training (middle) and change in gain (after – before) during training (right). OKR adaptation significantly increased OKR gain independent of the presence of a mutation (Fig. 2A). VOR adaptation through mismatch stimulation with OKR can be done in 2 directions: increase or decrease. Both were completed successfully by all three mutants, without significant differences with their littermates (Fig. 2B-C).

basic motor performance. Basic eye movement tests showed that both amplitudes (gain) and timing (phase) of the optokinetic reflex (OKR) and visual VOR in the mutants were not significantly worse ($p > 0.3$ for all values; ANOVA repeated measurements) from those in their wild type littermates over a range of stimulus frequencies varying from 0.2 Hz to 1.0 Hz (Fig. 1b, c and d). These data were comparable to those obtained in the LTD-deficient mutants in which one of the kinases PKC, PKG or α CamKII/IV are affected (De Zeeuw et al., 1998; Feil et al., 2003; Boyden et al., 2006; Hansel et al., 2006). Next to find out whether the GluR2K882A KI, GluR2D7 KI, and PICK1 KO also have the same deficits in motor learning as the kinase mutants, we subjected

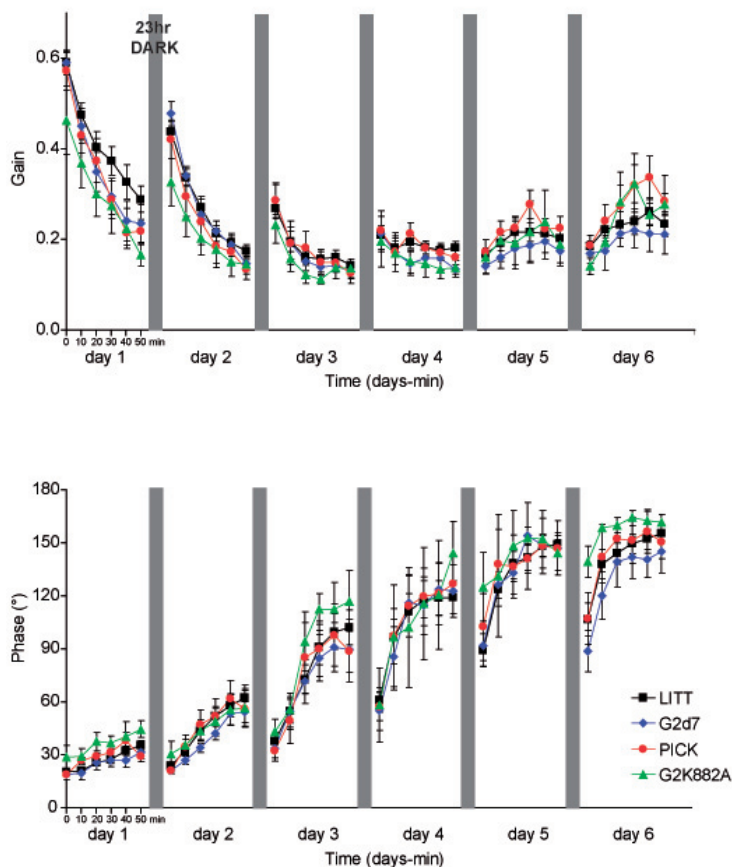


Figure 3. Long, multiple days, VOR phase adaptation was not affected in the mutated mice. Over a period of 6 days with 5 times 10 min of training each, mice had to reverse their VOR phase (reach a value of 180°). Again all three types of LTD-deficient mutant mice were perfectly capable of performing this learning-task.

them to various short-term adaptation tests including VOR gain-up and VOR gain-down adaptation as well as OKR gain-up adaptation (Fig. 2). After being exposed for one hour to different forms of visuovestibular training all mutants showed significant adaptation for all three paradigms ($p < 0.02$ for all paradigms, one-sample t-test) and none of the mutants showed any sign of impairment compared to the adaptation levels in wild types ($p > 0.1$ for all parameters, ANOVA for repeated measurements).

The outcomes of these tests stand in marked contrast to those of the kinase mutants (De Zeeuw et al., 1998; Feil et al., 2003; Boyden et al., 2006; Hansel et al., 2006), in which clear deficits of motor learning are apparent. In theory, possible differences among the GluR2K882A KI, GluR2D7 KI, and PICK1 KO mutants and their wild type littermates could become apparent when they are subjected to a longer, more robust training paradigm (see also Blazquez et al., 2004; De Zeeuw and Yeo, 2005). We therefore also employed a six day in phase visuovestibular training paradigm, which has resulted in very prominent gain and phase learning changes in wild types, but not in the LTD-deficient kinase mutants (eg. Van Alphen and De Zeeuw, 2002; Schonewille et al., 2007). However, here too both VOR gain and VOR phase values of all GluR2K882A KI, GluR2D7 KI, and PICK1 KO mutants adapted significantly and equally as well as their wild type littermates with comparable learning curves (Fig. 3). Thus, if one blocks LTD induction by directly

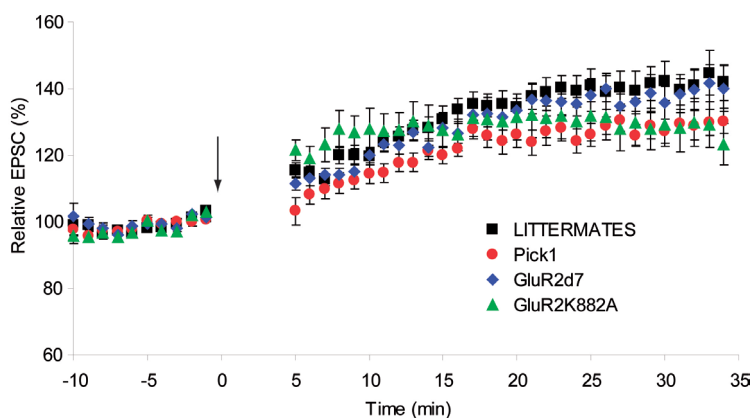


Figure 4. LTD-deficient mice show normal parallel fiber – Purkinje cell LTP. Parallel fiber–Purkinje cell LTP is not altered in slices of adult PICK1, GluR2D7 and GluR2K882A mice. PF-PC LTP was induced by PF stimulation alone at 1 Hz for 5 min (arrow). Error bars indicate SEM.

impairing endocytosis of the AMPA-receptors, no deficits in cerebellar motor learning can be observed neither after 3 different types of short-term training nor following an extremely strong form of long-term training.

Discussion

These data provide strong evidence against the reported role of PF-PC LTD in VOR adaptation and they raise two important questions. First, do the GluR2K882A KI, GluR2D7 KI, and PICK1 KO mutants show secondary compensations that may rescue the behavioral phenotype without affecting the loss of LTD induction? In theory, changes in LTP induction might partially compensate for impaired LTD induction (Lev-Ram et al., 2003; Coesmans et al., 2004). To exclude this possibility we investigated induction of postsynaptic LTP at the parallel fiber to Purkinje cell synapse in the mutant mice (Fig. 4). No significant difference in LTP ($p > 0.4$; ANOVA for repeated measurements) was found among the GluR2K882A KI, GluR2D7 KI, and PICK1 KO mutants and wild type littermates indicating that the loss of PF-PC LTD is not compensated by an altered capacity for PF-PC LTP. Second, if the blockage of PF-PC-LTD induction in the PKC, PKG and CamKII mutants is not the main cause for their deficits in VOR adaptation (De Zeeuw et al., 1998; Feil et al., 2003; Boyden et al., 2006; Hansel et al., 2006), which mechanism then is causing their impairments in motor learning? Since the genetic defects were specific for Purkinje cells in the L7-PKCi and L7-PKG/- mutants (De Zeeuw et al., 1998; Feil et al., 2003) as well as L7- α CamKII mutants (unpublished observations De Jeu and De Zeeuw), it appears unlikely that their behavioral deficits were caused by global genetic effects in the vestibulo-cerebellar eye movement system. However, in principle it appears possible that inactivation of kinases in Purkinje cells can affect, apart from PF-LTD, also plasticity at their inhibitory synaptic inputs from molecular layer interneurons. For example, activation of PKC may modulate the efficacy of their GABA receptors by influencing their surface density and sensitivity to positive allosteric modulators and/or by modifying chloride conductance (Song and Messing, 2005), while activation of CamKII may directly induce rebound potentiation at these GABAergic inputs (Kano et al., 1996). Similarly, recently it has been shown that Purkinje cells can also show signs of intrinsic plasticity, which may directly affect their firing rate (Hosy et al., 2007). Such a process, which involves active insertion and/

or endocytosis of multiple types of ion channels in the Purkinje cell membrane may well require one or more kinases. Thus, possible deficits in plasticity at the inhibitory synapses and/or in intrinsic plasticity provide interesting alternative pathways to explain the behavioral phenotypes observed in the Purkinje cell specific PKC, PKG and α CamKII mutants (De Zeeuw et al., 1998; Feil et al., 2003; Boyden et al., 2006; Hansel et al., 2006).

Taken together, the current study in which we employed three different mutant mice in which PF-LTD is directly blocked at its site of expression, provides strong evidence against the Marr-Albus-Ito hypothesis and it is difficult to draw any other conclusion than that PF-LTD is not necessary for any form of VOR adaptation.

Reference list

- Aiba A, Kano M, Chen C, Stanton ME, Fox GD, Herrup K, Zwingman TA, Tonegawa S (1994) Deficient cerebellar long-term depression and impaired motor learning in mGluR1 mutant mice. *Cell* 79:377-388.
- Albus JS (1971) A theory of cerebellar function. *Math Biosci* 10:25-61.
- Bear MF, Linden DJ (2000) The mechanisms and meaning of long-term synaptic depression in the mammalian brain. In: *Synapses* (Cowan WS, T. C.; Stevens, C. F., ed), pp 455-517. Baltimore: Johns Hopkins University Press.
- Blazquez PM, Hirata Y, Highstein SM (2004) The vestibulo-ocular reflex as a model system for motor learning: what is the role of the cerebellum? *Cerebellum* 3:188-192.
- Boyden ES, Katoh A, Pyle JL, Chatila TA, Tsien RW, Raymond JL (2006) Selective engagement of plasticity mechanisms for motor memory storage. *Neuron* 51:823-834.
- Chung HJ, Steinberg JP, Huganir RL, Linden DJ (2003) Requirement of AMPA receptor GluR2 phosphorylation for cerebellar long-term depression. *Science* 300:1751-1755.
- Coesmans M, Weber JT, De Zeeuw CI, Hansel C (2004) Bidirectional parallel fiber plasticity in the cerebellum under climbing fiber control. *Neuron* 44:691-700.
- De Zeeuw CI, Yeo CH (2005) Time and tide in cerebellar memory formation. *Curr Opin Neurobiol* 15:667-674.
- De Zeeuw CI, Hansel C, Bian F, Koekkoek SK, van Alphen AM, Linden DJ, Oberdick J (1998) Expression of a protein kinase C inhibitor in Purkinje cells blocks cerebellar LTD and adaptation of the vestibulo-ocular reflex. *Neuron* 20:495-508.
- Feil R, Hartmann J, Luo C, Wolfgruber W, Schilling K, Feil S, Barski JJ, Meyer M, Konnerth A, De Zeeuw CI, Hofmann F (2003) Impairment of LTD and cerebellar learning by Purkinje cell-specific ablation of cGMP-dependent protein kinase I. *J Cell Biol* 163:295-302.
- Goossens HH, Hoebeek FE, Van Alphen AM, Van Der Steen J, Stahl JS, De Zeeuw CI, Frens MA (2004) Simple spike and complex spike activity of floccular Purkinje cells during the optokinetic reflex in mice lacking cerebellar long-term depression. *Eur J Neurosci* 19:687-697.
- Hansel C, de Jeu M, Belmeguenai A, Houtman SH, Buitendijk GH, Andreev D, De Zeeuw CI, Elgersma Y (2006) α CaMKII is essential for cerebellar LTD and motor learning. *Neuron* 51:835-843.
- Hosy E, Belmeguenai A, Bengtsson F, De Zeeuw CI, Pedroarena CM, Jorntell H, Hansel CR (2007) Activity-dependent increases in the intrinsic excitability of cerebellar

- Purkinje cells. *Abstr Soc Neurosci* 364.7/N6.
- Ito M (1982) Cerebellar control of the vestibulo-ocular reflex--around the flocculus hypothesis. *Annu Rev Neurosci* 5:275-296.
- Kano M, Kano M, Fukunaga K, Konnerth A (1996) Ca^{2+} -induced rebound potentiation of gamma-aminobutyric acid-mediated currents requires activation of Ca^{2+} /calmodulin-dependent kinase II. *Proc Natl Acad Sci U S A* 93:13351-13356.
- Kemp BE, Pearson RB (1990) Protein kinase recognition sequence motifs. *Trends Biochem Sci* 15:342-346.
- Kim JJ, Thompson RF (1997) Cerebellar circuits and synaptic mechanisms involved in classical eyeblink conditioning. *Trends Neurosci* 20:177-181.
- Koekkoek SK, Hulscher HC, Dortland BR, Hensbroek RA, Elgersma Y, Ruigrok TJ, De Zeeuw CI (2003) Cerebellar LTD and learning-dependent timing of conditioned eyelid responses. *Science* 301:1736-1739.
- Lev-Ram V, Mehta SB, Kleinfeld D, Tsien RY (2003) Reversing cerebellar long-term depression. *Proc Natl Acad Sci U S A* 100:15989-15993.
- Linden DJ, Connor JA (1995) Long-term synaptic depression. *Annu Rev Neurosci* 18:319-357.
- Marr D (1969) A theory of cerebellar cortex. *J Physiol* 202:437-470.
- Nagao S (1989) Behavior of floccular Purkinje cells correlated with adaptation of vestibulo-ocular reflex in pigmented rabbits. *Exp Brain Res* 77:531-540.
- Raymond JL, Lisberger SG (1997) Multiple subclasses of purkinje cells in the primate floccular complex provide similar signals to guide learning in the vestibulo-ocular reflex. *Learn Mem* 3:503-518.
- Schonewille M, Wulff P, Renzi M, Wisden W, Farrant M, De Zeeuw CI (2007) Interneurons in the molecular layer of the cerebellum are required for consolidation of motor learning. *Abstr Soc Neurosci* 190.13/TT30.
- Song M, Messing RO (2005) Protein kinase C regulation of GABAA receptors. *Cell Mol Life Sci* 62:119-127.
- Steinberg JP, Takamiya K, Shen Y, Xia J, Rubio ME, Yu S, Jin W, Thomas GM, Linden DJ, Huganir RL (2006) Targeted in vivo mutations of the AMPA receptor subunit GluR2 and its interacting protein PICK1 eliminate cerebellar long-term depression. *Neuron* 49:845-860.
- Van Alphen AM, De Zeeuw CI (2002) Cerebellar LTD facilitates but is not essential for long-term adaptation of the vestibulo-ocular reflex. *Eur J Neurosci* 16:486-490.
- Wang YT, Linden DJ (2000) Expression of cerebellar long-term depression requires postsynaptic clathrin-mediated endocytosis. *Neuron* 25:635-647.
- Welsh JP, Yamaguchi H, Zeng XH, Kojo M, Nakada Y, Takagi A, Sugimori M, Llinas RR (2005) Normal motor learning during pharmacological prevention of Purkinje cell long-term depression. *Proc Natl Acad Sci U S A* 102:17166-17171.
- Xia J, Chung HJ, Wihler C, Huganir RL, Linden DJ (2000) Cerebellar long-term depression requires PKC-regulated interactions between GluR2/3 and PDZ domain-containing proteins. *Neuron* 28:499-510.

Chapter 4

Paragraph 2

Role of Calcineurin in Pf-PC LTP and Cerebellar Motor Learning

M. Schonewille, S.H. Houtman, G. Ohtsuki, H.J. Boele, A. Badura, A. Belmeguenai, S. Tonegawa, S.K. Koekkoek, Y. Elgersma, C.H. Hansel and C.I. De Zeeuw.

Abstract

Cerebellar motor learning is required to obtain proper procedural skills such as learning how to walk or to follow and reach a target. Recent models on the function of the cerebellum postulate that postsynaptic plasticity at its parallel fiber (Pf) synapses contribute to learning by employing the temporal coding of simple spike activities of Purkinje cells (PC) (Shin et al., 2007; Steuber et al., 2007; De Zeeuw et al., 2008). So far, all behavioral studies on plasticity at this site have been focused on the potential role of long-term depression (LTD) (for reviews see Ito, 2001). Here, we investigated the role of long-term potentiation at the same synapse (Pf-PC LTP) by creating and testing a Purkinje cell specific knockout mouse of Ca^{2+} -activated protein phosphatase 2B (PP2B or calcineurin). The selective deletion of PP2B indeed abolished Pf-PC LTP, whereas their LTD was unaffected. Moreover, the mutants showed both impaired adaptation of their vestibulo-ocular reflex (VOR) following visuo-vestibular mismatch training and impaired classical delay conditioning of their eyeblink response to a tone. As predicted by our model, the simple spike activities of the LTP deficient mutants showed an increased level of regularity (i.e., reduced CV_2) and a reduced number of long interspike intervals (i.e., > 20 ms), while their average firing frequency was unaffected. Thus, our data indicate that calcineurin-mediated Pf-PC LTP may contribute to the formation of temporal patterns of simple spike activities and thereby to cerebellar motor learning.

Introduction

As Pf-PC LTD is not the key element in motor learning it was hypothesized to be, new candidates should be considered. A prominent candidate can be found in the potentiation of the same synapse. For instance, the many parallel fiber to Purkinje cell synapses that appear silent could be reactivated by Pf-PC LTP. However, LTP is a relatively new phenomenon; little is known about its components. Recent studies revealed the requirement for phosphatase PP2B in the induction of LTP (Belmeguenai and Hansel, 2005), providing an opportunity to study the role of LTP in cerebellar motor learning.

Experimental procedures

Generation of L7-PP2B mice

Mutant mice in which calcineurin was selectively deleted from Purkinje cells were obtained by crossing the Cre-loxP-system (L7-PP2B mutant) heterozygous for PP2B-lox mice (Zeng et al., 2001) with mice heterozygous for the L7-Cre transgene (Barski et al., 2000). Littermates of the following genotypes were used for the experiments: PP2B-lox^{+/+} x L7Cre ^{+/+} (L7-PP2B) and PP2B-lox^{+/+} x L7Cre ^{-/-}, PP2B-lox^{-/-} x L7Cre ^{+/+} and PP2B-lox^{-/-} x L7Cre ^{-/-} (littermate controls).

Immunohistochemistry and electron microscopy

Immunocytochemistry of L7-PP2B was performed on free-floating 40 μm thick frozen sections from 3-5 month's old mice, employing a standard avidin-biotin-immunoperoxidase complex method (ABC, Vector Laboratories, USA) with PP2B as the primary antibody and diaminobenzidine (0.05%) as the chromogen (Jaarsma et al., 2001). For electron microscopy, sections were stained for calbindin immunocytochemistry with rabbit anti-calbindin antibody (Swant), osmicated, embedded in Durcupan, and processed for

electron microscopy (De Zeeuw et al., 1989).

In vitro electrophysiology

Sagittal slices of the cerebellar vermis (200-250 μ m) of 10-30 weeks old mice were kept in ACSF containing (in mM): 124 NaCl, 5 KCl, 1.25 Na₂HPO₄, 2 MgSO₄, 2 CaCl₂, 26 NaHCO₃, and 10 D-glucose aerated with 95%O₂ and 5% CO₂. 20 μ M bicuculline methiodide was added for the recordings to block GABA_A receptors. Whole-cell patch-clamp recordings were performed at room temperature using an EPC-10 amplifier (HEKA Electronics, Germany). Recording electrodes were filled with a solution containing (in mM): 9 KCl, 10 KOH, 120 K-gluconate, 3.48 MgCl₂, 10 HEPES, 4 NaCl, 4 Na₂ATP, 0.4 Na₃GTP and 17.5 sucrose (pH 7.25). All drugs were purchased from Sigma. Currents were filtered at 3kHz and digitized at 8kHz. For extracellular stimulation, glass pipettes were filled with external saline. Test responses were evoked at a frequency of 0.05 Hz using ca. 0.5-4 μ A pulses that were applied for 500 (LTP) or 700 μ s (LTD). Holding potentials in the range of -60 to -75 mV were chosen to prevent spontaneous spike activity. In all experiments, cells were switched to current-clamp mode for tetanization. Recordings were excluded from the study if the series or input resistance varied by >15% over the course of the experiment.

The role of calcineurin in PF-LTD and PF-LTP was addressed using whole-cell patch-clamp recordings from PCs. PF-LTD was induced by paired PF and climbing fiber (CF) stimulation at 1Hz for 5min in current-clamp mode, and measured by test responses recorded in voltage-clamp mode. PF-LTP was induced by PF stimulation at 1Hz for 5min.

To test whether CF elimination was delayed in L7-PP2B mice, we recorded CF-EPSCs in voltage-clamp mode. As CF-EPSCs preserve the all-or-none character that is typical for complex spikes recorded in current-clamp mode, one can determine the number of innervating CFs by stepwise increasing the stimulus intensity and counting the number of all-or-none steps in the EPSC amplitude.

Eye movement recordings

All mice for eye movement recordings were between 12 and 30 weeks of age and were surgically prepared for experiments under general anesthesia of a mixture of isoflurane (Rhodia Organique Fine Ltd, Bristol, UK) and oxygen. A construct consisting of two nuts was attached to the frontal and parietal bones using Optibond prime and adhesive (Kerr, Bioggio, Switzerland) and Charisma (Heraeus Kulzer, Armonk, NY, USA). After a recovery period of 5 days the mouse was placed in a restrainer, with its head bolted to a bar. The restrainer was fixed onto the centre of the turntable. A cylindrical screen (diameter 63 cm) with a random-dotted pattern (each element 2°) surrounded the turntable (diameter 60 cm). The OKR and (V)VOR were evoked by rotating the surrounding screen and turntable, respectively, with an amplitude of 5° at different frequencies. The surrounding screen and the turntable were driven independently by AC servo-motors (Harmonic Drive AG, The Netherlands). The table and drum position signal were measured by potentiometers, filtered, digitized (CED Limited, UK), and stored on disk for off-line analysis. A CCD camera was fixed to the turntable in order to monitor the mouse's eyes. The eye movements were recorded at 240 Hz using an eye-tracking device (ISCAN Inc.). Video calibrations and subsequent eye movement computations were performed as described previously (Stahl et al., 2000; Hoebeek et al., 2005).

Eyeblink conditioning.

The L7-PP2B mutants (C57Bl/6 background; $n = 9$) and wild type littermates ($n = 9$) were anesthetized with the use of an oxygenated mixture of nitrous oxide and halothane and a pre-made connector (SamTec; www.samtec.com) was placed with a pedestal of dental cement on the skull (for details see Koekkoek et al., 2003). A magnet embedded in silicon was implanted in a pocket dissected in the eyelid and a GMR sensor chip was placed over the upper eyelid such that the distance between the magnet and sensor in the eyelid closed situation was 2 mm and that the axis of sensitivity was aligned with the north-south axis of the magnet in the halfway closed position. Two insulated copper wires with a diameter of 30 μm were placed underneath the skin close to the lateral corner of the eyelids to provide the US. The US electrodes were connected to computer controlled stimulus isolation units (Dagan S910; www.dagan.com), which created biphasic constant current electrical shocks (30 ms, 166 Hz pulses) the strength of which was controlled by an unconditioned response based feedback mechanism (max 1 mA) to prevent fear conditioned responses.

The eyelid responses of the wild type mice and L7-PP2B mutants were conditioned to a tone as the CS (10 kHz, gradually increased over 40 ms to 78 dB) during daily training sessions of 8 blocks of 8 trials. The blocks consisted of 1 US-alone trial, 6 paired trials, and 1 CS-alone trial, and the trials were separated by a random inter-trial interval in the range of 20 to 40 s. In the first group of experiments the onsets of the CS and US were separated by an ISI of 350 ms.

In vivo electrophysiology

All mice for *in vivo* electrophysiological recordings were between 12 and 30 weeks of age and were surgically prepared under general anesthesia of a mixture of isoflurane, nitrous oxide, and oxygen for chronic neurophysiological experiments by mounting a pedestal as described above (Hoebeek et al., 2005). A recording chamber was built around craniotomies in both left and right occipital bones with a maximal diameter of 3 mm (Goossens et al., 2004). Mice were placed in the setup as described above.

Extracellular Purkinje cell activity was recorded using borosilicate glass electrodes (OD 2.0 mm, ID 1.16 mm, 2 M NaCl, 4-8 M Ω). Electrodes were advanced into the cerebellum by a hydraulic micro-drive (Narishige, Tokyo, Japan). Recordings were made from left and right Crus I and II, paramedian lobule, and (para)floculus. Purkinje cells were identified by the brief pause in simple spike activity following each complex spike. The raw electrode signal was amplified, filtered (CyberAmp, CED, Cambridge, UK), digitized (CED) and stored on disk for off-line analysis. Following each recording session the brain was covered with gramicidin-containing ointment and the chamber was sealed with bone wax.

Data Analysis

Off-line analysis of eye movements and *in vivo* recordings was performed in Matlab (MathWorks, Natick, MA) (Goossens et al., 2004). The gain and the phase of the eye movements were determined by fitting sine functions to the slow-phase eye velocity traces. Gain was computed as the ratio of eye velocity to stimulus velocity, whereas phase was expressed as the difference (in degrees) between the eye velocity and stimulus velocity traces. Baseline data are from 23 control and 15 L7-PP2B mice; gain up, gain down and non training data from 13- 14, 13-10 and 7-5 WT and L7-PP2B mice, respectively.

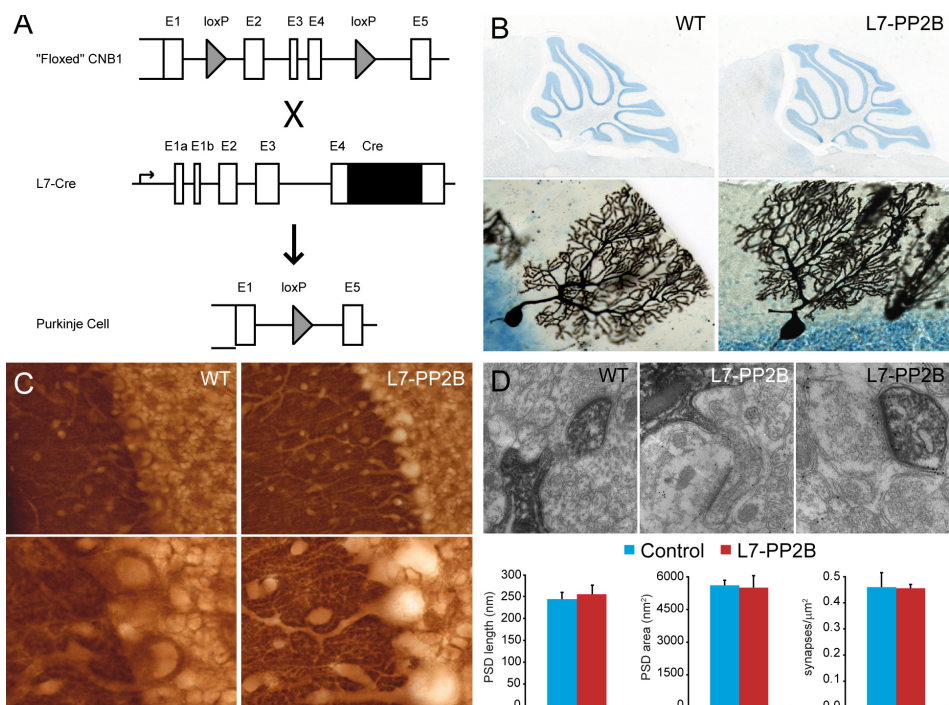


Figure 1. Cerebellar morphology is normal in L7-PP2B mutants.

The L7-PP2B mutant mice were created by crossing a floxed calcineurin line with an L7-Cre line (A). Calcineurin stainings of the cerebellar cortex confirm the selective deletion of PP2B from Purkinje cells en Purkinje cell dendrites extending into the molecular layer (ml) (B). Thionin and Golgi stainings of sagittal sections through the vermis showed no morphological or cytoarchitectural differences between control and L7-PP2B mice, respectively (C). Electron micrographic quantification of synaptic contacts with Calbindin stained Purkinje cell dendrites in the proximal and distal molecular layer revealed no differences between control and L7-PP2B mice (D). ml, molecular layer; pcl, Purkinje cell layer; gcl, granule cell layer. Scale bars: B) top, 1 mm; bottom, 25 μm; C) 25 μm and 50 μm.

In vivo recorded simple spikes and complex spikes were discriminated using custom-made routines based on principal component analysis. The interspike interval (ISI) distribution of each Purkinje cell was characterized by calculating the mean, CV (standard deviation divided by the mean) and CV_2 . The CV indicates the relative width of the distribution, the CV_2 is defined as the mean of $2 |ISI_{n+1} - ISI_n| / (ISI_{n+1} + ISI_n)$ and is a measure for the regularity of firing on small timescales (Holt et al., 1996; Shin et al., 2007).

Statistical analyses

Statistical tests were performed with SPSS 13 (SPSS Inc., Chicago, IL). Data were compared with two-tailed un-paired Student's *t*-tests or two-way repeated-measures ANOVA, as appropriate. The level of significance was set at $p < 0.05$.

Results

To investigate the potential role of Pf-PC LTP in cerebellar motor learning (Suppl. Fig. S1) we developed mutant mice in which calcineurin was selectively deleted from Purkinje cells using the Cre-loxP-system (L7-PP2B mutant) (Fig. 1a) (Barski et al., 2000; Zeng et al.,

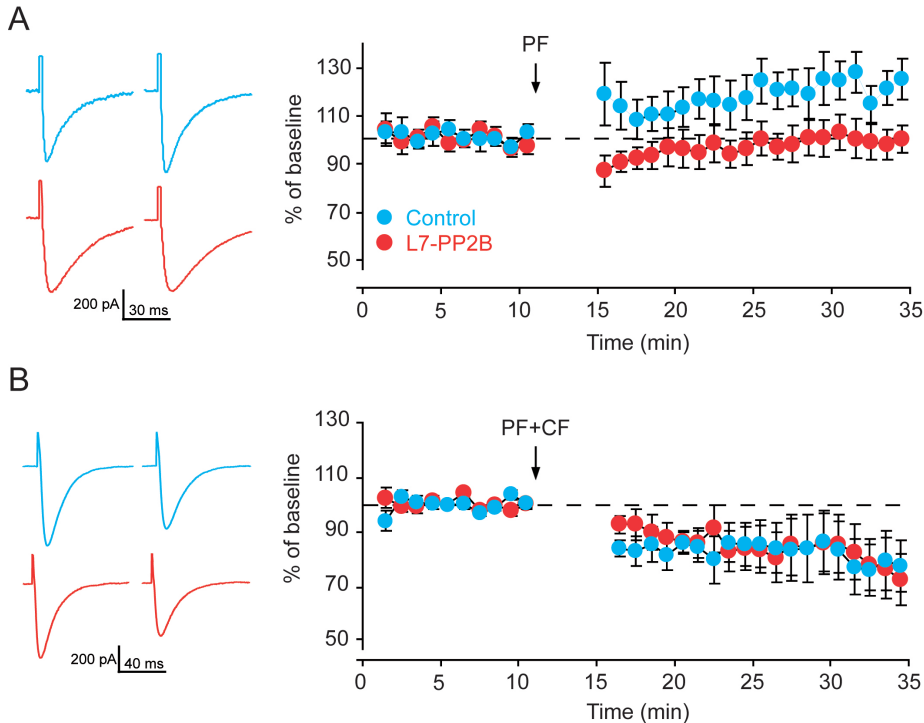
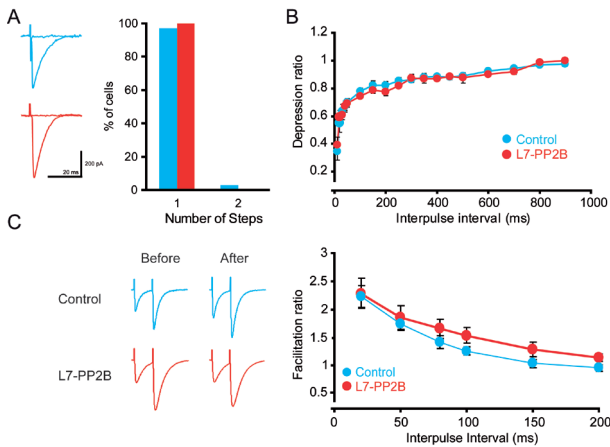


Figure 2. L7-PP2B mice show impaired parallel fiber – Purkinje cell LTP.

Parallel fiber – Purkinje cell LTP (A), but not LTD (B), is impaired in slices of adult L7-PP2B mice. PF-PC LTP was induced by PF stimulation alone at 1 Hz for 5 min and paired PF and CF stimulation at 1 Hz for 5 min was used to induce LTD. Traces show EPSCs before (dashed) and after LTD/LTP induction. Numbers between brackets indicate the number of cells. Error bars indicate SEM.

2001). Immunocytochemical analysis of these mutants confirmed that PP2B was indeed specifically deleted in their Purkinje cells (Fig. 1b). The mutation did not cause any overt morphological aberration in that thionine stainings and Golgi stainings revealed a normal foliation of the cerebellar cortex and cyto-architecture of Purkinje cells, respectively (Fig. 1c). Moreover, electron microscopic examinations of calbindin stained Vibrotome sections of the cerebellar cortex of the L7-PP2B mutants showed that the number and size of synaptic inputs from the parallel fibers, climbing fibers, and interneurons onto Purkinje cells were not significantly different from those in littermate controls (in all cases $p > 0.2$; t-tests) (Fig. 1d).

We designed the L7-PP2B mutants based upon our previous cell physiological experiments in rat cerebellar slices in which induction of postsynaptic LTP in Purkinje cells was blocked following pharmacological application of PP2B inhibitor cyclosporin A (Belmeguenai and Hansel, 2005). Cell physiological examination of the L7-PP2B mutants indeed showed that Pf-PC LTP induction was completely blocked ($p = 0.027$; t-test), whereas LTD induction at the same synapse was unaffected ($p > 0.9$; t-test) (Fig. 2). Since the presence or absence of climbing fiber activity is critical for the induction of LTD and LTP, respectively (Lev-Ram et al., 2003; Coesmans et al., 2004), we also examined whether deletion of PP2B in Purkinje cells can lead, just like that of kinases such as PKC and α CamKII (De Zeeuw et al., 1998; Hansel et al., 2006), to an abnormal climbing fiber

**Suppl. Figure 1.**

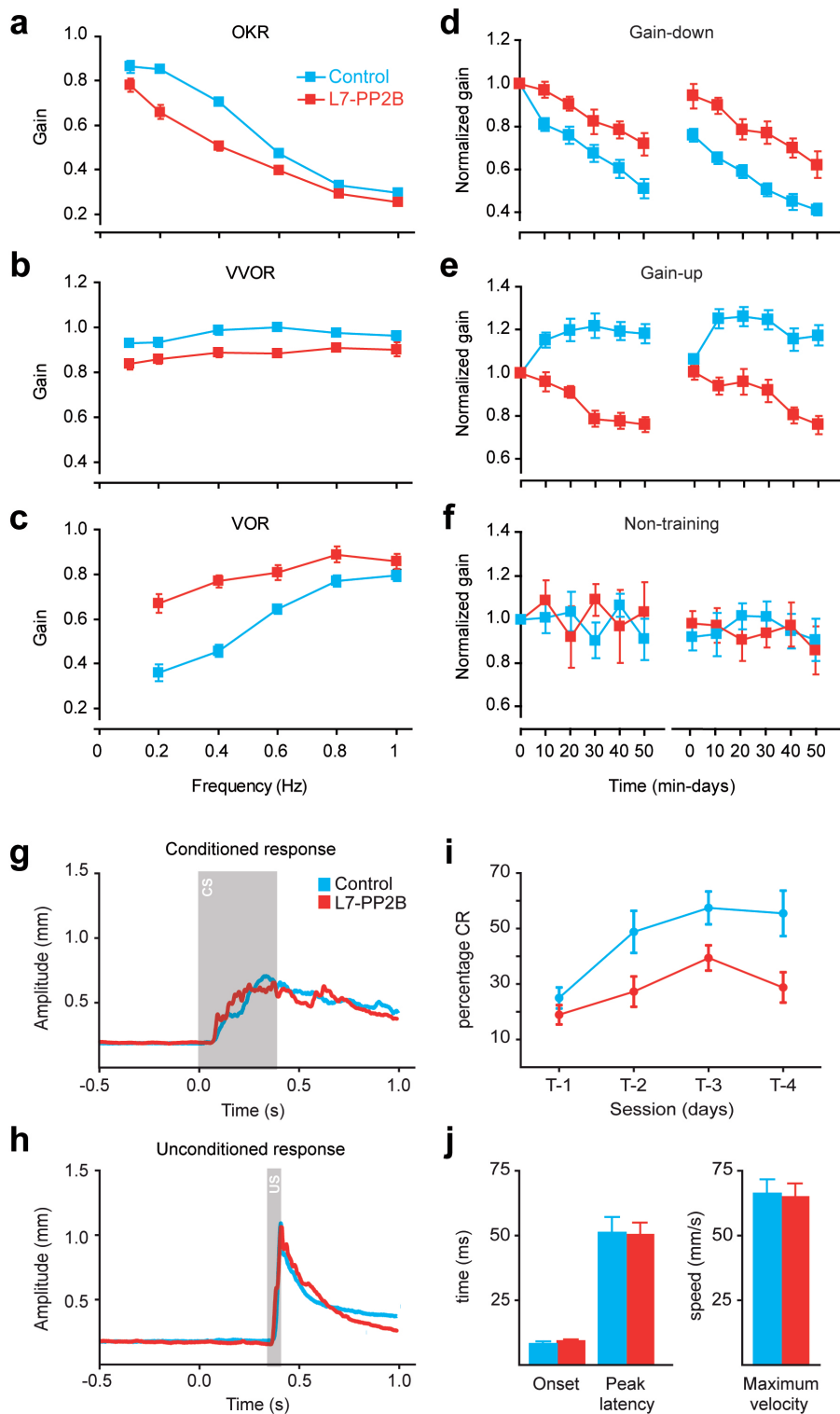
Climbing fiber elimination is not affected in L7-PP2B mutant mice. All-or-none climbing fiber EPSCs were evoked at increasing stimulus intensities. Traces show EPSCs above and below threshold. Climbing fiber elimination is nearly complete in Purkinje cells of both wild-type and L7-PP2B mice at 20-24 wks (wild-type, $n = 33$ cells from 12 mice; mutant, $n = 12$ cells from 3 mice).

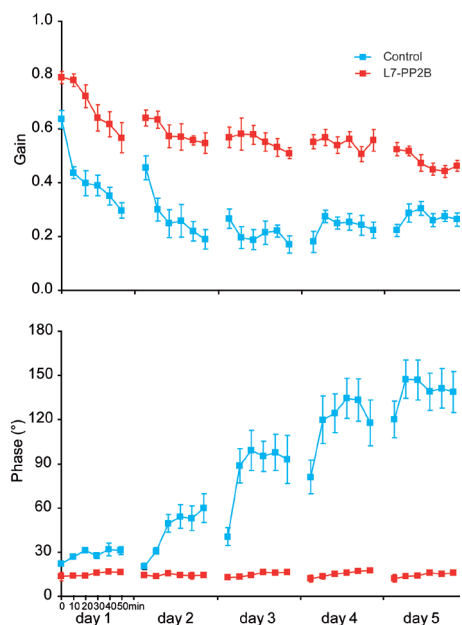
(B) Paired-pulse facilitation (PPF) is normal in L7-PP2B mice. PPF ratios were determined for the indicated stimulus intervals in both wild-type ($n = 8$) and mutant mice ($n = 5$). Traces show facilitation at 50 ms interpulse intervals. Error bars indicate SEM.

innervation. Suppl. Fig. S2 shows that the development of climbing fiber elimination in L7-PP2B mutant mice is normal and can therefore not cause the impaired induction of Pf-PC LTP.

The animals did not show any gross sign of ataxia; to find out whether the selective blockage of LTP induction in Purkinje cells leads to a specific cerebellar motor coordination deficit, we subjected them to compensatory eye movement tests, which allow us to discriminate abnormalities in motor performance and motor learning (De Zeeuw et al., 1998; Hoebeek et al., 2005; Hansel et al., 2006). The basic measurements of gain (amplitude) and phase (timing) of the optokinetic reflex (OKR) and/or VOR showed that their motor performance was slightly, but significantly, affected (for gain values all p values < 0.001 , ANOVA for repeated measurements; for phase data all p values < 0.01 , data not shown) (Fig. 3a-c). The ability of the LTP-deficient mice to learn new motor behaviors was much more severely affected. In a two-day visuo-vestibular mismatch paradigm aimed at reducing the gain of the VOR, learning was significantly less in the mutants (Fig. 3d) ($p < 0.002$ for both days, ANOVA for repeated measurements). In the opposite training paradigm, which was aimed at increasing the gain, the gain values of the mutants even showed a decrease (Fig. 3e; comparison among mutants and controls $p < 0.0001$ for both days, ANOVA for repeated measurements). Control experiments showed that this decrease was not due to effects of fatigue, because exposure of a normal, no-mismatch combination of optokinetic and vestibular stimulation for the same duration did not induce any decrease (Fig. 3f). The ability of the mutants to learn was affected in such a profound way that they were also completely unable to reverse their phase during phase reversal training (Suppl. Fig. S3). In contrast, controls were able to reverse their phase by 150 degrees in five consecutive training sessions (5th day, comparison among mutants and controls $p < 0.0001$, ANOVA for repeated measurements). Thus, the Purkinje cell specific, LTP-deficient mutants were affected in all forms of VOR adaptation tested.

Still, one might argue that these deficits in cerebellar motor learning might have been partly caused by a mild deficit in eye movement performance rather than the other way around. Therefore, we also subjected the animals to a cerebellar learning paradigm, which is aimed at acquiring a motor skill that normally does not occur: delay conditioning of an eyeblink response to a tone using an air-puff as the unconditioned





Suppl. Figure 3. Long-term VOR adaptation is dramatically impaired in L7-PP2B mutants.

L7-PP2B mice performed significantly worse during four consecutive days of mismatch training to reverse the phase of the VOR phase. In fact, L7-PP2B mutant mice were completely unable to change their VOR phase. Reversal training data are from 8 WT and 8 L7-PP2B mice. Vertical error bars denote SEM.

stimulus (Koekkoek et al., 2003). After 4 paired training sessions (T-1 to T-4) the L7-PP2B mutants showed significantly less conditioned responses than their wild type littermates (comparison among mutants and controls $p < 0.015$, ANOVA for repeated measurements), while this difference was absent during the first training sessions (Fig. 3g). The difference in cerebellar motor learning was not due to a difference in motor performance, because the kinetics of the unconditioned eyeblink response in the L7-PP2B mutants was indistinguishable from that in controls (Fig. 3h). Taken together our behavioral data indicate that Purkinje cell specific impairment of LTP induction at their parallel fiber synapses result in deficits in cerebellar motor learning.

Current models indicate that changes in the temporal patterns of the simple spike activities of Purkinje cells should be sufficient to affect cerebellar motor learning (Shin et al., 2007; Steuber et al., 2007; De Zeeuw et al., 2008). We therefore recorded Purkinje

cell activities in awake behaving animals. The average firing frequency of both the simple spike and complex spike activities in the PP2B mutants did not differ from those in controls (comparison among mutants and controls both $p > 0.5$, t-tests). In contrast, the temporal patterns of the simple spike activities, but not of the complex spike activities, differed significantly (Fig 4). The simple spike activities of the LTP-deficient PP2B mutants showed an enhanced level of regularity compared to controls; their CV_2 value, which is the coefficient of variation for consecutive interspike intervals, was significantly lower (comparison among mutants and controls $p < 0.0001$, t-test). Thus, together our data suggest that PP2B-dependent Pf-PC LTP influences the regularity of Purkinje cell activity and thereby cerebellar motor performance and motor learning.

Figure 3. Motor learning is impaired in L7-PP2B mutants.

Motor performance during the optokinetic reflex (OKR) (a) as well as during the vestibulo-ocular reflex in the light (VVOR) (b) and in the dark (VOR) (c) revealed significant but slight gain aberrations in L7-PP2B mice. L7-PP2B mice performed significantly worse during two days of mismatch training to either decrease (d) or increase (e) the VOR gain. Without training stimulus no differences were observed (f), contradicting a-specific problems to be the cause of results in (d-e). Motor learning problems were confirmed in a delay conditioning of an eyeblink response to a tone. L7-PP2B mice demonstrated significantly less conditioned responses over four days of training sessions (g). This was not due the result of motor performance problems, as the kinetics of the unconditioned eyeblink response were not different. Baseline eye movement data are from 23 control and 15 L7-PP2B mice; gain up, gain down and non training data from 13 / 14, 13 / 10 and 7 / 5 WT / L7-PP2B mice, respectively. Eyeblink data are from 9 control and 9 L7-PP2B mice. Vertical error bars denote SEM.

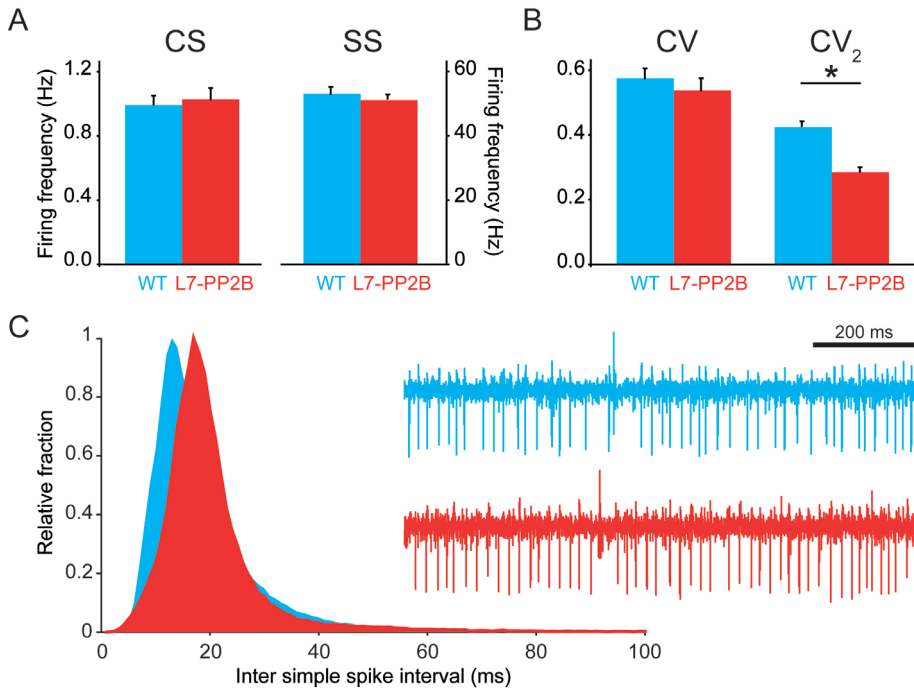


Figure 4. Purkinje cell simple spike activity is more regular in L7-PP2B mutants.

In vivo extracellular recordings of single unit Purkinje cells in awake mice revealed no difference in frequency of simple and complex spike activities (A). Detailed analysis of the regularity of simple spike trains however, confirms current hypotheses on the importance of temporal patterns. Overall regularity is not affected (CV), but local regularity (CV₂) was significantly lower in L7-PP2B mutants (B). Inter simple spike interval distributions indicate that the increased regularity in L7-PP2B mutants is caused by a loss of both shorter and longer intervals (C).

Discussion

The current study is the first to specifically address the role of PP2B and Pf-PC LTP in cerebellar motor learning. Historically, virtually all studies aimed at elucidating the molecular and cellular mechanisms underlying cerebellar motor learning focused on the role of depression rather than potentiation of the Pf-PC synapse (Albus, 1971; Ito, 1982, for review see Ito, 2000). Many studies provided supportive evidence that kinases such as PKC, PKG or CaMKII contribute to the induction of Pf-PC LTD as well as to one or more form(s) of cerebellar motor learning (De Zeeuw et al., 1998; Boyden and Raymond, 2003; Feil et al., 2003; Hansel et al., 2006). The behavioral phenotypes that we observed in the LTP-deficient PP2B mutant were similar to and at least as robust as those that we observed in Purkinje cell specific LTD-deficient mutants. These data indicate that Pf-PC LTD is not the only cellular phenomenon that may be required for cerebellar motor learning. In fact, they suggest that LTD and LTP together may shape the spatiotemporal patterns of the simple spike activities and thereby together optimize the settings for memory formation and retrieval in the cerebellar nuclei and cerebellar cortex (Shin et al., 2007; Steuber et al., 2007; De Zeeuw et al., 2008). Interestingly, in the hippocampus similar interactions may occur at the systems level even though LTP and LTD are mediated by molecular processes that are opposite to those in the cerebellum (for review see Jorntell and Hansel, 2006). In contrast to that in cerebellar Purkinje cells,

induction of LTP in hippocampal pyramidal cells is mediated by kinase pathways such as that of α CamKII, whereas LTD in these cells is dependent on phosphatases such as PP2B (Zeng et al., 2001). Yet, here too, both LTP-deficient mutants and LTD-deficient mutants can show similar deficits in hippocampal dependent learning (Zeng et al., 2001; Jorntell and Hansel, 2006). Thus, in a learning system operating in vivo LTP and LTD may act much more concomitantly than one might expect from the bidirectional synaptic switch mechanisms that can be observed in cerebellar and hippocampal tissue in vitro (Zeng et al., 2001; Coesmans et al., 2004). Therefore, LTP and LTD may neither be the selective cell physiological correlates for learning and forgetting in the hippocampus, nor for forgetting and learning in the cerebellum. Instead, they may both contribute to both behavioral processes by shaping simultaneously the efficacies of individual synapses, which in turn together may integrate into specific spatiotemporal spiking patterns of its neurons downstream.

Reference list

- Albus JS (1971) A theory of cerebellar function. *Math Biosci* 10:25-61.
- Barski JJ, Dethleffsen K, Meyer M (2000) Cre recombinase expression in cerebellar Purkinje cells. *Genesis* 28:93-98.
- Belmeguenai A, Hansel C (2005) A role for protein phosphatases 1, 2A, and 2B in cerebellar long-term potentiation. *J Neurosci* 25:10768-10772.
- Boyden ES, Raymond JL (2003) Active reversal of motor memories reveals rules governing memory encoding. *Neuron* 39:1031-1042.
- Coesmans M, Weber JT, De Zeeuw CI, Hansel C (2004) Bidirectional parallel fiber plasticity in the cerebellum under climbing fiber control. *Neuron* 44:691-700.
- De Zeeuw CI, Hoebeek FE, Schonewille M (2008) Causes and consequences of oscillations in the cerebellar cortex. *Neuron* 58:655-658.
- De Zeeuw CI, Holstege JC, Ruigrok TJ, Voogd J (1989) Ultrastructural study of the GABAergic, cerebellar, and mesodiencephalic innervation of the cat medial accessory olive: anterograde tracing combined with immunocytochemistry. *J Comp Neurol* 284:12-35.
- De Zeeuw CI, Hansel C, Bian F, Koekkoek SK, van Alphen AM, Linden DJ, Oberdick J (1998) Expression of a protein kinase C inhibitor in Purkinje cells blocks cerebellar LTD and adaptation of the vestibulo-ocular reflex. *Neuron* 20:495-508.
- Feil R, Hartmann J, Luo C, Wolfgruber W, Schilling K, Feil S, Barski JJ, Meyer M, Konnerth A, De Zeeuw CI, Hofmann F (2003) Impairment of LTD and cerebellar learning by Purkinje cell-specific ablation of cGMP-dependent protein kinase I. *J Cell Biol* 163:295-302.
- Goossens HH, Hoebeek FE, Van Alphen AM, Van Der Steen J, Stahl JS, De Zeeuw CI, Frens MA (2004) Simple spike and complex spike activity of floccular Purkinje cells during the optokinetic reflex in mice lacking cerebellar long-term depression. *Eur J Neurosci* 19:687-697.
- Hansel C, de Jeu M, Belmeguenai A, Houtman SH, Buitendijk GH, Andreev D, De Zeeuw CI, Elgersma Y (2006) α CaMKII is essential for cerebellar LTD and motor learning. *Neuron* 51:835-843.
- Hoebeek FE, Stahl JS, van Alphen AM, Schonewille M, Luo C, Rutteman M, van den

- Maagdenberg AM, Molenaar PC, Goossens HH, Frens MA, De Zeeuw CI (2005) Increased noise level of purkinje cell activities minimizes impact of their modulation during sensorimotor control. *Neuron* 45:953-965.
- Holt GR, Softky WR, Koch C, Douglas RJ (1996) Comparison of discharge variability in vitro and in vivo in cat visual cortex neurons. *J Neurophysiol* 75:1806-1814.
- Ito M (1982) Questions in modeling the cerebellum. *J Theor Biol* 99:81-86.
- Ito M (2001) Cerebellar long-term depression: characterization, signal transduction, and functional roles. *Physiol Rev* 81:1143-1195.
- Jaarsma D, Rognoni F, van Duijn W, Verspaget HW, Haasdijk ED, Holstege JC (2001) CuZn superoxide dismutase (SOD1) accumulates in vacuolated mitochondria in transgenic mice expressing amyotrophic lateral sclerosis-linked SOD1 mutations. *Acta Neuropathol (Berl)* 102:293-305.
- Jorntell H, Hansel C (2006) Synaptic memories upside down: bidirectional plasticity at cerebellar parallel fiber-Purkinje cell synapses. *Neuron* 52:227-238.
- Koekkoek SK, Hulscher HC, Dortland BR, Hensbroek RA, Elgersma Y, Ruigrok TJ, De Zeeuw CI (2003) Cerebellar LTD and learning-dependent timing of conditioned eyelid responses. *Science* 301:1736-1739.
- Lev-Ram V, Mehta SB, Kleinfeld D, Tsien RY (2003) Reversing cerebellar long-term depression. *Proc Natl Acad Sci U S A* 100:15989-15993.
- Shin SL, Hoebeek FE, Schonewille M, De Zeeuw CI, Aertsen A, De Schutter E (2007) Regular patterns in cerebellar Purkinje cell simple spike trains. *PLoS ONE* 2:e485.
- Stahl JS, van Alphen AM, De Zeeuw CI (2000) A comparison of video and magnetic search coil recordings of mouse eye movements [In Process Citation]. *J Neurosci Methods* 99:101-110.
- Steuber V, Mittmann W, Hoebeek FE, Silver RA, De Zeeuw CI, Hausser M, De Schutter E (2007) Cerebellar LTD and pattern recognition by Purkinje cells. *Neuron* 54:121-136.
- Zeng H, Chattarji S, Barbarosie M, Rondi-Reig L, Philpot BD, Miyakawa T, Bear MF, Tonegawa S (2001) Forebrain-specific calcineurin knockout selectively impairs bidirectional synaptic plasticity and working/episodic-like memory. *Cell* 107:617-629.

Chapter 5

Role of GABAergic Interneurons in Cerebellar Motor Learning

M. Schonewille, P. Wulff, A. Badura, M. Renzi, M. Sassoè-Pognetto, Z. Gao, F.E. Hoebeek, W. Wisden, M. Farrant and C.I. De Zeeuw

Abstract

Studies on learning and memory have focused largely on the role of plasticity at excitatory synapses onto projecting neurons. Here we examined the role of synaptic feed-forward inhibition from molecular layer interneurons onto Purkinje cells in cerebellar motor learning. We investigated adaptation of the vestibulo-ocular reflex in a mouse model (PC- $\Delta\gamma 2$), in which the GABA_A receptor $\gamma 2$ subunit was selectively deleted from Purkinje cells, resulting in a loss of GABA_A receptor-mediated synaptic inhibition. While baseline motor performance in these mice was only mildly, but significantly impaired, motor learning was severely disrupted. Specifically, phase reversal learning as well as consolidation of both gain and phase adaptations of the vestibular ocular reflex were strongly compromised. The simple spike activities of Purkinje cells in PC- $\Delta\gamma 2$ mice showed abnormal temporal patterns, both during and in the absence of naturally evoked compensatory eye movements, whereas mean firing frequencies were unaffected. We used these experimental data to generate computer simulations of the vestibulo-cerebellar system. We propose that feed-forward inhibition from molecular layer interneurons, by controlling the temporal patterns of Purkinje cell activity, is necessary for the consolidation of cerebellar learning in downstream neurons of the cerebellar and vestibular nuclei.

Introduction

A fundamental tenet of modern neuroscience is that plasticity at excitatory synapses onto projecting neurons underlies various types of memory formation. Examples include the putative role of long-term potentiation (LTP) at the CA3 - CA1 synapse onto hippocampal pyramidal cells in declarative memory formation (Lisman and Raghavachari, 2006; Whitlock et al., 2006) and the possible role of long-term depression (LTD) at the parallel fiber to Purkinje cell synapse in procedural memory formation (Boyden et al., 2004 and 2006; De Zeeuw et al., 1998; Hansel et al., 2006). However, results described in chapter 4, together with these studies done on kinase mutation based LTD-deficient mice, demonstrate that although there is a clear role for kinases in motor learning, this role can not be confirmed with mutations downstream of kinases. This discrepancy could be caused by the rather general function of kinases, and consequently the involvement of other forms of kinase-dependent plasticity in motor learning cannot be excluded. For instance, the largely ignored feed-forward inhibition of molecular layer interneurons is equipped with a comparable plasticity mechanism (Kano et al., 1992), providing a possible additional pathway in motor learning. For both hippocampal and cerebellar learning, hypotheses have been generated as to how feed-forward inhibition from local inhibitory interneurons may contribute to network performance and eventual memory formation at excitatory synapses (Pouille & Scanziani, 2001 and 2004; Mittmann et al., 2005). In the hippocampus, inhibitory interneurons may re-route the excitatory signals of pyramidal cells, allowing pattern separation in spatial memory formation (Buzsaki, 2005), whereas in the cerebellum, molecular layer interneurons may act, in conjunction with plasticity at the parallel fiber to Purkinje cell synapse, to adjust the size and form of receptive fields of Purkinje cells or to mediate associative processing (Ekerot and Jorntell, 2003; Jorntell and Ekerot, 2002; Santamaria et al., 2006; Scelfo et al., 2008). However, for both hippocampal and cerebellar learning the role of inhibitory interneurons remains to be confirmed at the systems level in an intact, awake animal.

Here, using a Purkinje cell-specific genetic manipulation in mice, we examined whether and how cerebellar stellate and basket cells control procedural memory formation. These interneurons in the molecular layer of the cerebellar cortex make GABAergic synapses onto dendrites and somata of Purkinje cells, which in turn project onto neurons in the cerebellar and vestibular nuclei (Figure 1). Inhibition at the interneuron to Purkinje cell synapse is mediated by $\alpha 1\beta 2/3\gamma 2$ -type GABA_A receptors (Laurie et al., 1992; Wisden et al., 1996; Fritschy et al., 2006), and, as at other synapses, the $\gamma 2$ subunit is responsible for targeting receptors to the postsynaptic membrane (Schweizer et al., 2003). Thus, to investigate the role of GABA_A receptor-mediated feed-forward inhibition we used a genetic approach to selectively delete the $\gamma 2$ subunit, and thereby eliminate synaptic GABA_A receptors, from Purkinje cells (PC- $\Delta\gamma 2$ mice). After establishing *in vitro* that transmission at GABAergic synapses onto Purkinje cells was indeed selectively removed in these animals, we examined their behaviour. First, we investigated basic cerebellar motor performance by measuring the baseline amplitude (gain) and timing (phase) of their compensatory eye movements, including the optokinetic reflex (OKR) and vestibulo-ocular reflex (VOR) (Hoebeek et al., 2005); and next, we tested their capability for motor learning and its consolidation by measuring changes in amplitude and timing of their VOR during visuo-vestibular training paradigms over consecutive days (Boyden et al., 2004; De Zeeuw and Yeo, 2005; Gittis and du Lac, 2006; Ito, 1989).

Behavioural changes resulting from the functional removal of molecular layer interneurons must ultimately derive from altered activity of Purkinje cells, as they form the sole output of the cerebellar cortex. Thus, to determine the possible changes in signal coding that might cause the potential deficits in compensatory eye movements, we also investigated the simple spike and complex spike activities of Purkinje cells in the flocculus of the vestibulo-cerebellum, which is known to control the OKR and VOR (Ito, 1993; Lisberger, 1998; Schonewille et al., 2006a). Whereas complex spikes result directly from the activation of climbing fibers originating in the inferior olive (De Zeeuw et al., 1998a), simple spike activities reflect integration of Purkinje cell intrinsic excitability and the excitatory and inhibitory synaptic inputs from parallel fibers and molecular layer interneurons, respectively (Jorntell and Ekerot, 2002). By selectively ‘lesioning’ the fast GABAergic inputs onto Purkinje cells, and by investigating the resulting changes in the pattern of cell firing and consequent changes in motor behaviour, we provide strong evidence for a specific role of molecular layer interneurons in cerebellar signal coding and motor learning.

Experimental Procedures

Procedures involving experimental mice were performed in accordance with regulations of the European Union, the United Kingdom Animals (Scientific Procedures) Act 1986, the Animal Care and Use Committee of Turin University, or the Dutch Ethical Committee (DEC) for animal experiments.

Generation of PC- $\Delta\gamma 2$ mice

$\gamma 2^{177lox}$ mice were generated by flanking exon 4 of the GABA_A receptor $\gamma 2$ subunit gene by loxP sites, but the codon encoding F77 in exon 4 was changed to I, resulting in a neutral amino acid substitution (F77 to I). Mice homozygous for the $\gamma 2^{177lox}$ gene were crossed with mice heterozygous for $\gamma 2^{177lox}$ and heterozygous for an L7Cre transgene

(Barski et al., 2000; Wulff et al., 2007). Littermates of the following genotypes were used for the experiments: $\gamma 2177\text{lox}/\gamma 2177\text{lox}/\text{L7Cre}$ ($\text{PC-}\Delta\gamma 2$) and $\gamma 2177\text{lox}/\gamma 2177\text{lox}$ (littermate controls). Mice were genotyped by PCR analysis of genomic DNA from tail biopsies using the following primer pairs:

$\gamma 21x5'_{-s}$ (5'-GTCATGCTAAATATCCTACAGTGG-3') plus

$\gamma 21x5'_{-as}$ (5'-GGATAGTGCATCAGCAGACAATAG-3')

to test for the $\gamma 2177\text{lox}$ allele (213 bp band for WT, 250 bp band for $\gamma 2177\text{lox}$), and:

Cre1 (5'-GACCAGGTTCGTTCACTCATGG-3') plus

Cre2 (5'-AGGCTAAGTGCCTTCTCTACAC-3')

to test for the Cre recombinase transgene (250 bp band for L7Cre).

Immunofluorescence and confocal microscopy

Adult mice were anaesthetized with an intraperitoneal injection of 0.1 ml of a 1 to 1 mixture of ketamine (50 mg/ml) and xylazine (2.8 mg/ml), and subsequently perfused with 4% paraformaldehyde in phosphate-buffered saline (PBS; pH7.4). After postfixation in the same fixative for 2 hours, the cerebella were cryoprotected in sucrose (10%, 20% and 30% in PBS) and cut into 16- μm coronal sections with a cryostat. Sections containing the flocculi were collected on cold gelatin-coated slides and processed for double-immunofluorescence labelling (see Schneider-Gasser et al., 2006). Following a blocking step in normal goat serum (10% in PBS with 0.5% Triton X-100), the sections were incubated overnight with a monoclonal antibody against calbindin (1:10,000; Swant, Bellinzona, Switzerland) and one of the following antisera raised in rabbit: anti-VGAT (1:3000; Synaptic Systems, Göttingen, Germany), anti-VGLUT1 (1:1000; Synaptic Systems), anti-VGLUT2 (1:500; Synaptic Systems). The sections were then rinsed in PBS and incubated with the appropriate secondary antibodies, conjugated to either Alexa 488 (Molecular Probes, Eugene, OR) or the cyanine-derived Cy3 (Jackson ImmunoResearch, West Grove, PA). After rinsing, slides were coverslipped with Dako fluorescence mounting medium (Dako Italia, Italy). The sections were analyzed with a laser scanning confocal microscope (Zeiss LSM5 Pascal) with the use of the multi-channel acquisition mode to avoid fluorescence cross-talk. Stacks of 5-15 confocal sections spaced by 250-350 nm were acquired with either a x40 (1.3 NA) or a x100 (1.4 NA) oil-immersion objective and the pinhole set at 1 Airy unit. For display, images were processed with the image-analysis program Imaris (release 4.2; Bitplane, Zurich, Switzerland). Quantification of VGLUT2-positive puncta was done on segmented images spanning the entire length of the molecular layer. 8 confocal fields (13225 $\mu\text{m}^2/\text{field}$) were counted per animal ($n = 4$). For VGLUT1 and VGAT, images acquired at a magnification of 8.1×10^{-3} $\mu\text{m}^2/\text{pixel}$ (512 x 512 pixels) were segmented using a threshold that maximized the selection of immunofluorescent puncta over background labelling, and the number and density of puncta were then calculated with NIH Image J software (<http://rsb.info.nih.gov/ni-image>). For VGLUT1 6 confocal fields (2125 $\mu\text{m}^2/\text{field}$) were counted per animal ($n = 3$), for VGAT 8 confocal fields (2125 $\mu\text{m}^2/\text{field}$) per animal ($n = 4$). To quantify the number of Purkinje cells, a line was placed through the Purkinje cell layer of the flocculus and all calbindin-positive cells on the line were counted (4 sections per animal, $n = 4$). The density of molecular layer interneurons was calculated in 3-6 fields (5000 $\mu\text{m}^2/\text{field}$) in the flocculus of 3-5 Nissl-stained sections per animal ($n = 4$).

Electron microscopy

PC- $\Delta\gamma 2$ and control mice (2-3 months old, $n = 2$ per genotype) were perfused with 4% paraformaldehyde and 2.5% glutaraldehyde in phosphate buffer (PB, 0.1M, pH 7.4). The cerebella were removed from the skull and postfixed in the same solution overnight. Small blocks of tissue were postfixed in 1% osmium tetroxide (in 0.1M cacodylate buffer), dehydrated in ethanol and embedded in Epon-Araldite. Ultrathin sections were stained with uranyl acetate and lead citrate and analyzed with a JEM-1010 transmission electron microscope (Jeol, Japan) equipped with a side-mounted CCD camera (Mega View III, Soft Imaging System, Germany). In each mouse, 90 electron micrographs were taken randomly from the neuropil of the molecular layer at a magnification of $\times 30,000$ ($15.7 \mu\text{m}^2/\text{micrograph}$) to compare the density of parallel fiber to Purkinje cell synapses.

Slice preparation and in vitro electrophysiology

Male and female control and PC- $\Delta\gamma 2$ mice (10 – 25 weeks of age) were anaesthetized with isoflurane (IVAX Pharmaceuticals, Runcorn, UK) and decapitated. The brains were removed and dissected in cold ($0.5\text{--}4^\circ\text{C}$) oxygenated 'slicing' solution, containing (in mM): 85 NaCl, 2.5 KCl, 0.5 CaCl_2 , 4 MgCl_2 , 25 NaHCO_3 , 1.25 NaH_2PO_4 , 75 sucrose, 25 glucose, 0.01 D-(-)-2-amino-5-phosphonopentanoic acid (D-AP5); pH 7.4, when bubbled with 95% O_2 and 5% CO_2 . Parasagittal slices ($250\text{--}300 \mu\text{m}$) were cut from the cerebellar vermis (HM 650V; Microm International GmbH, Walldorf, Germany) and incubated at 32°C for 40 minutes and thereafter at room temperature. After 20 minutes of incubation, the sucrose containing slicing solution was gradually replaced by a normal 'external' solution containing (in mM): 125 NaCl, 2.5 KCl, 2 CaCl_2 , 1 MgCl_2 , 25 NaHCO_3 , 1.25 NaH_2PO_4 , and 25 glucose; pH 7.4, when bubbled with 95% O_2 and 5% CO_2 .

Slices were transferred to a submerged recording chamber and perfused with oxygenated external solution (1.5-2.5 ml/min). Patch-clamp recordings were made with Axopatch-200A or -200B amplifiers (Molecular Devices Corporation, Sunnyvale, CA) from Purkinje cells visualized under infrared differential interference contrast optics (Zeiss Axioscop; Zeiss, Oberkochen, Germany or Olympus BX51 WI; Olympus, London, UK). For single-channel recordings outside-out patches were excised from the soma of Purkinje cells. Whole-cell and single-channel currents were recorded at room temperature ($25 \pm 1^\circ\text{C}$). Simple spike activity was recorded at both room and near-physiological temperature ($34 \pm 2^\circ\text{C}$), in loose cell-attached mode with external solution in the recording pipette. Firing was recorded in voltage- or current-clamp with the pipette current set to zero (Häusser and Clark, 1997). In experiments investigating the effect of GABA_B receptor activation on firing, SR-95531 (20 μM), D-AP5 (20 μM), and 2,3-dioxo-6-nitro-1,2,3,4-tetrahydrobenzo[f]quinoxaline-7-sulfonamide (NBQX; 5 μM) were added to the perfusate. GABA_B receptors were activated with baclofen (10 μM) and the effects were reversed by CGP54626 (4 μM).

For single-channel recordings, GABA was applied at a high concentration (100-500 μM , typically 200 μM) sufficient to induce, in control patches, marked receptor desensitization. Under these conditions, GABA_A receptors entered long-lived closed states, and channel openings occurred as infrequent clusters (Brickley et al., 1999). Such isolated clusters were analyzed to determine the main conductance states of the channels. In patches from PC- $\Delta\gamma 2$ mice, where receptor desensitization was reduced, single-channel activity was studied after equilibration with agonist for 30-60 s. Only one patch was recorded per cell. Whole-cell and single-channel currents recorded under such conditions were completely blocked by 10-20 μM of the GABA_A receptor antagonist

SR 95531.

For whole-cell and loose cell-attached recordings, pipettes were pulled from thin-walled borosilicate glass tubing (1.5 mm o.d., 1.17 mm i.d; G150TF-3; Warner Instr. Inc., Hamden, CT, USA). For patch recordings, pipettes were pulled from thick-walled borosilicate glass tubing (1.5 mm o.d., 0.86 mm i.d; GC-150F; Harvard Apparatus Ltd, Edenbridge, UK). All pipettes were coated with Sylgard resin (Dow Corning 184) and fire polished to give a final resistance of 2-6 M Ω (whole-cell and loose cell-attached recordings) or 10-15 M Ω (single-channel recordings). The internal solution contained (in mM): CsCl, 140; NaCl, 4; CaCl₂, 0.5; N-2-hydroxyethylpiperazine-N'-2-ethanesulphonic acid (HEPES), 10; ethyleneglycol-bis (β -aminoethylether)-N,N,N',N'-tetraacetic acid (EGTA), 5; Mg-ATP, 2; pH 7.3 with CsOH. To block ionotropic glutamate receptors, 10 μ M D-AP5 and 5 μ M 6-cyano-7-nitroquinoxaline-2,3-dione (CNQX) were added to the perfusate. mIPSCs were recorded in the presence of 0.5-1 μ M tetrodotoxin (TTX).

Paired PF-EPSCs were evoked by stimuli delivered with a glass pipette (containing external solution) located within the molecular cell layer (in an fixed position ~100-150 μ m from the soma of the recorded Purkinje cell). Stimuli of 100 μ s duration were delivered at 0.2 Hz, with a 50 ms paired-pulse interval (Digitimer DS2 isolated stimulator, Digitimer Ltd., Welwyn Garden City, UK). The stimulation intensity was varied pseudo-randomly in 5V steps (10 sweeps each voltage). AMPAR-mediated PF-evoked EPSCs were recorded in the presence of strychnine (1 μ M), SR-95531 (40 μ M) and D-AP5 (50 μ M) after 60-70% series resistance compensation (typically 7 μ s lag-time). Recordings showing a >20 % increase of the series resistance were discarded.

Parallel fiber-evoked Purkinje cell simple spike responses were recorded in loose cell-attached mode and obtained using a similar approach (5-10 V stimulus intensity at 0.5 Hz). Recordings were made in the absence of added drugs and the effect of GABA_A receptor blockade was tested using SR-95531 (40 μ M). In cases where it was tested, NBQX completely blocked the parallel fiber evoked response (data not shown). All drugs were obtained from Tocris Bioscience (Bristol, UK) or Ascent Scientific (Weston-super-Mare, UK).

Long-term plasticity experiments were performed as previously described (Hansel et.al., 2006). In short, 200 μ m thick parasagittal sections were sliced in ice-cold ACSF (containing in mM: 124 NaCl, 5 KCl, 1.25 Na₂PO₄, 2 MgSO₄, 2 CaCl₂, 26 NaHCO₃ and 15 D-glucose, bubbled with 95% O₂ and 5% CO₂). All chemicals were purchased from Sigma. Experiments were performed at room temperature in the presence of bath-applied 100 μ M picrotoxin to block GABA_A receptors. Whole cell patch-clamp recordings of Purkinje cells were performed using an EPC-10 amplifier (HEKA electronics, Lambrecht, Germany). The resistance of patch pipettes were 4-5 M Ω when filled with intracellular solution containing (in mM): 120 K-gluconate, 9 KCl, 10 KOH, 3.48 MgCl₂, 4 NaCl, 10 HEPES, 4 Na₂ATP, 0.4 Na₃GTP and 17.5 sucrose (pH 7.25). Holding potentials were between -65 and -70mV. Cells in which the series or input resistance varied by >15% were discarded. Parallel fiber LTP was induced by parallel fiber stimulation at 1 Hz for 5 min in current-clamp mode and was measured by test responses recorded in voltage-clamp mode, while parallel fiber LTD was induced using combined parallel fiber and climbing fiber stimulation (Coesmans et al., 2004).

Eye movement recordings

All mice for eye movement recordings were between 12 and 30 weeks of age and were surgically prepared for experiments under general anesthesia of a mixture of isoflurane (Rhodia Organique Fine Ltd, Bristol, UK) and oxygen. A construct consisting of two nuts was attached to the frontal and parietal bones using Optibond prime and adhesive (Kerr, Bioggio, Switzerland) and Charisma (Heraeus Kulzer, Armonk, NY, USA). After a recovery period of 5 days the mouse was placed in a restrainer, with its head bolted to a bar. The restrainer was fixed onto the centre of the turntable. A cylindrical screen (diameter 63 cm) with a random-dotted pattern (each element 2°) surrounded the turntable (diameter 60 cm). The OKR and VVOR were evoked by rotating the surrounding screen and turntable, respectively, with an amplitude of 5° at different frequencies. The surrounding screen and the turntable were driven independently by AC servo-motors (Harmonic Drive AG, The Netherlands). The table and drum position signal were measured by potentiometers, filtered, digitized (CED Limited, UK), and stored on disk for off-line analysis. A CCD camera was fixed to the turntable in order to monitor the mouse's eyes. The eye movements were recorded at 240 Hz using an eye-tracking device (ISCAN Inc.). Video calibrations and subsequent eye movement computations were performed as described previously (Hoebeek et al., 2005; Stahl et al., 2000).

In vivo electrophysiology

All mice for *in vivo* electrophysiological recordings were between 15 and 40 weeks of age and were surgically prepared under general anesthesia of a mixture of isoflurane, nitrous oxide, and oxygen for chronic neurophysiological experiments by mounting a pedestal as described above (Hoebeek et al., 2005). A recording chamber was built around craniotomies in both left and right occipital bones with a maximal diameter of 3 mm. Mice were placed in the setup as described above.

Extracellular Purkinje cell activity was recorded using borosilicate glass electrodes (OD 2.0 mm, ID 1.16 mm, 2 M NaCl, 4-8 MΩ). Electrodes were advanced into the cerebellum by a hydraulic micro-drive (Narishige, Tokyo, Japan). Recordings were made from left and right Crus I and II, paramedian lobule, and (para)flocculus (all recordings during optokinetic stimulation were from floccular Purkinje cells). Purkinje cells were identified by the brief pause in simple spike activity following each complex spike. The raw electrode signal was amplified, filtered (CyberAmp, CED, Cambridge, UK), digitized (CED) and stored on disk for off-line analysis. Following each recording session the brain was covered with gramicidin-containing ointment and the chamber was sealed with bone wax.

Data Analysis

During *in vitro* experiment signals were recorded onto digital audiotape (DTR-1204; BioLogic, Claix, France; DC to 20 kHz); for analysis, replayed signals were filtered at 2 or 5 kHz (whole-cell and single-channel or loose cell-attached recordings, respectively; -3dB, 8-pole lowpass Bessel) and digitised at 10 kHz (Digidata 1200; Axotape, Molecular Devices). Miniature IPSCs were detected using a scaled template detection method (Clements and Bekkers, 1997) implemented in IGOR Pro 5.0 (Wavemetrics, Lake Oswego, OR) with NeuroMatic 1.91 (<http://www.neuromatic.thinkrandom.com>) (Wulff et al., 2007). The peak current amplitude and the total charge transfer of averaged parallel fiber-evoked EPSCs were estimated (for a 10 V stimuli) using NeuroMatic. The decay of synaptic currents was best described by the sum of two exponential functions according

to:

$$y = A_1 \exp\left(\frac{-(x - x_0)}{\tau_1}\right) + A_2 \exp\left(\frac{-(x - x_0)}{\tau_2}\right)$$

where x_0 is the decay onset, τ_1 and τ_2 are the decay time constants of the fast and slow components, and A_1 and A_2 are their respective amplitudes. The weighted time constant of decay (τ_w) was calculated according to:

$$\tau_w = \tau_1 \left(\frac{A_1}{A_1 + A_2} \right) + \tau_2 \left(\frac{A_2}{A_1 + A_2} \right)$$

To measure the mean phasic current produced by action potential-dependent release of GABA, recordings were made in the presence of CNQX and D-AP5 but in the absence of TTX. For each cell, an all-point amplitude histogram was generated from a short section of record (2 – 10 s) and a Gaussian fitted to the portion of the histogram corresponding to the baseline current (IGOR Pro 5.0). The fitted section was restricted to just beyond the apex of the initial peak of the distribution, thereby excluding contamination from phasic events (IPSCs or presumed spillover currents). The peak of the fitted Gaussian was taken as the mean baseline current and subtracted from the record. Summing the individual data points and dividing by the total number of points in the epoch gave the mean phasic current.

Single-channel currents from outside-out patches were analyzed by constructing all-point amplitude histograms (Fetchan; pCLAMP 8.1) from short selected epochs during which identified clusters of openings were present (Brickley et al., 1999). The mean single-channel current was determined from Gaussian fits to these amplitude distributions. Measurements were made at two or more potentials and the slope conductance estimated from the fit of the current-voltage relationship (assuming a reversal of 0 mV). In some patches, only single measurements of chord conductance were obtained; these were pooled with the slope conductance data to provide estimates of the single-channel conductance in each group of mice.

Purkinje cell simple spikes were detected by threshold-crossing, and inter-spike interval (ISI), autocorrelation histograms and peristimulus-time histograms (PSTHs) and were generated using NeuroMatic and IGOR Pro 5.0.

Off-line analysis of eye movements and *in vivo* recordings was performed in Matlab (MathWorks, Natick, MA) (Goossens et al., 2004). The gain and the phase of the eye movements were determined by fitting sine functions to the slow-phase eye velocity traces. Gain was computed as the ratio of eye velocity to stimulus velocity, whereas phase was expressed as the difference (in degrees) between the eye velocity and stimulus velocity traces.

In vivo recorded simple spikes and complex spikes were discriminated using custom-made routines based on principal component analysis. The interspike interval (ISI) distribution of each Purkinje cell was characterized by calculating the mean, CV (standard deviation divided by the mean) and CV2. The CV indicates the relative width of the distribution, the CV2 is defined as the mean of $2 |ISI_{n+1} - ISI_n| / (ISI_{n+1} + ISI_n)$ and is a measure for the regularity of firing on small timescales (Holt et al., 1996; Shin et al., 2007). Simple spike PSTH's (100 bins per cycle) were compiled at each stimulus frequency

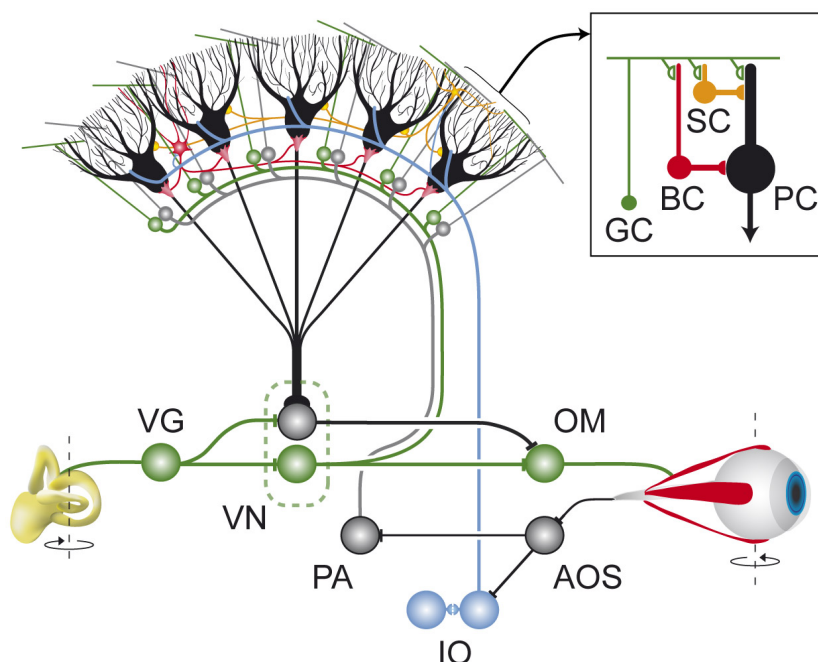


Figure 1. Connectivity of interneurons in the molecular layer of the cerebellar cortex and their relationship to the vestibulo-ocular system.

Purkinje cells (PC; black) in the flocculus of the vestibulo-cerebellum converge upon neurons in the vestibular nuclei (VN), through which they can influence the output of the oculomotor neurons (OM) that drive the eye movements. The Purkinje cells are innervated by two main inputs: they receive vestibular and eye movement signals through the mossy fiber-parallel fiber system (represented by green and grey inputs, respectively), and retinal slip signals through climbing fibers derived from the inferior olive (IO; blue). The parallel fibers, which all originate from the granule cells (GC), innervate the dendritic trees of both Purkinje cells and molecular layer interneurons (basket cells, BC: red and stellate cells, SC: yellow), thereby providing a feedforward inhibitory connection (see inset). The axons of both basket and stellate cells are oriented in the same sagittal plane as that of the dendritic trees of Purkinje cells. Therefore, short pauses in Purkinje cell activity induced by these interneurons may well occur coherently within an entire set of Purkinje cells within a particular sagittal zone. VG, AOS and PA indicate vestibular ganglion cells, accessory optic system, and pontine areas, respectively.

and fit by a sine function. Epochs containing quick phases were deleted from the trace (50 ms before until 150 ms after). Neuronal amplitude of modulation was calculated by dividing the amplitude of the sine wave fitted to the histogram of simple spike firing by its offset. The phase of the simple spike activity relative to the optokinetic stimulus position was calculated from the difference of the phase of the sinusoidal fits to firing rate and stimulus.

Model and simulations of vestibulo-cerebellar system

In the model, variable synaptic strengths are governed by coincidence rules for activity probabilities of parallel fibers, climbing fibers, molecular layer interneurons, Purkinje cells and vestibular nuclei neurons. Synapses are accordingly described by differential equations, which are coupled by linear relations that represent the vestibulo-cerebellar system. This formulation directly allows producing the plots shown in Figures 9 and 10. Figures 9C I and 9D I were produced by an integrate-and-fire model, while Figures 10C-E are the result of a phenomenological model using two exponential learning rates to

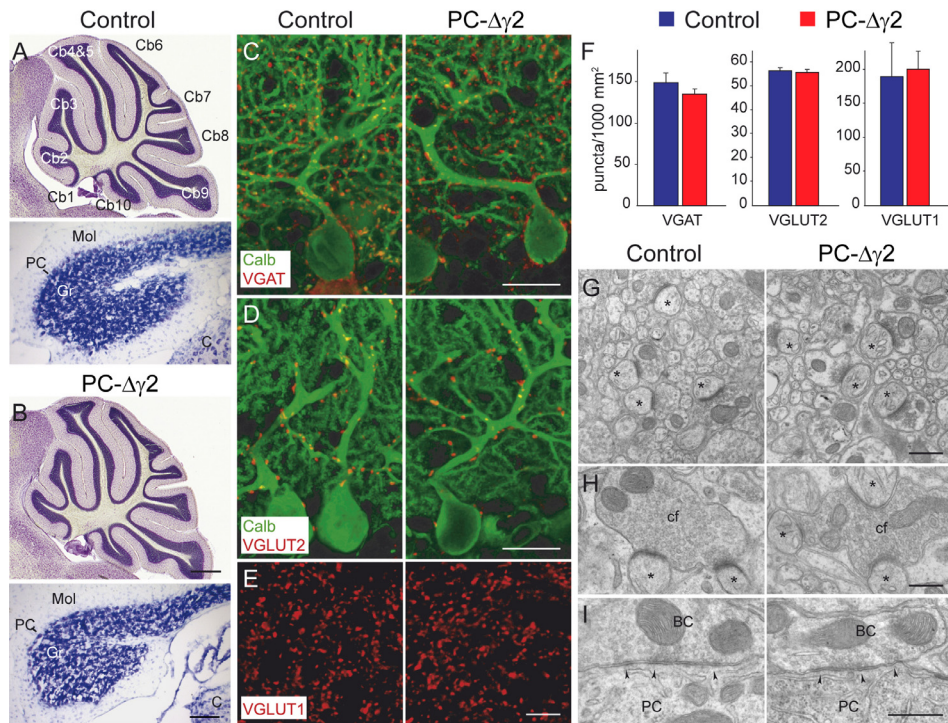


Figure 2. Unaltered cerebellar morphology and normal synaptic organization in PC- γ 2 mice.

(A, B) Nissl stains of sagittal sections through the vermis and coronal sections through the flocculus revealed no morphological differences between control (A) and PC- γ 2 (B) mice (Cb1-10, cerebellar lobules 1-10; Mol, molecular layer; PC, Purkinje cell layer; Gr, granule cell layer, C, cochlear nucleus). (C-E) Immunofluorescence labelling showed no differences in the distribution of the synaptic markers VGAT (C), VGLUT2 (D) and VGLUT1 (E) in the flocculus of control and PC- γ 2 mice. Purkinje cells were visualized by immunolabelling for calbindin. (F) Quantification of VGAT, VGLUT2 and VGLUT1 immunolabelling (number of puncta per 1000 μ m²) revealed no significant difference between the genotypes ($n = 4$ for both genotypes; $p > 0.25$ for all comparisons). (G-I) Electron micrographic examination of synaptic contacts in the molecular layer of PC- γ 2 and control mice. (G) Asymmetric synapses between parallel fibers and Purkinje cell spines (asterisks). (H) Examples of asymmetric synapses made by climbing fibers (cf). (I) Symmetric synapses (arrowheads) made by basket cell axons (BC) onto Purkinje cells dendrites (PC). Scale bars: (A) 250 μ m; (B) 50 μ m; (C, D) 20 μ m; (E) 5 μ m; (G) 500 nm; (H) 360 nm; and (I) 440 nm.

describe the experimentally observed VOR adaptation learning. The equations were solved by numerical integration using MATLAB's function ode45, which is a 4th order Runge-Kutta solver. The model equations were implemented in real-time simulations running with a 5 ms time-step. A visuo-vestibular training paradigm was used to train the network, both in the presence and absence of molecular layer interneurons. Details on constraints and formulas are presented in the Supplementary Material.

Statistical analyses

Statistical tests were performed with GraphPad Prism software (Prism 3.0, GraphPad Software Inc., CA) or with SPSS 11 (SPSS Inc., Chicago, IL). Unless stated otherwise, data were compared with two-tailed paired or un-paired Student's t-tests, as appropriate. We also used two-way repeated-measures ANOVA, and where data were non-normally distributed (Shapiro-Wilk test), the Mann-Whitney U-test was used. The level of significance was set at $p < 0.05$.

Results

PC-Δγ2 mice and morphological analysis

To remove GABA_A receptor-mediated synaptic input to Purkinje cells, we developed PC-Δγ2 mice, in which the GABA_A receptor γ2 subunit was selectively deleted from Purkinje cells using the Cre/loxP-system (see Experimental Procedures). Mice carrying conditional alleles of the GABA_A receptor γ2 subunit (γ2I77lox, exon 4 flanked by loxP sites) were crossed with transgenic mice expressing Cre recombinase under the control of the Purkinje cell-specific L7 promoter (L7Cre) to obtain PC-Δγ2 mice (Barski et al., 2000; Wulff et al., 2007). In these mice Cre recombinase induced a Purkinje cell-specific deletion of the floxed γ2 subunit gene starting in the second postnatal week. To determine whether this ablation of synaptic GABA_A receptors from Purkinje cells altered cerebellar morphology, we compared Nissl stained brain sections of adult PC-Δγ2 and control mice. General cerebellar morphology including that of the vestibulo-cerebellum was unaltered in PC-Δγ2 mice (Figures 2A and 2B). The number of Purkinje cells (24.5 ± 2 vs. 23.9 ± 2.5 cells/mm²; $p = 0.75$) and molecular layer interneurons (2.36 ± 0.19 vs. 2.28 ± 0.18 cells/mm²; $p = 0.53$) in the flocculus did not differ between PC-Δγ2 and control mice.

To test whether postnatal deletion of synaptic GABA_A receptors from Purkinje cells influenced the density of GABAergic inputs, we quantified the density of vesicular γ-aminobutyric acid transporter (VGAT)-positive terminals in the molecular layer of the flocculus. Here too, we found no difference between PC-Δγ2 mice and littermate controls (Figures 2C and 2F) ($p = 0.27$). Next, we investigated potential structural alterations in the excitatory circuitry by quantifying the parallel fiber and climbing fiber terminals in the flocculus using vesicular glutamate transporter 1 (VGLUT1) and VGLUT2 immunohistochemistry, respectively (Hioki et al., 2003). The numbers of immunoreactive puncta (representing parallel fiber and climbing fiber terminals) were similar in PC-Δγ2 and control animals (Figures 2D-F) ($p = 0.68$ and 0.62 , respectively). Moreover, further electron microscopic analyses of excitatory terminals in the molecular layer did not reveal any obvious difference in the density of parallel fiber to Purkinje cell synapses ($33.0/100 \mu\text{m}^2$ in PC-Δγ2 mice vs $32.9/100 \mu\text{m}^2$ in control animals; $n = 2$ per genotype) or in the morphological characteristics of parallel and climbing fiber synapses (Figures 2G and 2H). Finally, inhibitory synapses were present on Purkinje cells despite the loss of postsynaptic GABA_A receptors (Figure 2I).

Purkinje cell-specific loss of synaptic GABA_A receptors

To characterize GABA_A receptor-mediated synaptic transmission in these animals we made patch-clamp recordings from cells in acute slices of cerebellar vermis from adult mice. Recordings were made in the presence of D-2-amino-5-phosphonopentanoic acid (D-AP5; 10 μM) and 6-cyano-7-nitroquinoxaline-2,3-dione (CNQX; 5 μM) to block ionotropic glutamate receptors. Under these conditions in control mice, spontaneous fast GABA_A receptor-mediated inhibitory postsynaptic currents (sIPSCs) occurred at high frequency. In all cells tested these currents were blocked by the GABA_A receptor antagonist SR-95531 (20 μM; data not shown). In accord with previous studies (Wall and Usowiz, 1997; Fritschy et al., 2006), we found no evidence for tonic activation of (extrasynaptic) GABA_A receptors in Purkinje cells.

sIPSCs were present in all recordings from Purkinje cells of control mice ($n = 21$), but were absent from Purkinje cells of PC-Δγ2 mice ($n = 19$) (Figure 3A). In some PC-Δγ2 cells ($n = 12$), although fast-rising sIPSCs were not detected, less frequent small slow-

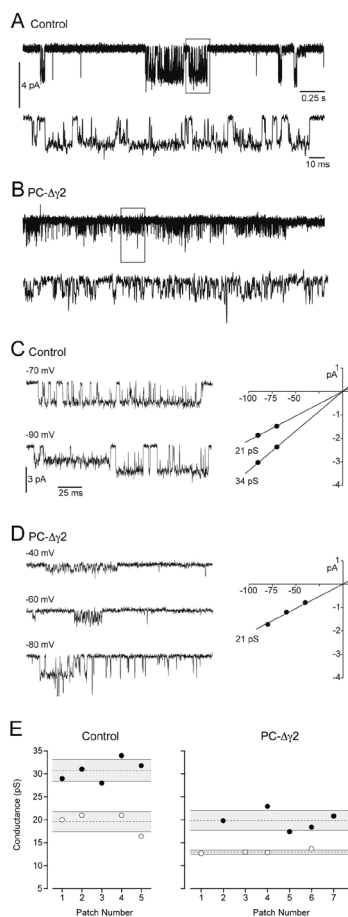


Figure S1. Purkinje cells of PC- $\Delta\gamma 2$ mice have extrasynaptic GABA_A receptors with properties characteristic of receptors lacking the $\gamma 2$ subunit.

(A) Single-channel events in an outside-out patch taken from a Purkinje cell of a control mouse (200 μ M GABA, -70 mV); clusters of channel openings are separated by long closed periods. The lower trace is an expansion of the boxed region. All patches ($n = 9$) from control mice were responsive to GABA, and in the continued presence of GABA the channels entered long-lived closed states characteristic of desensitization clusters (Brickley et al., 1999). (B) A recording of currents in a patch taken from a Purkinje cell of a PC- $\Delta\gamma 2$ mouse (-60 mV). All patches ($n = 8$) from PC- $\Delta\gamma 2$ mice were responsive to GABA (100–500 μ M), often showing clear macroscopic responses on initial application, but the receptors exhibited a lower single-channel conductance and reduced desensitization. (C) Representative clusters from a single patch of a control Purkinje cell at two membrane voltages. To the right is the current-voltage relationship for this patch indicating the slope conductances of the two main conductance states observed. (D) Representative channel clusters recorded at three membrane voltages in a patch taken from a PC- $\Delta\gamma 2$ Purkinje cell. To the right is the corresponding current-voltage relationship. In this patch, and in 5 others, only a single main conductance state was detected; in 2 other patches two conductance states were present. (E) Plot showing the distribution of main conductance states among different patches from Purkinje cells of control and PC- $\Delta\gamma 2$ mice. Filled symbols represent the higher- and open symbols the lower conductance states. Dashed lines indicate the mean, and shaded areas the standard deviation, of conductance values from each group.

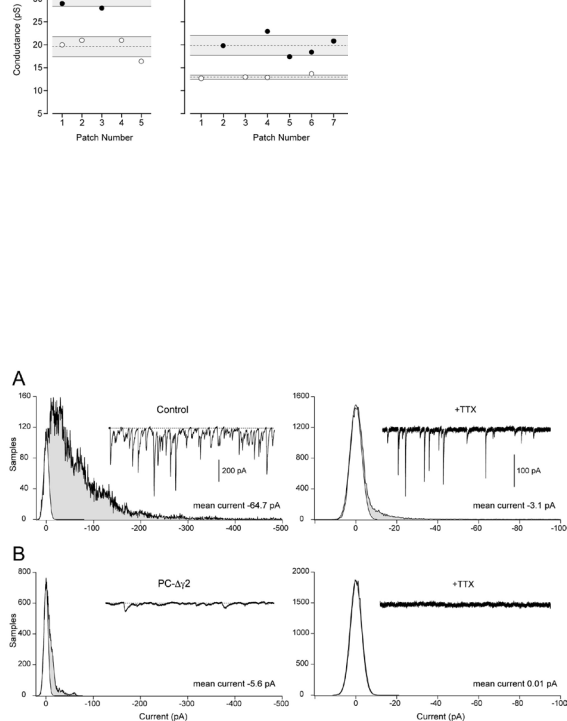


Figure S2. Quantification of mean phasic current in Purkinje cells of control and PC- $\Delta\gamma 2$ mice.

(A) A 2.5 s record of sIPSCs recorded from a Purkinje cell of a control mouse in the presence of CNQX and D-AP5 at -70 mV. The left-hand peak (most positive current values) of the associated all-point amplitude histogram, corresponding to the baseline current noise, is fitted with a single-sided Gaussian (white). The peak of the histogram is taken as the zero current value (dotted line in inset). The filled grey area of the histogram corresponds to all sample points other than those within the baseline noise, and thus represents the current produced by phasic synaptic events. In this cell, the mean of this current is -64.7 pA. The right-hand panel shows a 2.5 s record from the same cell in the presence of TTX. The grey area of the all-point-amplitude histogram is greatly reduced (mean current -3.1 pA). Note the different scaling of the current record and the abscissa of the all-point histogram. (B) Corresponding data from a Purkinje cell from a PC- $\Delta\gamma 2$ mouse (same scaling as A). Note that in the absence of TTX the infrequent slow events contribute a mean current of only -5.6 pA. On average, this current was $< 2\%$ of that seen in control mice (see Results). The right-hand panel is from the same cell in the presence of TTX and shows the complete absence of any phasic events (mean current $+0.01$ pA).

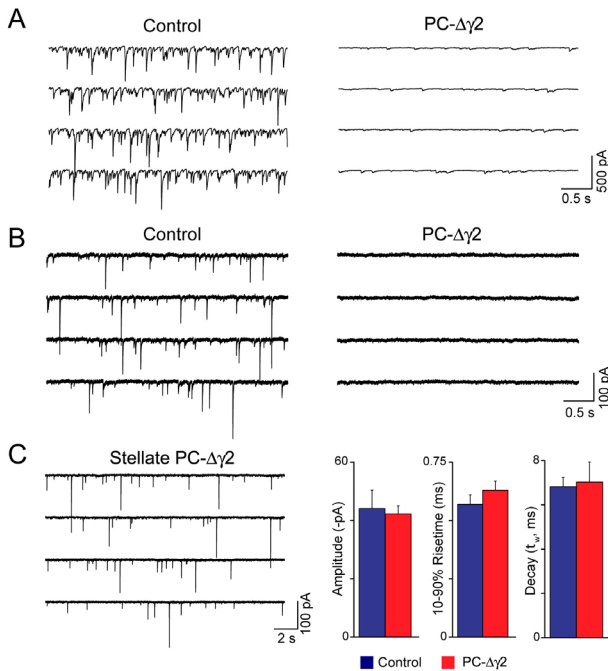


Figure 3. Selective loss of GABA_A receptor-mediated synaptic inhibition from Purkinje cells in PC-Δγ2 mice.

(A) Representative contiguous segments of whole-cell recordings (-70 mV) from Purkinje cells of a control mouse (left) and a PC-Δγ2 mouse (right). In the presence of CNQX and D-AP5, to block ionotropic glutamate receptors, spontaneous fast IPSCs were seen in all cells from control mice but in none of the PC-Δγ2 cells examined. Slow SR-95531-sensitive currents were seen in $\sim 60\%$ of PC-Δγ2 cells. (B) Contiguous segments of whole-cell recordings in the presence of TTX from Purkinje cells of a control mouse (left) and a PC-Δγ2 mouse (right), showing the absence of mIPSCs in the latter. (C) For comparison, contiguous segments of a recording in TTX from a molecular layer interneuron (presumptive stellate cell) of a PC-Δγ2 mouse showing frequent mIPSCs. On the right are pooled data from interneurons, showing that the properties of mIPSCs from control and PC-Δγ2 mice did not differ ($n = 4$ and 5 , respectively; peak amplitude $p = 0.78$, rise time $p = 0.31$, decay $p = 0.85$).

rising currents were seen. As these currents were also blocked by SR-95531, and were absent following inhibition of presynaptic action potentials with tetrodotoxin (TTX), they could reflect spillover of synaptically released GABA onto extrasynaptic receptors that contain only α and β subunits – the $\alpha\beta$ subunit combination forms low-conductance GABA_A receptors that cannot cluster at the synapse (Brickley et al. 1999; Lorez et al. 2000; Mortensen & Smart, 2006; see Figure S1 and Supplementary Information for more detail). Although these $\alpha\beta$ receptors clearly endow Purkinje cells in PC-Δγ2 mice with some sensitivity to GABA, their activation by action potential-dependent release of GABA (Figure 3A) produced, on average, less than 2% of the phasic (synaptic) current seen in Purkinje cells of control animals. The mean phasic current (see Experimental Procedures) was reduced from 149.6 ± 46.1 pA in control Purkinje cells ($n = 8$) to 2.4 ± 1.3 pA in Purkinje cells from PC-Δγ2 mice ($n = 15$; $p < 0.0002$; Mann-Whitney U -test) (see Figure S2 in the Supplementary Data). Consistent with this massive reduction in responsiveness to GABA, recordings from PC-Δγ2 mice made in the presence of TTX confirmed the complete absence of synaptic GABA_A receptors; miniature IPSCs (mIPSCs) were present in all Purkinje cells from control mice but were never detected in cells from PC-Δγ2 mice (Figure 3B). Importantly, this loss of synaptic GABA_A receptors was restricted to Purkinje cells: mIPSCs in molecular layer interneurons were unaffected. Thus, their peak amplitude (42.3 ± 2.7 pA), 10-90% risetime (626 ± 41 μ s) and decay (7.0 ± 0.9 ms τ_w , see Experimental Procedures) were indistinguishable from those of mIPSCs in interneurons from control mice (peak amplitude 44.1 ± 6.3 pA $p = 0.78$, rise time 565 ± 35 μ s $p = 0.31$, decay 6.8 ± 0.4 ms $p = 0.85$; $n = 4$ and 5 , respectively) (Figure 3C).

Motor performance is mildly, but significantly, affected in PC-Δγ2 mice

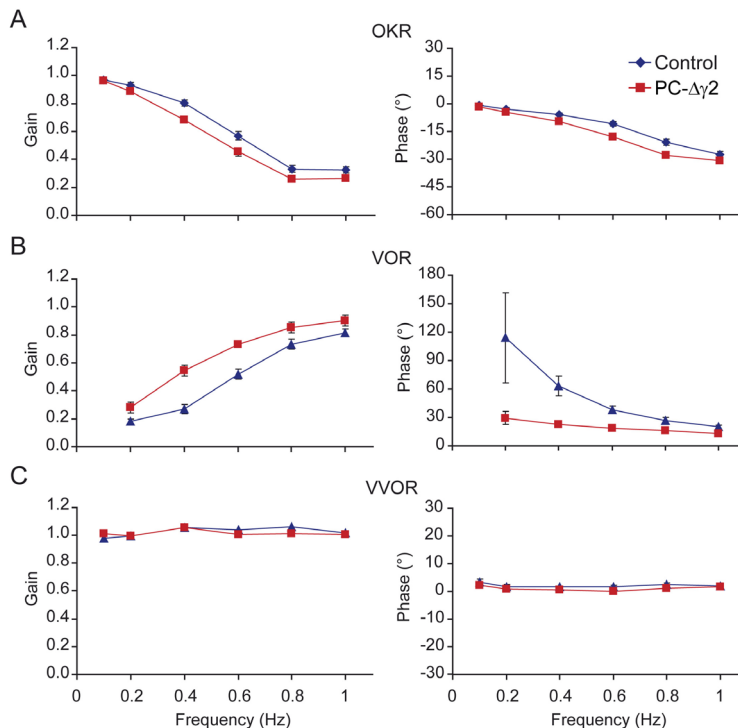


Figure 4. Motor performance during the optokinetic reflex (OKR) (A) as well as during the vestibulo-ocular reflex in the dark (VOR) (B) and the light (VVOR) (C). Stimulus frequencies of optokinetic drum and turntable were varied from 0.1 Hz to 1.0 Hz. Stimulus amplitude was fixed at 5° for both drum and table. Note significant but slight gain and/or phase aberrations in PC-Δγ2 mice during OKR ($p < 0.05$ for both gain and phase values; two-way repeated-measures ANOVA) and VOR ($p < 0.05$ for gain and phase values; two-way repeated-measures ANOVA), but not during VVOR. Data are from 8 control and 9 PC-Δγ2 mice. Vertical error bars denote SEM.

PC-Δγ2 mice appeared healthy, had a normal weight range and showed no sign of ataxia, tremor or any obvious neurological abnormality. To allow a sensitive probing of cerebellar performance and learning, we performed extensive analyses of their compensatory eye movements. Adult male PC-Δγ2 mice and littermate controls were exposed to whole-field visual stimuli to test the amplitude (gain) and timing (phase) of their OKR and/or tested with turntable stimulation to investigate the same parameters of their vestibulo-ocular reflex in the dark (VOR) and light (visual VOR or VVOR). During OKR the PC-Δγ2 mice showed a small, but significant, deficit in motor performance in that there was a slight reduction in gain and a slight lag in phase compared to those of controls ($p < 0.05$ in both cases; two-way repeated-measures ANOVA) (Figure 4A). Similarly, during VOR the compensatory eye movements of PC-Δγ2 mice were also slightly affected, but in this paradigm gain values and phase leads were larger and smaller, respectively, than those of controls ($p < 0.05$ in both cases; two-way repeated-measures ANOVA) (Figure 4B). By contrast, no significant differences in baseline performance values were observed between the genotypes during VVOR (Figure 4C). Thus, we conclude that the PC-Δγ2 mice show small, but significant, abnormalities in motor performance when the visual and vestibular systems are investigated separately, but not when they operate together, as they would under natural conditions or during visuo-vestibular training (see also Figure S3 in Supplementary Material).

PC-Δγ2 mice show marked deficits in procedural learning

Removal of GABA_A receptor-mediated inhibitory synaptic input onto Purkinje cells had

much more profound effects on specific aspects of cerebellar motor learning. Gain and phase learning capabilities were studied by applying a protocol that was aimed at reducing the gain of the VOR on day 1 and subsequently reversing its phase on days 2, 3 and 4. Gain adaptation on day 1 was studied by subjecting the mice to 5 x 10 min periods of sinusoidal, in phase drum and table rotation at 0.6 Hz (both with an amplitude of 5°). Phase reversal adaptations on days 2, 3 and 4 were studied by subjecting the animals to 5 x 10 min periods of sinusoidal *in phase* drum and table rotation at 0.6 Hz, but with drum amplitudes of 7.5° (day 2) and 10° (days 3 and 4), while the amplitude of the turntable remained 5°. To measure consolidation of gain and phase adaptations, the animals were kept in the dark in between all recording days.

The paradigm provided on day 1 did not reveal any significant difference in gain-decrease between PC- $\Delta\gamma 2$ and control mice (when measured at the end of the training $p = 0.11$; two-way repeated-measures ANOVA) (Figures 5A and 5B). However, when the measurements were resumed the next day, the degree of gain reduction carried forward from the previous day's learning was significantly smaller in PC- $\Delta\gamma 2$ mice as compared with controls ($p < 0.001$) (Figures 5A, 5B and 5E). This effect on consolidation was apparent at a wide range of frequencies (Figure 5D) and was not caused by non-specific effects of fatigue in PC- $\Delta\gamma 2$ mice, since in non-adapting paradigms both control and PC- $\Delta\gamma 2$ mice showed minimal decreases in VOR over time, and none over consecutive days (see Figure S3 in Supplementary data).

The phase-reversal paradigm provided on days 2, 3 and 4 immediately revealed significant learning deficits in PC- $\Delta\gamma 2$ mice starting 10 - 20 min after the initiation of visuo-vestibular training (e.g. at 20 min $p < 0.01$) (Figure 5C). Further, similar to the lack of consolidation observed in the gain-decrease paradigm, prominent differences were observed in the consolidation of phase changes between PC- $\Delta\gamma 2$ and controls (e.g. from day 2 to day 3 $p < 0.006$) (Figures 5C and 5E). Moreover, in this paradigm the lack of consolidation also occurred at a wide range of frequencies (Figure 5D) and adaptation differences were also not caused by visual problems in PC- $\Delta\gamma 2$ mice. Analysis of compensatory eye movements recorded during the adaptation sessions showed that PC- $\Delta\gamma 2$ mice were capable of perceiving the reversed movement of the visual stimulus (see Supp Fig. 4).

In conclusion, PC- $\Delta\gamma 2$ mice showed a relatively normal capacity for gain-decrease motor learning but a profound lack of phase reversal learning and a general deficit in consolidation of both gain and phase adaptation.

Abnormal temporal patterns of Purkinje cell simple spike activities

How can we explain the deficits of PC- $\Delta\gamma 2$ mice in consolidation of cerebellar motor learning? The impact of any loss of feed-forward inhibitory synaptic input from stellate and basket cells on cerebellar motor learning must ultimately be reflected in changes in the simple spike activities of Purkinje cells, as these cells provide the sole output of the cerebellar cortex (see Figure 1). We thus investigated Purkinje cell activities both *in vitro* and *in vivo*. Indeed, when examined *in vitro*, the temporal pattern of spontaneous simple spike activity in Purkinje cells from PC- $\Delta\gamma 2$ mice differed from that of control mice, in that the variability of firing was significantly decreased (Figure 6). The mean firing rate of Purkinje cells from the two groups was not different (control 12.3 ± 1.6 vs PC- $\Delta\gamma 2$ 13.7 ± 0.6 Hz, $n = 26$ and 9 ; $p = 0.062$, Mann-Whitney U-test), but the coefficient of variation (CV; SD/mean) of the inter-spike interval (ISI) was reduced in PC- $\Delta\gamma 2$ mice

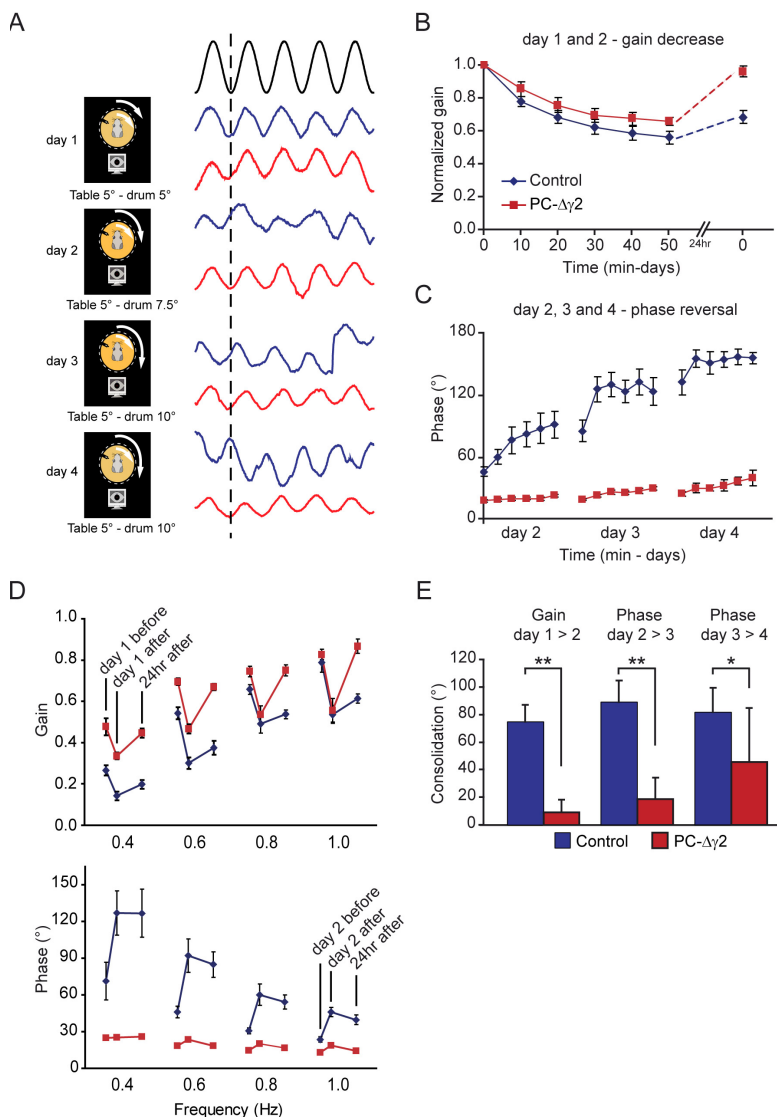


Figure 5. Consolidation of motor learning and phase reversal are severely affected in PC-Δγ2 mice during a four-day training paradigm.

(A) On day 1 gain-down adaptation was studied using in phase, drum and table stimulation (rotating sinusoidally in the same direction and both at 5° amplitude). On days 2, 3 and 4 phase reversal adaptation was studied by rotating the drum 7.5° (day 2) or 10° (days 3 and 4) in phase with the table, which rotated at 5°. Thus, in this training paradigm normal mice tend to move their eyes during the vestibulo-ocular reflex in the same direction as the table instead of the opposite direction. Gain and phase parameters were evaluated 5 times at 10 min intervals for both the gain-down and phase reversal training paradigm; examples of eye movement traces are shown for each day (control, blue; PC-Δγ2, red). (B) During gain-down training on day 1 no differences in gain reduction were observed among PC-Δγ2 and control mice ($p = 0.11$), but a clear difference became apparent in the first test on day 2 ($p < 0.001$). (C) During phase reversal training controls learned far better than PC-Δγ2 mice (on day 4 $p < 0.00001$). (D) Differences in both gain consolidation and phase reversal between PC-Δγ2 and control mice occurred over a wide range of frequencies. Day “x” before and day “x” after indicate values just before and after training on day “x”, respectively; 24hr after indicates value on next day just before new measurement on subsequent day. (E) Differences in consolidation (i.e. the percentage of gain reduction or phase reversal carried forward from the previous days learning) among PC-Δγ2 and control mice for gain from day 1 to 2 and for phase from day 2 to 3 as well as from day 3 to 4. For all panels, pooled data are from 10 controls and 9 PC-Δγ2 mice. Vertical error bars denote SEM; * and ** denote $p < 0.05$ and 0.01, respectively.

(0.20 ± 0.03 in control vs 0.10 ± 0.01 in PC- $\Delta\gamma 2$; $p = 0.018$, Mann-Whitney U-test) (Figure 6C). The coefficient of variation of adjacent intervals (CV_2 ; mean value of $2 |ISI_{n+1} - ISI_n| / (ISI_{n+1} + ISI_n)$; Holt et al., 1996) also differed. CV_2 was 0.19 ± 0.02 in control vs 0.10 ± 0.01 in PC- $\Delta\gamma 2$ mice ($p = 0.018$; Mann-Whitney U-test). Blockade of GABA_A receptors with SR-95531 decreased the CV of the ISI in every control Purkinje cell tested (0.20 ± 0.04 vs 0.13 ± 0.02 in SR-95531; $p = 0.024$, $n = 8$). By contrast, SR-95531 failed to alter the CV of the ISI in cells from PC- $\Delta\gamma 2$ mice (0.13 ± 0.02 vs 0.13 ± 0.04 , $n = 3$). Similar results were obtained at near-physiological temperature (34°C ; Figure 6B and C).

Although these changes in the spontaneous activity of Purkinje cells in vitro are consistent with a loss of synaptic inhibition in PC- $\Delta\gamma 2$ mice (see also Raman and Bean, 1997; Häusser and Clark, 1997; Walter et al., 2006), they may not accurately predict the in vivo situation, given the absence in brain slices of ongoing parallel- and climbing fiber-mediated excitatory synaptic input. We therefore also investigated the activity of Purkinje cells in awake behaving mice responding to natural stimuli. Since Purkinje cells in the flocculus of the cerebellum control adaptation of compensatory eye movements (Ito, 1993; Lisberger, 1998; Schonewille et al., 2006b), we investigated whether the floccular Purkinje cells in PC- $\Delta\gamma 2$ mice showed differences in firing during optokinetic stimulation as compared to control mice (Figure 7). Single units of Purkinje cells that responded optimally to stimulation around the vertical axis were identified by creating tuning curves of the complex spike responses and by identifying a clean climbing fiber pause (Hoebeek et al., 2005; Schonewille et al., 2006b; Simpson et al., 1996). None of the basic simple spike parameters, including average firing frequency, phase relative to

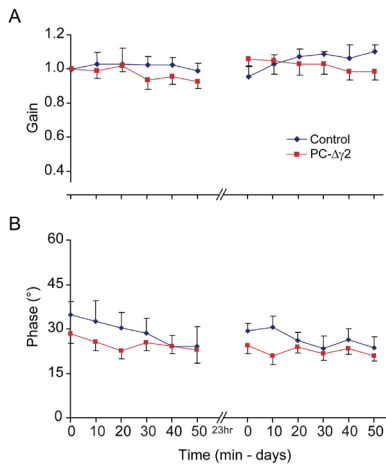
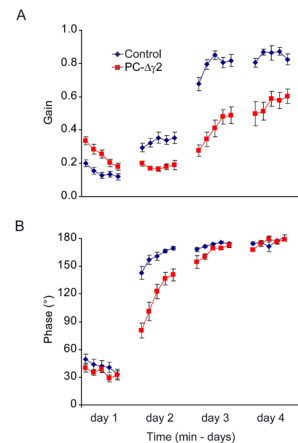


Figure S4. Phase changes in PC- $\Delta\gamma 2$ mice argue against the possibility that observed differences in behaviour are the result of differences in perception of the adaptation stimulus.

(A) Gain of compensatory eye movements recorded during the adaptation sessions shows that on day 1 PC- $\Delta\gamma 2$ mice were capable of decreasing the gain of their VOR when the visual stimulus rotates in phase with the table. (B) Furthermore, PC- $\Delta\gamma 2$ mice were capable of perceiving the reversed movement of the visual stimulus on days 2-4. The reversed stimulus (starting on day 2) requires the eyes to move with a phase of 180° ; this was fully achieved by all mice by the end of day 2.

Figure S3. VOR gain decrease in PC- $\Delta\gamma 2$ is the result of the adaptation stimulus. VOR gain (A) and phase (B) were recorded in sessions with no adaptation-requiring stimulus but all other settings the same. In this non-adapting paradigm, both control and PC- $\Delta\gamma 2$ mice show a minimal decrease in VOR over time, and none over consecutive days. This is significantly different from the results obtained during the actual adaptation sessions (all $p < 0.001$ for control and PC- $\Delta\gamma 2$,



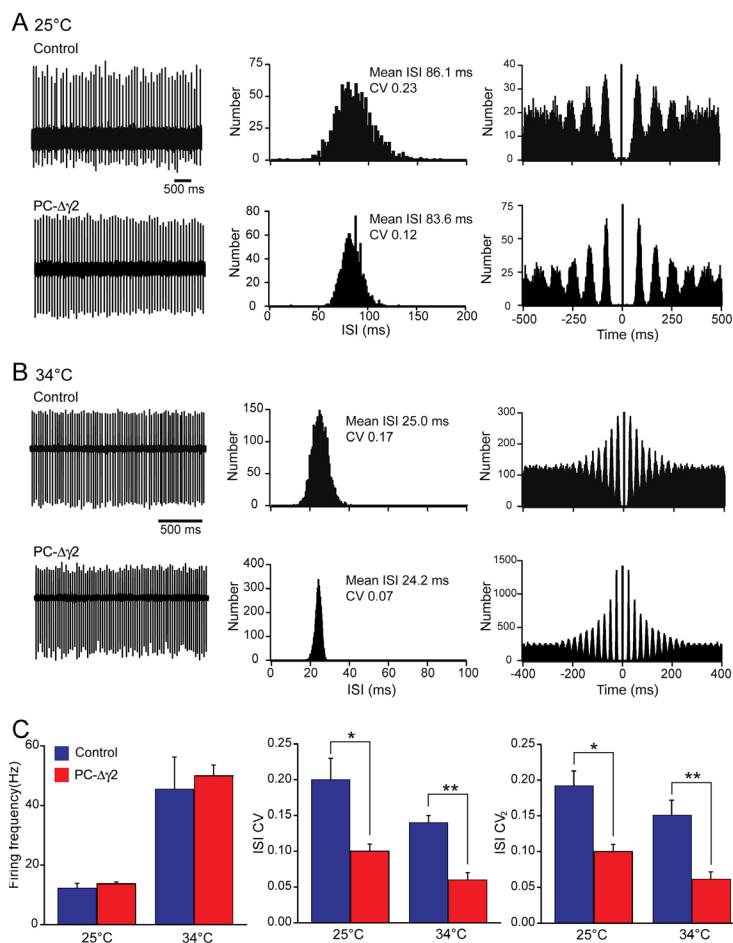


Figure 6. Removal of fast synaptic GABA_A receptor-mediated inhibition in PC-Δγ2 mice results in reduced variability of simple spike firing in vitro. Spontaneous firing was recorded in 61 of 68 Purkinje cells in slices from 3 control and 3 PC-Δγ2 mice. (A) Representative cell-attached records of simple spike activity, inter-spike interval (ISI) histograms and autocorrelation histograms from a control and PC-Δγ2 mouse at room temperature. (B) Corresponding data from two different cells at near-physiological temperature. (C) Pooled data. The mean firing rate of Purkinje cells from the two groups was not significantly different, either at room temperature or near physiological temperature. However, the coefficient of variation (CV) of the ISI and the coefficient of variation of adjacent intervals (CV₂) was significantly different (* denotes $p < 0.05$, ** $p < 0.01$; see text for details).

stimulus and modulation amplitude, was different between PC-Δγ2 and control mice (Figure 7B). By contrast, the regularity of Purkinje cell firing was affected, as predicted by the in vitro recordings. For floccular simple spike activities, the CV of the ISIs was significantly reduced during visual stimulation in PC-Δγ2 mice as compared to controls ($p = 0.008$; PC-Δγ2: $n = 55$, controls: $n = 60$) (Figure 7C). Mostly this difference reflected specific changes in temporal patterning, because the CV₂ was also significantly lower for floccular Purkinje cells during natural optokinetic stimulation in the PC-Δγ2 mice ($p < 0.0001$) (Figure 7C; for probability distributions of ISIs see also Figure S5 in Supplementary Material). If the differences in the temporal pattern of Purkinje cell activities contribute to the differences in memory consolidation after the training periods, we would expect that these differences would also be found outside the periods of optokinetic stimulation. Indeed, both the CV and CV₂ of Purkinje cell simple spikes were also significantly reduced in the absence of this form of natural stimulation (for CV $p = 0.022$ and for CV₂ $p < 0.0001$; PC-Δγ2: $n = 41$, controls: $n = 43$) (Figure 7C). In contrast, the patterns of complex spike activities of Purkinje cells did not differ between PC-Δγ2 and control mice during

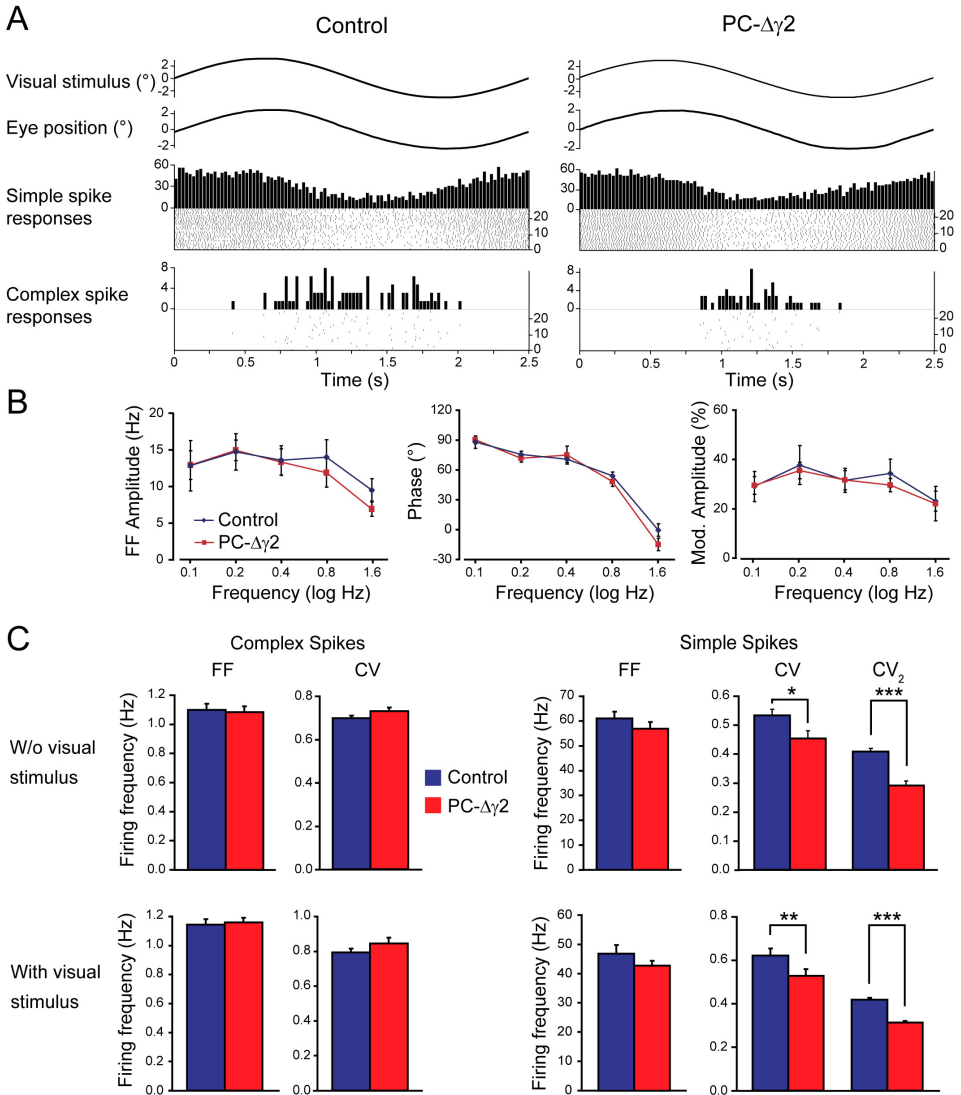


Figure 7. Temporal patterns of simple spike activities of floccular Purkinje cells are specifically affected in PC- $\Delta\gamma 2$ mice, both during compensatory eye movement behaviour and during spontaneous behaviour. (A) Representative single unit activity recorded from Purkinje cells in the flocculus of a control and a PC- $\Delta\gamma 2$ mouse during fixed velocity ($8^{\circ}/s$, 0.2 Hz) OKR stimulation. The visual stimulus and eye position are shown together with histograms of simple spike and complex spike frequencies and corresponding raster plots. (B) Firing frequency, phase relative to stimulus and amplitude of modulation (see Experimental Procedures) of floccular simple spike activities during optokinetic stimulation ($8^{\circ}/s$, $0.1 - 1.6$ Hz) were not significantly different among PC- $\Delta\gamma 2$ and control mice. (C) Although average firing frequency of simple and complex spike activity did not differ between PC- $\Delta\gamma 2$ and control mice, the coefficient of variation (CV) of simple spikes in PC- $\Delta\gamma 2$ mice was significantly reduced in recordings both with and without visual stimuli ($p = 0.008$ and $p = 0.022$, respectively). Also, CV₂ values of simple spikes were significantly lower than those of controls in both conditions. Vertical error bars denote SEM, * denotes $p < 0.05$, ** $p < 0.01$ and *** $p < 0.0001$.

any of the recordings (Figures 7A and C; see also Figure S6 in Supplementary Material).

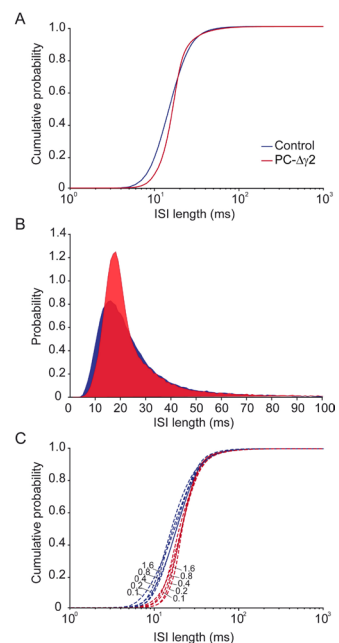
PF-evoked excitatory input, but not GABA_B responsiveness, is altered in PC-Δγ2 mice

Despite the lack of fast synaptic GABA_A receptor-mediated inhibition of Purkinje cells in the PC-Δγ2 mice, the average firing frequency and modulation amplitude of their simple spike activities were normal both *in vitro* and in intact behaving animals. As acute GABA_A receptor blockade in cerebellar slices can increase Purkinje cell simple spike firing frequency by about 40% (Häusser and Clark, 1997), our findings suggest that the loss of GABA_A receptors from Purkinje cells in PC-Δγ2 mice was partly compensated for. Although not the only possible mechanisms, such compensation could result either from an enhanced activity of another inhibitory input or through a reduction in excitatory input to Purkinje cells. We therefore performed control experiments to establish whether postsynaptic metabotropic GABA_B receptor inhibition (mediated by activation of an inwardly rectifying K⁺ current; Tabata et al., 2005) was altered and/or whether excitatory postsynaptic currents were changed at the parallel fiber to Purkinje cell synapse.

To determine whether GABA_B receptor-mediated inhibition of Purkinje cells was altered, we examined the action of the GABA_B receptor agonist baclofen on the simple spike firing rate of Purkinje cells. Baclofen reduced the firing rate to $43.9 \pm 10.0\%$ in PC-Δγ2 mice ($p < 0.001$, $n = 8$) and to $45.9 \pm 9.3\%$ in littermate control mice ($p < 0.005$, $n = 9$). These changes in firing rate were not significantly different between the two groups of mice ($p = 0.89$) (Figure S7 in Supplementary Data). Moreover, restoring the firing rate by application of the GABA_B receptor antagonist CGP54626 was equally successful in PC-Δγ2 and control mice. Firing rate was restored to $105.7 \pm 9.0\%$ in PC-Δγ2 mice ($p = 0.71$, $n = 8$) and to $95.8 \pm 12.1\%$ in control littermate mice ($p = 0.43$; Wilcoxon matched pairs test, $n = 9$); these changes were not significantly different between the two groups of mice ($p = 0.17$; Mann-Whitney U test) (Figure S7). Together, our data indicate that GABA_B receptor action was not altered in the PC-Δγ2 mice.

Figure S5. Simple spike ISI distributions are sharper in PC-Δγ2 mice.

(A) Histograms of individual ISI values pooled from all Purkinje cells recorded without any stimulus (control, blue; PC-Δγ2, red) indicates that PC-Δγ2 mouse Purkinje cell firing is more pronouncedly focused around a preferred interval, whereas in control mice the range of intervals is broader. Inset shows corresponding cumulative probability curves. The later rise and steeper slope indicate the relative absence of short intervals, and thus high frequency, in PC-Δγ2 mice together with a relative abundance of 'normal' intervals. (B) Recordings from floccular Purkinje cells during compensatory eye movements evoked with visual stimulation demonstrate that this phenomenon is also present during motor performance. Shown are cumulative probability plots of ISI values recorded with visual stimuli at various frequencies (0.1 – 1.6 Hz)



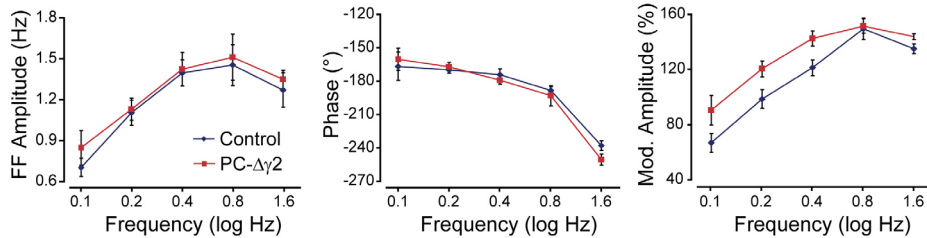


Figure S6. Removal of fast synaptic inhibition from PC- $\Delta\gamma 2$ mice did not alter climbing fiber responses to visual stimuli. Complex spike modulation was analyzed in a manner similar to that for simple spikes (Fig. 7). Modulation parameters were determined by fitting a sine wave through the peri-stimulus histogram. None of the parameters, including firing rate, phase and modulation amplitude, were found to be significantly different between control and PC- $\Delta\gamma 2$ mice. Since climbing fiber activity in the flocculus is considered to carry predominantly the error signal from the retina (retinal slip), these results provide strong evidence that the loss of synaptic inhibition did not affect the processing of visual input before it reached the flocculus.

To determine whether there might be any change in excitatory input to Purkinje cells mediated by parallel fiber activation of AMPA-type glutamate receptors, we measured the EPSC charge transfer evoked in response to increasing stimulus voltages (see Methods, also Matsushita et al., 2002). In Purkinje cells ($n = 14$) from PC- $\Delta\gamma 2$ mice, the slope of the relationship between stimulus voltage and charge transfer was significantly reduced compared to that seen with cells ($n = 13$) from control mice ($p = 0.0025$; ANOVA) (Figure 8). In addition, the weighted time constant (τ_w) of EPSC decay was significantly smaller in PC- $\Delta\gamma 2$ mice ($p = 0.018$), while the paired-pulsed ratio was slightly, but significantly increased ($p = 0.0099$; Mann-Whitney U-test) (Figure 8). Thus, the alteration in parallel fiber-evoked EPSCs could represent a compensatory response to the lack of fast synaptic inhibition.

In principle, the changes in excitatory input described above might affect induction of LTD and/or LTP at the parallel fiber to Purkinje cell synapse, which in turn could contribute to the differences in memory formation we observed between control and PC- $\Delta\gamma 2$ mice. We therefore investigated both LTD and LTP in PC- $\Delta\gamma 2$ ($n = 5$) and control mice ($n = 6$). However, these experiments showed that neither LTD ($p = 0.6$; Mann-Whitney U-test) nor LTP ($p = 0.3$; Mann-Whitney U-test) were significantly affected (Figure S8 in Supplementary Material).

Model, simulations and predictions

Our experiments show (1) that Purkinje cells in PC- $\Delta\gamma 2$ mice are characterized by a relatively low degree of variability in their simple spike activities (Figures 6 and 7); (2) that PC- $\Delta\gamma 2$ mice are able to adapt the gain of their VOR during a gain-down training session, whereas they are unable to fully carry forward this learned decrease in gain to the following day (Figure 5); and (3) that PC- $\Delta\gamma 2$ mice are unable to reverse the phase of their VOR during a multiple-day training paradigm (Figure 5). To elucidate the cellular mechanisms that could underlie these observations, we interpreted our data within the framework of a ‘distributed memory’ model. This model is based on the following accepted ideas: (A) the direct VOR pathway runs through the vestibular nuclei neurons, whose activity can be modulated by an indirect pathway relayed through the cerebellar cortex (De Zeeuw and Yeo, 2005; see Fig. 1); (B) initial acquisition of new VOR skills takes place in the cerebellar cortex (Boyden et al., 2004; De Zeeuw et al., 1998b; Ito, 1982); and (C) memory of recently acquired VOR skills undergoes a form of ‘system

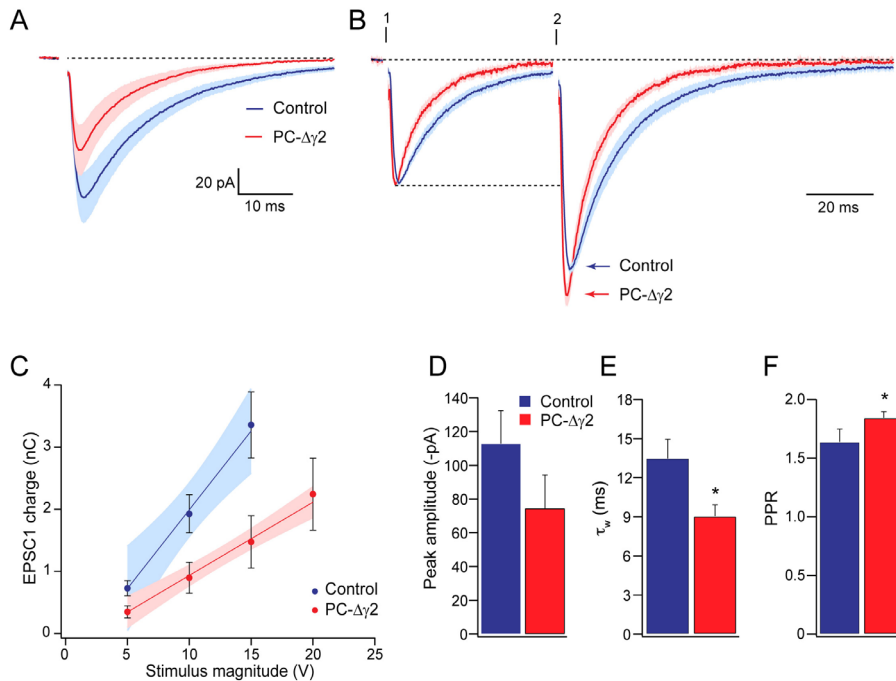


Figure 8. PF-evoked excitatory input is altered in Purkinje cells lacking phasic synaptic inhibition. (A) Parallel fiber-evoked EPSCs (-60 mV) recorded from PC- $\Delta\gamma 2$ mice (red) and 10 V stimulus, 50 ms interval; traces show global averages and shaded areas represent \pm SEM ($n = 14$ PC- $\Delta\gamma 2$ and 10 control cells). The average current was scaled to the peak of EPSC1. Dashed lines illustrate the baseline current and the peak of EPSC1. (C) Relationship between parallel fiber stimulus voltage (0.1 ms pulse duration) and EPSC1 charge transfer, for PC- $\Delta\gamma 2$ mice (red) and littermate controls (blue). Symbols denote mean, error bars denote SEM, and shaded areas the 90% confidence limits for the linear fits. The slopes of the fits are significantly different ($p = 0.0025$). D, E and F, Pooled data showing the peak amplitude (D), decay kinetics (τ_w) of EPSC1 (E) and PPR (F). Bars denote mean and error bars denote SEM. Asterisks indicate significant differences (PPR $p = 0.0099$, Mann Whitney U-test; τ_w $p = 0.018$). For each cell, PPR was calculated as the mean of ratios (EPSC2/EPSC1) obtained at multiple voltages.

consolidation' in that cortical activity guides, during several days of ongoing training, the partial transfer of memory from the cerebellar cortex to the vestibular nuclei for long-term consolidation (Broussard and Kassardjian, 2004; Kassardjian et al., 2005; Miles and Lisberger, 1981; Raymond et al., 1996). The aim of the modeling was three-fold: first, to provide a possible explanation for the altered simple spike ISI distribution in PC- $\Delta\gamma 2$ Purkinje cells; second, to assess the potential impact of changed Purkinje cell firing on plasticity at synapses onto vestibular target neurons; and third, to analyze the role of this modulation at the behavioural level.

Acute drug-induced changes of inhibitory input can result in net changes in Purkinje cell excitation and altered behaviour (Miyashita and Nagao, 1984; Wulff et al., 2007). By contrast, the genetic removal of inhibition in PC- $\Delta\gamma 2$ mice did not alter simple spike frequency (Figures 6 and 7) and only slightly affected baseline motor behaviour (Figure 4). Thus, we assumed that PC- $\Delta\gamma 2$ mice could partially compensate for the loss of feed-forward inhibition. These observations were incorporated into our model, as schematically illustrated in Fig. 9A, with compensation for genetic removal of inhibition shown as maintenance of the integrated simple spike response. The observation that the PF-evoked charge transfer of EPSCs in PC- $\Delta\gamma 2$ mice is reduced *in vitro* (Figure 8)

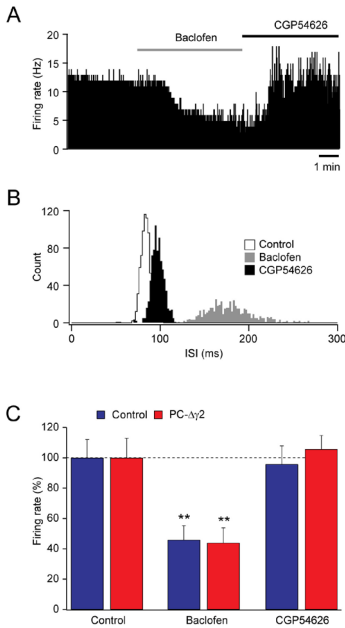


Figure S7. Effect of baclofen on firing rate of Purkinje cells from PC-Δγ2 and control littermate mice.

(A) Firing rate record of a Purkinje cell in a slice from a control mouse. Application of baclofen (10 μM; grey bar) caused a reduction in firing rate from 12 to 6 Hz. Subsequent addition of the GABA_B antagonist CGP54626 (4 μM; black bar) restored firing to near control rates (10 Hz). (B) Histograms of inter-spike interval (ISI) for the cell shown in A (2 ms bin-width). ISI analysis was performed over ~1 min epochs at the end of the respective control or treatment period. (C) Pooled data showing the effect of baclofen in PC-Δγ2 (n = 8) and control mice (n = 9), and the reversal of its actions by CGP54626. Bars show mean and error bars SEM. Asterisks denote significant difference from control firing rate (** p < 0.01).

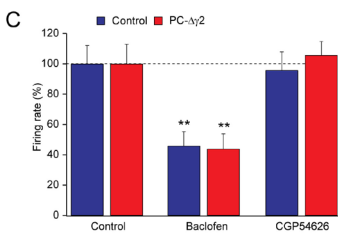
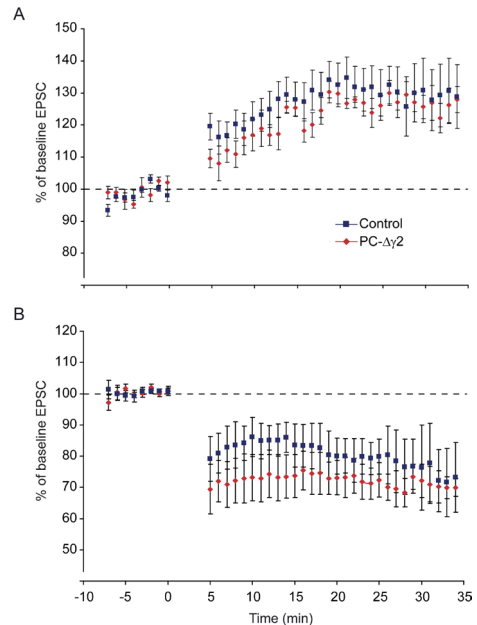


Figure S8. Parallel fiber-Purkinje cell LTP and LTD are not altered in PC-Δγ2 mice.

(A) To test if the loss of inhibition onto Purkinje cells modifies plasticity at others synapses, parallel fiber to Purkinje cell LTP was induced in acute sagittal cerebellar slices by parallel fiber stimulation only (5 min, 5 Hz). This protocol caused a significant increase in EPSC amplitude in PC-Δγ2 mice (n = 4, red) that was comparable to that found in control mice (n = 7, blue) (both p < 0.005 vs baseline, p = 0.257 control vs PC-Δγ2). (B) Parallel fiber to Purkinje cell LTD was induced using 5 min of combined climbing and parallel fiber stimulation at 1 Hz. Following such stimulation, both PC-Δγ2 (n = 5) and control (n = 4) EPSC amplitudes were significantly depressed (both p < 0.05 vs baseline), but no difference was observed between the two groups (p = 0.624).



supports this approach. However, while the average simple spike firing rate may be largely recovered by this compensatory mechanism, the temporal fidelity of the Purkinje cell simple spike responses to parallel fiber input will be reduced (Figure 9A; panel IV). Thus, the model predicts that in PC-Δγ2 mice the parallel fiber-evoked simple spikes will show greater temporal dispersion (increased 'jitter'). This prediction is confirmed by the experimental data shown in Figure 9B, in which the jitter of the evoked response was quantified as the standard deviation of spike latency, measured in a 10 ms window following stimulation (control: 0.81 ± 0.14 ms; PC-Δγ2: 1.80 ± 0.10 ms, p < 0.0001, n = 12 and 11, respectively). Moreover, acute blockade of GABA_A receptors with SR-95531 significantly increased spike jitter in Purkinje cells from control mice (to 1.45 ± 0.14 ms, p = 0.0011; see also Mittmann et al., 2005), whilst, as expected, having no effect in PC-Δγ2 cells (1.76 ± 0.10 ms with SR-95531, p = 0.605).

As described above, the absence of inhibitory input results in different time

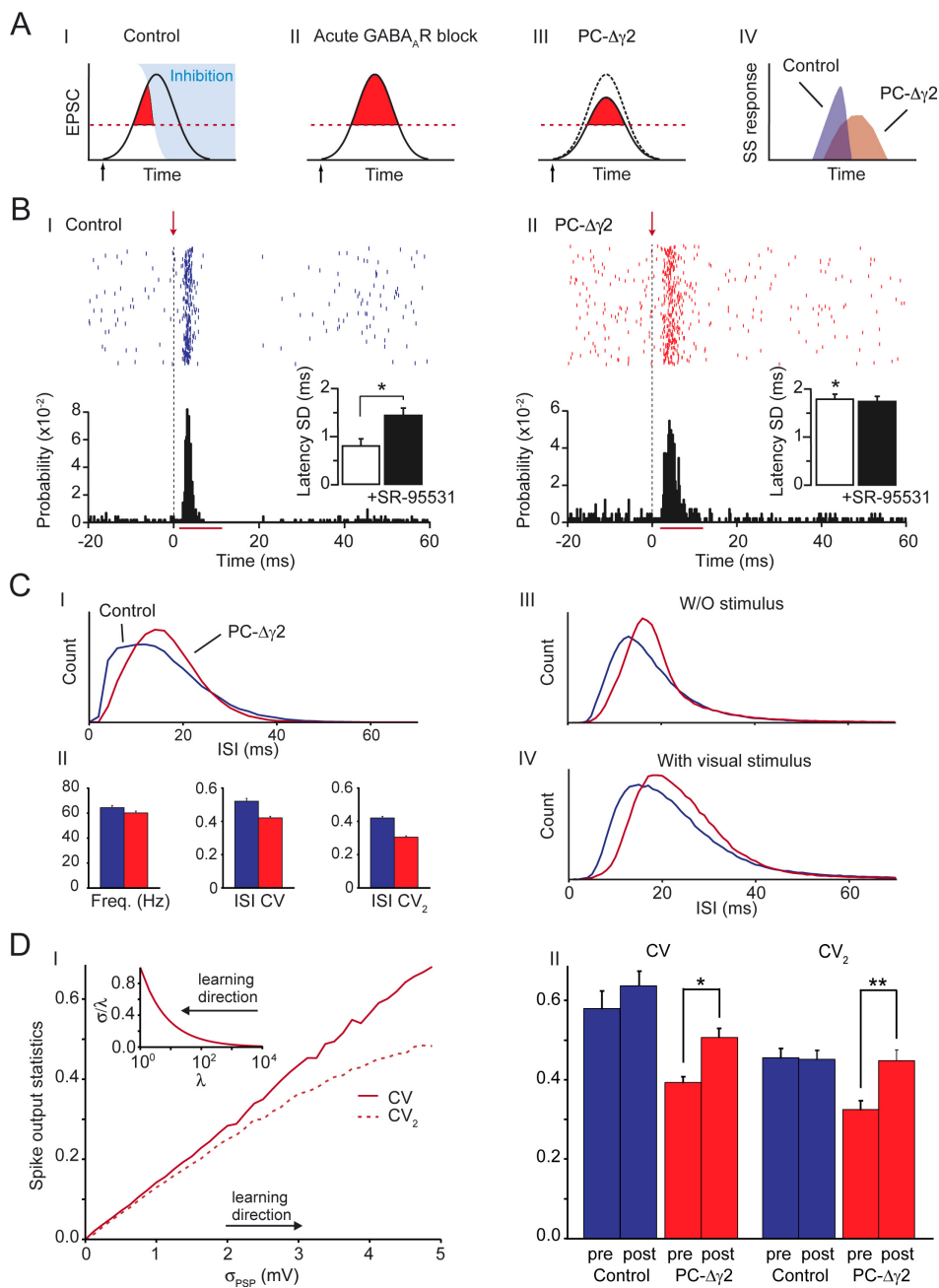


Figure 9. Model, simulations and predictions on spiking activities. (A) Schematic illustration of the presumed relationship between excitatory and inhibitory influences on simple spike responses. A burst of excitatory synaptic activity (black Gaussian curve) elicits simple spike responses in the Purkinje cell when the post-synaptic current crosses an activation threshold (red dashed line). The red area represents the temporal distribution of the simple spike response. The black arrow indicates the start of the excitatory input. (I) In control cells, feed-forward inhibition (blue area) sets the time window for spike generation. (II) Acute block of inhibition results in a large increase in simple spike response, manifested as an increase in Purkinje cell average firing rate. (III) In PC- $\Delta\gamma 2$ mice the EPSC charge is reduced until the red area is again equal to that in control, providing compensation for the loss of inhibition. (IV) Resulting schematic peristimulus-time histograms (PSTHs) of simple spike (SS)

averaged statistical properties of simple spike activity (see also Jaeger et al., 1997; Steuber et al., 2007). Specifically, the ISI distribution and the CV and CV_2 values of PC- $\Delta\gamma 2$ Purkinje cells *in vivo* differed from those in controls, in that the ISI variability was lower in the PC- $\Delta\gamma 2$ mice, both with and without visual stimulation (Figures 7 and 9C; Supplementary Figure S5). Corresponding simple spike ISI distributions and values of CV and CV_2 could be reproduced in our simple spiking model, as shown in Figure 9C. Moreover, the model predicts that the variability of simple spike firing in the PC- $\Delta\gamma 2$ mice alters during visuo-vestibular training (Figure 9D I); in effect, their ‘learning’ can be modeled as the selection of only a set of excitatory synapses, thereby automatically increasing the overall variability of synaptic input (inset of Figure 9D I). This prediction was confirmed by comparing Purkinje cell activities recorded before and after visuo-vestibular training; these experiments showed that both CV and CV_2 values increase in the PC- $\Delta\gamma 2$ mice ($p < 0.01$ and $p < 0.005$), but not in the controls ($p = 0.4$ and $p = 0.6$) (Figure 9D II).

The question remains, how do changes in the temporal patterns of simple spike activities lead to changes in plasticity at downstream synapses in the cerebellar and vestibular nuclei? In the second part of our model (Figure 10 and Supplementary Material), we propose that the induction of plasticity in the vestibular nuclei, necessary for the partial transfer of memory from the cortex, is less efficient in the PC- $\Delta\gamma 2$ mice (Figure 10A). The impairment in plasticity may be due to its putative dependence on the precise spike timing of Purkinje cell inhibitory input with respect to that of the mossy fiber collaterals (Gittis and du Lac, 2006; see also Aizenman et al., 1998). Such ‘system consolidation’ through plasticity in the vestibular nuclei, which is coordinated by Purkinje cell output, could involve changes in efficacy of synapses from mossy fiber collaterals (Pugh and Raman, 2006; Zhang and Linden, 2006). Conceivably, correlations between mossy fiber activity and Purkinje cell output would determine the polarity of synaptic weight change in the nuclei (Masuda and Amari, 2007) (Figure 10A). Mossy fiber input reaches the vestibular nuclei directly via collateral fibers and indirectly, with a time delay T_i via the cerebellar cortex. Thus, as the temporal fidelity of Purkinje cell simple spike responses in PC- $\Delta\gamma 2$ Purkinje cells is disrupted, the nature of the correlation between the two signals will be different, thereby impairing the system transfer of memory to

responses to the excitatory burst. (B) *In vitro* study of simple spike responses evoked by parallel fiber activation. The data show the difference between evoked simple spikes in a Purkinje cell from (I) a control and (II) a PC- $\Delta\gamma 2$ mouse. Upper panels show raster plots (400 sweeps at 0.5 Hz) and lower panels the corresponding PSTHs (0.2 ms bin-width). Arrows and dashed lines indicate the time of stimulation. Note the difference in variability of evoked spike latency, which corresponds to the predictions presented in panel A. Insets show SD of spike latency measured in a 10 ms window following stimulation (red bars; 12 control and 11 PC- $\Delta\gamma 2$ cells; error bars denote SEM). In PC- $\Delta\gamma 2$ cells, spike jitter was significantly greater than that in control cells (* $p < 0.0001$). As predicted, acute blockade of GABA_A receptors with SR-95531 (40 μ M; filled columns) had no effect in PC- $\Delta\gamma 2$ cells, but significantly increased jitter in control cells (* $p = 0.0011$). (C) Results of a basic integrate-and-fire model, with pace-maker activity of ~ 50 Hz. The ISI distributions (I) and time-averaged statistics (II) of control (blue) and PC- $\Delta\gamma 2$ (red) simple spikes closely resemble those observed *in vivo* (III and IV also see Fig. 7C). (D) Predictions of changes in variability due to cerebellar learning. (I) For the distribution of events in a Poisson process, the ratio of standard deviation to mean (σ/λ) increases with decreasing λ , as shown in the inset. For PC- $\Delta\gamma 2$ mice, we assume that learning will reduce the number of synaptic inputs per unit of time (λ) via LTD, but each input will have a stronger post-synaptic effect (due to LTP), thereby preserving the mean postsynaptic potential while the standard deviation (σ_{psp}) is increased. Both the CV and CV_2 value of the simple spike ISI distribution positively depend on σ_{psp} , thus predicting an increase of these values after cerebellar adaptation in PC- $\Delta\gamma 2$ mice. (II) Experimental changes in spike variability due to cerebellar learning. Extracellular recordings from Purkinje cells in the flocculus were obtained in mice subjected to vestibular stimulation in the dark (0.6 Hz VOR) both before and after phase reversal training. As predicted, regularity of firing decreased after training in PC- $\Delta\gamma 2$ mice (CV $p < 0.01$; CV_2 $p < 0.005$). By contrast, the temporal patterns were unchanged in control mice that reversed their phase. For details see Supplementary Material.

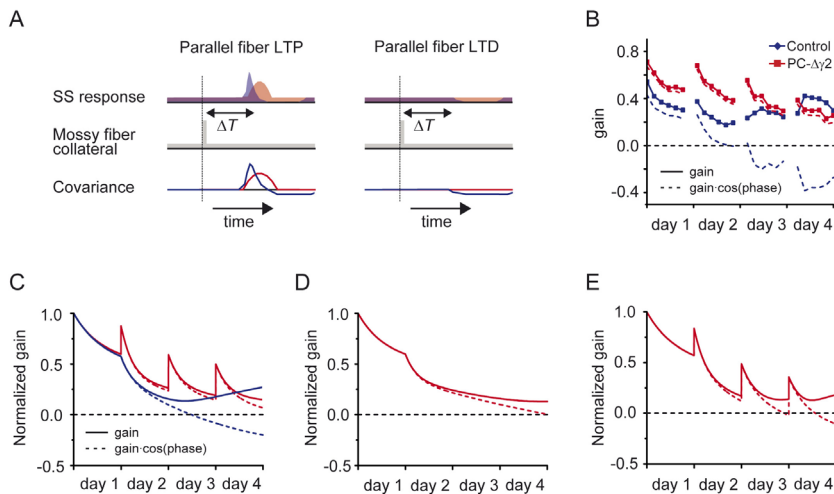


Figure 10. Model, simulations and predictions of plasticity and eye movement behaviour. (A) Schematic illustration of presumed dependency of Purkinje cell simple spike output on parallel fiber plasticity. Mossy fiber signals reach the nuclei directly, via collaterals, and indirectly, with a time delay T , via the cerebellar cortex (i.e. via MF-GC, GC-PC, and PC-VN connections). The simple spike output of the Purkinje cells depends on whether the relevant GC-PC synapses are potentiated (left side) or depressed (right side), and this output can be correlated to that of the mossy fiber collaterals over time (shown as covariance). These correlations in turn may set the polarity of plastic change in the nuclei, involved in ‘system consolidation’ of a motor memory. ‘System consolidation’ in PC- $\Delta\gamma 2$ mice can be impaired due to altered correlations as compared to controls. (B) Experimental data of VOR adaptation in PC- $\Delta\gamma 2$ mice (red) and controls (blue) during a four-day training paradigm: gain down training on the first day, followed by three days of phase reversal training. The dashed curves indicate the extent of phase-shift in the VOR. (C) VOR adaptation was simulated by two learning rates on different timescales, involved in a form of ‘system consolidation’ (see Text and Supplementary Materials for details). These simulations describe the data presented in B well. (D) The inability of PC- $\Delta\gamma 2$ mice to reverse the phase of their VOR during the four-day training paradigm can be accounted for by assuming a reduced rate of plasticity induction in the nuclei, as depicted in (A). (E) The inability of PC- $\Delta\gamma 2$ mice to carry a learned decrease in gain forward to the next training day can be accounted for by incorporating impaired consolidation of cortical memory. In this case, phase reversal is still possible (the dashed line crosses zero), although the cortical signal has to be relearned at the beginning of each training day. Incorporating both impairments (D and E) in the simulations yields the red curve shown in (C). For details see Supplementary Material.

the nuclei.

The proposed model can explain how functional removal of feed-forward inhibition by molecular layer interneurons in the cerebellar cortex may result in impaired plasticity in the vestibular nuclei, but how will such a deficit affect long-term consolidation of a motor memory? To assess whether the behavioural phenotype in PC- $\Delta\gamma 2$ mice is compatible with impaired ‘system consolidation’ at the cellular level, we simulated our VOR adaptation data (Figure 10B) using two superimposed exponential learning rates (Figures 10C-E): a rate constant in the order of ~ 10 minutes, to represent initial acquisition in the cortex, and a rate constant in the order of hours, to represent gradual memory transfer to the nuclei. The VOR gain and phase adaptation during a four-day training paradigm in wild-types can be described well by such a model (Figure 10C, blue curves).

Within the framework of this model, plastic adaptation in the nuclei is an important factor in accomplishing VOR phase reversal. Slowing down the rate of memory transfer to the nuclei in the model (to simulate the impairment discussed above) prevents phase reversal from occurring within the modeled four-day paradigm (Figure 10D). Thus, this outcome indicates that impairment in phase reversal might be directly related to impaired

plasticity in the vestibular nuclei, resulting from absent cortical inhibition. The inability to consolidate a decrease in gain, however, indicates that memory initially acquired in the cortex is lost during the post-learning periods between the training sessions. PC- $\Delta\gamma 2$ mice need to re-acquire the new VOR gain at the beginning of each session, and do so every time at more or less the same rate (as illustrated in Figure 5). Why might such post-learning molecular consolidation processes not function properly in the absence of inhibition? Normal cortical activity in the 1-2 hour period directly following learning has been shown to be crucial for memory consolidation to occur (Cooke et al., 2004). By incorporating a partial loss of cortical memory in between training sessions, the gain curve in Figure 10E can be generated and this corresponds closely to the experimental gain curve. Moreover, combining both impairments in the model, i.e. a partial loss of cortical memory in between sessions and a less efficient memory transfer to the nuclei, provides a good description of the overall experimental data on multiple day VOR adaptation in PC- $\Delta\gamma 2$ mice (Figure 10C, red curves).

Thus, taken together our data indicate that functional removal of the output of molecular layer interneurons in PC- $\Delta\gamma 2$ mice leads to altered temporal patterns of simple spike activities, which in turn may result in reduced induction of plasticity in the nuclei downstream, and thereby contribute to impaired consolidation of motor learning.

Discussion

Given that the majority of cell types in the cerebellar cortex is inhibitory, it is surprising that the functional roles of GABAergic interneurons in the molecular layer of the cerebellum have been relatively neglected over the past decades. As a consequence, the significance of these cells at the behavioural level has remained, to a large extent, enigmatic. Here we show that a key role of cerebellar molecular layer interneurons, and by implication of feed-forward inhibition, is to enable the consolidation of procedural memories. This role in motor learning is of such prominence that early postnatal elimination of GABAergic input to Purkinje cells cannot be compensated for during subsequent development, with the consequence that motor performance is slightly, but permanently, affected. Our electrophysiological data and computer simulations indicate that the molecular layer interneurons exert their influence on cerebellar motor learning by shaping the temporal patterns of simple spike responses of Purkinje cells, a role that we suggest is critical for plasticity and consolidation in the cerebellar and vestibular nuclei.

Purkinje cell recurrent collaterals

Although our study was aimed at elucidating the role of molecular layer interneurons, we cannot exclude the possibility that recurrent collaterals of Purkinje cell axons also contribute to the motor functions described above. In the PC- $\Delta\gamma 2$ mouse, we eliminated all synaptic GABA_A receptors from Purkinje cells, and thereby we also affected any input from recurrent collaterals of the Purkinje cells themselves. Yet, several arguments suggest that the phenotypes we observed largely reflect the impact of a loss of input from molecular layer interneurons. First, the total number of GABAergic terminals onto Purkinje cells that derive from basket and stellate cells is vastly more than that from the recurrent collaterals (Palay and Chan-Palay, 1974). Second, the basket cells strategically synapse at cell bodies of Purkinje cells and here too they outnumber terminals from recurrent collaterals (Palay and Chan-Palay, 1974). Third, during phylogeny, inhibition

provided by recurrent collaterals of Purkinje cells has been gradually replaced by that from molecular layer interneurons (Llinas, 1969; Alvarez-Otero et al., 1995; Gao et al., 2006; Leto et al., 2006). Thus, even though recurrent collaterals might contribute to some extent (Watt et al., 2006; University College London, Proc Physiol Soc 3, C108), it is parsimonious to conclude that the feed-forward inhibition provided by the basket and stellate cells has a dominant role in cerebellar learning and simple spike patterning in mammals.

Signal coding mechanism

Our experimental findings and model simulations, which indicate that molecular layer interneurons support motor learning by controlling the temporal pattern of simple spike activities, are in line with several recent observations. Specifically, GABAergic interneurons in the cerebellar cortex have ample possibilities to induce and express plasticity at both the level of their synaptic input and output (Duguid & Smart, 2004; Ekerot and Jorntell, 2003; Jorntell and Ekerot, 2002; Kano et al., 1992, Smith and Otis, 2005). Moreover, simple spike trains of Purkinje cells show significantly more temporal patterns than would be expected based upon random activation (Shin et al., 2007), and these patterns can be influenced by natural stimuli (Steuber et al., 2007). Finally, the proposed mechanism of temporal coding also provides a possible explanation for some of the cyto-architectural aspects of the cerebellar network the possible function of which has remained unclear. For example, stellate cells and basket cells are electrically coupled by gap junctions and their axons are oriented in the sagittal plane controlling a zone of Purkinje cells (Mann-Metzer and Yarom, 1999; Van der Giessen et al., 2006) (Figure 1). This configuration will promote the occurrence of temporal activity patterns in ensembles of Purkinje cells within the same zone, which are known to project to the same cerebellar or vestibular nucleus (Schonewille et al., 2006b). The activity patterns of individual Purkinje cells in such an ensemble might thus enhance each other and induce plasticity at the level of their target neurons in the cerebellar and vestibular nuclei (Blazquez et al., 2006; Gittis and du Lac, 2006; Lisberger, 1998; Shin and De Schutter, 2006; Steuber et al., 2007), which in turn could, as explained in our model, serve as the main locus for the consolidation process itself (see also Kassardjian et al., 2005).

Prominent behavioural impact of feed-forward inhibition on consolidation of motor memories

PC- $\Delta\gamma 2$ mice show no overt signs of ataxia or tremor, unlike knock-outs of the GABA_A receptor $\alpha 1$ subunit gene (Kralic et al., 2005; see also Wulff et al., 2007). As the loss of synaptic GABA_A receptors in PC- $\Delta\gamma 2$ Purkinje cells is permanent, beginning in the second postnatal week (Barski et al., 2000), it appears likely that the system partially compensated for the functional loss of input from molecular layer interneurons (Miyashita and Nagao, 1984). Indeed, we know from our previous studies, in which we made Purkinje cell GABA_A receptors (and thus stellate/basket cell synapses) selectively sensitive to the positive modulator zolpidem, that ongoing feed-forward inhibition from molecular layer interneurons onto Purkinje cells does engage prominently in real-time control of baseline motor performance (Wulff et al., 2007). However, this ongoing GABA input is dispensable, in as much as compensatory changes appear capable of maintaining near-normal function if removal of inhibition is permanent, as in PC- $\Delta\gamma 2$ mice. In marked contrast, this GABAergic input is indispensable for consolidation of VOR gain adaptation

and phase reversal. Apparently, the role of interneurons in this process is so critical that their loss cannot be overcome by adaptive changes. We therefore suggest that facilitating the consolidation of motor memories is one of the principal functions of molecular layer interneurons.

The phenotype of the PC- $\Delta\gamma 2$ mice differs from that of other mouse lines in which LTD induction at the parallel fiber to Purkinje cell synapse is impaired (De Zeeuw et al., 1998a; Feil et al., 2003; van Alphen and De Zeeuw, 2002; Hansel et al., 2006). In these mice, which include the L7-PKCi, L7-PKG^{-/-}, and α -CaMKII lines, acute motor learning is more severely affected than in PC- $\Delta\gamma 2$ mice, whereas motor performance and consolidation over multiple days of training are less affected (cf. Boyden et al., 2006). The trend emerging from these phenotypes suggests that the ultimate baseline motor performance depends to a greater extent on the consolidation of motor memory formation mediated by the molecular layer interneurons and GABA_A receptor-mediated feed-forward inhibition, than it does on the acute effects of motor training mediated by parallel fiber LTD. On the other hand, it should be noted that our simulations indicate that co-induction of LTP at the parallel fiber to Purkinje cell synapse appears less dispensable than LTD. Indeed, this hypothesis is supported by experimental evidence from Strata and colleagues, who found that adequate levels of both plasticity at the inhibitory synapses onto Purkinje cells and LTP at the parallel fiber to Purkinje cell synapse were required for associative fear conditioning (Scelfo et al., 2008). Thus, in this scenario, the potentiation of GABAergic synapses may balance the LTP of excitatory inputs in a form of scaling, which in turn may be essential for memory consolidation downstream in the target neurons of the Purkinje cells.

General functional implications

To the best of our knowledge, the current study provides one of the most compelling pieces of evidence that inhibitory interneurons can play a profound role in procedural learning. In the field of cerebellar learning, our study complements numerous previous behavioural studies that have addressed the role of the excitatory parallel fiber to Purkinje cell synapse. These studies have provided mostly, but not exclusively, supportive evidence that parallel fiber LTD may be required for forms of motor learning such as eye-blink conditioning, locomotion learning, or adaptation of the VOR (Aiba et al., 1994; De Zeeuw et al., 1998; Koekkoek et al., 2003; Shibuki et al., 1996; cf. Welsh et al., 2005). Our findings suggest that it may also be instructive to further examine how feed-forward inhibition might control declarative learning processes. Research in this field has tended to emphasize the importance of hippocampal LTP. In the hippocampal and neocortical circuitry, where the diversity of GABAergic interneurons is also very high (Somogyi and Klausberger, 2005), some interneuron types may serve functions similar to those we have identified in the cerebellum. For example, feed-forward inhibitory interneurons in the stratum radiatum of the hippocampus may promote the temporal fidelity of synaptic integration and action potential generation in pyramidal cells during memory encoding (Lamsa et al., 2005; Smith and Mizumori, 2006; see also Pouille & Scanziani, 2001 and 2004), while administration of GABA targeting drugs in this region can affect spatial memory consolidation (McGaugh, 2000). Thus, GABAergic interneurons in different brain circuits might play a general role in memory formation by controlling the temporal activity patterns of projecting neurons.

Acknowledgements

This work was initiated while PW and WW were at the Dept of Clinical Neurobiology, University of Heidelberg; we thank H. Monyer for support during that time. We thank M. Rutteman, R. Avila Freire, E. Dalm and J. v.d. Burg for their excellent technical assistance, D. Andersson and L. Kelly for participation in initial electrophysiological studies. We were supported by the J. Ernest Tait Estate Aberdeen (WW), the University of Aberdeen (PW & WW), the Medical Research Council (PW & WW), the Institute Pasteur-Fondazione Cenci Bolognetti (MR), a Wellcome Trust Programme Grant (MF), Regione Piemonte and Compagnia di San Paolo (MSP), the Dutch Organization for Medical Sciences (CIDZ), Life Sciences (CIDZ), Senter (Neuro-Bsik, CIDZ), Prinses Beatrix Fonds (CIDZ), and the SENSOPAC program of the European Community (CIDZ).

Reference List

- Aiba, A., Kano, M., Chen, C., Stanton, M. E., Fox, G. D., Herrup, K., Zwingman, T. A., and Tonegawa, S. (1994). Deficient cerebellar long-term depression and impaired motor learning in mGluR1 mutant mice. *Cell* 79, 377-388.
- Aizenman, C. D., Manis, P. B., Linden, D. J. (1998) Polarity of long-term synaptic gain change is related to postsynaptic spike firing at a cerebellar inhibitory synapse. *Neuron* 21, 827-35.
- Alvarez-Otero, R., Perez, S.E., Rodriguez, M.A., Adrio, F., and Anadon, R. (1995) GABAergic neuronal circuits in the cerebellum of the dogfish *Scyliorhinus canicula* (Elasmobranchs): an immunocytochemical study. *Neurosci Lett.* 187, 87-90.
- Barski, J. J., Dethleffsen, K., and Meyer, M. (2000). Cre recombinase expression in cerebellar Purkinje cells. *Genesis* 28, 93-98.
- Blazquez, P. M., Hirata, Y., and Highstein, S. M. (2006). Chronic changes in inputs to dorsal Y neurons accompany VOR motor learning. *J Neurophysiol* 95, 1812-1825.
- Boyden, E. S., Katoh, A., and Raymond, J.L. (2004). Cerebellum-dependent learning: the role of multiple plasticity mechanisms. *Annu. Rev. Neurosci.* 27, 581-609.
- Boyden, E. S., Katoh, A., Pyle, J. L., Chatila, T. A., Tsien, R. W., and Raymond, J. L. (2006). Selective engagement of plasticity mechanisms for motor memory storage. *Neuron* 51, 823-834.
- Broussard, D.M., and Kassardjian, C.D. (2004). Learning in a simple motor system. *Learn. Mem.* 11, 127-136.
- Brickley, S. G., Cull-Candy, S. G., and Farrant, M. (1999). Single-channel properties of synaptic and extrasynaptic GABAA receptors suggest differential targeting of receptor subtypes. *J Neurosci* 19, 2960-2973.
- Broussard, D.M., and Kassardjian, C.D. (2004). Learning in a simple motor system. *Learn. Mem.* 11, 127-136.
- Buzsaki, G. (2005). Neuroscience. Similar is different in hippocampal networks. *Science* 309, 568-569.
- Clements, J. D. and Bekkers, J. M. (1997) Detection of spontaneous synaptic events with an optimally scaled template. *Biophys. J.* 73, 220-229.
- Coessmans, M., Weber, J. T., De Zeeuw, C. I., and Hansel, C. (2004). Bidirectional parallel fiber plasticity in the cerebellum under climbing fiber control. *Neuron* 44, 691-

- 700.
- Cooke, S. F., Attwell, P. J., and Yeo, C. H. (2004). Temporal properties of cerebellar-dependent memory consolidation. *J. Neurosci.* 24, 2934-2941.
- De Zeeuw, C. I., Simpson, J. I., Hoogenraad, C. C., Galjart, N., Koekkoek, S. K., Ruigrok T. J. (1998a). Microcircuitry and function of the inferior olive. *Trends Neurosci.* 21, 391-400.
- De Zeeuw, C. I., Hansel, C., Bian, F., Koekkoek, S. K., van Alphen, A. M., Linden, D. J., and Oberdick, J. (1998b). Expression of a protein kinase C inhibitor in Purkinje cells blocks cerebellar LTD and adaptation of the vestibulo-ocular reflex. *Neuron* 20, 495-508.
- De Zeeuw, C. I., and Yeo, C. H. (2005). Time and tide in cerebellar memory formation. *Curr Opin Neurobiol* 15, 667-674.
- Duguid, I. C., and Smart, T. G. (2004). Retrograde activation of presynaptic NMDA receptors enhances GABA release at cerebellar interneuron-Purkinje cell synapses. *Nat Neurosci* 7, 525-533.
- Eccles, J. C., Sasaki, K., and Strata, P. (1967). A comparison of the inhibitory actions of Golgi cells and of basket cells. *Exp Brain Res* 3, 81-94.
- Ekerot, C. F., and Jorntell, H. (2003). Parallel fiber receptive fields: a key to understanding cerebellar operation and learning. *Cerebellum* 2, 101-109.
- Fritschy, J. M., Panzanelli, P., Kralic, J. E., Vogt, K. E., and Sassoe-Pognetto, M. (2006). Differential dependence of axo-dendritic and axo-somatic GABAergic synapses on GABA_A receptors containing the $\alpha 1$ subunit in Purkinje cells. *J Neurosci* 26, 3245-3255.
- Gao W, Chen G, Reinert KC, Ebner TJ. (2006). Cerebellar cortical molecular layer inhibition is organized in parasagittal zones. *J Neurosci.* 26, 8377-87.
- Gittis, A. H., and du Lac, S. (2006). Intrinsic and synaptic plasticity in the vestibular system. *Curr Opin Neurobiol* 16, 385-390.
- Goossens, H. H., Hoebeek, F. E., Van Alphen, A. M., Van Der Steen, J., Stahl, J. S., De Zeeuw, C. I., and Frens, M. A. (2004). Simple spike and complex spike activity of floccular Purkinje cells during the optokinetic reflex in mice lacking cerebellar long-term depression. *Eur J Neurosci* 19, 687-697.
- Hansel, C., de Jeu, M., Belmeguenai, A., Houtman, S. H., Buitendijk, G. H., Andreev, D., De Zeeuw, C. I., and Elgersma, Y. (2006). α CaMKII is essential for cerebellar LTD and motor learning. *Neuron* 51, 835-843.
- Häusser, M., and Clark, B. A. (1997). Tonic synaptic inhibition modulates neuronal output pattern and spatiotemporal synaptic integration. *Neuron* 19, 665-678.
- Hioki, H., Fujiyama, F., Taki, K., Tomioka, R., Furuta, T., Tamamaki, N., and Kaneko, T. (2003). Differential distribution of vesicular glutamate transporters in the rat cerebellar cortex. *Neuroscience* 117, 1-6.
- Hoebeek, F. E., Stahl, J. S., van Alphen, A. M., Schonewille, M., Luo, C., Rutteman, M., van den Maagdenberg, A. M., Molenaar, P. C., Goossens, H. H., Frens, M. A., and De Zeeuw, C. I. (2005). Increased noise level of purkinje cell activities minimizes impact of their modulation during sensorimotor control. *Neuron* 45, 953-965.
- Holt, G. R., Softky, W. R., Koch, C., and Douglas, R. J. (1996). Comparison of discharge variability in vitro and in vivo in cat visual cortex neurons. *J Neurophysiol* 75, 1806-1814.
- Ito, M. (1982). Cerebellar control of the vestibulo-ocular reflex--around the flocculus

- hypothesis. *Annu Rev Neurosci* 5, 275-296.
- Ito, M. (1989). Long-term depression. *Annu Rev Neurosci* 12, 85-102.
- Ito, M. (1993). Cerebellar flocculus hypothesis. *Nature* 363, 24-25.
- Jaeger, D., and Bower, J. M. (1997). The role of synaptic and voltage-gated currents in the control of Purkinje cell spiking: a modeling study. *J. Neurosci.* 17, 91-106.
- Jorntell, H., and Ekerot, C. F. (2002). Reciprocal bidirectional plasticity of parallel fiber receptive fields in cerebellar Purkinje cells and their afferent interneurons. *Neuron* 34, 797-806.
- Kano, M., Rexhausen, U., Dreessen, J., and Konnerth, A. (1992). Synaptic excitation produces a long-lasting rebound potentiation of inhibitory synaptic signals in cerebellar Purkinje cells. *Nature* 356, 601-604.
- Kassardjian, C.D., Tan, Y.F., Chung, J.Y., Heskin, R., Peterson, M.J., Broussard, D.M. (2005). The site of a motor memory shifts with consolidation. *J Neurosci.* 25, 7979-85.
- Koekkoek, S. K., Hulscher, H. C., Dortland, B. R., Hensbroek, R. A., Elgersma, Y., Ruigrok, T. J., and De Zeeuw, C. I. (2003). Cerebellar LTD and learning-dependent timing of conditioned eyelid responses. *Science* 301, 1736-1739.
- Kralic, J. E., Criswell, H. E., Osterman, J. L., O'Buckley, T. K., Wilkie, M. E., Matthews, D. B., Hamre, K., Breese, G. R., Homanics, G. E., and Morrow, A. L. (2005). Genetic essential tremor in gamma-aminobutyric acidA receptor alpha1 subunit knockout mice. *J Clin Invest* 115, 774-779.
- Lorez, N., Benke, D., Luscher, B., Mohler, H., and Benson, J. A. (2000). Single-channel properties of neuronal GABA_A receptors from mice lacking the γ 2 subunit. *J Physiol* 527, 11-31.
- Lamsa, K., Heeroma, J. H., and Kullmann, D. M. (2005). Hebbian LTP in feed-forward inhibitory interneurons and the temporal fidelity of input discrimination. *Nat Neurosci* 8, 916-924.
- Laurie, D. J., Seeburg, P. H., and Wisden, W. (1992). The distribution of 13 GABA_A receptor subunit mRNAs in the rat brain. II. Olfactory bulb and cerebellum. *J Neurosci* 12, 1063-1076.
- Leto K., Carletti B., Williams I.M., Magrassi L., Rossi F. (2006). Different types of cerebellar GABAergic interneurons originate from a common pool of multipotent progenitor cells. *J Neurosci.* 26, 11682-94.
- Llinas, R.R. (1969). *Neurobiology of Cerebellar Evolution and Development: Proceedings of the First International Symposium of the Institute for Biomedical Research.* Published by American Medical Association; Chicago, pp. 1-941.
- Lisberger, S. G. (1998). Cerebellar LTD: a molecular mechanism of behavioural learning? *Cell* 92, 701-704.
- Lisman, J., and Raghavachari, S. (2006). A unified model of the presynaptic and postsynaptic changes during LTP at CA1 synapses. *Sci STKE* 2006, re11.
- Mann-Metzer, P., and Yarom, Y. (1999). Electrotonic coupling interacts with intrinsic properties to generate synchronized activity in cerebellar networks of inhibitory interneurons. *J Neurosci* 19, 3298-3306.
- Masuda, N., and Amari, S.I. (2008). A computational study of synaptic mechanisms of partial memory transfer in cerebellar vestibulo-ocular-reflex learning. *J. Comput. Neurosci.* 24, 137-56.
- Matsushita, K., Wakamori, M., Rhyu, I.J., Arai, T., Oda, S., Mori, Y., Imoto, K. et al., (2002). Bidirectional alterations in cerebellar synaptic transmission of tottering and rolling

- Ca²⁺ channel mutant mice. *J Neurosci* 22, 4388-4398.
- McGaugh, J.L. (2000). Memory - a century of consolidation. *Science* 287, 248-251.
- Miles, F.A., and Lisberger, S.G. (1981). Plasticity in the vestibulo-ocular reflex: a new hypothesis. *Annu. Rev. Neurosci.* 4, 273-299.
- Mittmann, W., Koch, U., and Häusser, M. (2005). Feed-forward inhibition shapes the spike output of cerebellar Purkinje cells. *J Physiol* 563, 369-378.
- Mortensen, M., and Smart, T. G. (2006). Extrasynaptic alphabeta subunit GABA_A receptors on rat hippocampal pyramidal neurons. *J Physiol* 577, 841-856.
- Miyashita, Y., and Nagao S. (1984). Contribution of cerebellar intracortical inhibition to Purkinje cell response during vestibulo-ocular reflex of alert rabbits. *J Physiol.* 351, 251-262.
- Palay, S.L., and Chan-Palay, V. (1974). Cerebellar cortex, cytology and organization. Springer Verlag, Berlin Heidelberg New York.
- Pouille, F., and Scanziani, M. (2001). Enforcement of temporal fidelity in pyramidal cells by somatic feed-forward inhibition. *Science* 293, 1159-1163.
- Pouille, F., and Scanziani, M. (2004). Routing of spike series by dynamic circuits in the hippocampus. *Nature* 429, 717-723.
- Pugh, J.R., and Raman, I.M. (2006). Potentiation of mossy fiber EPSCs in the cerebellar nuclei by NMDA receptor activation followed by postinhibitory rebound current. *Neuron* 51, 113-123.
- Raman, I. M., and Bean, B. P. (1997). Resurgent sodium current and action potential formation in dissociated cerebellar Purkinje neurons. *J Neurosci* 17, 4517-4526.
- Rancillac, A., and Crepel, F. (2004). Synapses between parallel fibres and stellate cells express long-term changes in synaptic efficacy in rat cerebellum. *J. Physiol* 554, 707-720.
- Raymond, J.L., Lisberger, S.G., and Mauk, M.D. (1996). The cerebellum: a neuronal learning machine? *Science* 272, 1126-1131.
- Santamaria, F., Tripp, P. G. and Bower, J. M. (2007). Feed-forward inhibition controls the spread of granule cell-induced Purkinje cell activity in the cerebellar cortex. *J Neurophysiol* 97, 248-263.
- Scelfo, B., Sacchetti, B., and Strata, P. (2008). Learning-related long-term potentiation of inhibitory synapses in the cerebellar cortex. *Proc Natl Acad Sci USA* 105, 769-774.
- Schneider Gasser, E. M., Straub, C. J., Panzanelli, P., Weinmann, O., Sassoe-Pognetto, M., and Fritschy, J. M. (2006). Immunofluorescence in brain sections: simultaneous detection of presynaptic and postsynaptic proteins in identified neurons. *Nat Protoc* 1, 1887-1897.
- Schonewille, M., Khosrovani, S., Winkelman, B. H., Hoebeek, F. E., De Jeu, M. T., Larsen, I. M., Van der Burg, J., Schmolesky, M. T., Frens, M. A., and De Zeeuw, C. I. (2006a). Purkinje cells in awake behaving animals operate at the upstate membrane potential. *Nat Neurosci* 9, 459-461.
- Schonewille, M., Luo, C., Ruigrok, T. J., Voogd, J., Schmolesky, M. T., Rutteman, M., Hoebeek, F. E., De Jeu, M. T., and De Zeeuw, C. I. (2006b). Zonal organization of the mouse flocculus: physiology, input, and output. *J Comp Neurol* 497, 670-682.
- Schweizer, C., Balsiger, S., Bluethmann, H., Mansuy, I. M., Fritschy, J. M., Mohler, H., and Luscher, B. (2003). The gamma 2 subunit of GABA(A) receptors is required for maintenance of receptors at mature synapses. *Mol Cell Neurosci* 24, 442-450.
- Shibuki, K., Gomi, H., Chen, L., Bao, S., Kim, J. J., Wakatsuki, H., Fujisaki, T., Fujimoto,

- K., Katoh, A., Ikeda, T., et al. (1996). Deficient cerebellar long-term depression, impaired eyeblink conditioning, and normal motor coordination in GFAP mutant mice. *Neuron* 16, 587-599.
- Shin, S.-L., and De Schutter, E. (2006). Dynamic synchronization of Purkinje cell simple spikes. *J Neurophysiol* 96, 3485-3491.
- Shin, S.-L., Rotter, S., Aertsen, A. and De Schutter, E. (2007). Stochastic description of complex and simple spike firing in cerebellar Purkinje cells. *Eur J Neurosci* 25, 785-794.
- Shin, S. L., Hoebeek, F. E., Schonewille, M., De Zeeuw, C. I., Aertsen, A., and De Schutter, E. (2007). Regular patterns in cerebellar Purkinje cell simple spike trains. *PLoS ONE* 2, e485.
- Smith, D. M., and Mizumori, S. J. (2006). Learning-related development of context-specific neuronal responses to places and events: the hippocampal role in context processing. *J Neurosci* 26, 3154-3163.
- Smith, S. L., and Otis, T. S. (2005). Pattern-dependent, simultaneous plasticity differentially transforms the input-output relationship of a feedforward circuit. *Proc Natl Acad Sci U S A* 102, 14901-6.
- Somogyi, P., and Klausberger, T. (2005). Defined types of cortical interneurone structure space and spike timing in the hippocampus. *J Physiol* 562, 9-26.
- Stahl, J. S., van Alphen, A. M., and De Zeeuw, C. I. (2000). A comparison of video and magnetic search coil recordings of mouse eye movements. *J Neurosci Methods* 99, 101-110.
- Steuber V., Mittmann, W., Hoebeek, F. E., Silver, R. A., De Zeeuw, C. I., Häusser, M. and De Schutter, E. (2007). Cerebellar LTD and pattern recognition by Purkinje cells: computer simulations and experiments. *Neuron* 54, 121-136.
- Tabata, T., Haruki, S., Nakayama, H., Kano, M. (2005). GABAergic activation of an inwardly rectifying K⁺ current in mouse cerebellar Purkinje cells. *J Physiol* 563, 443-57.
- van Alphen A.M., and De Zeeuw, C.I. (2002). Cerebellar LTD facilitates but is not essential for long-term adaptation of the vestibulo-ocular reflex. *Eur J Neurosci* 16, 486-90.
- Van Der Giessen, R. S., Maxeiner, S., French, P. J., Willecke, K., and De Zeeuw, C. I. (2006). Spatiotemporal distribution of Connexin45 in the olivocerebellar system. *J Comp Neurol* 495, 173-184.
- Wall, M. J. and Usowicz, M. M. (1997). Development of action potential-dependent and independent spontaneous GABA_A receptor-mediated currents in granule cells of postnatal rat cerebellum. *Eur J Neurosci* 9, 533-548.
- Walter, J. T., Alvina, K., Womack, M. D., Chevez, C. and Khodakhah, K. (2006). Decreases in the precision of Purkinje cell pacemaking cause cerebellar dysfunction and ataxia. *Nat Neurosci* 9, 389-397.
- Welsh, J. P., Yamaguchi, H., Zeng, X. H., Kojo, M., Nakada, Y., Takagi, A., Sugimori, M., and Llinas, R. R. (2005). Normal motor learning during pharmacological prevention of Purkinje cell long-term depression. *Proc Natl Acad Sci U S A* 102, 17166-17171.
- Whitlock, J. R., Heynen, A. J., Shuler, M. G., and Bear, M. F. (2006). Learning induces long-term potentiation in the hippocampus. *Science* 313, 1093-1097.
- Wisden, W., Korpi, E. R., and Bahn, S. (1996). The cerebellum: a model system for studying GABA_A receptor diversity. *Neuropharmacology* 35, 1139-1160.
- Wulff, P., Goetz, T., Leppa, E., Linden, A. M., Renzi, M., Swinny, J. D., Vekovischeva, O. Y., Sieghart, W., Somogyi, P., Korpi, E. R., Farrant, M., and Wisden, W. (2007). From

synapse to behaviour: rapid modulation of defined neuronal types with engineered GABA_A receptors. Nat Neurosci 10, 923-929.

Zhang, W., and Linden, D.J. (2006). Long-term depression at the mossy fiber-deep cerebellar nucleus synapse. J. Neurosci. 26, 6935-6944.

Integrate-and-fire model and simulations

Simple spike simulation

The absence of inhibitory interneuron input to Purkinje cells deprives the cerebellar cortex of a mechanism for dynamic control of Purkinje cell simple spike firing. During ongoing cerebellar control of precisely timed movements, molecular layer interneurons might be responsible for setting the integration window for EPSPs by actively suppressing EPSPs that fall outside this time window, thereby increasing the temporal fidelity of Purkinje cell simple spikes (Mittmann et al., 2005). We suggest that in PC- $\Delta\gamma 2$ mice, the loss of this function might have been compensated for by a decreased Purkinje cell activation, as described in Fig. 9A. This hypothesis is supported by the observed decrease in charge transfer arising from parallel fiber-evoked EPSCs (Fig. 8). This could explain why the overall motor performance of PC- $\Delta\gamma 2$ appears relatively normal, although slight impairments are observed in OKR and VOR baseline performance (Fig. 4). Such compensation is also compatible with the fact that the average firing frequencies of PC- $\Delta\gamma 2$ Purkinje cells are the same as those of controls (Figs. 6 and 7).

As a direct result of the acute removal of inhibitory input to Purkinje cells, the ISI distribution of the simple spikes is altered (Hausser and Clark, 1997; Jaeger et al., 1997; see also Text). Such a change was also observed following chronic loss of inhibition in the PC- $\Delta\gamma 2$ mutants (Figs. 6 and 7). We investigated this using a simple integrate-and-fire model that captured some of the macroscopic properties of simple spike firing by assuming a Gaussian distribution of synaptic input (Fig. 9C).

Synaptic input

The occurrence of parallel fiber synaptic activity was modeled as a homogeneous Poisson process with I_I and I_E being, respectively, the average inhibitory and excitatory synaptic input arriving within a time step Δt . For a large number of inputs the Poisson distribution approaches a Gaussian distribution with standard deviation $s = \sqrt{I}$. The post-synaptic effect of synaptic input is characterized by transmission factors a and b for excitatory and inhibitory input, respectively. Although, in reality, the summation of EPSPs and IPSPs is highly non-linear, this assumption should not influence the analysis presented here, which relies only on the existence of a positive relation between synaptic input and simple spike output. The mean effect on the post-synaptic potential (PSP) is given by

$m_{PSP} = aI_E - bI_I$ with standard deviation $s_{PSP} = \sqrt{a^2 I_E + b^2 I_I}$. In the case of the PC- $\Delta\gamma 2$ mice $b = 0$, and the PSP characteristics simplify to $m_{PSP} = aI_E$, with standard deviation

$s_{PSP} = a\sqrt{I_E}$. As Purkinje cells show significantly more regular patterns than would be expected based on random activation (Shin et al., 2007), the synaptic input was low-pass filtered with time-constant t_{PSP} and gain 1 to introduce random patterning. The synaptic PSP S_{PSP} is thus characterized by three independent variables: S_{PSP} , m_{PSP} and t_{PSP} .

Simple spike output

The outputs of the simulation were simple spike trains, characterized by three (interdependent) time-averaged ISI properties: mean, CV and CV_2 . The transformation of the input space, characterized by S_{PSP} , m_{PSP} and t_{PSP} to the output space was performed

by means of a basic leaky integrate-and-fire model, which fired a spike when an artificial membrane potential V_m crossed a threshold. The membrane potential had time constant $t_v = 1$ ms and was reset to $V_{rest} = -65$ mV after the occurrence of a spike. It decayed to resting potential $V_{rest} = -45$ mV, due to a leak current with time constant $t_v = 29$ ms. The firing threshold had resting value T_{rest} and time constant $t_r = 2$ ms and was reset to $T_{refract} = -40$ mV after a spike occurred, to mimic the refractory period. The intrinsic spike frequency is given by $f = (t_v \ln[(V_{rest} - V_{reset}) / (V_{rest} - T_{rest})])^{-1}$, which resulted in $f = 50$ Hz pace-maker activity for $T_{rest} = -55$ mV. The firing threshold was modulated by the synaptic PSPs as $T = T_{rest} + S_{PSP}$. The simulations were performed with time step $\Delta t = 1$ ms, using MATLAB.

Learning

Purkinje cells have been proposed to act as ‘adaptive filters’ for parallel fiber input, depressing, via LTD, synapses that carry unwanted information and enhancing, via LTP, synapses with relevant information. After transition from a ‘naive’ state to a ‘learned’ state a Purkinje cell will then be very responsive to a small set of specific synapses, while the majority of other synapses will be depressed. A ‘naive’ state in the current model corresponds to parallel fiber synaptic input characterized by an overall average transmission factor a . Learning, as described above, does not affect the overall synaptic transmission via adaptation of a , but instead decreases the number of active synapses (corresponding to I_E) by a factor d , through LTD, while increasing the post-synaptic effect of the selected active synapses through LTP. Assuming the average firing frequency does

not change due to ‘learning’, the mean PSP after learning is still $m_{PSP} = da \frac{I_E}{d} = a I_E$

while the standard deviation has increased to $s_{PSP} = da \sqrt{\frac{I_E}{d}} = a \sqrt{d} \sqrt{I_E}$, i.e. by a factor \sqrt{d} . This provides a possible explanation for the observed increase in variability of simple spikes in PC- $\Delta y2$ mice after four days of VOR training (Fig. 9D). In controls, the interaction between inhibitory and excitatory synaptic input complicates a macroscopic interpretation of the effects of learning on ISI statistics, especially as inhibitory inputs are also susceptible to plastic changes (Hansel et al., 2001; Jorntell and Ekerot, 2002; Rancillac and Crepel, 2004).

Consolidation

On a longer time scale, Purkinje cell output could guide the induction of various kinds of synaptic and/or intrinsic plasticity at the level of their target nuclei (Aizenman and Linden, 1999; Aizenman and Linden, 2000; Gittis and du Lac, 2006). These plastic changes might be involved in ‘system consolidation’ of cerebellar motor memory; a ‘learned state’ in the cerebellar cortex might serve as an instruction signal for plasticity in the target nuclei, driven by activity in mossy fiber collaterals (Medina et al., 2001; Miles and Lisberger, 1981). The polarity of plastic adaptation might be governed by similar covariance rules as are known, for example, to govern parallel fiber LTD and LTP (Coesmans et al., 2004; Masuda and Amari, 2008). Thus, the functional absence of cerebellar cortical interneurons could impair ‘system consolidation’ by shifting the preference for one direction of plastic adaptation in the nuclei (see also Fig. 10A).

Conclusions

Some of the macroscopic properties of Purkinje cell simple spike firing can be described by a simple integrate-and-fire model. The ISI distributions of the simulated spike trains resemble those observed in control and PC- $\Delta\gamma 2$ mice, providing a possible explanation for the effects of VOR learning on simple spike variability.

Simulation of VOR adaptation

Several lines of evidence indicate that the acquisition of cerebellar motor memory is characterized by different stages, where memory is stored in distributed locations through a form of 'system consolidation'. Memory formation is believed to take place initially in the cerebellar cortex, after which it is partly transferred to a downstream site for long-term consolidation during several days of ongoing training (Broussard and Kassardjian, 2004; Kassardjian et al., 2005; Raymond et al., 1996). Likely candidate sites for consolidation are the deep cerebellar nuclei for the eyeblink and nictitating membrane (NM) response (Medina et al., 2001) and the vestibular nuclei for VOR adaptation (Lisberger, 1994). Regulation of plasticity at these sites could be instructed by specific modulation of inhibitory input that is learned by Purkinje cells (Miles and Lisberger, 1981). These findings are strengthened by the variety of different forms of intrinsic and synaptic plasticity that have been described in vestibular (Gittis and du Lac, 2006) and deep cerebellar nucleus neurons (Aizenman et al., 1998; Aizenman and Linden, 2000; Pugh and Raman, 2006; Zhang and Linden, 2006).

Model implementation

Results of VOR adaptation experiments in the current study are interpreted here within the framework of the model described above. Initial acquisition of a gain down paradigm was achieved within 30-50 minutes of training, comparable to values found by other groups (Boyden et al., 2006). Within the framework of the model, this timescale defines the rate of acquisition in the cerebellar cortex. The second timescale, defining the rate of 'system consolidation', was shown to be in the order of days when training trials are repeated daily (Kassardjian et al., 2005). These observations are incorporated in a schematic polar plot representation of a 4-day VOR adaptation paradigm consisting of one day of gain down training followed by three days of phase reversal training (Fig. S9A). Head (\vec{H}) and target (\vec{T}) have fixed amplitude and phase during training, and therefore have a fixed position in the polar diagram. For convenience the VOR is initially perfect, i.e. eye movement (\vec{E}) has the same gain but opposite phase as compared to head movement. Initial adaptation in the cerebellar cortex (\vec{C}) is represented by the blue arrow, driven by the mismatch between eye and target positions (by 'position', we mean position in the diagram). System consolidation in the nuclei (\vec{N}) is represented by the gradual adaptation of the red arrow, driven by the signal from the cortex. The eye position is calculated as $\vec{E} = -(\vec{N} - \vec{C})$. Details and formulas are presented below. Figure S9B plots the VOR gain $|\vec{E}|$ in blue for a simulated control animal. Despite the simplified nature of the model, it does describe the data well (compare to Figs. 5 / 10).

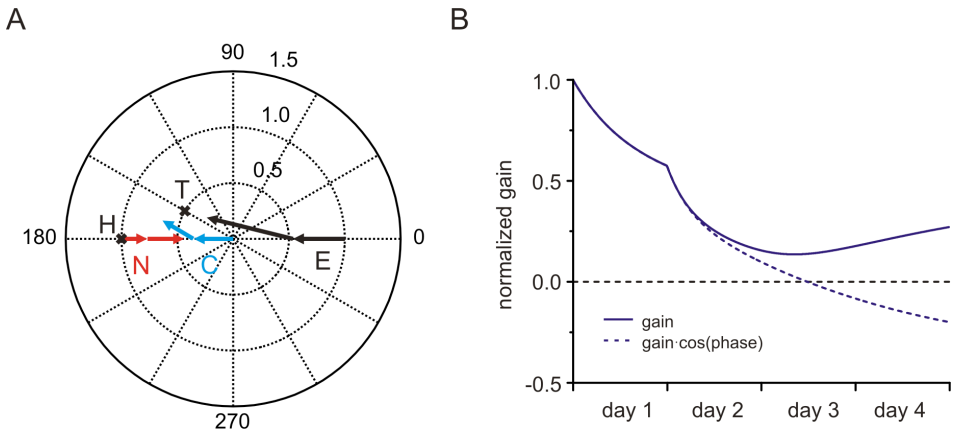


Figure S9. (A) VOR adaptation model in a polar diagram representation. (B) Simulated VOR gain (solid curve) and phase corrected gain (dashed curve).

PC- $\Delta\gamma 2$ mice display some abnormalities in VOR adaptation: 1) memory of an acquired skill partly disappears overnight, and 2) they are unable to reverse the phase of their VOR during the 4 day training exercise. Since the rate of initial adaptation in a gain down training in these mice is similar to controls (Fig. 5), it appears within the framework of the model that acquisition in the cortex is relatively normal. The fact, however, that part of the learned behavior has disappeared on the following day, indicates that memory is lost in the cortex, since little adaptation will have taken place in the vestibular nuclei after 30-50 minutes of training.

As to the second observation, the inability of PC- $\Delta\gamma 2$ mice to reverse the phase of their VOR might well be related to impaired plasticity in the vestibular nuclei (see also section 1.5). Plastic adaptation in the nuclei is an important prerequisite for phase reversal in the current model; therefore, impairment of this plasticity could slow down or prevent phase reversal in PC- $\Delta\gamma 2$ mice. Figure S9 (a recapitulation of Fig. 10 C-E) shows the model interpretation of PC- $\Delta\gamma 2$ VOR adaptation data. In Fig. S10A, settings are as in Fig. S9B, with the added feature that a portion of the memory in the cortex is abolished after each training session, to explain observation 1 (above). In Fig. S10B settings are also as in Fig. S9B, with the added feature that the rate of plastic adaptation in the nuclei is half that used for Fig. S9, to explain observation 2 (above). Finally, in Fig. S10C, both features are included, resulting in an accurate description of the experimental data.

Conclusions

Interpretation of VOR adaptation data in the framework of the distributed memory model indicates that the functional removal of cerebellar molecular layer interneurons could disrupt the consolidation of motor memory in both the cortex and vestibular nuclei. Regarding loss of learned adaption overnight (observation 1), motor learning in the cerebellar cortex is most commonly assumed to take place at the parallel fiber to Purkinje cell synapse. The initial acquisition in VOR adaptation in PC- $\Delta\gamma 2$ mice appears to be normal, which is supported by the finding that parallel fiber LTD and LTP induction are not impaired in vitro (Fig. S8). The overnight loss of acquired memory, however, indicates that the post-learning molecular consolidation of parallel fiber LTD and/or LTP might

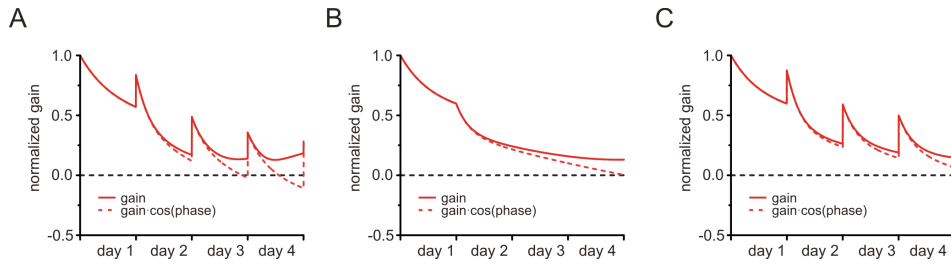


Figure S10. Simulated PC- Δy_2 VOR gain (solid curves) and phase corrected gain (dashed curves). (A) Cortical memory is partially removed after each trial. (B) The rate of system consolidation is reduced. (C) Both impairments described in (A) and (B) combined.

be impaired. Although the involvement of GABAergic inhibition in these post-learning processes is not well known, it has been shown that the post-learning application of the GABA agonist muscimol into the cerebellar cortex abolishes a previously learned motor response (when given within 2 hours after training; Cooke et al., 2004). This result indicates that normal GABA_A receptor-mediated signaling within this post-learning period is crucial for the molecular consolidation process. Moreover, in hippocampal pyramid cells, it is known that the different stages of LTP induction and maintenance relate to the different stages of memory acquisition and consolidation in a spatial learning task (Pastalkova et al., 2006; Whitlock et al., 2006). The administration of drugs acting on GABA_A receptors can impair or enhance spatial memory consolidation (McGaugh, 2000). Since cerebellar parallel fiber synaptic plasticity is almost a mirror image of the hippocampal process (Jorntell and Hansel, 2006), it seems likely that GABAergic signaling could serve a similar important function in consolidation of a motor memory, albeit with a reversed polarity.

Model details

Phase and gain of the VOR components were represented by positions in a polar diagram, with coordinates [phase, gain]. The positions of head and target were given by head $\vec{H} = [180, 1]$, target $\vec{T} = [0, 0.5]$ for the first session of gain down training, and $\vec{T} = [150, 0.5]$ for the last three sessions of phase reversal training. The initial conditions of the cortex and nuclei were $\vec{C}_{init} = [0, 0]$ and $\vec{N}_{init} = [180, 1]$. The position of the eye at all times was calculated as $\vec{E} = -(\vec{N} - \vec{C})$, and thus had initial value eye $\vec{E} = [0, 1]$. The cortex was assumed to be able to generate all phase elements, whereas the nucleus was restricted to the phase of the head (Masuda and Amari, 2007; Raymond and Lisberger, 1998).

The initial mismatch between eye position and target position drives adaptation in the cortex:

$$\begin{aligned}\dot{\bar{C}}_{plast} &= \frac{1}{t_c} (\bar{T} - \bar{E}), \\ \bar{C}_{plast}(2) &= 2 \cdot s_c \cdot \text{sigmoid} \{ \bar{C}_{plast}(2) - 0.5 \}, \\ \bar{C} &= \bar{C}_{init} + \bar{C}_{plast}.\end{aligned}$$

$\dot{\bar{C}}_{plast}$ is the time derivative and t_c is the time constant (measured in simulation steps)

of cortex adaptation. The function sigmoid was defined as $\text{sigmoid}\{x\} = \frac{1}{1+e^{-x}}$ and was used to set the limit for cortical capacity for memory storage at s_c .

Nucleus plasticity is driven by the signal from the cortex:

$$\begin{aligned}\dot{\bar{N}}_{plast} &= -\frac{\bar{C}}{t_N}, \\ \bar{N}_{plast}(2) &= 2 \cdot s_N \cdot \text{sigmoid} \{ \bar{N}_{plast}(2) - 0.5 \}, \\ \bar{N} &= \bar{N}_{init} + \bar{N}_{plast}.\end{aligned}$$

$\dot{\bar{N}}_{plast}$ is the time derivative and t_N is the time constant of nucleus adaptation.

Simulations consisted of 4 trials of 1000 steps each, representing the four days of the experimental paradigm. Parameter values were carried on from one trial to the next without modifications in control simulations, but for PPC- $\Delta\gamma 2$ simulations the value of \bar{C} was reduced after each trial by 80% as $\bar{C}_{day+1} = 0.2 \cdot \bar{C}_{day}$. Further settings were $t_c = 200$, $s_c = 0.65$ and $s_N = 0.75$. For controls $t_N = 1000$, and for PC- $\Delta\gamma 2$: $t_N = 2000$.

Reference list

- Aizenman, C.D., and Linden, D.J. (1999). Regulation of the rebound depolarization and spontaneous firing patterns of deep nuclear neurons in slices of rat cerebellum. *J. Neurophysiol.* 82, 1697-1709.
- Aizenman, C.D., and Linden, D.J. (2000). Rapid, synaptically driven increases in the intrinsic excitability of cerebellar deep nuclear neurons. *Nat. Neurosci.* 3, 109-111.
- Aizenman, C.D., Manis, P.B., and Linden, D.J. (1998). Polarity of long-term synaptic gain change is related to postsynaptic spike firing at a cerebellar inhibitory synapse. *Neuron* 21, 827-835.
- Boyden, E.S., Katoh, A., Pyle, J.L., Chatila, T.A., Tsien, R.W., and Raymond, J.L. (2006). Selective engagement of plasticity mechanisms for motor memory storage. *Neuron* 51, 823-834.
- Broussard, D.M., and Kassardjian, C.D. (2004). Learning in a simple motor system. *Learn.*

Mem.11, 127-136.

- Coesmans,M., Weber,J.T., De Zeeuw,C.I., and Hansel,C. (2004). Bidirectional parallel fiber plasticity in the cerebellum under climbing fiber control. *Neuron* 44, 691-700.
- Cooke,S.F., Attwell,P.J., and Yeo,C.H. (2004). Temporal properties of cerebellar-dependent memory consolidation. *J. Neurosci.* 24, 2934-2941.
- Gittis,A.H., and du Lac,S. (2006). Intrinsic and synaptic plasticity in the vestibular system. *Curr. Opin. Neurobiol.* 16, 385-390.
- Hansel,C., Linden,D.J., and D'Angelo,E. (2001). Beyond parallel fiber LTD: the diversity of synaptic and non-synaptic plasticity in the cerebellum. *Nat. Neurosci.* 4, 467-475.
- Häusser, M., and Clark, B. A. (1997). Tonic synaptic inhibition modulates neuronal output pattern and spatiotemporal synaptic integration. *Neuron* 19, 665-678.
- Jaeger,D., De,S.E., and Bower,J.M. (1997). The role of synaptic and voltage-gated currents in the control of Purkinje cell spiking: a modeling study. *J. Neurosci.* 17, 91-106.
- Jorntell,H., and Ekerot,C.F. (2002). Reciprocal bidirectional plasticity of parallel fiber receptive fields in cerebellar Purkinje cells and their afferent interneurons. *Neuron* 34, 797-806.
- Jorntell,H., and Hansel,C. (2006). Synaptic memories upside down: bidirectional plasticity at cerebellar parallel fiber-Purkinje cell synapses. *Neuron* 52, 227-238.
- Kassardjian, C.D., Tan, Y.F., Chung, J.Y., Heskin, R., Peterson, M.J., and Broussard, D.M. (2005). The site of a motor memory shifts with consolidation. *J. Neurosci.* 25, 7979-7985.
- Lisberger,S.G. (1994). Neural basis for motor learning in the vestibuloocular reflex of primates. III. Computational and behavioral analysis of the sites of learning. *J. Neurophysiol.* 72, 974-998.
- Masuda,N., and Amari,S.I. (2008). A computational study of synaptic mechanisms of partial memory transfer in cerebellar vestibulo-ocular-reflex learning. *J. Comput. Neurosci.* 24, 137-56.
- McGaugh,J.L. (2000). Memory--a century of consolidation. *Science* 287, 248-251.
- Medina,J.F., Garcia,K.S., and Mauk,M.D. (2001). A mechanism for savings in the cerebellum. *J. Neurosci.* 21, 4081-4089.
- Miles,F.A., and Lisberger,S.G. (1981). Plasticity in the vestibulo-ocular reflex: a new hypothesis. *Annu. Rev. Neurosci.* 4, 273-299.
- Mittmann,W., Koch,U., and Häusser,M. (2005). Feed-forward inhibition shapes the spike output of cerebellar Purkinje cells. *J. Physiol* 563, 369-378.
- Pastalkova,E., Serrano, P., Pinkhasova, D., Wallace, E., Fenton, A.A., and Sacktor, T.C. (2006). Storage of spatial information by the maintenance mechanism of LTP. *Science* 313, 1141-1144.
- Pugh,J.R., and Raman,I.M. (2006). Potentiation of mossy fiber EPSCs in the cerebellar nuclei by NMDA receptor activation followed by postinhibitory rebound current. *Neuron* 51,113-123.
- Rancillac,A., and Crepel,F. (2004). Synapses between parallel fibres and stellate cells express long-term changes in synaptic efficacy in rat cerebellum. *J.*

Physiol 554,707-720.

Raymond,J.L., Lisberger,S.G., and Mauk,M.D. (1996). The cerebellum: a neuronal learning machine? Science 272, 1126-1131.

Shin,S.L., Hoebeek,F.E., Schonewille,M., De Zeeuw,C.I., Aertsen,A., and De,S.E. (2007). Regular patterns in cerebellar Purkinje cell simple spike trains. PLoS. ONE. 2, e485.

Whitlock,J.R., Heynen,A.J., Shuler,M.G., and Bear,M.F. (2006). Learning induces long-term potentiation in the hippocampus. Science 313, 1093-1097.

Zhang,W., and Linden,D.J. (2006). Long-term depression at the mossy fiber-deep cerebellar nucleus synapse. J. Neurosci. 26, 6935-6944.

Chapter 6

Discussion

Discussion

The present thesis describes electrophysiological and behavioural studies in a large number of genetically manipulated mice. The combined recording of performance and adaptation of compensatory eye movement and Purkinje cell activity with and without sensorimotor stimulation in the present work has cumulated to the overview as presented in Table 1. A few basic principles can be suggested based on this table.

6.1 Basic principles in Purkinje cell activity and motor learning

First, strong disruption of normal simple spike firing leading to an increase in irregularity (*tottering* mice) is accompanied by very poor motor performance (Ch. 3.3). Interestingly, this is also the only mouse mutant with a significant change in simple spike firing rate presented here. Further evidence supporting this link was recently obtained in BK channel knockout mice, that have a lower simple spike frequency (Sausbier et al., 2004). Deleting Purkinje cells or (part of) the cerebellum leads to comparable motor problems, most clearly in the acute situation (see also Van Alphen, 2002). In *tottering* mice (Ch. 3.3) we found no difference between before and several days after lesion indicating that Purkinje cell dysfunction can result in motor problems at least as severe as, but possibly even worse, in a situation without cerebellum or Purkinje cells.

	Pf-PC plasticity LTD / LTP	Simple spike			Motor performance	Motor learning
		frequency	regularity	modulation		
<i>Tottering</i>	? / ?	↑	↓	N	↓↓	↓(↓)
Anesthetized		N	↓	↓	↓↓↓	?
PICK1 GluR2delta7 GluR2K882A	↓ / N	?	?	?	N	N
L7-PP2B	N / ↓	N	↑	?	↓	↓↓
L7-gamma2	N / N	N	↑	N	↓	↓

Table 1. Summary of the cellular, electrophysiological and behavioral phenotypes observed in the different experiments described in this thesis, except motor learning in *tottering* (Stahl et al., 2006).

The second principle that arises from the work presented in this thesis and summarized in Table 1 is related to the -traditionally considered- key element in motor learning, Pf-PC LTD. We tested plasticity of the parallel fibre to Purkinje cells synapse in five different mutant mice strains. In contrast to the majority of literature on this subject that report a correlation between impaired Pf-PC LTD and impaired motor learning (Aiba et al., 1994; De Zeeuw et al., 1998; Feil et al., 2003; Boyden et al., 2006; Hansel et al., 2006), we find both impaired LTD without motor learning problems (Ch. 4.1), as well as normal LTD with impaired motor learning (Chs. 4.2 and 5). Together, these data provide substantial

evidence against Pf-PC LTD being an absolute requirement for motor learning. We therefore explored two other pathways in an attempt to direct future studies. The results with L7-PP2B mutant mice (Ch. 4.2) suggest Pf-PC LTP plays a major role in motor learning but, considering the experiences with Pf-PC LTD deficient mice, obviously further experiments need to be done. Downstream pathways and involved proteins affected by phosphatases are largely unknown, but deletion of their genes will have to clarify the significance of the pathway. An interesting factor here is formed by the molecular layer interneurons, as both the role of inhibition of Purkinje cells and plasticity of this inhibition is largely unclear. A recent study has demonstrated that the incoming vestibular afferent activity is reciprocal to the outgoing activity of the Purkinje cells receiving that input. The switch is suggested to be caused by stellate and basket cells, again emphasizing the strong influence of molecular layer interneurons on Purkinje cell activity (Barmack and Yakhnitsa, 2008). The finding that CaMKII is required for induction of this plasticity of inhibition indicates that kinase mutant behavioural results may have been confounded by a concomitant loss of inhibitory input plasticity (Kano et al., 1992). Recent evidence also suggests that the result of simultaneous parallel and climbing fibre stimulation on Purkinje cell output strongly depends on the ratio between inhibitory and excitatory input (Mittmann and Hausser, 2007). The fact that only consolidation is affected in mice with Purkinje cell inhibition, however, confirms that other, plastic, synapses are involved.

Finally, a pattern can be seen in the results obtained in mice without Pf-PC LTP (Ch. 4.2) and mice without inhibitory input onto Purkinje cells (Ch. 5). Although the mutations affect apparently very different parts of the cerebellar network (Pf-PC plasticity vs. MLI-PC contact) the resulting phenotype is comparable in several aspects. Both cause an impaired motor performance with a small but significant effect on OKR and an increase in VOR gain, impaired motor learning and a change in inter simple spike interval distributions towards more regular firing, particularly on small timescales that were measured by calculating CV_2 . Despite the apparent difference between the two types of mutations, there might be one or more common pathway(s). First, it is possible that the mutations are in fact not that different. Although phosphatase 2B in Purkinje cells is primarily known to be involved in LTP, a role in other pathways cannot be excluded. In fact, the striking observation that 'kinase mutations' delete Pf-PC LTD and motor learning but mutations downstream delete Pf-PC LTD but do not affect motor learning could be interpreted as evidence for an alternative pathway for the effects of kinases and perhaps also phosphatases. For example, the former has been implicated in the induction of rebound potentiation, which is the potentiation of GABAergic inhibition onto Purkinje cells by concomitant climbing fibre stimulation (Kano et al., 1992; Kano et al., 1996). Since kinases and phosphatases are believed to counteract each other (Lisman, 1989; Lisman and Zhabotinsky, 2001; Belmeguenai and Hansel, 2005), deletion of phosphatases could also influence (plasticity of) MLI inhibition of Purkinje cells. In theory, this could ultimately have an effect comparable to that seen in mice without Purkinje cell inhibition, where the additional features of the phenotype in L7-PP2B may be explained by the effect of phosphatase deletion on parallel fibre to Purkinje cell synapses.

Alternatively, the mutation may be very different but may result in the same effect on the output of the cell. Assuming that inter simple spike interval (ISSI) distributions are

strongly linked to behaviour (Ch. 3.2, 3.3, 4.2 and 5), the mutations could thereby cause the same effect on motor control. Without Pf-PC LTP parallel fibre input will generally be weaker, most likely resulting in a lower number of short inter simple spike intervals. In contrast the loss of inhibition putatively causes a lower number of long inter simple spike intervals, as molecular layer interneuron activity removes single simple spikes rather than decreasing firing rate for a longer period (Hausser and Clark, 1997). However, as mentioned before, Purkinje cells appear to have a preferred firing rate of ~50-60 Hz with the only exceptions found in ataxic mice. Therefore one could assume that compensatory mechanisms are present to retain this frequency. This compensation would in turn lead to comparably shaped ISSI distributions in otherwise very different mutant mice. The factors controlling Purkinje cell activity and the consequences of Purkinje cell activity on deep cerebellar nuclei neurons are discussed below.

6.2 Causes of Purkinje cell activity

Although the firing frequency is the predominant parameter for Purkinje cell simple spike firing pattern analysis, various recent studies show that there must be more information in the Purkinje cell firing patterns than just frequency. For instance, theoreticians have recognized that the impact of noise levels (i.e. regularity of firing) in neuronal network models (Mar et al., 1999; Steinmetz et al., 2001; Tiesinga et al., 2002; De Zeeuw et al., 2008) greatly influence the transport of information. Various phenomena influence the temporal spike coding, and this thesis provides evidence that the disturbance of this coding minimizes the effect of modulation by Purkinje cells (Ch. 3.3).

Thus, in theory a basis exists for a discussion on the role of exact timing of simple spike firing. In this thesis several studies have implicated the relevance of simple spike timing in relation to motor behaviour: Ch. 3.2 demonstrated an increase in the regularity of simple spike firing in response to tactile stimulation, Ch 3.3 showed that when the irregularity is permanently higher the impact of modulation in response to sensorimotor behaviour is minimized and Chs. 4.2 and 5 demonstrate more subtle changes in regularity in combination with motor learning problems. These studies indicate that not only the average firing frequency, which has been the popular measure for characterizing the simple spike firing pattern, but also the regularity of simple spike firing is important for the transfer of information. Below we review possible causes of irregular simple spike firing as well as the possible consequences.

Simple spike firing of Purkinje cells *in vivo* has always been considered to be quite irregular (C.V. ~ 0.5, this thesis), but we found it to consist of many shorter regular periods with CV < 0.2 for several consecutive ISSIs (Ch. 3.2). Purkinje cell firing *in vivo* can become highly irregular as a result of certain anaesthetics (Ch. 3.1) or a particular genetic mutation (Ch. 3.3). Deregulation of simple spike firing can be caused by numerous endogenous and exogenous variables. The regular action potential firing of Purkinje cells *in vitro* becomes more irregular upon application of particular pharmacological agents (Williams et al., 2002), and through inhibitory input (Hausser and Clark, 1997). In addition, we demonstrated how various intracellular mechanisms as well as the use of various anaesthetics affect the regularity of simple spike firing (Ch. 3). These and other influences will be reviewed below in order to shed a light on what the possible causes of disturbances in the regularity of simple spike firing are.

In chapter 3.3 we demonstrate that regularity of simple spike firing is grossly affected by mutations in a P/Q-type voltage-gated Ca²⁺-channel mutant called *tottering*

(Ch. 3.3). These mice are characterized by a single, spontaneous point mutation in the CACNA1A gene, which codes for the α_{1A} -subunit of the P/Q-type channel (Fletcher et al., 1996). In wild type mice this channel gates >90% of high-voltage-activated Ca^{2+} -influx whereas in *tottering* the P/Q-type current density is ~45% lower (Wakamori et al., 1998). We hypothesized that the decrease in P/Q-type function leads to an irregular simple spike firing through increased GABAergic input from inhibitory interneurons and decreased Ca^{2+} -activated K^+ -channel function. The increased input from inhibitory interneurons is illustrated by the fact that GABA_B -receptor activation has a direct effect on P/Q-type Ca^{2+} -influx (Mintz and Bean, 1993). In addition, *in vitro* experiments showed that 1) bath application of GABAergic antagonists cause more regular action potential firing in Purkinje cells, and 2) single action potentials of cerebellar inhibitory interneuron delays single action potentials in Purkinje cells (Hausser and Clark, 1997). These results show that the activation of GABA-receptors induces irregular action potential firing in Purkinje cells *in vitro* and thus could be causal to the increased irregularity of simple spike firing as found in *tottering*. Interestingly, Zhou et al. showed increased influence of inhibitory interneurons on the neurotransmitter release from parallel fibre terminals in *tottering* (Zhou et al., 2003), which acts additional to the decreased postsynaptic excitation following parallel fibre stimulation in increasing inhibitory influence (Matsushita et al., 2002). This correlation between increased influence of inhibition and irregularity fits the one between decreased inhibition and irregularity, as observed in Chapter 5. The common denominator in irregular simple spike firing patterns could thus very well be found in the GABAergic input to cerebellar Purkinje cells.

Pathogenic alterations of the Purkinje cell's intracellular excitability and inhibitory synaptic input as found in CACNA1A mutants are not the sole source of irregular simple spike firing patterns. Highly irregular action potential firing patterns have been described in various types of neurons in various species (Heyward et al., 2001; Egorov et al., 2002) and have also been linked to shifts in the membrane potential between multiple preferred states, which can be sustained without any synaptic input and result in either action potential firing ('up-state') or silence ('down-state'). Loewenstein and colleagues (2005) performed *in vivo* recordings in whole-cell configuration in the cerebellum of anesthetized rats and guinea pigs and showed that in Purkinje cells the switch between the two states could be triggered by injecting a current pulse or by a sensory activation of climbing fibre activity ('toggling') and that 24 out of 24 Purkinje cells recorded under ketamine / xylazine anaesthesia showed bistable membrane potential and spike output. Since anaesthetics can affect the membrane potentials directly and indirectly (MacIver and Kendig, 1991; Franks and Lieb, 1994), we further investigated the phenomenon in awake and behaving animals under physiological conditions. After convincingly showing that every extracellularly recorded simple spike consistently corresponds to an intracellularly recorded action potential we showed that bistability hardly occurs in awake animals and that natural sensory stimulation, motor performance, or motor learning does not increase the occurrence, while it is prominently present under isoflurane or ketamine / xylazine anaesthesia. However, Chapter 3.2 shows that the number of long (>10) regular simple spike patterns was significantly higher in anesthetized mice and rats when compared to awake animals. The origin of the apparent conflict in data can be found in the chosen length of the considered time interval. When CV is calculated all ISSIs are used to determine regularity, independent of their temporal order, and thus a limited

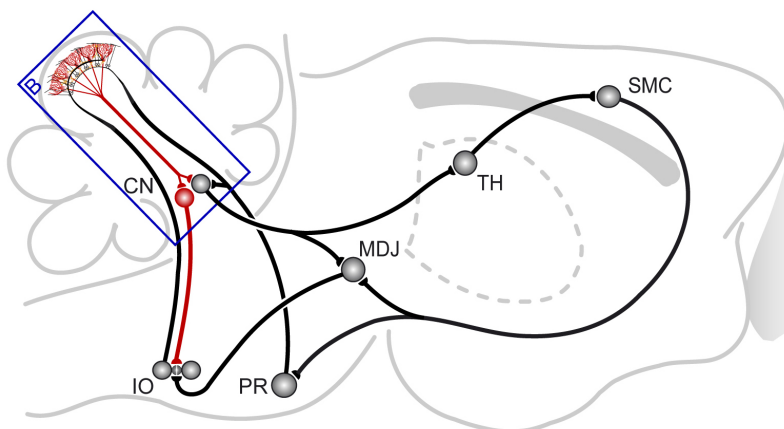


Figure 1. Schematic drawing of intra- and extracerebellar connections.

The cerebellar cortex receives main excitatory inputs (black) from the inferior olive (IO) and pontine regions (PR), and provides via the Purkinje cell axons an inhibitory feedback (grey) to the vestibular and cerebellar nuclei (VN and CN, respectively). The outputs of VN and CN create a short loop by inhibiting the IO and two longer loops by exciting the mesodiencephalic junction (MDJ) and thalamus (TH). The TH excites various parts of the cerebral cortex among which the sensorimotor cortex (SMC), which in turn provides descending projections back to the PR and via the MDJ to the IO.

number of very long pauses will strongly increase the calculated value (resulting in the high values described in Ch. 3.1). When short time intervals are chosen -by calculating CV_2 as done in Chapter 3.1- bistable Purkinje cells could be considered regular since the regular firing in upstates contributes relatively more. The validity of the statement that certain anaesthetics increase irregular Purkinje cell firing therefore depends on the length of the time interval that is considered.

As mentioned above, one of the first influences on simple spike firing was identified as the input of molecular layer interneurons. Hausser and Clark (1997) described how molecular layer interneuron activity rather than decreasing the average firing rate, ‘takes out’ single simple spikes. This has a clearly different effect on for instance the regularity (CV or CV_2), which is not that much effected by a slow decrease of firing rate, but strongly effected by the absence or delay of a single spike. In addition, it also creates a pause that could have a pronounced effect in the DCN, which will be discussed later. This *in vitro* study was confirmed *in vivo* and correlated to a phenotype in mutant mice in which selectively in Purkinje cells the $\gamma 2$ subunit of the GABA_A receptor was knocked out (Ch. 5). When motor behaviour was tested using compensatory eye movement reflexes, these mice displayed minor performance problems, a poor consolidation over night of adapted reflexes and (thus) an inability to complete a complex multiple day training paradigm. In vivo recordings of Purkinje cell activity confirmed the higher regularity of simple spike firing (CV and CV_2 both ~20% lower) in mice lacking Purkinje cell inhibition.

Although the study described in Chapter 5 to the best of our knowledge is the first example of a genetic deletion of inhibition, several studies have implicated the importance for inhibition in the cerebellar cortex in motor performance. The effect of local application of inhibition blockers on Purkinje cell modulation caused by VOR stimulus

was inconsistent, but modulation shifted more often towards the in phase than the out phase type (Miyashita and Nagao, 1984). Interesting too here is the work of Jorntell and Ekerot who first demonstrated that receptive fields (on the forelimb) for climbing fibre and parallel fibre of local Purkinje cells differ, but are similar for interneurons and climbing fibres, most probably caused by bidirectional CF-specific PF plasticity (Ekerot and Jorntell, 2001; Jorntell and Ekerot, 2002). Further experiments suggested an important role for granule cells and/or the parallel fibre to interneuron synapse in this plasticity (Jorntell and Ekerot, 2003). In a series of studies Mittmann and colleagues have, adapted from studies in the hippocampus, provided evidence for the role of MLIs in controlling precise simple spike timing in Purkinje cells (Mittmann et al., 2004; Mittmann et al., 2005). Subsequently, they demonstrated that concomitant parallel and climbing activity induced LTD both at the parallel fibre and the interneuron to Purkinje cell synapse (Mittmann and Hausser, 2007), the latter being in sharp contrast with earlier findings (Kano et al., 1992). Consequently, the ultimate effect of concomitant climbing and parallel fibre activity on Purkinje cell output will depend on the balance of excitatory and inhibitory input to that Purkinje cell. Steuber and colleagues (2007) suggested, based on a model confirmed with experimental data, that the duration of the pause after parallel fibre-induced burst as the ideal criterion to distinguish learned patterns. Moreover, in a classical conditioning paradigm Purkinje cell activity was inhibited during the acquisition and disinhibited during extinction, again suggestive of a role for Purkinje cell inhibition (Jirenhed et al., 2007). All together these data emphasize the significance of molecular layer interneuron activity during motor learning; a theory that requires further investigation.

6.3 Consequences of Purkinje cell activity

Both the Purkinje cell axon and its terminal separately affect the information transfer downstream of Purkinje cells. Purkinje cell axons transmit simple spikes as single action potentials and complex spikes as bursts of action potentials (Ito and Simpson, 1971). Recent findings by several laboratories show a possible consequence of irregular firing pattern for action potential propagation along the Purkinje cell axon (Khaliq and Raman, 2005; Monsivais et al., 2005). These studies indicate that the propagation of a burst of action potentials caused for instance by the activation of a climbing fibre is incomplete; only one or two spikes propagated, contradicting observations *in vivo* (Ito and Simpson, 1971). Furthermore, Monsivais et al. showed that action potential propagation through the Purkinje cell axon is limited to ≤ 260 Hz, with Na^+ -channel inactivation as the limiting factor (Monsivais et al., 2005). These findings are in line with evidence showing that small reductions in Na^+ -current can increase the refractory period, reduce maximal firing frequency (Madeja, 2000), and inhibit propagation of action potentials in axons (Kopysova and Debanne, 1998). Note however that in *tottering* and $\text{BK}^{-/-}$ mice, both affected by an altered Ca^{2+} -homeostasis, instantaneous firing frequencies reach up to 500 Hz (Ch. 3.3) (Sausbier et al., 2004), suggesting that Ca^{2+} -homeostasis is crucial for the refractory period and thus for the maximum firing rate.

One of the prominent questions in the field concerns the effect of (irregular) simple spike firing on target neurons in the cerebellar nuclei (Fig. 1). The convergence of synaptic inputs on Purkinje target neurons needs to be known to answer this question. Palkovits et al. (1977) stated that inhibitory synaptic inputs show a large convergence of 1000:1. In addition they stated that the number of Purkinje cell contacts per cerebellar

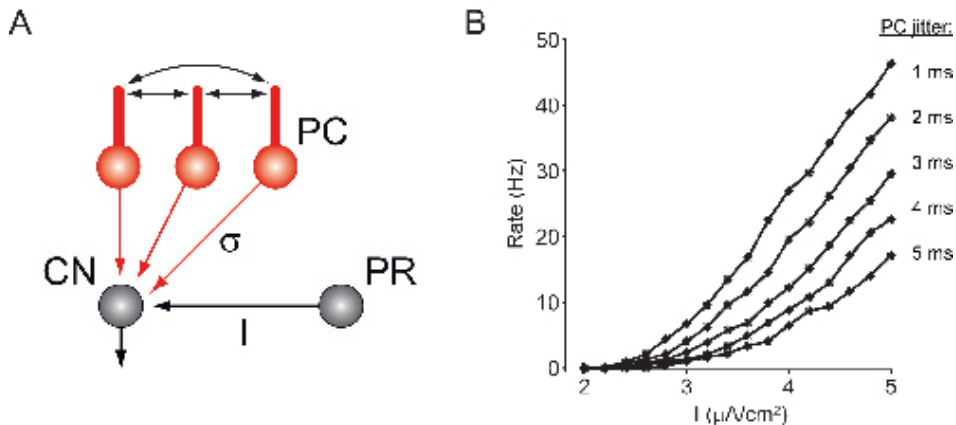


Figure 2. Inhibitory gain control on excitatory transmission.

Firing rate gain in the cerebellar nucleus (CN) following excitation (I) by the mossy fiber collaterals from the pontine region (PR) may be regulated by synchronous, high frequency oscillations in the inhibitory activities of the Purkinje cells. The PC spike-time dispersion (σ) is inversely related to the synchrony of this network oscillation. B) The CN firing rate versus mossy fiber collateral (mfc) input current (I) plots are shown for different values of the Purkinje cell (PC) jitter. As the jitter is decreased from 5 to 1 ms (from bottom to top), the gain of the CN responses to the excitatory mfc inputs is dramatically increased. This interaction between mfc inputs and PC synchrony might be one of the potential mechanisms by which high frequency oscillations in the cerebellar cortex exert their effects. Adapted with permission from Tiesinga et al., 2004 and Sejnowski and Paulsen, 2006).

nucleus neuron was ~ 13 and that the number of boutons made by single Purkinje cell axons on single cerebellar nuclei neurons ranges between 1 and 50, a statement that was later confirmed by (Pedroarena and Schwarz, 2003). Additionally, locally projecting small inhibitory GABAergic interneurons have been found in the cerebellar nuclei (Batini et al., 1992), which add up to the massive inhibitory input (75% of the total synaptic input) (De Zeeuw et al., 1995) cerebellar nuclei neurons receive.

Obviously, in addition to convergence synchrony, the occurrence of spikes nearly simultaneously in different Purkinje cells, can have a great influence on information transfer downstream of Purkinje cells (see also Fig. 2A). The fact that a sagittal array of Purkinje cells can be contacted by the same climbing fibre and/or MLI(s) and contact the same cerebellar nucleus neuron emphasizes to the possible relevance of synchrony in Purkinje cell activity. It has to be stated that the occurrence and level of Purkinje cell synchronous firing has been a matter of debate for decades, with several studies providing evidence supporting (Bell and Grimm, 1969; De Zeeuw et al., 1997; Heck et al., 2007) and against (Ebner and Bloedel, 1981; Jaeger, 2003) the existence. In Chapter 3.2 we describe how regular patterns coincide in nearby Purkinje cells, without precise simple spike synchronization. Additional support could be considered to come from studies demonstrating the occurrence of (low to very high frequency) oscillations in the cerebellar cortex (Middleton and Strick, 1994; Hansel et al., 2001; Courtemanche and Lamarre, 2005; de Solages et al., 2008; Van Der Giessen et al., 2008), but the enhanced oscillations in an ataxic mouse mutant could be interpreted as contradictory support (as reviewed by Cheron et al., 2008; De Zeeuw et al., 2008).

The complexity of afferent synaptic input on cerebellar nuclei neurons is extended by the fact that large numbers of excitatory fibres contact these neurons too. Palkovitz et al. and Chan-Palay postulated that ~ 2000 excitatory synapses contact a

single neuron in the cerebellar nuclei (Chan-Palay, 1977; Palkovits et al., 1977). These inputs originate in various precerebellar nuclei and the inferior olive in the brainstem and innervate cerebellar nuclei neurons through collaterals of mossy fibres and climbing fibres, respectively. Each fibre may form multiple synaptic contacts and Gauck and Jaeger estimated the convergence to be around 200:1, meaning that each fibre makes 10 synaptic contacts (Gauck and Jaeger, 2003). As cerebellar nuclei neurons receive both the direct mossy fibre input and the indirect mossy fibre activity containing Purkinje cell output, their firing pattern will thus reflect the sum of all computations that are performed in the cerebellar system.

But what do these cerebellar nuclei neurons do with this massive synaptic input and what is the effect of synchrony of the inhibitory input? Work in the visual cortex has led to the hypothesis that synchronized inhibition can provide gain control of the target neuron, where synchronized activity resulted in a higher firing rate with the same excitatory input (Fig. 2) (Tiesinga et al., 2004; Sejnowski and Paulsen, 2006). The work of Gauck and Jaeger also has been particularly informative on this matter (Gauck and Jaeger, 2000, 2003). They showed that when cerebellar nuclei neurons that were recorded in vitro using a dynamic current clamp conformation (Robinson and Kawai, 1993), creating the possibility to mimic synaptic input, DCN neurons showed reproducible spiking patterns in response to synchronized inhibitory input. It must be noted though, that Gauck and Jaeger ignored the possible effects of transient decreases and increases in the input activity, i.e., firing frequency of the both excitatory and inhibitory afferent fibres. These characteristics are of great importance for understanding the effect of Purkinje cell input on DCN neurons and are directly related to how irregular Purkinje cell firing can affect the downstream information transfer.

However, one should be careful drawing conclusions considering the fact that recent literature on Purkinje cell – cerebellar nucleus neuron contacts does not provide a conclusive image of what the possible effects of increased irregularity could be on the information transfer. The results described in chapter 3.2, using theoretical modelling and Purkinje cell recordings, indicate that information transfer, i.e. synaptic transmission, is most prominent when the regularity is highest. In contrast, the results described in chapter 5 emphasize that the regularity can also be too high. This suggests there is an ideal level of regularity, at which information transfer and thereby cerebellar function is optimal. But the relevance of these results can only become evident when it is shown what the individual Purkinje cell firing patterns are of all Purkinje cells that project onto a single cerebellar nucleus neuron.

6.4 Conclusions and perspectives

So is there more in the simple spike data than just the average firing frequency? The data in this thesis provide direct and indirect evidence that firing frequency is not the sole simple spike parameter that carries information downstream of the cerebellar cortex, but that the level of regularity of firing is equally as important. Both increased (Ch. 3.3) and decreased (Ch. 4.2 and 5) regularity has been found in relation to affected motor behaviour, indicating the existence of an optimal range of firing regularity. The exact requirements of simple spike firing pattern need to be further elucidated, for instance through careful examination of the Purkinje cell activity of during adaptation in both learning and non-learning mice. Combined recordings from the deep cerebellar or vestibular nuclei could significantly aid this research.

Reference List

- Aiba A, Kano M, Chen C, Stanton ME, Fox GD, Herrup K, Zwingman TA, Tonegawa S (1994) Deficient cerebellar long-term depression and impaired motor learning in mGluR1 mutant mice. *Cell* 79:377-388.
- Barmack NH, Yakhnitsa V (2008) Functions of interneurons in mouse cerebellum. *J Neurosci* 28:1140-1152.
- Batini C, Compoin C, Buisseret-Delmas C, Daniel H, Guegan M (1992) Cerebellar nuclei and the nucleocortical projections in the rat: retrograde tracing coupled to GABA and glutamate immunohistochemistry. *J Comp Neurol* 315:74-84.
- Bell CC, Grimm RJ (1969) Discharge properties of Purkinje cells recorded on single and double microelectrodes. *J Neurophysiol* 32:1044-1055.
- Belmeguenai A, Hansel C (2005) A role for protein phosphatases 1, 2A, and 2B in cerebellar long-term potentiation. *J Neurosci* 25:10768-10772.
- Boyden ES, Katoh A, Pyle JL, Chatila TA, Tsien RW, Raymond JL (2006) Selective engagement of plasticity mechanisms for motor memory storage. *Neuron* 51:823-834.
- Chan-Palay V (1977) *Cerebellar Dentate Nucleus*: Springer-Verlag.
- Cheron G, Servais L, Dan B (2008) Cerebellar network plasticity: from genes to fast oscillation. *Neuroscience* 153:1-19.
- Courtemanche R, Lamarre Y (2005) Local field potential oscillations in primate cerebellar cortex: synchronization with cerebral cortex during active and passive expectancy. *J Neurophysiol* 93:2039-2052.
- de Solages C, Szapiro G, Brunel N, Hakim V, Isope P, Buisseret P, Rousseau C, Barbour B, Lena C (2008) High-frequency organization and synchrony of activity in the purkinje cell layer of the cerebellum. *Neuron* 58:775-788.
- De Zeeuw CI, Hoebeek FE, Schonewille M (2008) Causes and consequences of oscillations in the cerebellar cortex. *Neuron* 58:655-658.
- De Zeeuw CI, Koekkoek SKE, Wylie DRW, Simpson JJ (1997) Association between dendritic lamellar bodies and complex spike synchrony in the olivocerebellar system. *J Neurophysiol* 77:1747-1758.
- De Zeeuw CI, Van der burg J, Wylie DR, DiGiori PL, Ruigrok TJ, Teune T, Simpson JJ (1995) Morphological evidence for interzonal inhibition by Golgi cells in the rabbit vestibulo-cerebellum. *Eur J Morphol* 33:328-329.
- De Zeeuw CI, Hansel C, Bian F, Koekkoek SK, van Alphen AM, Linden DJ, Oberdick J (1998) Expression of a protein kinase C inhibitor in Purkinje cells blocks cerebellar LTD and adaptation of the vestibulo-ocular reflex. *Neuron* 20:495-508.
- Ebner TJ, Bloedel JR (1981) Correlation between activity of Purkinje cells and its modification by natural peripheral stimuli. *J Neurophysiol* 45:948-961.
- Egorov AV, Hamam BN, Fransen E, Hasselmo ME, Alonso AA (2002) Graded persistent activity in entorhinal cortex neurons. *Nature* 420:173-178.
- Ekerot CF, Jorntell H (2001) Parallel fibre receptive fields of Purkinje cells and interneurons are climbing fibre-specific. *Eur J Neurosci* 13:1303-1310.
- Feil R, Hartmann J, Luo C, Wolfgruber W, Schilling K, Feil S, Barski JJ, Meyer M, Konnerth A, De Zeeuw CI, Hofmann F (2003) Impairment of LTD and cerebellar learning by Purkinje cell-specific ablation of cGMP-dependent protein kinase I. *J Cell Biol* 163:295-302.

- Fletcher CF, Lutz CM, O'Sullivan TN, Shaughnessy JD, Jr., Hawkes R, Frankel WN, Copeland NG, Jenkins NA (1996) Absence epilepsy in tottering mutant mice is associated with calcium channel defects. *Cell* 87:607-617.
- Franks NP, Lieb WR (1994) Molecular and cellular mechanisms of general anaesthesia. *Nature* 367:607-614.
- Gauck V, Jaeger D (2000) The control of rate and timing of spikes in the deep cerebellar nuclei by inhibition. *J Neurosci* 20:3006-3016.
- Gauck V, Jaeger D (2003) The contribution of NMDA and AMPA conductances to the control of spiking in neurons of the deep cerebellar nuclei. *J Neurosci* 23:8109-8118.
- Hansel C, Linden DJ, D'Angelo E (2001) Beyond parallel fiber LTD: the diversity of synaptic and non-synaptic plasticity in the cerebellum. *Nat Neurosci* 4:467-475.
- Hansel C, de Jeu M, Belmeguenai A, Houtman SH, Buitendijk GH, Andreev D, De Zeeuw CI, Elgersma Y (2006) α CaMKII is essential for cerebellar LTD and motor learning. *Neuron* 51:835-843.
- Hausser M, Clark BA (1997) Tonic synaptic inhibition modulates neuronal output pattern and spatiotemporal synaptic integration. *Neuron* 19:665-678.
- Heck DH, Thach WT, Keating JG (2007) On-beam synchrony in the cerebellum as the mechanism for the timing and coordination of movement. *Proc Natl Acad Sci U S A* 104:7658-7663.
- Heyward P, Ennis M, Keller A, Shipley MT (2001) Membrane bistability in olfactory bulb mitral cells. *J Neurosci* 21:5311-5320.
- Ito M, Simpson JJ (1971) Discharges in Purkinje cell axons during climbing fiber activation. *Brain Res* 31:215-219.
- Jaeger D (2003) No parallel fiber volleys in the cerebellar cortex: evidence from cross-correlation analysis between Purkinje cells in a computer model and in recordings from anesthetized rats. *J Comput Neurosci* 14:311-327.
- Jirenhed DA, Bengtsson F, Hesslow G (2007) Acquisition, extinction, and reacquisition of a cerebellar cortical memory trace. *J Neurosci* 27:2493-2502.
- Jorntell H, Ekerot CF (2002) Reciprocal bidirectional plasticity of parallel fiber receptive fields in cerebellar Purkinje cells and their afferent interneurons. *Neuron* 34:797-806.
- Jorntell H, Ekerot CF (2003) Receptive field plasticity profoundly alters the cutaneous parallel fiber synaptic input to cerebellar interneurons in vivo. *J Neurosci* 23:9620-9631.
- Kano M, Rexhausen U, Dreessen J, Konnerth A (1992) Synaptic excitation produces a long-lasting rebound potentiation of inhibitory synaptic signals in cerebellar Purkinje cells. *Nature* 356:601-604.
- Kano M, Kano M, Fukunaga K, Konnerth A (1996) Ca^{2+} -induced rebound potentiation of gamma-aminobutyric acid-mediated currents requires activation of Ca^{2+} /calmodulin-dependent kinase II. *Proc Natl Acad Sci U S A* 93:13351-13356.
- Khaliq ZM, Raman IM (2005) Axonal propagation of simple and complex spikes in cerebellar Purkinje neurons. *J Neurosci* 25:454-463.
- Kopysova IL, Debanne D (1998) Critical role of axonal A-type K^{+} channels and axonal geometry in the gating of action potential propagation along CA3 pyramidal cell axons: a simulation study. *J Neurosci* 18:7436-7451.
- Lisman J (1989) A mechanism for the Hebb and the anti-Hebb processes underlying

- learning and memory. *Proc Natl Acad Sci U S A* 86:9574-9578.
- Lisman JE, Zhabotinsky AM (2001) A model of synaptic memory: a CaMKII/PP1 switch that potentiates transmission by organizing an AMPA receptor anchoring assembly. *Neuron* 31:191-201.
- Loewenstein Y, Mahon S, Chadderton P, Kitamura K, Sompolinsky H, Yarom Y, Hausser M (2005) Bistability of cerebellar Purkinje cells modulated by sensory stimulation. *Nat Neurosci* 8:202-211.
- MacIver MB, Kendig JJ (1991) Anesthetic effects on resting membrane potential are voltage-dependent and agent-specific. *Anesthesiology* 74:83-88.
- Madeja M (2000) Do neurons have a reserve of sodium channels for the generation of action potentials? A study on acutely isolated CA1 neurons from the guinea-pig hippocampus. *Eur J Neurosci* 12:1-7.
- Mar DJ, Chow CC, Gerstner W, Adams RW, Collins JJ (1999) Noise shaping in populations of coupled model neurons. *Proc Natl Acad Sci U S A* 96:10450-10455.
- Matsushita K, Wakamori M, Rhyu IJ, Arai T, Oda S, Mori Y, Imoto K (2002) Bidirectional alterations in cerebellar synaptic transmission of tottering and rolling Ca²⁺ channel mutant mice. *J Neurosci* 22:4388-4398.
- Middleton FA, Strick PL (1994) Anatomical evidence for cerebellar and basal ganglia involvement in higher cognitive function. *Science* 266:458-461.
- Mintz IM, Bean BP (1993) GABAB receptor inhibition of P-type Ca²⁺ channels in central neurons. *Neuron* 10:889-898.
- Mittmann W, Hausser M (2007) Linking synaptic plasticity and spike output at excitatory and inhibitory synapses onto cerebellar Purkinje cells. *J Neurosci* 27:5559-5570.
- Mittmann W, Chadderton P, Hausser M (2004) Neuronal microcircuits: frequency-dependent flow of inhibition. *Curr Biol* 14:R837-839.
- Mittmann W, Koch U, Hausser M (2005) Feed-forward inhibition shapes the spike output of cerebellar Purkinje cells. *J Physiol* 563:369-378.
- Miyashita Y, Nagao S (1984) Contribution of cerebellar intracortical inhibition to Purkinje cell response during vestibulo-ocular reflex of alert rabbits. *J Physiol* 351:251-262.
- Monsivais P, Clark BA, Roth A, Hausser M (2005) Determinants of action potential propagation in cerebellar Purkinje cell axons. *J Neurosci* 25:464-472.
- Palkovits M, Mezey E, Hamori J, Szentagothai J (1977) Quantitative histological analysis of the cerebellar nuclei in the cat. I. Numerical data on cells and on synapses. *Exp Brain Res* 28:189-209.
- Pedroarena CM, Schwarz C (2003) Efficacy and short-term plasticity at GABAergic synapses between Purkinje and cerebellar nuclei neurons. *J Neurophysiol* 89:.
- Robinson HP, Kawai N (1993) Injection of digitally synthesized synaptic conductance transients to measure the integrative properties of neurons. *J Neurosci Methods* 49:157-165.
- Sausbier M, Hu H, Arntz C, Feil S, Kamm S, Adelsberger H, Sausbier U, Sailer CA, Feil R, Hofmann F, Korth M, Shipston MJ, Knaus HG, Wolfer DP, Pedroarena CM, Storm JF, Ruth P (2004) Cerebellar ataxia and Purkinje cell dysfunction caused by Ca²⁺-activated K⁺ channel deficiency. *Proc Natl Acad Sci U S A* 101:9474-9478.
- Sejnowski TJ, Paulsen O (2006) Network oscillations: emerging computational principles. *J Neurosci* 26:1673-1676.

- Stahl JS, James RA, Oommen BS, Hoebeek FE, De Zeeuw CI (2006) Eye movements of the murine P/Q calcium channel mutant tottering, and the impact of aging. *J Neurophysiol* 95:1588-1607.
- Steinmetz PN, Manwani A, Koch C (2001) Variability and coding efficiency of noisy neural spike encoders. *Biosystems* 62:87-97.
- Steuber V, Mittmann W, Hoebeek FE, Silver RA, De Zeeuw CI, Hausser M, De Schutter E (2007) Cerebellar LTD and pattern recognition by Purkinje cells. *Neuron* 54:121-136.
- Tiesinga PH, Fellous JM, Jose JV, Sejnowski TJ (2002) Information transfer in entrained cortical neurons. *Network* 13:41-66.
- Tiesinga PH, Fellous JM, Salinas E, Jose JV, Sejnowski TJ (2004) Inhibitory synchrony as a mechanism for attentional gain modulation. *J Physiol Paris* 98:296-314.
- Van Der Giessen RS, Koekkoek SK, van Dorp S, De Gruijl JR, Cupido A, Khosrovani S, Dortland B, Wellershaus K, Degen J, Deuchars J, Fuchs EC, Monyer H, Willecke K, De Jeu MT, De Zeeuw CI (2008) Role of olivary electrical coupling in cerebellar motor learning. *Neuron* 58:599-612.
- Wakamori M, Yamazaki K, Matsunodaira H, Teramoto T, Tanaka I, Niidome T, Sawada K, Nishizawa Y, Sekiguchi N, Mori E, Mori Y, Imoto K (1998) Single tottering mutations responsible for the neuropathic phenotype of the P-type calcium channel. *J Biol Chem* 273:34857-34867.
- Williams SR, Christensen SR, Stuart GJ, Hausser M (2002) Membrane potential bistability is controlled by the hyperpolarization-activated current I(H) in rat cerebellar Purkinje neurons in vitro. *J Physiol* 539:469-483.
- Zhou YD, Turner TJ, Dunlap K (2003) Enhanced G protein-dependent modulation of excitatory synaptic transmission in the cerebellum of the Ca²⁺ channel-mutant mouse, tottering. *J Physiol* 547:497-507.

Summary

This thesis attempts to correlate cerebellar Purkinje cell spiking activities to motor performance and motor learning. To do so we evoked compensatory eye movements in mice by visual and/or vestibular stimulation, and recorded the eye movements and floccular Purkinje cell activity. The relationship between the flocculus and eye movements has been previously established in several species, and a zonal organization has been described in for instance the cat (Groenewegen and Voogd, 1977) and the rabbit (Van der Steen et al., 1994). Though recordings have been made from the mouse flocculus, no studies have focused on the organization of the flocculus in mice.

In chapter 2 we demonstrate that the flocculus in the mouse has five zones: two vertical axis (VA), two horizontal axis (HA) and a non-responsive zone(s), comparable to the rabbit. Additionally, we show that discrete regions in the inferior olive send climbing fibres to the flocculus, and that floccular projections also adhere to the system of separate modules. This study forms the basis for the subsequent chapters on motor performance and motor learning in relation to Purkinje cell activity.

In the next chapter we focus on the simple spikes and their temporal distribution. First, we provide strong evidence against the acclaimed role for Purkinje cell membrane potential bistability. We demonstrated with intracellular recordings that during the hyperpolarized downstate no simple spikes are fired, while in the depolarized upstate there always is simple spike activity, thereby permitting the use of extracellular recordings to test the occurrence of bistability *in vivo*. We then recorded Purkinje cells under several conditions and in normal and mutant mice and found that Purkinje cells in awake behaving animals are virtually always in the upstate, and downstates can only be observed in anesthetized mice and/or mice with genetic mutations. Next, we focus on Purkinje cell activity patterns and find that simple spike activities occur regularly when examined on small timescales, in contrast to the highly irregular activity over longer periods. The fact that regular patterns coincide in nearby Purkinje cells, taken together with the modelled effect on the DCN, suggest that PCs may transfer information, at least in part, in regular spike patterns to downstream DCN neurons. Third, we demonstrate the importance of simple spike firing patterns for motor behaviour using the *tottering* natural mutant. These mice with a mutation of voltage gated calcium channels -most abundantly present in Purkinje cells- suffer from severe ataxia. We show that motor performance in *tottering* mice is very poor, and is not further impaired by ablation of the flocculus. Simple spike firing activity is highly irregular, but still shows 'normal' average modulation when a visual stimulus is given. These contradictory results stress the devastating effect of noise in simple spike firing and the importance of the spike regularity for normal motor behaviour.

In Chapter 4 we go into a major question in cerebellar research, the exact locus of motor learning. First we provide strong evidence against the role of Pf-PC LTD in motor learning, by studying VOR adaptation in three different mouse mutants with mutations downstream of the kinase pathway that has been strongly implicated motor learning, as described in further detail in the introduction (Chapter 1). All three mutant mice adapted normally in both short and long term learning paradigms, contradicting the longstanding hypothesis that Pf-PC LTD is the key element in cerebellar motor learning, at least for VOR adaptation. Next, we tested the role of calcineurin and the phosphatase

pathway, which, when activated, counteracts the kinase pathway and leads to Pf-PC LTP. In cerebellar slices of mutant mice with a Purkinje cell specific ablation of calcineurin or phosphatase 2B (PP2B), we found that PP2B is required for Pf-PC LTP but not for LTD. Mice without PP2B in Purkinje cells have mild motor performance problems and severe short and long term motor learning problems, but LTD is not affected. Additionally, we observed a distinct change in the shape of the interspike interval distributions with significantly less higher and lower frequencies, and thus more regular firing, in the mutant mice.

In Chapter 5 we investigated a relatively unexplored area in cerebellar research: the role of molecular layer interneurons (MLIs) in motor behaviour. To do so we used mice with Purkinje cell specific mutation that keeps GABA_A receptors outside the synapse, thereby rendering the molecular layer interneurons ineffective. These mutants showed a clear phenotype: motor performance was slightly affected and particularly long-term motor learning and the inter simple spike interval distributions were severely affected. The simple spike activity of Purkinje cells in the mutant mice showed abnormal temporal patterns, both during and in the absence of naturally evoked compensatory eye movements, whereas mean firing frequencies were unaffected. We used these experimental data to generate computer simulations of the vestibulo-cerebellar system. Based on the experimental data and computer simulations we propose that feed-forward inhibition from molecular layer interneurons, by controlling the temporal patterns of Purkinje cell activity, is necessary for the consolidation of cerebellar learning in downstream neurons of the cerebellar and vestibular nuclei.

All in all, the present thesis describes electrophysiological and behavioural studies in a large number of genetically manipulated mice. Although individual mutant mouse strains often lead to interesting hypotheses, ultimately the features found using molecular, electrophysiological and behavioural analysis of a spectrum of genetically or pharmacologically manipulated mice will have to lead to the general understanding of cerebellar learning rules and codes.

Samenvatting

Dit proefschrift tracht cerebellaire Purkinje cel activiteit te correleren aan motorisch gedrag en motorisch leren. Ten einde dit doel te bereiken, hebben we compensatoire oogbewegingen opgewekt in muizen met visuele en vestibulaire stimulatie, en de oogbewegingen en Purkinje cel activiteit in de flocculus gemeten. De sterke relatie tussen de flocculus en oogbewegingen eerst eerder uitgebreid beschreven in meerdere diersoorten, en een gezonde organisatie is beschreven voor de kat (R) en het konijn (R). Alhoewel metingen in de flocculus van de muis al eerder gedaan zijn, is de organisatie van de flocculus in de muis nog niet onderzocht. In hoofdstuk 2 tonen we aan dat de flocculus in de muis 5 zones heeft: twee verticale as (VA), twee horizontale as (HA) en een zone die niet reageert op visuele stimulatie. Daarnaast tonen we aan dat specifieke gebieden in de inferieure olijf klimvezels sturen naar de flocculus en dat de flocculaire projecties zich ook aan deze scheiding van modules houden. Deze studie vormt deze basis voor de hierop volgende hoofdstukken over motorisch gedrag en motorisch leren in relatie tot Purkinje cel activiteit.

In het volgende hoofdstuk richten we ons op de simple spikes en hun temporele distributie. In paragraaf 1 leveren bewijs tegen de geclaimde rol van membraan potentiaal bistabiliteit van Purkinje cellen. Door middel van intracellulaire metingen tonen we aan dat tijdens 'downstates' geen actiepotentialen gevuurd worden, terwijl er in de 'upstate' altijd simple spike activiteit is. Dit maakt het mogelijk extracellulaire metingen te gebruiken om het voorkomen van bistabiliteit in vivo te bestuderen. Vervolgens hebben de Purkinje cel activiteit gemeten onder verschillende omstandigheden en in normale en mutant muizen en vonden dat Purkinje cellen in wakkere, actieve muizen zo goed als altijd in de 'upstate' verkeren en dat 'downstates' vrijwel alleen in geanesthezeerde en/of mutant muizen. Vervolgens richten we ons op Purkinje cel vuurpatronen en tonen aan dat simple spikes zeer regelmatig zijn op kleine tijdschalen, terwijl ze over grotere perioden juist onregelmatig zijn. Het feit dat regelmatige patronen in nabij gelegen Purkinje cellen gelijktijdig voorkomen, samen met het gemodelleerde effect hiervan op de diep cerebellaire kernen (DCN), suggereert dat Purkinje cellen tenminste ten dele informatie doorgeven aan de DCN cellen door middel van regelmatige patronen. Ten derde tonen we met behulp van de *tottering* muis het belang aan van simple spikes vuurpatronen in motorisch gedrag. Deze muizen hebben een heterozygote mutatie van een voltage-gevoelig calcium kanaal, welke voornamelijk tot expressie komt in Purkinje cellen, en leiden aan een ernstige vorm van ataxie. We tonen aan dat motorisch gedrag bijzonder sterk aangedaan is in tottering muizen, zo sterk dat verwijdering van de flocculus geen invloed meer heeft. Simple spike vuurpatronen zijn bijzonder onregelmatig, maar herhaalde visuele stimulatie leidt nog steeds tot een 'normale' gemiddelde response. Deze tegenstrijdigheid benadrukt het desastreuze effect van ruis in simple spike vuurpatronen en het belang van regelmatigheid van Purkinje cel vuren voor normaal motorisch gedrag.

In hoofdstuk 4 onderzoeken we een belangrijk vraagstuk in cerebellair onderzoek, de exacte plaats waar het motorisch leren plaats vindt. We trekken de bestaande hypothese draaiend om de rol van Pf-PC LTD in twijfel, door de VOR adaptatie te bestuderen in drie verschillende transgene muizen, allen met mutatie in eiwitten downstream in het kinase-pad dat sterk gekoppeld is aan motorisch leren. Alle drie de transgenen leren

vergelijkbaar met de controle muizen in zowel het korte als lange termijn adapteren. Dit weersprekt, in ieder geval voor VOR adaptatie, dat de oude hypothese dat Pf-PC LTD het belangrijkste element in motorisch leren is. Vervolgens hebben we de rol van calcineurin en daarmee het phosphatase-pad bestudeerd, het pad dat wanneer geactiveerd het kinase-pad tegenwerkt en leidt tot Pf-PC LTP. In plakjes van het cerebellum van de transgene muizen met een Purkinje cel specifieke deletie van calcineurin (PP2B) tonen we aan dat PP2B noodzakelijk is voor Pf-PC LTP maar niet LTD. Muizen zonder PP2B in hun Purkinje cellen hebben een licht motorisch gedragsprobleem, en ernstige korte en lange termijn adaptatieproblemen. Daarnaast vonden we een scherpe verandering in de vorm van de inter simple spike interval distributies met significant grote en kleine intervallen, en dus meer regelmatigheid, in de transgene muizen.

In hoofdstuk 5 onderzoeken we een relatief onontgonnen terrein in het cerebellaire onderzoek: de rol van inhibitie van moleculaire laag interneuronen. Hiervoor hebben we gebruik gemaakt van muizen met een Purkinje cel specifieke mutatie die voorkomt dat de GABA_A-receptor in de synapse samenkomen, waardoor de moleculaire laag interneuronen hun functie verliezen. Deze transgenen vertoonden een duidelijk fenotype: motorisch gedrag was licht aangedaan, en voornamelijk lange termijn motorisch leren en de inter simple spike interval distributies zijn sterk aangedaan. Het simple spike vuurgedrag van de transgenen vertonen abnormale patronen, zowel in rust als tijdens visuele of vestibulaire stimulatie, terwijl de gemiddelde vuurfrequentie niet is aangedaan. Met behulp van experimentele data hebben we computer simulaties gemaakt van het vestibulo-cerebellaire systeem. Op basis van de experimentele data en computer simulaties komen we tot de volgende hypothese: feed-forward inhibitie van moleculaire laag interneuronen is, door middel van controle op Purkinje cel vuurpatronen, noodzakelijk voor de consolidatie van cerebellair leren in de cellen downstream van de flocculus.

Over het geheel genomen beschrijft dit proefschrift elektrofysiologische en gedragsstudies in een groot aantal genetisch gemanipuleerde muizen. Hoewel individuele muismodellen vaak leiden tot interessante hypothesen, zal uiteindelijk de volledige karakterisering op moleculair, elektrofysiologisch en gedragsniveau van een spectrum aan genetisch of farmacologisch gemanipuleerde muizen moeten leiden tot het algemene begrip van de cerebellaire leerregels en -coderingen.

Dankwoord

Dit zijn misschien wel de meest gelezen pagina's van dit boekje, en voor de leek in ieder geval de meest leesbare pagina's. Helaas voor mij ook de lastigste om te schrijven. Toch ga ik mijn best doen om te eren wie er toe komt en hopelijk duidelijk te maken dat er veel mensen aan dit proefschrift hebben bijgedragen. Bij voorbaat mijn excuses aan de mensen die ik onverhoopt ben vergeten, onthouden is nog steeds niet mijn sterkste eigenschap.

Als eerste gaat mijn dank natuurlijk uit naar Chris. Vanaf de eerste dag had ik het gevoel dat ik in Rotterdam goed zat en dat is zeker niet in de laatste plaats door jou gekomen. Ik vond het wat vreemd dat je tijdens mijn 'sollicitatie-lunch' meer interesse leek te hebben in mijn voetbalverleden dan in mijn wetenschappelijke activiteiten. Pas later begreep ik het belang van dit soort eigenschappen bij het zoeken naar nieuwe mensen. Eén van de vele wetenschappelijke en niet-wetenschappelijke dingen die ik van je heb geleerd. Bedankt voor het vertrouwen, de steun en de drive die je me gaf. Ik hoop deze nog lang te ondervinden.

Daarnaast natuurlijk mijn enorme dank aan Freek, mijn copromotor! Je leerde me alle tips en tricks van het meten van oogbewegingen en het tegelijk afleiden van Purkinje cellen. Maar boven alles leerde je me tussen de regels door om niet te veel te "ja, maar"-en en dat er maar één manier is om een experiment succesvol af te ronden, doorrammen. Je stond en staat altijd open voor vragen, of het nou werk is of privé, zelfs nu we langzaam aan andere dingen zijn gaan doen. Ik hoop dat we nog vele jaren zo verder kunnen, het bevalt mij zeer goed. Bedankt gast!

Vervolgens wil ik mijn kleine commissieleden graag bedanken: Hans, Tom en Maarten. Alle drie hebben jullie vooral in het begin van mijn AIO-periode me wegwijs gemaakt op de jullie eigen gebieden. Hans, bedankt voor de introductie in het vestibulaire systeem, de leuke werkbesprekingen en de gezelligheid. Het projectie-project gaan we zeker een keer afmaken! Tom, jouw schijnbaar eindeloze kennis van de anatomie is van grote waarde geweest voor mij. Met alle vragen kon ik bij je terecht en zelfs nu nog was je zo scherp op alles wat maar enigszins anatomisch gerelateerd is in dit proefschrift dat je er oude foutjes uit hebt weten te halen. Bedankt! Maarten, het lastig exact te duiden waar ik je precies voor wil danken. Problemen van allerlei soort, algemene vragen en discussies, voor alles kon ik bij je terecht. Bedankt voor die altijd leuke en interessante gesprekken!

Daarnaast wil ik hier mijn dank betuigen aan Marcel, de drijvende kracht achter veel van de experimenten die in dit proefschrift beschreven staan. Het briefje "niet storen" heb ik vaak genegeerd, en toch was je altijd bereid te helpen. Ik hoop dat we de goede samenwerking voort kunnen zetten!

Jerry! A special 'thank you' to the man with whom I spent many many hours talking about all sorts of things, many not related to science at all. It has always been a pleasure, and has been highly educational too. I do hope to be able to visit you in New York one

day and for you to visit us in our new house.

Natuurlijk mag de andere Hans niet ontbreken in de lijst. Bedankt voor het helpen repareren van de opstelling, het ontwikkelen van de operatietechnieken, mijn eerste echte lessen in elektrische circuits, het maken van stapels dual-recording pipetten, het niet doorberekenen van al mijn minpunten en bovenal de zeer nodige afleiding met foute grappen. Eén van de belangrijkste redenen dat ik het meten en opereren zo mis, is dat ik nu niet meer elke dag even mag komen zeuren omdat iets niet werkt. Daar ga ik na mijn promotie verandering in brengen!

Mijn dank gaat ook uit naar Elize, Erika en Mandy. Elize voor de mooie EM plaatjes en lekkere borrels en Erika voor alle hulp bij de histologie en het gezellige buurten. Mandy, bedankt voor al het breedten en genotyperen, en vooral de hulp bij het regelen van de altijd leuke imports. Bovenal alle drie enorm bedankt voor alle gezelligheid en een luisterend oor in tijden van chaos.

Ook wil ik Edith en Loes bedanken voor alle hulp bij allerhande problemen en bij het mogelijk maken van deze promotie. Daarbij weet ik zeker dat het zonder al die extra suikers die ik bij jullie gehaald heb niet was gelukt. Bedankt!

Veel dank ook voor Eddie, voor de mooie EM plaatjes en de hulp bij het bestellen, installeren en onderhouden van de inmiddels flinke lijst aan computers.

Annette, Kenneth, Ria en Jurgen bedankt voor de hulp bij allerhande financiële zaken, dingen die er vaak bij in schieten in alle drukte.

Aleksandra, in English of toch maar gewoon in het Nederlands? Ik denk dat we vanaf nu maar over moeten op Nederlands, dat beheers je toch meer dan goed genoeg. Net als de taal heb je de werkzaamheden in het lab heel snel eigen gemaakt. Je leert snel en hebt in zeer korte tijd je plek in het lab gevonden. Daarom weet ik zeker dat ook jij je promotie met succes zult afronden. Er staan nog een paar heel mooie experimenten gepland, waar ik je (ons) heel veel succes mee wens.

Dan kan ik natuurlijk niet om Rogerio heen. Je hebt me enorm veel werk uit handen genomen en inmiddels zijn we zo op elkaar ingespeeld dat ik met een gerust hart voor langere tijd op vakantie kan. Jouw stabiele manier van werken is ideaal voor de experimenten en gaat hopelijk in de toekomst nog veel meer mooie resultaten opleveren. Bedankt!

Na een vrij rustig begin waren daar de laatste jaren ineens een aantal (top)masterstudenten, die ik het één en ander mocht bijbrengen en die vervolgens daarmee aan de slag zijn gegaan. Wardell, het project waar je aan ging werken was al zeker een jaar of 2 bezig, maar mede dankzij jouw enorme inzet gaat het nu eindelijk afgerond worden. Ik denk dat we er beiden zeer veel van hebben geleerd. Laurens, het feit dat je nu als AIO bent begonnen met het bouwen van je eigen opstelling, zegt genoeg denk ik. Je kwam hier, ging aan de slag en ik moest mijn best doen om je nog een beetje begeleiding te kunnen geven. Ik hoop dat je het goede werk van hier voort kunt zetten in Amsterdam en dat we intensief kunnen blijven samenwerken. Caroline en Thijs, het laatste half jaar is voor mij heel snel gegaan, en daardoor heb ik niet altijd de tijd voor jullie gehad, die ik had willen hebben. Desondanks is het jullie toch heel goed afgegaan, vooral door jullie

enorme inzet. Ik ben erg blij met de nieuwe richting van jullie projecten en hoop dat we daar succesvol aan kunnen blijven werken. Thomas, weliswaar nog geen master, maar ik ga er vanuit dat dat nog komt, zodat we dan eindelijk het mosvezel project af kunnen maken. Voor nu bedankt voor de gezelligheid en tot ziens dus!

Oud-collega's Arjan, Luo, Corina, Sara en Ruben wil ik ook in het bijzonder bedanken voor de nuttige, interessante of gewoon gezellige gesprekken. Arjan, bedankt voor de hulp bij het leren werken met de opstelling en de nodige cynische commentaren die me hebben voorbereid op alle mislukte experimenten. Jouw werk was de basis voor groot deel van dit boekje. Luo, mijn eerste kamergenoot, bedankt voor gezelligheid en goede samenwerking. We moeten nodig eens een 'borrel' doen. Corina, we zijn tegelijk begonnen, maar ik was niet snel genoeg om samen te eindigen. Ik heb enorm veel respect en bewondering voor wat je hier gepresteerd hebt en ook wat je nu doet. Bedankt voor alles! Sara, bedankt voor de vaak vrolijke noot, de leuke samenwerking en de heel leuke trip naar Pavia. Ik zal nooit meer naar Bruce kunnen luisteren zonder daar aan te denken. Ruben, ondanks dat we nooit een echt project samen hebben gedaan, hebben we elkaar toch goed kunnen helpen met technieken. Wie weet kunnen we dat project in de toekomst nog eens op poten zetten.

Also I would like to thank Christian for the nice discussions on LTD and its role in life, for your pictures I used in this thesis and for keeping the eternal soccer rivalry alive. Ype, bedankt voor de goede samenwerking en de nuttige commentaren. Zoals gezegd, ik ben erg enthousiast over de voor mij nieuwe richting met de meer klinisch relevante muismodellen. Bas, bedankt voor alle hulp bij het verhelpen van opstellingsproblemen, en het bouwen van nieuwe opstellingen. Daarnaast ben ik je ook zeer erkentelijk voor de prachtige plaatjes, die ook veelvuldig in dit proefschrift terug te vinden zijn. Dick, bedankt voor de regelmatige update over het ALS-veld, en alle leuke uren lesgeven in de snijzaal. Hopelijk zullen er nog vele volgen.

Beerend en Bart bedankt voor de samenwerking, de gezelligheid in Rotterdam en in Bergen aan Zee en de hulp in geval van nood. Succes met de laatste loodjes, waar het kan, help ik graag.

Simone, vooral het laatste jaar was erg gezellig met een voor mij in ieder geval onverwachte samenwerking. Ik hoop dat ons project het mooie einde krijgt dat het verdient, je privé project is in ieder geval heel goed gelukt.

Ook Geeske en Petra wil ik bedanken. Geeske voor de leuke gesprekken en langzaam groeiende samenwerking, die mij heel goed bevalt. Petra omdat het altijd gezellig is, en nu je nog dichterbij komt werken kan het alleen maar leuker worden!

Because of the tight collaboration with Freek and Marcel I have spent a quite some time with Gao, Andreea, Elisa and Paolo. I wish you all the best of luck and hope to continue working with you.

I want to thank Peer, Bill, Erik, Soon-Lim, Rick and David for the studies we did together, the results of which can be found in this thesis. I hope we can continue and extend these fruitful collaborations.

Tot slot wil ik natuurlijk de mensen die mij buiten werk enorm gesteund hebben bedanken. Pap, Mam, Marie-Louise, Pascal, Margriet, bedankt voor jullie liefde en onvoorwaardelijke steun die dit alles mogelijk hebben gemaakt. Cees, Marianne, Jessika, Johan, Fiona en John bedankt voor de warme ontvangst en de hulp bij van alles. Wijnand en Hanneke, Bart en Marja, Martijn en Annemieke bedankt voor de gezelligheid en ontspanning in lunchpauzes en buiten werktijd.

En zoals elke dag is het laatste woord natuurlijk voor Amanda.

Amanda, dit alles was om zoveel redenen niet zo gegaan zonder jou. Het feit dat jij al in Rotterdam zat had natuurlijk niets te maken met mijn keuze om hier te gaan werken... Bedankt voor je steun als ik thuis kwam na een zware dag, je begrip als ik weer eens in het weekend moest werken en je lieve zorgen als het even wat minder ging. Bij jouw stralende lach vergeet ik alle tegenslag meteen. Daarom deel ik deze titel met liefde met jou!

Curriculum Vitae

Martijn Schonewille

30 september 1978	geboren te Rotterdam
1990-1996	VWO, C.S.G. Blaise Pascal te Spijkenisse
1996-2002	Biomedische Wetenschappen, Universiteit Utrecht
2002	Wetenschappelijk onderzoeker, Afd. Sportgeneeskunde en Medische Fysiologie, Universiteit Utrecht
2003-2008	AIO Afd. Neurowetenschappen Erasmus MC
2008-	Postdoc Afd. Neurowetenschappen Erasmus MC

List of publications

F.E. Hoebeek, J.S. Stahl, A.M. van Alphen, M. Schonewille, C. Luo, M. Rutteman, A.M. van den Maagdenberg, P.C. Molenaar, H.H. Goossens, M.A. Frens, C.I. De Zeeuw.
Increased noise level of Purkinje cell activities minimizes impact of their modulation during sensorimotor control.
Neuron. 2005 Mar 24;45(6):953-65.

M. Schonewille, C. Luo, T.J. Ruigrok, J. Voogd, M.T. Schmolesky, M. Rutteman, F.E. Hoebeek, M.T. De Jeu, C.I. De Zeeuw.
Zonal organization of the mouse flocculus: physiology, input, and output.
J Comp Neurol. 2006 Aug 1;497(4):670-82.

M. Schonewille, S. Khosrovani, B.H. Winkelman, F.E. Hoebeek, M.T. De Jeu, I.M. Larsen, J. Van der Burg, M.T. Schmolesky, M.A. Frens, C.I. De Zeeuw.
Purkinje cells in awake behaving animals operate at the upstate membrane potential.
Nat Neurosci. 2006 Apr;9(4):459-61.

S.L. Shin, F.E. Hoebeek, M. Schonewille, C.I. De Zeeuw, A. Aertsen, E. De Schutter.
Regular patterns in cerebellar Purkinje cell simple spike trains.
PLoS ONE. 2007 May 30;2(5):e485.

C.I. De Zeeuw, F.E. Hoebeek, M. Schonewille.
Causes and consequences of oscillations in the cerebellar cortex.
Neuron. 2008 Jun 12;58(5):655-8.

M. Schonewille, P. Wulff, M. Renzi, L. Viltono, M. Sassoè-Pognetto, A. Badura, Z. Gao, F.E. Hoebeek, S. van Dorp, W. Wisden, M. Farrant and C.I. De Zeeuw.
Role of GABAergic interneurons in cerebellar motor learning
Submitted

M. Schonewille, S.H. Houtman, G. Othsuki, H.J. Boele, A. Badura, A. Belmeguenai, S. Tonegawa, S.K. Koekkoek, Y. Elgersma, C.H. Hansel and C.I. De Zeeuw.
Role of calcineurin in Pf-PC LTP and cerebellar motor learning
Submitted

M. Schonewille, Z. Gao, F.E. Hoebeek, W. Amerika, M. de Jeu, D. Linden, R. Huganir and C.I. De Zeeuw.
Challenging the Marr-Albus-Ito Hypothesis
Submitted

F.E. Hoebeek, B.B. Todorov, E. Galliano, A. Pop, Z. Gao, M. Schonewille, E. D'Angelo, A.M. van den Maagdenberg, C.I. De Zeeuw.
Granule cells mediate cerebellar learning by altering regularity of Purkinje cell firing
In preparation

L. Witter, S. Khosrovani, M. Schonewille, C.I. De Zeeuw.

A look inside cerebellar cortical neurons: linking electrophysiology to morphology
In preparation

M. Schonewille, J.J. Kuo, T. Siddique, A.N. Schults, R. Fu, P.R. Bär, R. Anelli, C.J. Heckman, A.B. Kroese.

Hyperexcitability of cultured spinal motoneurons from presymptomatic ALS mice.
J Neurophysiol. 2004 Jan;91(1):571-5.